

ISSN 1563 – 0277
eISSN 2617 – 4871

ӘЛ-ФАРАБИ атындағы ҚАЗАҚ ҰЛТТЫҚ УНИВЕРСИТЕТІ

ХАБАРШЫ

Математика, механика, информатика сериясы

КАЗАХСКИЙ НАЦИОНАЛЬНЫЙ УНИВЕРСИТЕТ имени АЛЬ-ФАРАБИ

ВЕСТНИК

Серия математика, механика, информатика

AL-FARABI KAZAKH NATIONAL UNIVERSITY

Journal of Mathematics, Mechanics and Computer Science

№1 (121)

Алматы
«Қазақ университеті»
2024

Зарегистрирован в Министерстве информации и коммуникаций Республики Казахстан, свидетельство №16508-Ж от 04.05.2017 г. (Время и номер первичной постановки на учет №766 от 22.04.1992 г.). Язык издания: английский. Выходит 4 раза в год.

Тематическая направленность: теоретическая и прикладная математика, механика, информатика.

Редакционная коллегия

научный редактор – Б.Е. Кангужин, д.ф.-м.н., профессор, КазНУ им. аль-Фараби,
заместитель научного редактора – Д.И. Борисов, д.ф.-м.н., профессор, Институт математики с
вычислительным центром Уфимского научного центра РАН, Башкирский государственный педагогический
университет им. М. Акмуллы, Россия
ответственный секретарь – С.Е. Айтжанов, к.ф.-м.н., доцент, КазНУ им. аль-Фараби

Гиви Пэйман (США); Моханрадж Муругесан (Индия); Эльбаз Ибрагим Мохаммед Абу Эльмагд (Египет);
Кабанихин С.И. (Россия); Майнке М. (Германия); Малышкин В.Э. (Россия); Ракишева З.Б. (Казахстан);
Ружанский М. (Бельгия); Сагитов С.М. (Швеция); Сукочев Ф.А. (Австралия); Тайманов И.А. (Россия);
Темляков В.Н. (США); Шиничи Накасука (Япония); Моханрадж Муругесан (Индия); Гиви Пейман (США);
Дарибаев Беимбет Серикович (Казахстан); Иманкулов Тимур Сакенович (Казахстан); Сергей Горлач (Гер-
мания); Триго Пауло (Португалия); Минсу Хан (Южная Корея); Эжилчелван Пол Девадосс (Великобрита-
ния); Кантони Вирджинио (Италия); Феррейра Хорхе (Бразилия); Мохаммед Отман (Малайзия); Альбер-
то Кабада (Испания)

Индексируется и участвует:



Научное издание
Вестник КазНУ. Серия “Математика, механика, информатика”, № 1 (121) 2024.
Редактор – С.Е. Айтжанов. Компьютерная верстка – С.Е. Айтжанов

ИБ N 15309
Формат 60 × 84 1/8. Бумага офсетная. Печать цифровая. Объем 11,0 п.л.
Заказ N 623. Издательский дом “Қазақ университеті”
Казахского национального университета им. аль-Фараби. 050040, г. Алматы, пр.аль-Фараби, 71, КазНУ.

1-бөлім

Раздел 1

Section 1

Математика

Математика

Mathematics

IRSTI 27.39.21

DOI: <https://doi.org/10.26577/JMMCS202412111>

М.Е. Akhymbek , Р.А. Tastankul*  Б.О. Ozbekbay 
Institute of Mathematics and Mathematical Modeling, Kazakhstan, Almaty
*e-mail: ramazan.tastankul@mail.ru

SPECTRUM OF THE HILBERT TRANSFORM ON ORLICZ SPACES OVER \mathbb{R}

In this paper, we investigate the spectrum of the classical Hilbert transform on Orlicz spaces L_Φ over the real line \mathbb{R} , extending Widom's and Jörgens's results in the context of L^p spaces [3, 8], since the classical Lebesgue spaces are particular examples of Orlicz spaces when the N -function $\Phi = x^p/p$. Our motivation to do so is due to the classical result of Boyd [1] which says that the Hilbert transform is bounded on certain Orlicz spaces and the fact that the spectrum of the bounded linear operator is not an empty set. We first present an auxiliary result from the general theory of Banach algebras and results from general theory of Banach spaces, which further helps us to give a full description of the fine spectrum of the Hilbert transform on Orlicz spaces over the real line \mathbb{R} . We also present a resolvent set of the Hilbert transform on Orlicz spaces over the real line \mathbb{R} as well as its resolvent operator.

Key words: Hilbert transform, spectrum, point spectrum, Orlicz space.

М.Е. Ахымбек, Р.А. Тастанқұл*, Б.О. Озбекбай
Математика және математикалық модельдеу институты, Қазақстан, Алматы қ.
*e-mail: ramazan.tastankul@mail.ru

\mathbb{R} жиынындағы Орлич кеңістіктерінде анықталған Гильберт түрлендіруінің спектрі

Бұл мақалада біз, Уидом және Йоргенстің L^p кеңістіктерінің контекстіндегі нәтижелерін [3, 8] кеңейте отырып, \mathbb{R} нақты түзуінде анықталған L_Φ Орлич кеңістіктеріндегі классикалық Гильберт түрлендіруінің спектрін зерттейміз, себебі классикалық Лебег кеңістіктері Φ N -функциясы $\Phi = x^p/p$ болған кезде Орлич кеңістіктерінің ерекше мысалдары болып табылады. Зерттеу жүргізудегі негізгі мотивациямыз Бойдтың кейбір Орлич кеңістіктеріндегі Гильберт түрлендіруінің шенелгендігі туралы классикалық нәтижесі [1] және жалпы шенелген сызықты операторлардың спектрі бос жиын емес екендігімен байланысты. Біріншіден, біз Банах алгебраларының жалпы теориясынан көмекші нәтижені ұсынамыз, ол әрі қарай \mathbb{R} нақты түзуінде анықталған Орлич кеңістіктеріндегі Гильберт түрлендіруінің дәл спектрін толық сипаттауға көмектеседі. Біз сондай-ақ \mathbb{R} нақты түзуінде анықталған Орлич кеңістіктеріндегі Гильберт түрлендіруінің резольвентті жиынын, сонымен қатар оның резольвенттік операторын анықтаймыз.

Түйін сөздер: Гильберт түрлендіруі, спектр, нүктелік спектр, Орлич кеңістігі.

М.Е. Ахымбек, Р.А. Тастанқұл*, Б.О. Озбекбай
Институт математики и математического моделирования, Казахстан, г. Алматы
*e-mail: ramazan.tastankul@mail.ru

Спектр преобразования Гильберта в пространствах Орлича над \mathbb{R}

В данной статье мы исследуем спектр классического преобразования Гильберта в пространствах Орлича L_Φ над вещественной прямой \mathbb{R} , расширяя результаты Видома и Йоргенса в контексте L^p пространств [3, 8], поскольку классические пространства Лебега являются частными примерами пространств Орлича, когда N -функция $\Phi = x^p/p$. Наша мотивация в исследовании, обусловлена классическим результатом Бойда [1] об ограниченности преобразования Гильберта в некоторых пространствах Орлича и к тому, что спектр ограниченного линейного оператора не является пустым множеством.

Сначала приведем вспомогательный результат из общей теории банаховых алгебр, который в дальнейшем поможет нам дать полное описание тонкого спектра преобразования Гильберта в пространствах Орлича над вещественной прямой \mathbb{R} . Мы также представляем резольвентное множество преобразования Гильберта в пространствах Орлича над вещественной прямой \mathbb{R} , а также его резольвентный оператор.

Ключевые слова: преобразование Гильберта, спектр, точечный спектр, пространство Орлича.

1 Introduction

Let $L_\Phi(\mathbb{R})$ be an Orlicz space over the real line \mathbb{R} . Define the Hilbert transform \mathcal{H} on the space $L_\Phi(\mathbb{R})$ by the formula

$$\mathcal{H}f(t) := \frac{1}{\pi i} p.v. \int_{-\infty}^{\infty} \frac{f(s)}{t-s} ds, \quad t \in \mathbb{R}, \quad (1)$$

where the integral is understood as Cauchy principal value. Boundedness of \mathcal{H} acting on $L_\Phi(\mathbb{R})$ obtained by D.W.Boyd in [1, Theorem 5.8]. In the same work, Boyd demonstrated that the necessary condition for the boundedness of the Hilbert Transform is the reflexivity of the Orlicz space, which coincides with the condition of non-triviality of Boyd indices. According to the fundamental principles of spectral theory for linear operators on Banach spaces, it is established that if a linear operator is bounded, then its spectrum must necessarily be non-empty. Hence, the purpose of this paper is to investigate the spectrum of the Hilbert transform, including the classification of points within the spectrum. The spectrum of the Hilbert Transform on $L^p(-1, 1)$, $1 < p < \infty$ was completely identified by Widom in 1960. Additionally, he provided a decomposition of the spectrum into its point spectrum, denoted as $\sigma_{pt}(\mathcal{H})$, continuous spectrum $\sigma_c(\mathcal{H})$, and residual spectrum $\sigma_r(\mathcal{H})$ [8, §5]. In 2021 Guillermo P.Curbera, Susumu Okada and Werner J.Ricker extended Widom's results to any rearrangement invariant Banach spaces over $(-1, 1)$ [9]. They investigated the spectrum and fine spectra of the finite Hilbert transform acting on rearrangement invariant spaces over $(-1, 1)$ with non-trivial Boyd indices. Jörgens demonstrated the spectrum and point spectrum of the Hilbert Transform in the context of $L^p(\mathbb{R})$ and $L^p(\mathbb{R}_+)$, where $1 < p < \infty$, as presented in [3]. In our research, we applied the identical methodology, which also relies on the theory of Banach algebras.

2 Preliminaries

In this section, we provide certain definitions and notations from the theory of Banach algebras and from the theory of linear bounded operators on Banach spaces.

Definition 1 A complex normed space \mathcal{A} is called a normed algebra if for any elements A, B of \mathcal{A} there is defined a product $AB \in \mathcal{A}$ with the following properties

- *associativity*: $A(BC) = (AB)C$;
- *distributivity*: $(A + B)C = AC + BC$, $A(B + C) = AB + AC$;
- *homogeneity*: $\alpha(AB) = (\alpha A)B = A(\alpha B)$, $\forall \alpha \in \mathbb{C}$.

The product satisfies the inequality $\|AB\| \leq \|A\|\|B\|$, where $\|\cdot\|$ is a norm of \mathcal{A} . If \mathcal{A} is a Banach space, then \mathcal{A} is called a *Banach algebra*. Moreover, if there exists in \mathcal{A} an element I with following properties $AI = IA = A, \forall A \in \mathcal{A}$ and $\|I\| = 1$ then \mathcal{A} is called a normed algebra with unit (respectively Banach algebra with unit). An element $A \in \mathcal{A}$ is called *regular* if there exists $B \in \mathcal{A}$ such that $AB = BA = I$. The element B is the inverse of A and accordingly is denoted by A^{-1} . If an element is not regular, then it is called singular. For every $A \in \mathcal{A}$ we define the resolvent set $\rho(A)$ as the set of all $\lambda \in \mathbb{C}$ such that $(\lambda I - A)$ is regular. For all $\lambda \in \rho(A)$ we defined the *resolvent operator* $R_\lambda(A) = (\lambda I - A)^{-1}$. The complement of $\rho(A)$ is called the spectrum of A and denoted by $\sigma(A)$.

Definition 2 An element $A \in \mathcal{A}$ is called algebraic if there exists a polynomial

$$p(\lambda) = \sum_{i=0}^m \alpha_i \lambda^i \quad (2)$$

with coefficients $\alpha_i \in \mathbb{C}$ and $\alpha_m \neq 0$ such that

$$p(A) = \sum_{i=0}^m \alpha_i A^i = 0. \quad (3)$$

A minimal polynomial of A is a monic polynomial (whose highest-degree coefficient equals 1) $p(x)$ of the lowest degree such that $p(A) = 0$

First note that a minimal polynomial is unique. Indeed, if there are two minimal polynomials, denoted as $p(x)$ and $q(x)$, both of degree m , then, $(p-q)(A) = p(A) - q(A) = 0$. Note that, the degree of the resulting polynomial $(p-q)(x)$ is less than m , contradicting their minimality. Thus, it follows that $p = q$. Additionally, recognize that the minimal polynomial $p(x)$ is irreducible, i.e. it cannot be expressed as the product of two polynomials. To illustrate, if $p(x) = r(x)t(x)$, where both $r(x)$ and $t(x)$ have degrees lower than that of $p(x)$, then $0 = p(A) = r(A)t(A)$. Consequently, either $r(A) = 0$ or $t(A) = 0$, contradicting the minimality of $p(x)$. It is also known that any polynomial $q(x)$ with $q(A) = 0$ is divisible by the minimal polynomial of A . In other words, if there exists a polynomial $q(x)$ satisfying $q(A) = 0$, then $q(x) = p(x)r(x)$, where $p(x)$ is the minimal polynomial of A .

Now we introduce some definitions from the theory of bounded linear operators on Banach spaces. Let X be a Banach space. For Banach space X we denote by $\mathcal{B}(X)$, the set of all bounded operators from X into itself. It is known that $\mathcal{B}(X)$ is a Banach algebra [2].

Definition 3 Let $T \in \mathcal{B}(X)$. The spectrum of T is the set of all $\lambda \in \mathbb{C}$ for which the operator $\lambda I - T$ does not have an inverse that is a bounded linear operator, denoted as $\sigma(T)$. The resolvent set $\rho(T)$ of T in X is defined as complement of the spectrum: $\mathbb{C} \setminus \sigma(T)$. In other words, the resolvent set of T is the set of all $\lambda \in \mathbb{C}$ for which the operator $\lambda I - T$ have an inverse that is a bounded linear operator.

Definition 4 [7, Definition 1.13] Let $T \in \mathcal{B}(X)$. Define

$$\sigma_{pt}(T) = \{\lambda \in \mathbb{C} : \lambda I - T \text{ is not injective} \Leftrightarrow \text{Ker}(\lambda I - T) \neq \{0\}\};$$

$$\sigma_c(T) = \left\{ \lambda \in \mathbb{C} : \lambda I - T \text{ is injective } \overline{\text{Im}(\lambda I - T)} = X, \text{ but } \text{Im}(\lambda I - T) \neq X \right\};$$

$$\sigma_r(T) = \left\{ \lambda \in \mathbb{C} : \lambda I - T \text{ is injective, but } \overline{\text{Im}(\lambda I - T)} \neq X \right\}.$$

$\sigma_{pt}(T)$, $\sigma_c(T)$ and $\sigma_r(T)$ are called respectively the point spectrum, the continuous spectrum and the residual spectrum of T in X .

It is known that $\sigma_{pt}(T)$, $\sigma_c(T)$ and $\sigma_r(T)$ are disjoint [7] and

$$\sigma(T) = \sigma_{pt}(T) \cup \sigma_c(T) \cup \sigma_r(T).$$

Since $\mathcal{B}(X)$ is a Banach algebra, the definition of the spectrum and resolvent set on Banach algebras and linear bounded operators on Banach spaces coincide. As usual, by $L^p(\mathbb{R})$ we denote the standard Lebesgue space.

Definition 5 [4, 5] A mapping $\Phi : \mathbb{R} \rightarrow \mathbb{R}_+$ is called an N -function if

- $\Phi(x) = 0$ iff $x = 0$ and $\Phi(x) > 0$ for $x > 0$;
- Φ is convex, continuous and even;
- $\lim_{x \rightarrow 0} \frac{\Phi(x)}{x} = 0$, $\lim_{x \rightarrow \infty} \frac{\Phi(x)}{x} = +\infty$.

We say that N -function Φ satisfies the Δ_2 -condition, if and only if there exists a constant $k > 0$ such that

$$\Phi(2x) \leq k\Phi(x), \text{ for all } x > 0.$$

For every N -function Φ and for every measurable function f on \mathbb{R} we can define a functional

$$M^\Phi(f) = \int_{\mathbb{R}} \Phi(|f|) dx$$

and set

$$\|f\|_{L_\Phi} = \inf \left\{ a > 0 : M^\Phi \left(\frac{f}{a} \right) \leq 1 \right\}.$$

Definition 6 *The set*

$$L_{\Phi} = \{f \in L : \|f\|_{L_{\Phi}} < \infty\}$$

equipped with the norm $\|\cdot\|_{L_{\Phi}}$ is called an Orlicz function space.

An Orlicz space is an example of rearrangement invariant spaces. Note that L^p spaces coincide with Orlicz spaces when the N-function has the form $\Phi(x) = x^p/p, p \in (1, \infty)$. For a more general information on Orlicz spaces L_{Φ} , see [2, 4, 5, 7].

Definition 7 *Let $L_{\Phi}(\mathbb{R})$ be reflexive. If $f \in L_{\Phi}(\mathbb{R})$, then the classical Hilbert transform \mathcal{H} is defined by the principal-value integral*

$$\mathcal{H}f(t) := \frac{1}{\pi i} p.v. \int_{-\infty}^{\infty} \frac{f(s)}{t-s} ds, \quad \forall f \in L_{\Phi}(\mathbb{R}),$$

(see, e.g. [2, Chapter III. 4]).

The Hilbert transform \mathcal{H} is bounded on $L_{\Phi}(\mathbb{R})$ if and only if $L_{\Phi}(\mathbb{R})$ is reflexive (see, for example, [1, 2, 6]).

3 Methods and materials. Spectrum of the Hilbert transform on $L_{\Phi}(\mathbb{R})$

In this section, we find the spectrum of the Hilbert transform on $L_{\Phi}(\mathbb{R})$. First, we present a preliminary result from the theory of Banach algebras.

Proposition 1 *[3, Exercize 4.10] Let A be an algebraic element of \mathcal{A} (cf. Definition 2). Then*

1. *The resolvent of A has the form*

$$R_{\lambda}(A) = \frac{1}{p(\lambda)} \sum_{i=0}^{m-1} \lambda^i B_i$$

where

$$B_j = \sum_{k=i+1}^m \alpha_k A^{k-i-1}.$$

2. *The spectrum $\sigma(A)$ is contained in the set of zeros of p :*

$$p_0 = \{\lambda \in \mathbb{C} \mid p(\lambda) = 0\} \supset \sigma(A)$$

3. *If p is a minimal polynomial for A , then*

$$p_0 = \sigma(A).$$

Proof. 1. We know that

$$R_\lambda(A) = \frac{1}{p(\lambda)}(B_0 + \lambda B_1 + \lambda^2 B_2 + \dots + \lambda^{m-1} B_{m-1})$$

and

$$B_0 = \alpha_1 I + \alpha_2 A + \dots + \alpha_m A^{m-1};$$

$$B_1 = \alpha_2 I + \alpha_3 A + \dots + \alpha_m A^{m-2};$$

$$B_2 = \alpha_3 I + \alpha_4 A + \dots + \alpha_m A^{m-3};$$

...

$$B_{m-2} = \alpha_{m-1} I + \alpha_m A;$$

$$B_{m-1} = \alpha_m I.$$

Then we have

$$\begin{aligned} p(\lambda)R_\lambda(A) &= (\alpha_1 I + \alpha_2 A + \dots + \alpha_m A^{m-1}) \\ &\quad + \lambda(\alpha_2 I + \alpha_3 A + \dots + \alpha_m A^{m-2}) \\ &\quad + \lambda^2(\alpha_3 I + \alpha_4 A + \dots + \alpha_m A^{m-3}) \\ &\quad + \dots + \lambda^{m-2}(\alpha_{m-1} I + \alpha_m A) + \lambda^{m-1} \alpha_m I. \end{aligned}$$

Therefore,

$$\begin{aligned} p(\lambda)R_\lambda(A) &= \alpha_1 I + \alpha_2(\lambda I + A) + \alpha_3(\lambda^2 I + \lambda A + A^2) \\ &\quad + \alpha_4(\lambda^3 I + \lambda^2 A + \lambda A^2 + A^3) + \dots \\ &\quad + \alpha_{m-1}(\lambda^{m-2} I + \lambda^{m-3} A + \dots + \lambda A^{m-3} + A^{m-2}) \\ &\quad + \alpha_m(\lambda^{m-1} I + \lambda^{m-2} A + \dots + \lambda A^{m-2} + A^{m-1}) \\ &= \alpha_1(\lambda I - A)(\lambda I - A)^{-1} + \alpha_2((\lambda I)^2 - A^2)(\lambda I - A)^{-1} + \dots \\ &\quad + \alpha_{m-1}((\lambda I)^{m-1} - A^{m-1})(\lambda I - A)^{-1} + \alpha_m((\lambda I)^m - A^m)(\lambda I - A)^{-1} \\ &= (\lambda I - A)^{-1}(\alpha_1(\lambda I - A) + \alpha_2((\lambda I)^2 - A^2) + \dots \\ &\quad + \alpha_{m-1}((\lambda I)^{m-1} - A^{m-1}) + \alpha_m((\lambda I)^m - A^m)) \\ &= (\lambda I - A)^{-1}(p(\lambda) - p(A)) = p(\lambda)(\lambda I - A)^{-1}. \end{aligned}$$

If $p(\lambda) \neq 0$, then

$$R_\lambda(A) = (\lambda I - A)^{-1},$$

and

$$R_\lambda(A)(\lambda I - A) = (\lambda I - A)R_\lambda(A) = I.$$

2. We demonstrate that $\sigma(A)$ is a subset of $p_0 = \{\lambda \in \mathbb{C} : p(\lambda) = 0\}$. Choose any $\lambda \in \sigma(A)$. It follows that $p(\lambda) = 0$, meaning that λ belongs to p_0 . To argue this, assume the opposite, i.e., suppose $p(\lambda) \neq 0$. In such a case, based on the preceding reasoning, a resolvent $R_\lambda(A)$ exists, implying that $\lambda \in \rho(A)$. This assumption leads to a contradiction, compelling the conclusion that $p(\lambda) = 0$. Consequently, we establish that $\sigma(A)$ is a subset of p_0 .

3. Let $p(x)$ be the minimal polynomial of A . Assume that $\sigma(A)$ is a subset of p_0 . Then choose $\lambda_0 \in p_0 \setminus \sigma(A)$. Then, by the preceding arguments, there would exist a resolvent $R_{\lambda_0}(A)$ which has the form

$$R_{\lambda_0}(A) = \frac{1}{q(\lambda_0)} \sum_{i=0}^{m-1} \lambda_0^i B_i,$$

for some polynomial $q(x)$ with $q(A) = 0$. Since $p(x)$ is the minimal polynomial, the polynomial $q(x)$ can be expressed as follows $q(x) = r(x)p(x)$. We know that $\lambda_0 \in p_0$, i.e. $p(\lambda_0) = 0$, therefore, $q(\lambda_0) = r(\lambda_0)p(\lambda_0) = 0$, which contradicts the existence of the resolvent $R_{\lambda_0}(A)$. The contradiction proves the fact that $p_0 = \sigma(A)$.

Before proceeding to the main result of this paper we present some technical lemmas. The proofs can be found in their respective references.

Lemma 1 [10, Lemma 2.1] *Let $X(\mathbb{R})$ be a separable Banach function space. Then the set $L^2(\mathbb{R}) \cap X(\mathbb{R})$ is dense in $X(\mathbb{R})$.*

Lemma 2 [4, 5] *The following statements are equivalent:*

- (a) *N -function Φ satisfies Δ_2 -condition;*
- (b) *$L_\Phi(\mathbb{R})$ is reflexive;*
- (c) *$L_\Phi(\mathbb{R})$ is separable.*

Let $L_\Phi(\mathbb{R})$ be a reflexive Orlicz space, then as stated earlier the Hilbert transform is bounded linear operator on $L_\Phi(\mathbb{R})$. In other words, we have that $\mathcal{H} \in \mathcal{B}(L_\Phi(\mathbb{R}))$. Since $L_\Phi(\mathbb{R})$ is a Banach space, $\mathcal{B}(L_\Phi(\mathbb{R}))$ is a Banach algebra.

Lemma 3 *Let $L_\Phi(\mathbb{R})$ be a reflexive Orlicz space, then $\mathcal{H}^2 f = f$, for any $f \in L_\Phi(\mathbb{R})$.*

Proof. It is a known [3], [11, Chapter 4] that $\mathcal{H}^2 = I$ for all $f \in L^p(\mathbb{R})$, $1 < p < \infty$. Let $p = 2$. Hence, one can obviously see that $\mathcal{H}^2 f = f$ for every $f \in L^2(\mathbb{R}) \cap L_\Phi(\mathbb{R})$. By Lemma 2, one has that $L_\Phi(\mathbb{R})$ is separable. Hence, by Lemma 1, $L^2(\mathbb{R}) \cap L_\Phi(\mathbb{R})$ is dense in $L_\Phi(\mathbb{R})$. Therefore noting that the integrals involved in the Hilbert transform are finite, passing to the limit, we have $\mathcal{H}^2 f = f$ for every $f \in L_\Phi(\mathbb{R})$, which completes the proof.

The following theorem is the main result of this paper, which extends Widom's result [3].

Theorem 1 *Let $L_\Phi(\mathbb{R})$ be a reflexive Orlicz space and let \mathcal{H} be the Hilbert transform on $L_\Phi(\mathbb{R})$. Then,*

- (i) $\sigma(\mathcal{H}) = \sigma_p(\mathcal{H}) = \{\pm 1\}$.
- (ii) $\rho(\mathcal{H}) = \mathbb{C} \setminus \{\pm 1\}$ and the resolvent has the following form

$$R_\lambda(\mathcal{H}) = \frac{1}{2}(\lambda + 1)^{-1}(I - \mathcal{H}) + \frac{1}{2}(\lambda - 1)^{-1}(I + \mathcal{H}).$$

Proof. (i). Note that, by Lemma 3, $\mathcal{H}^2 = I$ and obviously there is no polynomial $q(\cdot)$ of degree 1 such that $q(\mathcal{H}) = 0$. Hence, the minimal degree of the polynomials is 2:

$$p(\mathcal{H}) = I - \mathcal{H}^2 = 0.$$

Therefore, by Proposition 1, we have

$$\sigma(\mathcal{H}) = \{\lambda \in \mathbb{C} : \lambda^2 - 1 = 0\} = \{\pm 1\}.$$

Moreover, for $\lambda = \pm 1$, one has

$$(I - \mathcal{H})(I + \mathcal{H})f = (\lambda^2 I - \mathcal{H}^2)f = 0, \quad f \in L_{\Phi}(\mathbb{R}).$$

Hence, $g = (I + \mathcal{H})f \in \text{Ker}\{I - \mathcal{H}\} \neq \emptyset$. Therefore, $\sigma(\mathcal{H}) = \sigma_p(\mathcal{H}) = \{\pm 1\}$.

(ii). By the definition of the resolvent, it easily follows that $\rho(\mathcal{H}) = \mathbb{C} \setminus \sigma(\mathcal{H}) = \mathbb{C} \setminus \{\pm 1\}$. Since

$$p(\lambda) = \lambda^2 - 1, \alpha_0 = -1, \alpha_2 = 1, \alpha_k = 0, \quad k = 1, 3, 4, \dots$$

Then, by Proposition 1, we obtain

$$B_0 = \mathcal{H}, B_1 = I$$

and

$$R_{\lambda}(\mathcal{H}) = \frac{\lambda I + \mathcal{H}}{\lambda^2 - 1} = \frac{1}{2}(\lambda + 1)^{-1}(I - \mathcal{H}) + \frac{1}{2}(\lambda - 1)^{-1}(I + \mathcal{H}).$$

Remark 1 *Since the point spectrum, continuous spectrum and residual spectrum are disjoint sets, it easily follows from Theorem 1 that $\sigma_c(\mathcal{H}) = \sigma_r(\mathcal{H}) = \emptyset$.*

4 Conclusion

In this paper, we investigated the spectrum of the Hilbert transform on Orlicz spaces over the real line. Our findings revealed that the spectrum of \mathcal{H} on $L_{\Phi}(\mathbb{R})$ consists two points, specifically $\sigma(\mathcal{H}_{L_{\Phi}(\mathbb{R})}) = \{-1, 1\}$, and this spectrum coincides with the point spectrum. We also determined the resolvent set $\rho(\mathcal{H})$ and the resolvent $R_{\lambda}(\mathcal{H})$ of the Hilbert transform on the spaces $L_{\Phi}(\mathbb{R})$.

5 Acknowledgement

This research was partially supported by the grant NO.BR20281002 of the Ministry of Science and Higher Education of the Republic of Kazakhstan .

References

- [1] Boyd D. W., "The Hilbert transformation on rearrangement invariant Banach spaces." , *Canadian Journal of Mathematics*, 19 (1967): 599-616.
- [2] Bennett C., Sharpley R. C., "Interpolation of operators." *Academic press*, (1988).
- [3] Jörgens K., "Linear integral operators" , *Boston: Pitman Advanced Publishing Program*, 26.125-137 (1982).
- [4] Krasnoselskii M.A., Rutitskii Ya.B., "Convex Functions and Orlicz Spaces" , *Fizmatgiz, Moscow*(1958).
- [5] Rao M.M., Ren Z.D., "Theory of Orlicz spaces" , *Chapman & Hall Pure and Applied Mathematics*, (1991).
- [6] Boyd D. W., "The Hilbert Transformation on rearrangement invariant Banach spaces" , *Thesis, University of Toronto*, (1966).
- [7] Dowson H. R., "Spectral theory of linear operators" , *Academic Press*, No. 12. (1978).
- [8] Widom H., "Singular integral equations in L_p " , *Trans. Am. Math. Soc.* 97 (1960): 131–160.
- [9] Curbera G., Okado S. Ricker W., "Fine spectra of the finite Hilbert transform in function spaces" , *Advances in Mathematics* 380 (2021).
- [10] Fernandes C. A., Karlovich A. Yu., Karlovich Yu. I., "Calkin Images of Fourier Convolution Operators with Slowly Oscillating Symbols" , *Operator Theory, Functional Analysis and Applications* 282 (2021): 193-218.
- [11] King F.W. "Hilbert Transforms, vol.I," , *Cambridge: Cambridge University Press* 898 (2009)

IRSTI 27.35.17

DOI: <https://doi.org/10.26577/JMMCS202412112>

S. Burgumbayeva^{1*} , D. Zhussupova² , B. Koshkarova¹ 

¹L.N.Gumilyov Eurasian National University, Kazakhstan, Astana

²National Research University «Higher School of Economics», Russia, Moscow

*e-mail: burgumbayeva_sk@enu.kz

MATHEMATICAL MODELLING OF THE PROCESS OF NATURAL GAS TRANSPORTATION VIA PIPE NETWORKS USING CROSSING-BRANCH METHOD

This research is among the most relevant research on the problems of natural gas transportation via pipe networks. The increased demand for natural gas in Kazakhstan is associated with a greater level of environmental friendliness; as a result, many power-generating stations use natural gas as their main source of energy. Modernization of existing thermal power plants is necessary to improve the environmental situation in the country. There are three main groups of gas pipeline systems considered in the literature: collection, transmission, and distribution systems. In this article, we present detailed research on the transmission process and develop useful approaches. Over the past few years, a huge amount of research has been conducted on many problems of decision-making in the gas industry and, in particular, on optimizing the pipeline network. In this paper, we consider dynamical models, highlighting aspects of modelling and the most relevant solutions to date. This research can serve as a useful tool for understanding the evolution of many real-world applications and the most recent advances in solution methodologies emerging in this complex field of research. The results of this research can be used to develop technologies for automating calculations, planning, and optimizing natural gas transportation.

Key words: natural gas transportation, mathematical modelling, nonlinear model.

С. Бургумбаева^{1*}, Д. Жусупова², Б. Қошқарова¹

¹Л.Н. Гумилев ат. Еуразия ұлттық университеті, Қазақстан, Астана қ.

²Ұлттық зерттеу университеті, «Жоғары экономика мектебі», Ресей, Мәскеу қ.

*e-mail: burgumbayeva_sk@enu.kz

Қиылысу-тармақ әдісін қолдана отырып, табиғи газды құбыр желілері арқылы тасымалдау процесін математикалық модельдеу

Қарастырылып отырған зерттеу жұмысы табиғи газды құбыр желілері арқылы тасымалдау мәселелері бойынша ең өзекті зерттеулердің бірі болып табылады. Қазақстандағы табиғи газға деген сұраныстың артуы қоршаған ортаға зиянсыздық деңгейінің жоғарылауымен байланысты; нәтижесінде көптеген электр станциялары негізгі энергия көзі ретінде табиғи газды пайдаланады. Елдегі экологиялық жағдайды жақсарту үшін жұмыс істеп тұрған жылу электр станцияларын жаңғырту қажет. Әдебиеттерде қарастырылған газ құбырлары жүйелерінің үш негізгі тобы бар: жинау, тасымалдау және тарату жүйелері. Бұл мақалада біз тасымалдау процесі туралы егжей-тегжейлі зерттеулерді ұсынамыз және пайдалы тәсілдерді әзірлейміз. Соңғы бірнеше жылда газ саласындағы шешімдерді қабылдаудың көптеген мәселелері бойынша, атап айтқанда, құбыр желісін оңтайландыру бойынша үлкен көлемдегі зерттеулер жүргізілді. Бұл жұмыста біз динамикалық модельдерді қарастырамыз, модельдеудің аспектілерін және бүгінгі таңдағы ең өзекті шешімдерді атап өтеміз. Бұл зерттеу көптеген нақты әлем қолданбаларының эволюциясын және осы күрделі зерттеу саласында пайда болған шешім әдістемелеріндегі ең соңғы жетістіктерді түсіну үшін пайдалы құрал бола алады. Бұл зерттеулердің нәтижелерін есептеулерді автоматтандыру, жоспарлау және табиғи газды тасымалдауды оңтайландыру технологияларын әзірлеу үшін пайдалануға болады.

Түйін сөздер: табиғи газды тасымалдау, математикалық модельдеу, сызықты емес модель.

С. Бургумбаева^{1*}, Д. Жусупова², Б. Кошкарова¹

¹Евразийский национальный университет им. Л.Н. Гумилева, Казахстан, г. Астана

²Национальный исследовательский университет «Высшая школа экономики», Россия, г. Москва

*e-mail: burgumbayeva_sk@enu.kz

Математическое моделирование процесса транспортировки природного газа по трубопроводным сетям методом пересечения-ветви

Данное исследование относится к числу наиболее актуальных исследований по проблемам транспортировки природного газа по трубопроводным сетям. Повышенный спрос на природный газ в Казахстане связан с повышением уровня экологичности; в результате многие электростанции используют природный газ в качестве основного источника энергии. Модернизация существующих теплоэлектростанций необходима для улучшения экологической ситуации в стране. В литературе рассматриваются три основные группы газопроводных систем: системы сбора, транспортировки и распределения. В этой статье мы представляем подробное исследование процесса передачи и разрабатываем полезные подходы. За последние несколько лет было проведено огромное количество исследований по многим проблемам принятия решений в газовой отрасли и, в частности, по оптимизации трубопроводной сети. В данной статье мы рассматриваем динамические модели, освещая аспекты моделирования и наиболее актуальные на сегодняшний день решения. Это исследование может послужить полезным инструментом для понимания эволюции многих реальных приложений и последних достижений в методологиях решения, возникающих в этой сложной области исследований. Результаты исследования могут быть использованы при разработке технологий автоматизации расчетов, планирования и оптимизации транспортировки природного газа.

Ключевые слова: транспортировка природного газа, математическое моделирование, нелинейная модель.

1 Introduction

This research is intended to build mathematical and computer simulations of non-stationary modes with the optimization of the gas transportation process by choosing the most effective control strategy and control actions on the technological equipment of the main gas pipelines of the gas transmission system.

Over the past couple of centuries, fossil fuels have been the primary source of energy and essential to global economic growth. Originally, coal was the main source of energy, but oil later replaced it and became an important factor in maintaining civilization.

In the modern world, the rise in prices for non-renewable energy sources is breaking records in the entire history of their production. It is advisable to connect this with the deteriorating environmental situation in the world. A gradual transition to clean types of energy, such as solar, wind, etc., is planned by most developed countries. But immediate transformation of energy systems is impossible and takes time. Therefore, the most promising direction is less polluting energy sources such as natural gas.

Complex gas-dynamic processes occurring in a pipeline in transient conditions require a more comprehensive solution to problems such as management, design and operation of gas transmission systems. It should also be noted that gas transport is carried out in large diameter pipes and under high pressure.

The characteristics of the gas in the pipeline change in real time, which significantly complicates the modeling process and does not allow one to estimate the gas parameters well enough to make a decision. Gas dynamics is described by a system of three partial differential

equations based on the laws of conservation of energy, mass and momentum. But for practical purposes, the obtained numerical solutions of this system do not give satisfactory results.

An acute discussion about physical phenomena on graphs continues, particularly regarding the context of gas dynamics [1], [2] including the publications of the Pipeline Interest Group [3] or textbooks such as [4], [5].

In particular, accurate but computationally cheap prediction of gas dynamics in pipeline networks is a major industrial problem and has been studied for several years [6], [7]. In gas dynamics, the predominant physical phenomenon is pressure loss due to the effects of hydraulic friction on the pipe walls. Currently, there are several models that describe this effect with varying degrees of accuracy. Most of these models are given on isothermal Euler equations, i.e., a system of nonlinear partial differential equations for each pipe. The main difficulty lies in nonlinear dynamics, i.e., the nonlinearity of the system of differential equations, which limits the possibility of efficient and accurate modelling of pipelines and pipeline networks.

We consider the problem of modelling and simulating gas dynamics in pipes. The key point in modeling is the non-stationary nature of the process, which significantly affects the construction of optimal control, reducing the quality of the resulting solutions. Stationary modes are well studied and are often used in modeling natural gas transport, but they reduce the plausibility and reality of such processes, which leads to low confidence in the results obtained for management and decision-making.

Obtaining new capacity while maintaining emissions regulations is one of the difficult problems facing countries. The most optimal solution to switch to gas leads to the construction of gas-fired thermal power plants and gas power plants. The natural gas power generation vector is a reliable hedge against the variability of renewable energy sources such as wind and solar [8], [9]. Such conditions for energy supply are a challenge for gas transportation systems, since different volumes of consumption must be included in the modes of the gas transportation process in order to provide the necessary capacities in a timely manner. New approaches should be considered to replace those that existed in conditions of stable gas supplies, when gas from the field was supplied to consumers in accordance with established volumes [10], [11].

Such contracts ensured a nearly constant supply of gas [12]. Modeling and optimization of the transportation process was limited to the consideration of stationary processes [13], [14]. But now, consideration of the stationary case for gas-dynamic systems is becoming unsatisfactory. Several approaches to such research are encompassed in [15], [16].

The article is structured as follows:

- Section 2 represents the description and statement of methods.
- Section 3 provides a description of the main computational procedures and their relationship. The results of the calculations obtained using the dynamical model are shown in graphs.
- Section 4 discusses the meaning, importance, and relevance of the research results.
- Conclusions on the main outcomes of this study are finally presented in Section 5.

2 Methods

The following is a mathematical model that most fully describes the process of gas movement in a pipe, i.e., Newton's equation of motion

$$\frac{\partial P}{\partial x} + g\rho \frac{dh}{dx} + \frac{\lambda}{2DS^2} \frac{|M|M}{\rho} + \rho \frac{DW}{dt} = 0, \quad (1)$$

where P is pressure, g is acceleration due to gravity, ρ is density, $\frac{dh}{dx}$ is the slope of the pipeline, λ is the coefficient of hydraulic friction, D is the inner diameter, S is the cross-sectional area, M is mass flow rate,

$$\frac{DW}{dt} = \frac{\partial w}{\partial t} + w \frac{\partial w}{\partial x},$$

and x is the length of the pipe.

The continuity equation is as follows:

$$S \frac{\partial \rho}{\partial t} + \frac{\partial M}{\partial x} = 0, \quad (2)$$

and the energy equation is written in the form of temperature $\theta = \theta(x)$ under the assumption of zero temperature gradient over time. Also, the equation of state is

$$P = zR\theta\rho, \quad (3)$$

where R is the gas constant and z is the compressibility factor.

The coefficient of hydraulic friction can be calculated using Chen's formula [17], which is often used in practice:

$$\frac{1}{\sqrt{\lambda}} = -2 \log \left(\frac{\varepsilon/D}{3.7065} - \frac{5.0452}{N_{Re}} \log \left(\frac{1}{2.8257} \left(\frac{\varepsilon}{D} \right)^{1.1098} + \frac{5.8506}{0.8981 N_{Re}} \right) \right).$$

Here, N_{Re} is the Reynolds number, $N_{Re} = \rho u D / \mu$, μ is the dynamic viscosity of the gas, u is velocity, and ε is the roughness of the pipe.

Typically, isothermal models are used to model gas transport, ignoring temperature changes along the length of the pipeline and over time.

There are many formulas for calculating the compressibility coefficient; for example, see the source for an overview of existing methods [18]. Based on many studies, the standards for calculating the gas compressibility factor based on the parameters and composition of natural gas SGERG-88 [19], GERG-2004 [20], and the latest version of the standard GERG-2008 [21] were constructed; these take into account most of the dependent factors.

In accordance with [22], a simplified formula is used in practice; the compressibility coefficient of natural gas at a pressure of up to $15MPa$ and temperature in range of $250 - 400K$, z is calculated by the formula

$$z = 1 + A_1 P_{red} + A_2 P_{red}^2, \quad (4)$$

where

$$A_1 = -0.39 + 2.03T_{red} - 3.16T_{red}^2 + 1.0T_{red}^3,$$

$$A_2 = 0.0423 - 0.1812T_{red} + 0.2124T_{red}^2,$$

$$P_{red} = PP_{cr},$$

$$T_{red} = TT_{cr}.$$

The critical pressure and temperature of the gas mixture can also be determined from a known density under standard conditions ($T = 293.15K$, $P = 101325Pa$):

$$P_{cr} = 0.1737 \cdot (26.813 - \rho_{st}), \quad T_{cr} = 155.24 \cdot (0.564 + \rho_{st}),$$

where ρ_{st} is the gas density under standard conditions (set according to the gas passport).

The basis for all simplifications under the assumption of an isothermal process, and, therefore, also the classical dynamics of a gas in a pipe, is described by the Euler equations:

$$\rho_t + q_x = 0,$$

$$q_t + \left(\frac{q^2}{\rho} + a^2 \rho \right)_x = -\lambda \frac{q|q|}{2D\rho} - g\rho h_x.$$

Here, q is the gas flow, $q = \rho u$, and $a^2 = zRT$. The first equation is the law of conservation of mass, and the second equation describes momentum. The system represents a hyperbolic equilibrium law involving the effects of friction and gravity (described by gh_x). The computational complexity for modelling a pipeline network using these equations is high. The first approximation of this system can be obtained by performing an approximate estimate of the term $\partial(q^2/\rho)$ and excluding it from the equation. The resulting system is written as follows:

$$q_t \left(a^2 \rho \left(1 + \frac{q^2}{\rho^2 a^2} \right) \right)_x = -\lambda \frac{q|q|}{2D\rho} - g\rho h_x.$$

This system, known as the Weymouth equations, reduces to solving a linear system of hyperbolic partial differential equations for each pipe.

In the research implementation, we consider non-isothermal (1) - (3) models using the compressibility factor (4).

Adopting the space discretization according to Figure ??, the equation of motion (1) is represented as

$$\rho_{i+1} - \rho_i + \frac{\lambda_i |\hat{w}_i| L_i}{2D_i S_i \tilde{w}_{zi}^2} M_i + g \frac{\Delta h_i}{\tilde{w}_{zi}^2} \hat{\rho}_i + \frac{\tilde{\rho}_i + b^* \bar{\rho}_{i+1} \bar{\rho}_i}{\tilde{\theta}_i} \Delta \theta_i + \frac{L_i}{S_i \tilde{w}_{zi}^2} \frac{dM_i}{dt} = 0, \quad (i = 1, 2, \dots, n), \quad (5)$$

where

$$\hat{w}_i = \frac{\bar{M}_i}{S_i \bar{\rho}_i},$$

$$\tilde{w}_{zi}^2 = R \tilde{\theta}_i \bar{Z}_i \bar{Z}_{i+1},$$

$$\begin{aligned}\hat{\rho}_i &= \frac{\bar{p}_i + \bar{p}_{i+1}}{2R\bar{\theta}_i\sqrt{\bar{Z}_i\bar{Z}_{i+1}}}, \\ \tilde{\theta}_i &= 0.5(\bar{\theta}_i + \bar{\theta}_{i+1}), \tilde{\rho}_i = 0.5(\bar{\rho}_i + \bar{\rho}_{i+1}), \\ \bar{p}_i &= R\bar{\theta}_i\bar{Z}_i\bar{\rho}_i, \\ \bar{Z}_i &= \frac{1}{1 + \bar{\rho}_i(b^* - a^*\bar{\theta}_i)}, \Delta\theta_i = \theta_{i+1} - \theta_i, \\ \Delta h_i &= h_{i+1} - h_i, \frac{\hat{\rho}_i}{\tilde{w}_{zi}^2} = \frac{2\bar{\rho}_i\bar{\rho}_{i+1}}{(\bar{p}_i + \bar{p}_{i+1})\sqrt{\bar{Z}_i\bar{Z}_{i+1}}}.\end{aligned}$$

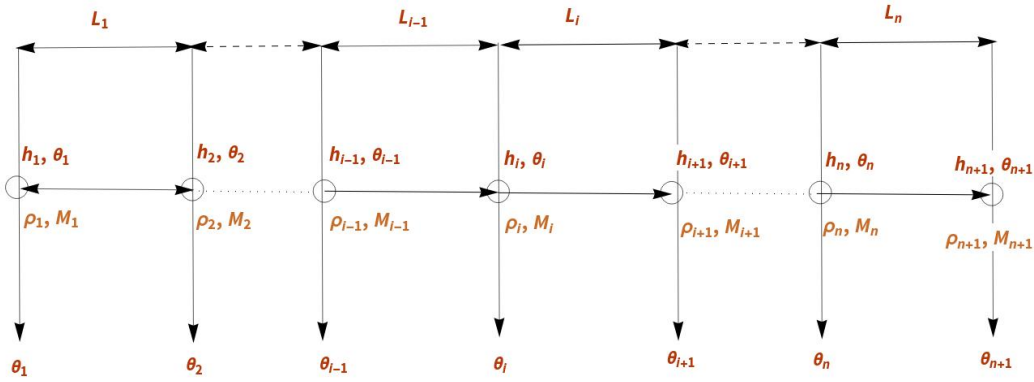


Figure 1: Discretization scheme by space

By following the paper [23], we write a discretized system of (2) - (3):

$$\begin{aligned}\frac{d\rho_1}{dt} + \frac{2}{L_1 S_1} M_1 &= -\frac{2}{L_1 S_1} Q_1, \\ \frac{d\rho_i}{dt} + \frac{2}{L_{i-1} S_{i-1} + L_i S_i} (M_i - M_{i-1}) &= -\frac{2}{L_{i-1} S_{i-1} + L_i S_i} Q_i, (i = 2, 3, \dots, n) \\ \frac{d\rho_{n+1}}{dt} + \frac{2}{L_n S_n} (-M_n) &= -\frac{2}{L_n S_n} Q_{n+1}.\end{aligned}\quad (6)$$

The integration is based on a modified implicit integration method [24] with a nonsymmetric difference:

$$\frac{Y_{n+1} - Y_n}{\Delta t} = A((1 - v)Y_{n+1} + vY_n) + \frac{1}{2}B(U_{n+1} + U_n), \quad (7)$$

where U_n and Y_n are the values at time t , U_{n+1} , Y_{n+1} are the values at time $t + \Delta t$ which is the integration time-step, and i is the coefficient of nonsymmetric difference.

We write the system of (5) - (6) for $i = 2$ in the following form:

$$\alpha_2 \frac{d}{dt} M_2 + \alpha_1 M_2 + \rho_3 - \rho_2 = r_2, \quad (8)$$

where the coefficients are written as follows:

$$\xi_{n-2} = \frac{a_{2n-2}}{c_{2n-1}}, \eta_{n-2} = \frac{f_{2n-1}}{c_{2n-1}}, \xi_i = \frac{a_i}{c_i - b_i \xi_{i+1}} \quad (i = 2n-3, 2n-4, \dots, 1).$$

Simplifying η_i ($i = 1, 2, \dots, n-1$), we obtain formulas for A , B , and C :

$$B = \frac{1}{c_1 - b_1 \cdot \xi_1}, \quad (17)$$

$$C = \frac{b_{2n-2}}{c_{2n-1}} \cdot \frac{b_{2n-3}}{c_{2n-2} - b_{2n-2} \cdot \xi_{2n-2}} \cdot \frac{b_{2n-4}}{c_{2n-3} - b_{2n-3} \cdot \xi_{2n-3}} \cdot \dots \cdot \frac{b_1}{c_2 - b_2 \cdot \xi_2} \cdot \frac{1}{c_1 - b_1 \cdot \xi_1}, \quad (18)$$

$$A = \left(\dots \left(\left(\left(b_{2n-2} \cdot \frac{f_{2n-3}}{c_{2n-1}} + f_{2n-2} \right) \cdot \frac{b_{2n-3}}{c_{2n-2} - b_{2n-2} \cdot \xi_{2n-2}} + f_{2n-3} \right) \times \right. \right. \quad (19)$$

$$\left. \left. \times \frac{b_{2n-4}}{c_{2n-3} - b_{2n-3} \cdot \xi_{2n-3}} + f_{2n-4} \right) \cdot \dots \cdot \frac{b_1}{c_2 - b_2 \cdot \xi_2} + f_1 \right) \cdot \frac{1}{c_1 - b_1 \cdot \xi_1}$$

Second, let us build formulas for the coefficients of (16) using the right tridiagonal matrix algorithm [25]:

$$\begin{cases} M_n = \beta_n, \\ \rho_i = \alpha_i M_{i+1} + \beta_i, \\ M_i = \alpha_i \rho_{i+1} + \beta_i, \quad (i = 1, 2, \dots, n-1) \end{cases},$$

where

$$\alpha_1 = \frac{b_1}{c_1}, \beta_1 = \frac{f_1}{c_1}, \alpha_{i+1} = \frac{b_i}{c_i - a_i \alpha_i} \quad (i = 1, 2, \dots, 2n-2).$$

Simplifying β_i , we obtain formulas for U , V , and W :

$$W = \frac{1}{c_{2n-1} - a_{2n-2} \cdot \alpha_{2n-2}} \quad (20)$$

$$V = \frac{a_1}{c_1} \cdot \frac{a_2}{c_2 - a_1 \cdot \alpha_1} \cdot \frac{a_3}{c_3 - a_2 \cdot \alpha_2} \cdot \dots \cdot \frac{a_{2n-2}}{c_{2n-2} - a_{2n-3} \cdot \alpha_{2n-3}} \cdot \frac{1}{c_{2n-1} - a_{2n-2} \cdot \alpha_{2n-2}} \quad (21)$$

$$U = - \left(\left(\left(\left(a_1 \cdot \frac{f_1}{c_1} + f_2 \right) \cdot \frac{a_2}{c_2 - a_1 \cdot \alpha_1} + f_3 \right) \cdot \frac{a_3}{c_3 - a_2 \cdot \alpha_2} + f_4 \right) \times \dots \times \right. \quad (22)$$

$$\left. \times \frac{a_{2n-2}}{c_{2n-2} - a_{2n-3} \cdot \alpha_{2n-3}} + f_{2n-1} \right) \cdot \frac{1}{c_{2n-1} - a_{2n-2} \cdot \alpha_{2n-2}}.$$

In general, these formulas can be written as follows:

$$M_{\alpha\beta} = A + B\rho_\alpha + C\rho_\beta, \quad (23)$$

$$-M_{\alpha\beta} = U + V\rho_\alpha + W\rho_\beta. \quad (24)$$

Here, $M_{\alpha\beta}$ elements describe crossing points in the transmission network (see Figure 3).

3 Numerical results

We use a model for gas dynamics in pipe networks by the crossing-branch method. We present the derivation of the model as well as numerical results illustrating its validity properties.

The calculation scheme consists of three main steps, as shown in Figure 2.

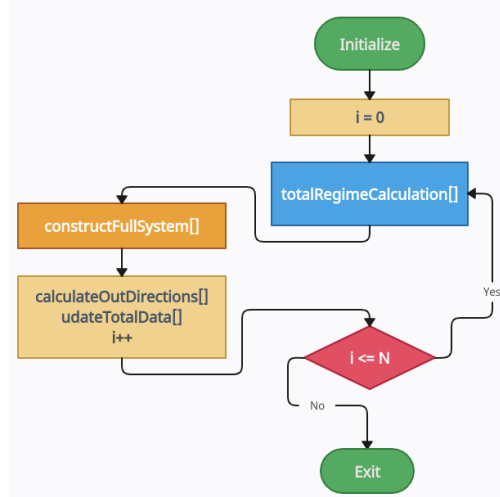


Figure 2: Calculation scheme by space and time

Next we present numerical results on an artificial sample network without compressors. Future work will be dedicated to the model considering compressors along the entire network.

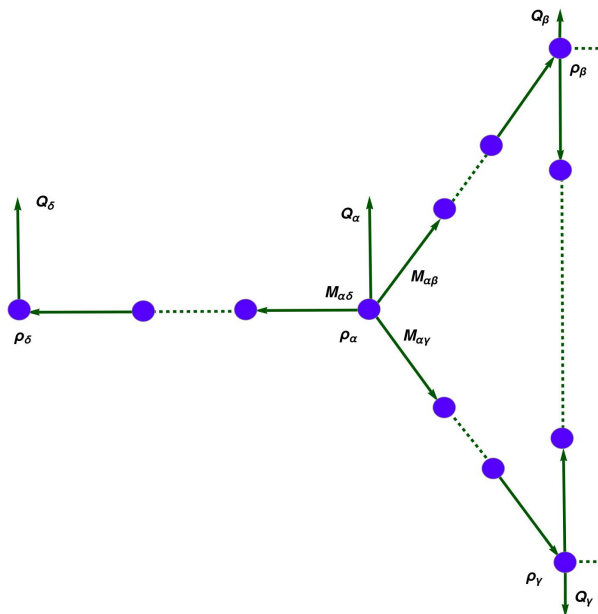


Figure 3: Crossing-branch scheme

To study the model, two calculation scenarios were built:

1. Building a steady state with stable input data.
2. Constructing a dynamic mode with the simulation of the growth of the gas flow at one inlet point of the main pipeline with a constant inlet pressure.

Using the crossing-branch method from [23]– [24] in Figure 3, we obtain numerical results for the artificial gas pipes network, as shown in Figure 4.

The method used in this study can be applied to pipeline networks without involving graphs. It is easy to see in the network figure that the mode of gas flow through pipes can be set as an array of sets of points following the given orientation of the gas flow. Then, we get an array of dimension 17, each element of which consists of a set of network points. For example, for our artificial network, we get the array in Table ??.

We present an example synthetic network in Figure 4 consisting of a tree with 29 nodes connected by 28 edges with a total length of 370.6 km, 3 gas fields, and 7 terminals or withdrawals, not containing compressors.

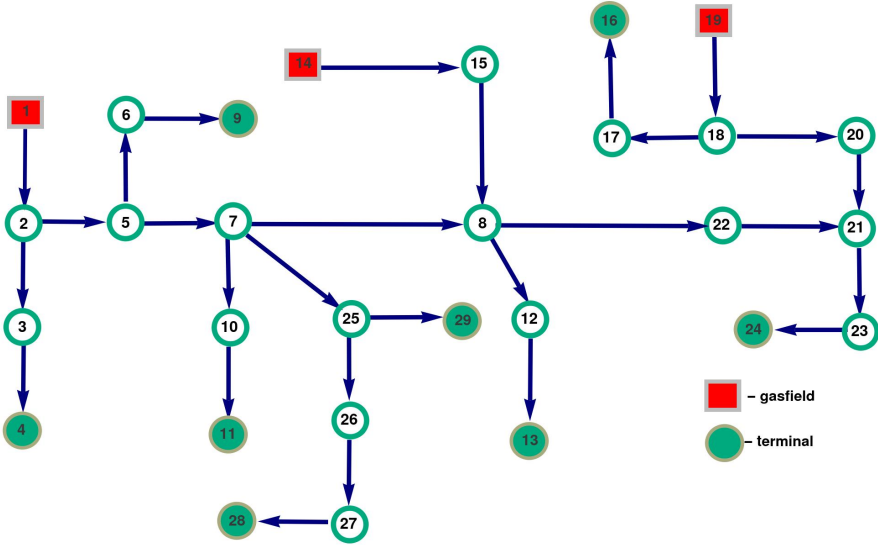


Figure 4: Gas pipelines network

Let us write the equation for the cross vertex α :

$$d_\alpha \rho_\alpha + \sum_{i \in Q_\alpha} M_{\alpha i} + Q_\alpha = e_\alpha, \tag{25}$$

where Q_α is the set of neighboring cross vertices. If we assume that the data on the output points are known, then we get an equation independent of ρ_δ . By combining all equations for cross vertices by applying formulas (17)–(24), we obtain the linear system with respect to vectors of unknown densities at the cross vertices of the graph:

$$S\rho = R. \tag{26}$$

`totalRegimeCalculation[]` constructs the initial regime using input data of the regime. According to the scheme in Figure 2, the procedure `constructFullSystem[]` builds matrix

S from (26) and solves the system. N depends on the simulation time, i.e., from the time interval of the modelling of the transportation process. As the compressors are not connected to the constructed gas pipeline network, the gas supply and the volume of consumption must be equal. Here, the loss of gas during transportation is considered insignificant due to micro-cracks in the pipes.

By ignoring gas parameters of output points of the network in (25), we must evaluate the separate numerical procedures for that like `calculateOutDirections[]`. This calculation is used a linear non-isothermal model [26].

The last block of calculations includes the procedure `updateTotalData[]`, which updates all gas parameters and applies appropriate conversions, such as density to pressure.

Table 1: Table of the regime

Table 1: Table of the regime					
Branch #	Set of points	Branch #	Set of points	Branch #	Set of points
1	{1, 2}	7	{7, 8}	13	{21, 23, 24}
2	{2, 3, 4}	8	{14, 15, 8}	14	{7, 25}
3	{2, 5}	9	{8, 12, 13}	15	{25, 26, 27, 28}
4	{5, 6, 9}	10	{18, 17, 16}	16	{25, 29}
5	{5, 7}	11	{19, 18}	17	{21, 22, 8}
6	{7, 10, 11}	12	{18, 20, 21}		

Numerical experiments were performed with time step $\tau = 0.01$ sec and $h = 1$ km and the duration of the simulation was 5.5 hours. Accounting for transient withdrawals, and accordingly the assumption of transient injections, we consider a regime with time-dependent dynamical information, where one of the injection point gas parameters, such as mass flow or pressure, is given dynamically.

Figures 5 and 6 show results for the numerical solution. Below are the calculated pressure values in the start point of branches and graphical form for each branch separately.

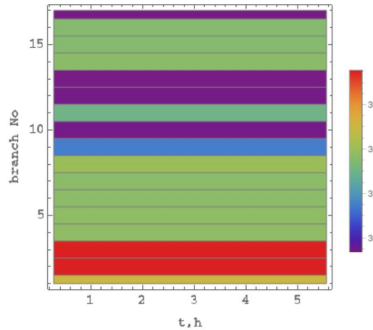


Figure 5: Pressure values in the start point of branches

The results for densities in crossing nodes $\{2, 5, 7, 25, 8, 18, 21\}$ are shown in Figures 7 and 8.

Calculations were performed using the software system Wolfram Mathematica. The computational procedures shown in scheme Figure 2 were implemented in various Wolfram

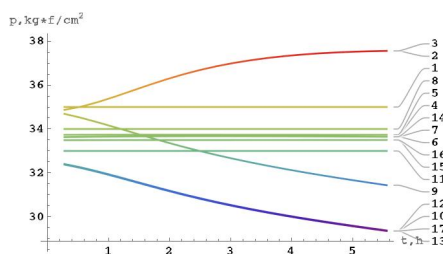


Figure 6: Pressure values in the graphical form for each branch separately

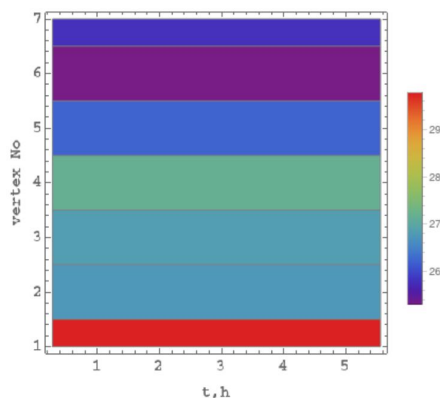


Figure 7: Density values in crossing points

notebooks, which can be instantly launched. The source code has been uploaded to GitHub and is available at the link [27].

4 Discussion

The outcomes of this research have provided insight into the investigation of the natural gas transportation process. Due to the unstable flow of natural gas into the pipeline system and changes in consumption, modeling the transportation process is a complicated problem. However using the considered dynamic model, we can obtain gas flow parameters at each point in the network dynamically. The crossing-branch method, which utilizes supply and consumption data, enables the development of the state of a dynamic system at a specific time.

Gas pipelines are often operated in transient modes due to the time-varying needs of consumers for natural gas and gas supplies. For a certain period of operation of the gas pipeline with specified gas parameters, depending on time, at the input and output points, pipeline dispatchers are faced with the task of optimizing the transition process to minimize fuel consumption at compressor stations in real time. For optimal management and control of the transport network, it is preferable to use dynamic models since they describe the dynamics of transient processes and allow efficient use of fuel gas.

Currently, the authors have conducted calculations to simulate the operation of gas compressor units, which will eventually be included in the complete transport network. The model discussed in this article will allow optimizing fuel consumption in such scenarios,

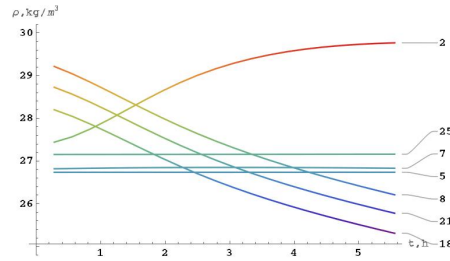


Figure 8: Density values in crossing points in the graphical form

reducing compressor speed, i.e. decreasing the load of these units while maintaining the equipment within the permissible operating range. These results should be considered when planning the implementation of gas transmission networks including equipment such as gas compressor units.

It should be noted that there is one important disadvantage of this model. As can be seen from formulas (18)-(19) and (21)-(22), it demands significant computational resources for large n . However for practical purposes (when n is less than 1000, mainly for real pipeline networks, since the number of vertices does not reach large values) this algorithm performs well and provides satisfactory computational results in an acceptable time.

5 Conclusions

The main problem is that gas movement without high pressure is impossible. If the gas enters with high pressure, then during movement, as a result of friction against the walls of the pipes, the pressure drops and the speed decreases. Therefore, compressor stations are installed in all onshore gas transportation networks. The main customers of this process are consumers and suppliers. The goal of this and future research is to control gas transportation in such a way as to meet the needs of consumers when operating compressors in economical mode, minimizing fuel gas consumption. The main element of the gas network is the pipe, followed by compressors to increase the gas pressure. The pipeline network contains many valves - regulators that can be opened and closed, which provide control and control of the direction and volume of gas. To get an idea of the size of such a gas transportation infrastructure, we consider the pipeline network of Kazakhstan. The total length of Kazakhstan's main gas pipelines is more than 19 thousand kilometers, on which 56 compressor stations operate, and 316 gas pumping units are installed [28]. Recently, many scientific papers have been devoted to theoretical studies of the optimization of gas network transients using mathematical optimization tools. After the gas consumption planning process, the operating modes of various main gas pipelines are built - the direction and volume of flows, the load on the network and the load of compressor stations that provide the gas with the required high pressure are taken into account. Specialist dispatchers monitor compressors and, based on their knowledge and experience, determine the loading of units for stable operation of the transport process.

Further research will be devoted to the construction of mathematical and computer modeling of non-stationary modes in order to optimize the gas transportation process by choosing the most optimal control policy and control influences on the technological

equipment of main gas pipelines.

Acknowledgments

This research was funded by the Science Committee of the Ministry of Science and High Education of the Republic of Kazakhstan (Grant Nos. AP14869558 and AP14871523).

References

- [1] Herty, M. and Mohring, J. and Sachers, V. "A new model for gas flow in pipe networks" , *Math Meth Appl Sci*, 33:1 (2010): 845-855.
- [2] Steinbach, M. *On PDE solution in transient optimization of gas networks* (Berlin: ZIB Berlin, 2004).
- [3] PSIG "Pipeline Simulation Interest Group" , <https://psig.org/>
- [4] White, F.M. *Fluid Mechanics* (New York: McGraw-Hill, 2002).
- [5] Osiadacz, A.J. *Dynamic optimization of high pressure gas networks using hierarchical systems theory* (Warsaw: Warsaw University of Technology, 2002).
- [6] Cameron, I. *Using an excel-based model for steady-state and transient simulation* (Ottawa: TransCanada Transmission Company, 2000).
- [7] Zhou, J. and Adewumi, M.A. "Simulation of transients in natural gas pipelines using hybrid TVD schemes" , *International Journal for Numerical Methods in Fluids*, 32:4 (2000): 407-437.
- [8] Li, T. "Interdependency of natural gas network and power system security" , *IEEE Trans. Power Systems*, 23:4 (2008): 1817-1824.
- [9] MITEI "Growing concerns, possible solutions: The interdependency of natural gas and electricity systems" , *MIT Energy Initiative Symposium*, Cambridge, United States, April 16, 2013.
- [10] Chertkov, M. and Backhaus, S. and Lebedev, V. "Cascading of Fluctuations in Interdependent Energy Infrastructures: Gas-Grid Coupling" , *Applied Energy*, 160:1 (2000): 541-551.
- [11] Chertkov, M. and Fisher, M. and Backhaus, S. and Bent, R. and Misra, S. "Measurement of energy market inefficiencies in the coordination of natural gas and power" , *In 47th Hawaii Internat. Conf. on System Sci.*, (2014): 2335-2343.
- [12] Tabors, R. and Adamson, S. "Measurement of energy market inefficiencies in the coordination of natural gas and power" , *In 47th Hawaii Internat. Conf. on System Sci.*, (2014): 2335-2343.
- [13] Rios-Mercado, R.Z. and Borraz-Sanchez, C. "Optimization problems in natural gas transportation systems: A state-of-the-art review" , *Applied Energy*, 147:1 (2015): 536-555.
- [14] Koch, T. and Hiller, B. and Pfetsch, M.E. and Schewe, L. *Evaluating Gas Network Capacities* (Philadelphia, United States: Society for Industrial and Applied Mathematics Philadelphia, 2015).
- [15] Zlotnik, A. and Chertkov, M. and Backhaus, S. "Optimal control of transient flow in natural gas networks" , *54th IEEE Conference on Decision and Control*, Osaka, Japan: 4563-4570.
- [16] Mak, T. and Van Hentenryck, P. and Zlotnik, A. and Bent, R. "Dynamic Compressor Optimization in Natural Gas Pipeline Systems" , *INFORMS Journal on Computing*, 31:1 (2019): 40-65.
- [17] Chen N.H. "An explicit equation for friction factor in pipe" , *Industrial and Engineering Chemistry Fundamentals*, 18:3 (1979): 296-297.
- [18] Elsharkawy, A. M. and Elsharkawy, L. A. "Predicting the compressibility factor of natural gases containing various amounts of CO2 at high temperatures and pressures" , *Journal of Petroleum and Gas Engineering*, 11:1 (2020): 19-36.
- [19] Koch, T. and Hiller, B. and Pfetsch, M.E. and Schewe, L. *SO 12213-3, Natural gas calculation of compression factor. Part 3: Calculation using physical properties. International Organization for Standardization, Technical Committee ISO/TC 193* (Natural gas, Sub committee SC1, Analysis of natural gas. Geneve, 1997).

- [20] Kunz, O. and Klimeck, R. and Wagner, W. and Jaeschke, M. *The GERG-2004 Wide-Range Equation of State for Natural Gases and Other Mixtures* (Düsseldorf: GERG Technical Monograph TM15, 2007).
- [21] Kunz, O. and Wagner, W. "The GERG-2008 Wide-Range Equation of State for Natural Gases and Other Mixtures: An Expansion of GERG-2004" , *Journal Chemical & Engineering Data*, 57:11 (2012): 3032-3091.
- [22] STOGazprom *Norms of technological design of main gas pipelines* (Moscow: Gazprom, 2006).
- [23] Kralik, J. and Stiegler, P. and Vostry, Z. and Zavorka, J. "The GERG-2008 Wide-Range Equation of State for Natural Gases and Other Mixtures: An Expansion of GERG-2004" , *Journal Chemical & Engineering Data*, 57:11 (2012): 3032-3091.
- [24] Kralik, J. and Stiegler, P. and Vostry, Z. and Zavorka, J. "A universal dynamic simulation model of gas pipeline networks" , *IEEE Transactions on Systems, Man, and Cybernetics*, SMC-14:4 (1984): 597-606.
- [25] Biswa, N. D. *Numerical Linear Algebra and Applications* (Philadelphia, United States: SIAM, 2010).
- [26] Osiadacz, A.J. and Chaczykowski, M. "Comparison of isothermal and non-isothermal pipeline gas flow models" , *Chemical Engineering Journal*, 81:1-3 (2001): 41-51.
- [27] zhus_dika *Github Repository* https://github.com/zhus-dika/natural_gas_transportation_through_pipeline_networks ([Online; open source], 2023).
- [28] QAZAQGAZ "qazaqgaz.kz" , <https://qazaqgaz.kz/>

IRSTI 27.31.15

DOI: <https://doi.org/10.26577/JMMCS202412113>M.T. Jenaliyev , A.S. Kassymbekova* 

Institute of Mathematics and Mathematical Modeling, Kazakhstan, Almaty

*e-mail: kasar1337@gmail.com

ON THE INITIAL BOUNDARY PROBLEM FOR HYPERBOLIC EQUATIONS WITH EXPONENTIAL DEGENERATION $t^{12/7}$

Degenerate equations have been and are the object of numerous studies. They have not only theoretical but also practical significance. Let us only point out the fact that they arise when modeling subsonic and supersonic processes flows in a gaseous environment, filtration processes and movement of groundwater, in climate forecasts, etc. Mathematically, the degeneracy of a differential equation can be different. In this paper we consider a degenerate equation of the form $\partial_t (t^\beta \partial_t u(x, t)) - \Delta u(x, t) = f(x, t)$. In a bounded cylindrical domain, when the degree of degeneracy $\beta = 12/7$, we have established the unique solvability of the Cauchy-Dirichlet problem for the considered degenerate hyperbolic equation. Based on the solution of the spectral problem for the Laplace operator with Dirichlet conditions are introduced spectral decompositions of the right side of the differential equation and the desired solution to the Cauchy-Dirichlet problem. For the Fourier coefficients we obtain a family of Cauchy problems for a degenerate second-order ordinary differential equation, moreover, the second initial the condition must be met with weight. The latter is determined by the degree of degeneracy of the equation. The solutions to each of the Cauchy problems are represented by using Bessel functions. A priori estimates are established, on the basis of which is established the solvability of the initial-boundary problems for a degenerate hyperbolic equation.

Key words: Degenerate equations, degree of degeneracy, hyperbolic equations, a priori estimate.

M.T. Жиенәлиев, А.С. Қасымбекова*

Математика және математикалық модельдеу институты, Қазақстан, Алматы қ.

*e-mail: kasar1337@gmail.com

Жойылым дәрежесі $t^{12/7}$ гиперболалық теңдеу үшін бастапқы шекаралық есеп туралы

Жойылмалы теңдеулер көптеген зерттеулердің объектісі болды да және болып табылады. Олардың тек теориялық емес, практикалық маңызы бар. Атап кететін болсақ олар газды ортадағы дыбысқа дейінгі және супер дыбыстық ағындар, сүзу және жер асты суларының қозғалысының үдерістерін модельдеу кезінде, климаттық болжамдарда және т.б. пайда болады. Математикалық тұрғыдан дифференциалдық теңдеудің жойылымдығы әртүрлі болуы мүмкін. Бұл жұмыста $\partial_t (t^\beta \partial_t u(x, t)) - \Delta u(x, t) = f(x, t)$ түріндегі жойылмалы теңдеуін қарастырамыз. Шектелген цилиндрлік облысында, жойылым дәрежесі $\beta = 12/7$ болғанда, қарастырылып отырған жойылмалы гиперболалық теңдеу үшін Коши-Дирихле есебінің бірмәнді шешімділігін орнаттық. Дирихле шарттары бар Лаплас операторы үшін спектрлік есептің шешімі негізінде, берілген функция болып табылатын дифференциалдық теңдеудің оң жағы мен Коши-Дирихле есебінің ізделінді шешімінің спектрлік жіктелуі енгізіледі. Фурье коэффициенттері үшін біз, екінші бастапқы шарты салмақтықпен орындалуы қажет болатын, жойылмалы екінші ретті қарапайым дифференциалдық теңдеулердің Коши есептерінің тобын аламыз. Соңғысы теңдеудің жойылым дәрежесімен анықталады. Коши есептерінің әрқайсысының шешімдері Бессель функциялары арқылы анықталады. Жұмыста сонымен қатар жойылмалы гиперболалық теңдеу үшін бастапқы шекаралық есептің шешімділігіне негіз болатын априорлы бағалаулар алынды.

Түйін сөздер: Жойылмалы теңдеулер, жойылым дәрежесі, гиперболалық теңдеу, априорлы бағалаулар.

М.Т. Дженалиев, А.С. Касымбекова*

Институт математики и математического моделирования, Казахстан, г. Алматы

*e-mail: kasar1337@gmail.com

**О начально-граничной задаче для гиперболического уравнения
со степенным вырождением $t^{12/7}$**

Вырождающиеся уравнения являлись и являются объектом многочисленных исследований. Они имеют не только теоретическую, но и практическую значимость. Укажем лишь на тот факт, что они возникают при моделировании процессов до-звуковых и сверх-звуковых течений в газовой среде, процессов фильтрации и движения подземных вод, в прогнозе климата и т.д. Математически, вырождение дифференциального уравнения может быть различным. В настоящей работе рассматривается вырождающееся уравнение вида $\partial_t(t^\beta \partial_t u(x, t)) - \Delta u(x, t) = f(x, t)$. В ограниченной цилиндрической области, когда степень вырождения $\beta = 12/7$, нами установлена однозначная разрешимость задачи Коши-Дирихле для рассматриваемого вырождающегося гиперболического уравнения. На основе решения спектральной задачи для оператора Лапласа с условиями Дирихле вводятся спектральные разложения заданных функций – правой части дифференциального уравнения и искомого решения задачи Коши-Дирихле. Для коэффициентов Фурье мы получаем семейство задач Коши для вырождающегося обыкновенного дифференциального уравнения второго порядка, причем второе начальное условие должно выполняться с весом. Последнее определяется степенью вырождения уравнения. Решения каждой из задач Коши представляется с помощью функций Бесселя. Установлены априорные оценки, на основе которых установлена разрешимость начально-граничной задачи для вырождающегося гиперболического уравнения.

Ключевые слова: Вырождающиеся уравнения, степень вырождения, гиперболическое уравнение, априорные оценки.

1 Introduction

Would like to note that the authors study degenerate equations and investigate the solvability of various initial-boundary value problems in degenerate domains [1]– [4]. The presented work is a continuation of these studies.

The following initial-boundary value problem for a model degenerate hyperbolic equation

$$\partial_t(t^\beta \partial_t u) - \Delta u = f \quad \text{in } Q = \Omega \times (0, T), \quad (1)$$

$$u = 0 \quad \text{on } \Sigma = \partial\Omega \times (0, T), \quad (2)$$

$$u(x, 0) = 0, \quad \lim_{t \rightarrow +0} t^\beta \partial_t u(x, t) = 0 \quad \text{in } \Omega, \quad (3)$$

was studied in the dissertation of N. Kaharman [5]. In particular, he established the following result:

Theorem 1 *Let $\beta \in [0, 1)$, $f \in L^2(Q)$, $(-\Delta)^{1-\nu} f \in L^2(Q)$. Then problem (1)–(3) is uniquely solvable, and there is an a priori estimate*

$$\begin{aligned} & \|u\|_{W^{2,2}(Q; t^\beta)}^2 \equiv \|u\|_{L^2(Q)}^2 + \|t^\beta \partial_t u\|_{W_2^1(0, T; L^2(\Omega))}^2 + \|\Delta u\|_{L^2(Q)}^2 \\ & \leq C \left[\|f\|_{L^2(Q)}^2 + \|(-\Delta)^{1-\nu} f\|_{L^2(Q)}^2 \right], \quad \text{where } \nu = \frac{1 - \beta}{2 - \beta}, \end{aligned} \quad (4)$$

that is, the parameter ν changes within the half-open segment: $\nu \in (0, 1/2]$.

As is known from [6], [7]– [12], if the degree of degeneracy $\beta \in [0, 1)$, then this is a case of weak degeneracy of the equation. If $\beta \in [1, 2]$, then this is a case of strong degeneracy. Thus, in the dissertation of N.Kaharman [5] the case of weak degeneracy is considered. The case of strong degeneracy is more difficult to study. Here, each value of the parameter β from the interval $[1, 2]$ requires separate consideration. In this paper we study the case $\beta = 12/7$, parameter $\nu = 5/2$.

2 Statement of the problem. Main result

Let $0 < T < \infty$, $\Omega \subset R^n$ is a bounded domain with the boundary $\partial\Omega \in C^2$, $Q = \Omega \times (0, T)$, $\Sigma = \partial\Omega \times (0, T)$. Consider the following initial boundary value problem

$$\partial_t(t^{12/7} \partial_t u) - \Delta u = f \text{ in } Q, \quad (5)$$

$$u = 0 \text{ on } \Sigma, \quad (6)$$

$$u(x, 0) = 0, \quad \lim_{t \rightarrow +0} t^{12/7} \partial_t u(x, t) = 0 \text{ in } \Omega. \quad (7)$$

The following result is valid.

Theorem 2 (Main result). *Let the following conditions be satisfied:*

$$f(x, t) \in L^2(Q), \quad \frac{f(x, t)}{t^\alpha} \in L^2(Q), \quad \frac{\Delta f(x, t)}{t^\alpha} \in L^2(Q), \quad \alpha > 23/14.$$

Then the problem (5)–(7) is uniquely solvable, and there is an a priori estimate

$$\begin{aligned} & \|u\|_{W(Q; t^{12/7})}^2 \equiv \|u\|_{L^2(Q)}^2 + \|t^{12/7} \partial_t u\|_{W_2^1(0, T; L^2(\Omega))}^2 + \|\Delta u\|_{L^2(Q)}^2 \leq \\ & \leq C \left[\|f(x, t)\|_{L^2(Q)}^2 + \left\| \frac{f(x, t)}{t^\alpha} \right\|_{L^2(Q)}^2 + \left\| \frac{\Delta f(x, t)}{t^\alpha} \right\|_{L^2(Q)}^2 \right]. \end{aligned} \quad (8)$$

3 Methods and materials. Proof of theorem2. A priori estimates

Applying the Fourier method to problem (5)–(7), namely $u(x, t) = \sum_{j=1}^{\infty} c_j(t) z_j(x)$ we obtain the Cauchy problem for the Fourier coefficients $c_j(t)$

$$(t^{12/7} c_j'(t))' + \lambda_j c_j(t) = f_j(t) \text{ in } (0, T), \quad (9)$$

$$c_j(0) = 0, \quad \lim_{t \rightarrow +0} t^{12/7} c_j'(t) = 0, \quad (10)$$

where $\{z_j(x), \lambda_j\}$ is a solution to the spectral problem:

$$-\Delta z(x) = \lambda z(x), \quad x \in \Omega, \quad z|_{\partial\Omega} = 0, \quad (11)$$

and let the solution has the form

$$\{z_j(x), \lambda_j, j = 1, 2, \dots\}, \text{ moreover, } 0 < \lambda_1 < \lambda_2 < \dots, \quad (12)$$

and the system of eigenfunctions $\{z_j(x), j = 1, 2, \dots\}$ is orthonormal.

Temporarily, for simplicity we will omit the index j . Let us rewrite equation (9) and the initial conditions (10) in the following form:

$$t^2 c''(t) + \frac{12}{7} t c'(t) + \lambda t^{2/7} c(t) = t^{2/7} f(t) \text{ in } (0, T). \quad (13)$$

$$c(0) = 0, \quad \lim_{t \rightarrow +0} t^{12/7} c'(t) = 0. \quad (14)$$

Let us find a general solution to the inhomogeneous equation (13). According to ([13], chapter 2, § 2.1.2, formula 62 or 127), the general solution to the homogeneous version of equation (13) has the form:

$$c_{\text{hom.eq.}}(t) = t^{-5/14} \left[A J_{5/2} \left(7\sqrt{\lambda} t^{1/7} \right) + B Y_{5/2} \left(7\sqrt{\lambda} t^{1/7} \right) \right], \quad t \in (0, T). \quad (15)$$

Since in (15) the Bessel functions have an index $\nu = 5/2$, then according to ([14], 10.1.1, 10.1.11–10.1.12 at $\nu = \frac{5}{2}$) for the homogeneous equation (13) (for $f(t) \equiv 0$) the fundamental solutions can be written in the following form

$$\begin{aligned} \varphi_1(t) &= \left(\frac{3}{[7\sqrt{\lambda} t^{1/7}]^3} - \frac{1}{7\sqrt{\lambda} t^{1/7}} \right) \sin(7\sqrt{\lambda} t^{1/7}) - \frac{3}{[7\sqrt{\lambda} t^{1/7}]^2} \cos(7\sqrt{\lambda} t^{1/7}), \\ \varphi_2(t) &= \left(-\frac{3}{[7\sqrt{\lambda} t^{1/7}]^3} + \frac{1}{7\sqrt{\lambda} t^{1/7}} \right) \cos(7\sqrt{\lambda} t^{1/7}) - \frac{3}{[7\sqrt{\lambda} t^{1/7}]^2} \sin(7\sqrt{\lambda} t^{1/7}), \\ \bar{\varphi}_1(z) &= \left(\frac{3}{z^2} - 1 \right) \sin z - \frac{3}{z} \cos z, \quad \bar{\varphi}_2(z) = \left(-\frac{3}{z^2} + 1 \right) \cos z - \frac{3}{z} \sin z, \end{aligned} \quad (16)$$

that is

$$\tilde{\varphi}_1(t) = \bar{\varphi}_1(z) \Big|_{z=7\sqrt{\lambda} t^{1/7}}, \quad \tilde{\varphi}_2(t) = \bar{\varphi}_2(z) \Big|_{z=7\sqrt{\lambda} t^{1/7}}, \quad (17)$$

therefore, the general solution (15) for the homogeneous equation (13) (for $f(t) \equiv 0$) is written as:

$$c_{\text{hom}}(t) = t^{-2/7} [A \varphi_1(t) + B \varphi_2(t)]. \quad (18)$$

Note, that the necessity for additional notations (16) will become evident later (formula(21)).

To find a general solution to the inhomogeneous equation (13) (where $f(t) \neq 0$) we use the method of variation of constants. We will have

$$c(t) = A(t) \varphi_1(t) + B(t) \varphi_2(t). \quad (19)$$

Let us write the system of algebraic equations in terms of the unknown functions $A'(t)$ and $B'(t)$:

$$\begin{cases} \varphi_1(t) A'(t) + \varphi_2(t) B'(t) = 0, \\ \varphi_1'(t) A'(t) + \varphi_2'(t) B'(t) = \frac{f(t)}{t^{12/7}}, \end{cases} \quad (20)$$

for which we calculate the Wronskian ([14], 10.1.6) and the corresponding determinants

$$W = W \{ \varphi_1(t), \varphi_2(t) \} = \begin{vmatrix} \varphi_1(t) & \varphi_2(t) \\ \varphi_1'(t) & \varphi_2'(t) \end{vmatrix} = \frac{1}{[7\sqrt{\lambda} t^{1/7}]^2},$$

$$W_A = \begin{vmatrix} 0 & \varphi_2(t) \\ \frac{f(t)}{t^{12/7}} & \varphi_2'(t) \end{vmatrix} = -\frac{f(t)}{t^{12/7}} \varphi_2(t), \quad W_B = \begin{vmatrix} \varphi_1(t) & 0 \\ \varphi_1'(t) & \frac{f(t)}{t^{12/7}} \end{vmatrix} = \frac{f(t)}{t^{12/7}} \varphi_1(t).$$

Hence, for the unknown coefficients of the general solution of equation (13) from (19), we, respectively, obtain

$$A'(t) = \frac{W_A}{W}, \quad B'(t) = \frac{W_B}{W},$$

that is,

$$A(t) = -7\sqrt{\lambda} \int_0^t \frac{f(\tau)}{\tau^{11/7}} \left[\left(-\frac{3}{[7\sqrt{\lambda} \tau^{1/7}]^2} + 1 \right) \cos(7\sqrt{\lambda} \tau^{1/7}) - \frac{3}{7\sqrt{\lambda} \tau^{1/7}} \sin(7\sqrt{\lambda} \tau^{1/7}) \right] d\tau + a,$$

$$B(t) = 7\sqrt{\lambda} \int_0^t \frac{f(\tau)}{\tau^{11/7}} \left[\left(\frac{3}{[7\sqrt{\lambda} \tau^{1/7}]^2} - 1 \right) \sin(7\sqrt{\lambda} \tau^{1/7}) - \frac{3}{7\sqrt{\lambda} \tau^{1/7}} \cos(7\sqrt{\lambda} \tau^{1/7}) \right] d\tau + b.$$

To satisfy the first initial condition from (14), it is necessary that $a = 0$, $b = 0$. Then for the general solution of equation (13) from (19) we obtain

$$c(t) = - \int_0^t \frac{f(\tau)}{t^{1/7} \tau^{11/7}} [\tilde{\varphi}_1(t) \tilde{\varphi}_2(\tau) - \tilde{\varphi}_1(\tau) \tilde{\varphi}_2(t)] d\tau, \quad (21)$$

where according to (16)–(17) the functions $\tilde{\varphi}_1(t)$, $\tilde{\varphi}_2(t)$ are defined by the following formulas

$$\tilde{\varphi}_1(t) = \left(\frac{3}{[7\sqrt{\lambda} t^{1/7}]^2} - 1 \right) \sin(7\sqrt{\lambda} t^{1/7}) - \frac{3}{7\sqrt{\lambda} t^{1/7}} \cos(7\sqrt{\lambda} t^{1/7}),$$

$$\tilde{\varphi}_2(t) = \left(-\frac{3}{[7\sqrt{\lambda} t^{1/7}]^2} + 1 \right) \cos(7\sqrt{\lambda} t^{1/7}) - \frac{3}{7\sqrt{\lambda} t^{1/7}} \sin(7\sqrt{\lambda} t^{1/7}).$$

For convenience of calculations, we introduce the functions $\bar{c}(z)$, $\bar{f}(z)$, $\bar{\varphi}_1(z)$, $\bar{\varphi}_2(z)$, so that the following equalities hold:

$$c(t) = \bar{c}(z) \Big|_{z=7\sqrt{\lambda} t^{1/7}}, \quad f(t) = \bar{f}(z) \Big|_{z=7\sqrt{\lambda} t^{1/7}}, \quad \tilde{\varphi}_1(t) = \bar{\varphi}_1(z) \Big|_{z=7\sqrt{\lambda} t^{1/7}}, \quad \tilde{\varphi}_2(t) = \bar{\varphi}_2(z) \Big|_{z=7\sqrt{\lambda} t^{1/7}}, \quad (22)$$

where

$$\bar{\varphi}_1(z) = \left(\frac{3}{z^2} - 1 \right) \sin z - \frac{3}{z} \cos z, \quad \bar{\varphi}_2(z) = \left(-\frac{3}{z^2} + 1 \right) \cos z - \frac{3}{z} \sin z. \quad (23)$$

Then from (21)–(23) for the solution $\bar{c}(z)$ we obtain

$$\begin{aligned} \bar{c}(z) &= -7^6 \lambda^{5/2} \int_0^z \frac{\bar{f}(\zeta)}{z \zeta^5} [\bar{\varphi}_1(z) \bar{\varphi}_2(\zeta) - \bar{\varphi}_1(\zeta) \bar{\varphi}_2(z)] d\zeta = \\ &= -7^6 \lambda^{5/2} \int_0^z \frac{\bar{f}(\zeta)}{z \zeta^5} \left\{ \left[\left(\frac{3}{z^2} - 1 \right) \sin z - \frac{3}{z} \cos z \right] \left[\left(-\frac{3}{\zeta^2} + 1 \right) \cos \zeta - \frac{3}{\zeta} \sin \zeta \right] - \right. \\ &\quad \left. \left[\left(\frac{3}{\zeta^2} - 1 \right) \sin \zeta - \frac{3}{\zeta} \cos \zeta \right] \left[\left(-\frac{3}{z^2} + 1 \right) \cos z - \frac{3}{z} \sin z \right] \right\} d\zeta, \end{aligned} \quad (24)$$

or

$$\begin{aligned} \bar{c}(z) &= -7^6 \lambda^{5/2} \int_0^z \frac{\bar{f}(\zeta)}{z \zeta^5} \cdot \frac{3(z-\zeta)}{\zeta^2} \left\{ \left(1 - 3 \frac{\zeta}{z} + \frac{\zeta^2}{z^2} \right) \frac{\sin(z-\zeta)}{z-\zeta} + \left(\frac{\zeta}{z} + \frac{3}{z^2} \right) \cos(z-\zeta) \right\} d\zeta = \\ &= -3 \cdot 7^6 \lambda^{5/2} \left[\int_0^z \frac{\bar{f}(\zeta)}{z \zeta^7} \left(1 - 3 \frac{\zeta}{z} + \frac{\zeta^2}{z^2} \right) \sin(z-\zeta) d\zeta - \int_0^z \frac{\bar{f}(\zeta)}{z^2 \zeta^7} (z \zeta + 3) \left(1 - \frac{\zeta}{z} \right) \cos(z-\zeta) d\zeta \right]. \end{aligned} \quad (25)$$

From (25), using formulas (21)–(24), we obtain:

$$\begin{aligned} |c(t)| &\leq K_1 \int_0^t \frac{|f(\tau)|}{t^{1/7} \tau^{13/7}} d\tau + K_2 \int_0^t \frac{|f(\tau)|}{t^{2/7} \tau^{13/7}} d\tau \leq \\ &\leq \left[\frac{K_1 t^{\alpha_1 - 3/2}}{\sqrt{2\alpha_1 - 3}} + \frac{K_2 t^{\alpha_2 - 23/14}}{\sqrt{2\alpha_2 - 23/7}} \right] \left\| \frac{f(\tau)}{\tau^\alpha} \right\|_{L^2(0,T)}, \quad \alpha = \max\{\alpha_1, \alpha_2\} > 23/14, \end{aligned} \quad (26)$$

where the constants K_1 and K_2 do not depend on λ , and satisfy the inequalities

$$K_1 \geq \frac{3}{7^2 \lambda}, \quad K_2 \geq \frac{3}{7^3 \lambda^{3/2}}. \quad (27)$$

From (26)–(27), we obtain the fulfillment of the first initial condition from (14).

Let us now verify the fulfillment of the second initial condition from (14). We will calculate the derivative with respect to z of the function $\bar{c}(z)$ (25):

$$\begin{aligned} \bar{c}'(z) &= -3 \cdot 7^6 \lambda^{5/2} \int_0^z \frac{\bar{f}(\zeta)}{z^2 \zeta^7} \left\{ \left(-z\zeta + \zeta^2 - 4 + 9 \frac{\zeta}{z} - 3 \frac{\zeta^2}{z^2} \right) \sin(z-\zeta) + \right. \\ &\quad \left. + \frac{1}{z} \left(z^2 - 4z\zeta + 3(\zeta^2 - 2) + 9 \frac{\zeta}{z} \right) \cos(z-\zeta) \right\} d\zeta. \end{aligned} \quad (28)$$

Furthermore, by using the formula

$$t^{12/7}c'(t) = \frac{z^{12}}{7^{12}\lambda^6} \bar{c}'(z) \Big|_{z=7\sqrt{\lambda}t^{1/7}} \frac{dz(t)}{dt} = \frac{z^6}{7^6\lambda^{5/2}} \bar{c}'(z) \Big|_{z=7\sqrt{\lambda}t^{1/7}}, \quad (29)$$

we establish

$$\begin{aligned} \frac{z^6}{7^6\lambda^{5/2}} \bar{c}'(z) &= -3z^4 \int_0^z \frac{\bar{f}(\zeta)}{\zeta^7} \left\{ \left(-z\zeta + \zeta^2 - 4 + 9\frac{\zeta}{z} - 3\frac{\zeta^2}{z^2} \right) \sin(z - \zeta) + \right. \\ &\left. + \frac{1}{z} \left(z^2 - 4z\zeta + 3(\zeta^2 - 2) + 9\frac{\zeta}{z} \right) \cos(z - \zeta) \right\} d\zeta. \end{aligned} \quad (30)$$

From relation (30), using formula (29), we, respectively, obtain

$$\begin{aligned} |t^{12/7}c'(t)| &\leq K_1^1 \int_0^t \frac{t^{10/7}|f(\tau)|}{\tau^{13/7}} d\tau + K_2^1 \int_0^t \frac{t^{9/7}|f(\tau)|}{\tau^{13/7}} d\tau \leq \\ &\leq \left[\frac{K_1^1 t^{\alpha_1 - 9/7}}{\sqrt{2\alpha_1 - 19/7}} + \frac{K_2^1 t^{\alpha_2 - 10/7}}{\sqrt{2\alpha_2 - 19/7}} \right] \left\| \frac{f(\tau)}{\tau^{\alpha_1}} \right\|_{L^2(0,T)}, \quad \alpha_1 > 19/14, \end{aligned}$$

where the constants K_1^1 and K_2^1 do not depend on λ , and satisfy the following inequalities

$$K_1^1 \geq \frac{3}{7^3 \lambda^{3/2}}, \quad K_2^1 \geq \frac{3}{7^4 \lambda^2}.$$

We have shown that the second initial condition from (14) also holds if there is the following requirement on the right-hand side of equation (13) $t^{-\alpha_1}f(t) \in L^2(0,T)$, $\alpha_1 > 19/14$.

So, we have shown that if the conditions of theorem 2 are met, function (21) satisfies Cauchy problem(13)–(14).

Let us proceed to establish the a priori estimate (8). For the solution $c(t)$ (21) according to (26) , we will have:

$$|c(t)| \leq \left[\frac{K_1 T^{\alpha_1 - 3/2}}{\sqrt{2\alpha_1 - 3}} + \frac{K_2 T^{\alpha_2 - 23/14}}{\sqrt{2\alpha_2 - 23/7}} \right] \left\| \frac{f(\tau)}{\tau^\alpha} \right\|_{L^2(0,T)}, \quad \alpha = \max\{\alpha_1, \alpha_2\} > 23/14. \quad (31)$$

From (31) we have

$$\|c(t)\|_{L^2(0,T)} \leq T^{1/2} \left[\frac{K_1 T^{\alpha_1 - 3/2}}{\sqrt{2\alpha_1 - 3}} + \frac{K_2 T^{\alpha_2 - 23/14}}{\sqrt{2\alpha_2 - 23/7}} \right] \left\| \frac{f(\tau)}{\tau^\alpha} \right\|_{L^2(0,T)}, \quad \alpha = \max\{\alpha_1, \alpha_2\} > 23/14. \quad (32)$$

Furthermore, from the equation (13), we obtain:

$$\left| (t^{12/7}c'(t))' \right| \leq |f(t)| + \lambda|c(t)|,$$

Using the last inequality and (32), we will have the following estimate

$$\left\| (t^{12/7} c'(t))' \right\|_{L^2(0,T)}^2 \leq K_3 \left[\|f(t)\|_{L^2(0,T)}^2 + \left\| \frac{\lambda f(t)}{t^\alpha} \right\|_{L^2(0,T)}^2 \right], \quad \alpha > 23/14. \quad (33)$$

Finally, using the relations

$$t^{12/7} c'(t) = \int_0^t (\tau^{12/7} c'(\tau))' d\tau, \quad |t^{12/7} c'(t)|^2 \leq T \int_0^T |(\tau^{12/7} c'(\tau))'|^2 d\tau$$

and the estimate (33), we obtain the following estimate

$$\|t^{12/7} c'(t)\|_{L^2(0,T)}^2 \leq K_4 \left[\|f(t)\|_{L^2(0,T)}^2 + \left\| \frac{\lambda f(t)}{t^\alpha} \right\|_{L^2(0,T)}^2 \right], \quad \alpha > 23/14. \quad (34)$$

Now, returning the indices j to the functions $c(t)$ and $f(t)$ we note, that these are the Fourier coefficients of the functions $u(x, t)$ and $f(x, t)$ in the expansions:

$$u(x, t) = \sum_{j=1}^{\infty} c_j(t) z_j(x), \quad f(x, t) = \sum_{j=1}^{\infty} f_j(t) z_j(x), \quad (35)$$

where $\{z_j(x), \lambda_j, j = 1, 2, \dots\}$ are solutions to the spectral problem (11)–(12).

As a result, using formulas (21) and (35), due to the Parseval-Stecklov equality and the estimate (32), we have the first a priori estimate:

$$\|u(x, t)\|_{L^2(Q)}^2 = \sum_{j=1}^{\infty} \|c_j(t)\|_{L^2(0,T)}^2 \leq K_5 \left\| \frac{f(x, t)}{t^\alpha} \right\|_{L^2(Q)}^2, \quad \alpha > 23/14. \quad (36)$$

Next, for $-\Delta u(x, t)$ according to (36), we obtain the second a priori estimate:

$$\|\Delta u(x, t)\|_{L^2(Q)}^2 = \sum_{j=1}^{\infty} \|\lambda_j c_j(t)\|_{L^2(0,T)}^2 \leq K_6 \left\| \frac{\Delta f(x, t)}{t^\alpha} \right\|_{L^2(Q)}^2, \quad \alpha > 23/14. \quad (37)$$

Now let us establish an estimate for the expression $\partial_t(t^{12/7} \partial_t u(x, t))$. First of all, from equation (5), we obtain equalities

$$\partial_t(t^{12/7} \partial_t u(x, t)) = f(x, t) + \Delta u(x, t), \quad (38)$$

$$t^{12/7} \partial_t u(x, t) = \int_0^t [f(x, \tau) + \Delta u(x, \tau)] d\tau. \quad (39)$$

From (38)–(39) and estimate (37) we have the third and fourth a priori estimates

$$\|\partial_t(t^{12/7} \partial_t u(x, t))\|_{L^2(Q)}^2 \leq K_7 \left[\|f\|_{L^2(Q)}^2 + \left\| \frac{\Delta f(x, t)}{t^\alpha} \right\|_{L^2(Q)}^2 \right], \quad \alpha > 23/14, \quad (40)$$

$$\|t^{12/7} \partial_t u(x, t)\|_{L^2(Q)}^2 \leq K_8 \left[\|f\|_{L^2(Q)}^2 + \left\| \frac{\Delta f(x, t)}{t^\alpha} \right\|_{L^2(Q)}^2 \right], \quad \alpha > 23/14. \quad (41)$$

The set of inequalities (36), (37), (40)–(41) is equivalent to the a priori estimate (8). Theorem 2 is completely proven.

4 Conclusion

In the work, sufficient conditions are found to be imposed on the right-hand side of the differential equation, which ensure in the Sobolev space the unique solvability of the homogeneous Cauchy-Dirichlet problem for one inhomogeneous degenerate hyperbolic equation, the degree of degeneracy β of which is determined by the relation: $\beta = 12/7$.

5 Acknowledgment

This research has been funded by the Science Committee of the Ministry of Science and Higher Education of the Republic of Kazakhstan (Grants No. AP23485369, No. AP19674862).

References

- [1] Jenaliyev M.T., Yergaliyev M.G., Assetov A.A., Kalibekova A.K. *On One Initial Boundary Value Problem for the Burgers Equation in a Rectangular Domain* // Bulletin of the Karaganda University. Mathematics Series, 2021. 104(4), P.74-88.
- [2] Jenaliyev M.T., Assetov A.A., Yergaliyev M.G. *On the Solvability of the Burgers Equation with Dynamic Boundary Conditions in a Degenerating Domain* // Lobachevskii Journal of Mathematic, 2021. 42(15), P. 3661-3674.
- [3] Jenaliyev M.T., Kassymbekova A.S., Yergaliyev M.G. *On a boundary value problem for a boussinesq-type equation in a triangle* // KazNU Bulletin. Mathematics, Mechanics, Computer Science Series, 2022. 115(3), P. 36-48.
- [4] Jenaliyev M.T., Kassymbekova A.S., Yergaliyev M.G., Assetov A.A. *An initial boundary value problem for the Boussinesq equation in a Trapezoid* // Bulletin of the Karaganda University. Mathematics Series, 2022. 106(2), P. 117-127.
- [5] Кахарман Н. *Азғындалған гиперболалық теңдеулер үшін жалпы регулярлы шеттік есептер.* – Алматы: Ғылым Ордасы-МММИ-ҚазҰУ. – 2023. – 77 б.
- [6] Дезин А.А. *Дифференциально-операторные уравнения. Метод модельных операторов в теории граничных задач, Труды МИАН, 229, МАИК «Наука/Интерпериодика».* – М.: Наука. – 2000. – 176 с.
- [7] Alabau-Boussouira F., Cannarsa P., Leugering G. *Control and stabilization of degenerate wave equations* // SIAM J.Control Optim., 2017. Vol. 55, No. 3. P. 2052–2087.
- [8] Cannarsa P., Martinez P., Urbani C. *Bilinear control of a degenerate hyperbolic equation* // arXiv: 21112.00636v1 [math.AP] 1 Dec 2021. 65 p.
- [9] Cannarsa P., Martinez P., Vancostenoble J. *The cost of controlling strongly degenerate parabolic equations* // ESAIM: Control, Optimization and Calculus of Variations, 2020. Vol. 26, No. 2. P. 1–50.
- [10] Cannarsa P., Martinez P., Vancostenoble J. *Global Carleman estimates for degenerate parabolic operators with applications.* Memoirs of the AMS. Volume 239, number 1133. 2016. 225 p.
- [11] Cannarsa P., Martinez P., and Vancostenoble J. *The cost of controlling weakly degenerate parabolic equations by boundary controls* // Math. Control Relat. Fields, 7(2):171-211, 2017.
- [12] Hussein M.S., Lesnic D., Kamynin V.L., Kostin A.B. *Direct and inverse source problems for degenerate parabolic equations* // J. of Inverse and Ill-Posed Problems, 2020. 28 (3). P. 425-448.
- [13] Зайцев В.Ф., Полянин А.Д. *Справочник по обыкновенным дифференциальным уравнениям.*– М.: ФизМатЛит. – 2001. – 576 с.
- [14] *Handbook of Mathematical Functions with Formulas, Graphs, and Mathematical Tables. Tenth Printing, with corrections* (Edited M. Abramovitz and I.A. Stegun) – Washington: National Bureau of Standards – 1972. – XIV+1046 p.

References

- [1] Jenaliyev M.T., Yergaliyev M.G., Assetov A.A., Kalibekova A.K. *On One Initial Boundary Value Problem for the Burgers Equation in a Rectangular Domain* // Bulletin of the Karaganda University. Mathematics Series, 104(4), (2021):74-88.
- [2] Jenaliyev M.T., Assetov A.A., Yergaliyev M.G. *On the Solvability of the Burgers Equation with Dynamic Boundary Conditions in a Degenerating Domain* // Lobachevskii Journal of Mathematic, 42(15), (2021): 3661-3674.
- [3] Jenaliyev M.T., Kassymbekova A.S., Yergaliyev M.G. *On a boundary value problem for a boussinesq-type equation in a triangle*// KazNU Bulletin. Mathematics, Mechanics, Computer Science Series, 115(3), (2022): 36-48.
- [4] Jenaliyev M.T., Kassymbekova A.S., Yergaliyev M.G., Assetov A.A. *An initial boundary value problem for the Boussinesq equation in a Trapezoid* // Bulletin of the Karaganda University. Mathematics Series, 106(2), (2022):117-127.
- [5] Kaharman N. *Azgyndalghan giperbolalyk tendeler ushin zhalpy reguljarly shettik esepter* [Generalized regular boundary value problems for degenerate hyperbolic equations], Almaty, Gylym Ordasy MMMI KazNU, (2023): 77 p. (in Kazakh).
- [6] Dezin A.A. *Differentsial'no-operatornyye uravneniya. Metod model'nyh operatorov v teorii granichnyh zadach* [Differential operator equations. Method of model operators in the theory of boundary value problems], Trudy MIAN, 229, MAIK Nauka/Interperiodika, M.- Nauka, (2000): 176 p. (in Russian).
- [7] Alabau-Boussouira F., Cannarsa P., Leugering G. *Control and stabilization of degenerate wave equations* // SIAM J.Control Optim., 55:3 (2017): 2052-2087.
- [8] Cannarsa P., Martinez P., Urbani C. *Bilinear control of a degenerate hyperbolic equation* // arXiv: 21112.00636v1 [math.AP] 1 Dec (2021): 65 p.
- [9] Cannarsa P., Martinez P., Vancostenoble J. *The cost of controlling strongly degenerate parabolic equations* // ESAIM: Control, Optimization and Calculus of Variations, 26:2 (2020): 1-50.
- [10] Cannarsa P., Martinez P., Vancostenoble J. *Global Carleman estimates for degenerate parabolic operators with applications*, Memoirs of the AMS. Volume 239, number 1133. (2016). 225p.
- [11] Cannarsa P., Martinez P., and Vancostenoble J. *The cost of controlling weakly degenerate parabolic equations by boundary controls* // Math. Control Relat. Fields, 7(2),(2017): 171-211.
- [12] Hussein M.S., Lesnic D., Kamynin V.L., Kostin A.B. *Direct and inverse source problems for degenerate parabolic equations* // J. of Inverse and Ill-Posed Problems, 28(3), (2020): 425-448.
- [13] Zajcev V.F., Poljanin A.D. *Spravochnik po obyknovennym differentsial'nyim uravnenijam* [Handbook of Ordinary Differential Equations], - M.:FizMatLit, (2001): 576 p. (in Russian).
- [14] *Handbook of Mathematical Functions with Formulas, Graphs, and Mathematical Tables. Tenth Printing, with corrections* (Edited M. Abramovitz and I.A. Stegun) – Washington: National Bureau of Standards, (1972): XIV+1046 p.

IRSTI 27.03.19

DOI: <https://doi.org/10.26577/JMMCS202412114>**A. Kabulov^{1*}**, **A. Baizhumanov²**, **M. Berdimurodov¹**¹Mirzo Ulugbek National University of Uzbekistan, Uzbekistan, Tashkent²O. Zhanibekov South Kazakhstan State Pedagogical University, Kazakhstan, Shymkent

*e-mail: Anvarkabulov1952@gmail.com

ON THE MINIMIZATION OF k -VALUED LOGIC FUNCTIONS IN THE CLASS OF DISJUNCTIVE NORMAL FORMS

In the world, research devoted to adjusting the results of heuristic methods based on forecasting, recognition, classification, and determining the absolute extremum of a multidimensional function is relevant and widely used in such fields as medicine, geology, hydrology, management, and computer technology. In this regard, it is important to construct optimal correctors of heuristic algorithms based on control materials. Therefore, checking the completeness of classes of k -valued logical functions and developing methods and algorithms for minimizing functions in the class of canonical normal forms, estimating the number of monotonic functions of k -valued logic, constructing minimal bases of special classes of correcting functions for correcting incorrect algorithms remains one of the important problems of computational and discrete science. mathematics. Currently, a lot of scientific research is being carried out around the world aimed at expanding the integration of science and industry, in particular the development of the theory of k -valued logical functions for correcting the results of heuristic algorithms. In this case, an important role is played by the construction of formulas in the class of canonical normal forms, the coding of elementary conjunctions and the application of the rules of gluing, absorption and idempotency for them, and checking the completeness of systems of correcting functions. Consequently, the development of effective numerical computational methods and algorithms for constructing correction functions based on k -valued logic to improve the accuracy of the results of heuristic methods is considered a targeted scientific research. The paper considers the representation of k -valued logical functions in the class of disjunctive normal forms. Various classes of monotone functions of k -valued logic are studied. Theorems are proved on the coincidence of abbreviated and shortest disjunctive normal forms of k -valued functions. For a certain class of k -valued monotone functions, we prove an estimate for the number of functions from this class. criteria for the absorption of elementary conjunctions by a first-order neighborhood of disjunctive normal forms of k -valued functions are proved.

Key words: k -valued, minimization, disjunctive normal form, rank, abbreviated d.n.f., monotone function.

А. Кабулов^{1*}, А. Байжуманов², М. Бердимуродов¹¹Мирзо Улугбек атындағы Өзбекстан Ұлттық университеті, Өзбекстан, Ташкент қ.²Ө. Жәнібеков атындағы Оңтүстік Қазақстан мемлекеттік педагогикалық университеті, Қазақстан, Шымкент қ.

*e-mail: Anvarkabulov1952@gmail.com

Дизъюнктивті нормалды формалар класындағы k -мәнді логикалық функцияларды минимизациялау туралы

Әлемде көп өлшемді функцияның абсолютті экстремумын болжау, тану, жіктеу және анықтау негізінде эвристикалық әдістердің нәтижелерін түзетуге арналған зерттеулер өзекті және медицина, геология, гидрология, менеджмент және компьютерлік технологиялар сияқты салаларда кеңінен қолданылады. Осыған байланысты бақылау материалдары негізінде эвристикалық алгоритмдердің оңтайлы корректорларын құру маңызды. Сондықтан k -мәнді логикалық функциялар кластарының толықтығын тексеру және канондық қалыпты формалар класындағы функцияларды минимизациялау әдістері мен алгоритмдерін әзірлеу,

k -мәнді логиканың монотонды функцияларының санын бағалау, арнайы функциялардың минималды негіздерін құру, қате алгоритмдерді түзетуге арналған түзету функцияларының кластары есептеу және дискретті математиканың маңызды мәселелерінің бірі болып қала береді. Қазіргі уақытта бүкіл әлемде ғылым мен өндірістің интеграциясын кеңейтуге бағытталған көптеген ғылыми зерттеулер жүргізілуде, атап айтқанда эвристикалық алгоритмдердің нәтижелерін түзету үшін k -мәнді логикалық функциялар теориясын жасауға бағытталған. Бұл жағдайда канондық қалыпты формалар класындағы формулаларды құру, элементар қосылыстарды кодтау және олар үшін желімдеу, сіңіру және идемпотенттілік ережелерін қолдану, түзету жүйелерінің толықтығын тексеру маңызды рөл атқарады. функциялары. Демек, эвристикалық әдістердің мен алгоритмдерін жасау мақсатты ғылыми зерттеу болып саналады. Жұмыста k -мәнді логикалық функциялардың дизъюнктивтік қалыпты формалар класында ұсынылуы қарастырылады. k -мәнді логиканың монотонды функцияларының әртүрлі кластары зерттеледі. k -мәнді функциялардың қысқартылған және ең қысқа дизъюнктивтік қалыпты түрлерінің сәйкестігі туралы теоремалар дәлелденген. k -мәнді монотонды функциялардың белгілі бір класы үшін біз осы сыныптағы функциялар санының болжамын дәлелдейміз. k -мәнді функциялардың дизъюнктивтік қалыпты формаларының бірінші ретті көршілестігімен элементар қосылыстарды жүту критерийлері дәлелденді.

Түйін сөздер: k -мәнді, минимизация, дизъюнктивтік қалыпты форма, ранг, қысқартылған д.к.ф., монотонды функция.

А. Кабулов^{1*}, А. Байжуманов², М. Бердимуродов¹

¹Национальный университет Узбекистана имени Мирзо Улугбека, Узбекистан, г. Ташкент

²Южно-Казахстанский государственный педагогический университет имени У. Жанибекова,

Казахстан, г. Шымкент

*e-mail: Anvarkabulov1952@gmail.com

О минимизации k -значных логических функций в классе дизъюнктивных нормальных форм

В мире исследования, посвященные корректировке результатов эвристических методов на основе прогнозирования, распознавания, классификации, определения абсолютного экстремума многомерной функции, актуальны и широко используются в таких областях, как медицина, геология, гидрология, менеджмент, вычислительной технике. В связи с этим важно построение оптимальных корректоров эвристических алгоритмов на основе контрольных материалов. Поэтому проверка полноты классов k -значных логических функций и разработка методов и алгоритмов минимизации функций в классе канонических нормальных форм, оценка количества монотонных функций k -значной логики, построение минимальных базисов специальных классов корректирующих функций для корректировки некорректных алгоритмов остается одной из важных задач вычислительной и дискретной математики. В настоящее время в мире проводится много научных исследований, направленных на расширение интеграции науки и промышленности, в частности развитие теории k -значных логических функций для коррекции результатов эвристических алгоритмов. При этом важную роль играет построение формул в классе канонических нормальных форм, кодирование элементарных конъюнкций и применение для них правил склеивания, поглощения и идемпотентности, проверка полноты систем корректирующих функций. Следовательно, разработка эффективных численных вычислительных методов и алгоритмов построения корректирующих функций на основе k -значной логики для повышения точности результатов эвристических методов считается целевым научным исследованием. В работе рассматривается представление k -значных логических функций в классе дизъюнктивных нормальных форм. Исследуются различные классы монотонных функций k -значной логики. Доказываются теоремы о совпадении сокращенных и кратчайших дизъюнктивных нормальных форм k -значных функций. Для определенного класса k -значных монотонных функций доказывается оценка числа функций из этого класса. Доказываются критерии поглощения элементарных конъюнкций окрестностью первого порядка дизъюнктивных нормальных форм k -значных функций.

Ключевые слова: k -значная, минимизация, дизъюнктивная нормальная форма, ранг, сокращенная д.н.ф., монотонная функция.

The function $f_\gamma(\tilde{x})$, which takes only two values (0 and γ), will be called quasi-Boolean, and the representation of the function $f(x_1, \dots, x_n)$ in the form of a (2)-quasi-Boolean representation of the multi-valued logical function $f(x_1, \dots, x_n)$.

We introduce the function

$$J_M(x) = \begin{cases} k-1, & \text{if } x \in M \\ 0, & \text{if } x \notin M \end{cases}, \text{ where}$$

$$M \subseteq E_k = \{0, 1, 2, \dots, k-1\} \quad (3)$$

An elementary conjunction (e.c.) is an expression

$$\mathfrak{A} = \min[J_{M_1}(x_1), \dots, J_{M_n}(x_n), \gamma], \text{ where}$$

$$\emptyset \neq M_j \subseteq E_k, (j = \overline{1, n}) \quad (4)$$

Further, for brevity, formulas $\max[\mathfrak{A}_1, \dots, \mathfrak{A}_m]$ will be conventionally denoted as $\mathfrak{A}_1 \vee \dots \vee \mathfrak{A}_m = \bigvee_{i=1}^m \mathfrak{A}_i$: if \mathfrak{A}_i is an analog of e.c., then this formula will be called disjunctive normal form (d.n.f.).

The area of truth of e.c. let's call \mathfrak{A} the region $N_{\mathfrak{A}}$ in which \mathfrak{A} takes the value γ . It is easy to see that the domain $N_{\mathfrak{A}} = \prod_{j=1}^n M_j$ is a sub lattice (a subset of the set E_n^k) of the lattice E_n^k .

With such a geometric consideration, the e.c. the sub lattice $N_{\mathfrak{A}}$ corresponds to the lattice E_n^k .

$$\text{Rank e.c. let's } \mathfrak{A} \text{ call a number } r(\mathfrak{A}) = \sum_{j=1}^n (k - |M_j|) = kn - \sum_{j=1}^n |M_j|.$$

The formula $\mathfrak{M} = \bigvee_{i=1}^t \mathfrak{A}_i$ where all $\mathfrak{A}_i, (i = \overline{1, t})$ are e.c. will be called the disjunctive normal form.

Note that each set-valued logic function $f(x_1, \dots, x_n)$ corresponds to a non-empty class of d.n.f. realizing the given function. The set of all intervals corresponding to e.c. a certain d.n.f. from this class determines the covering of N_f by sub lattices of the lattice E_n^k . Hence it follows that the subsets $M \subseteq E_n^k$ can be defined using the d.n.f.

Let $I = \{N_{\mathfrak{A}}\}$, be some subset of sub lattices from E_n^k .

A sub lattice $N_B \in I$ is said to be maximal with respect to M if there is no sub lattice $N_{\mathfrak{A}}$ in I such that $N_{\mathfrak{A}} \neq N_B$ and $N_{\mathfrak{A}} \supseteq N_B$.

To represent the function $f(x_1, \dots, x_n)$ in the form of a d.n.f. we considered its quasi-Boolean representation: $f = f_{\gamma_1} \vee \dots \vee f_{\gamma_m}$ and $\gamma_1 < \gamma_2 < \dots < \gamma_m$.

Note that for the same function $f(\tilde{x})$ there can be several equivalent quasi-Boolean representations. Indeed, $f = f_{\gamma_1} \vee \dots \vee f_{\gamma_m} = f^* = f_{\gamma_1}^* \vee \dots \vee f_{\gamma_m}^*$ where $N_{f_{\gamma_i}^*} = N_{f_{\gamma_i}} \cup Q_i$, $Q_i \subseteq \bigcup_{j>i} N_{\gamma_j}, (i = \overline{1, m})$.

We will consider only one "maximum" representation $f' = f'_{\gamma_1} \vee \dots \vee f'_{\gamma_m}$ where $N_{f'_{\gamma_i}} = \bigcup_{j=1}^n N_{f_{\gamma_j}}, (i = \overline{1, m})$.

Select all maximal sub lattices $N_{B_j^i}, (i = \overline{1, m})$ contained in $N_{f'_{\gamma_i}}$ that have non-empty intersection with $N_{f_{\gamma_i}}$ and such that the value of B_j^i is equal to γ_i in $N_{B_j^i}, (i = \overline{1, m})$. D.n.f.

$$\mathfrak{M} = \bigvee_{i=1}^m \bigvee_{j=1}^{I_i} B_j^i \text{ is called the reduced disjunctive normal form of the function } f(\tilde{x}).$$

A covering of a set N_f by maximal sub lattices is said to be irreducible if, after the removal of any of its sub lattices, it ceases to be a covering. A d.n.f. realizing a function f is called dead-end if it corresponds to an irreducible cover of the set N_f .

Consider a multivalued logic function $F(x_1, \dots, x_n)$ defined at $M \subseteq E_n^k : F(\tilde{x}) = \gamma_j$, if $\tilde{x} \in M_j$, ($j = \overline{1, m}$), $m < k$, $\gamma_j \in E_k$, $M = \bigcup_{i=0}^m M_i$ and $M_i \cap M_j = \emptyset$ at ($i \neq j$, $i, j = \overline{0, m}$). And $\gamma_1 < \dots < \gamma_m$, $\gamma_0 = 0$.

Thus, $F(x_1, \dots, x_n)$ is defined by specifying pairwise disjoint sets M_0, \dots, M_m . The function $F(\tilde{x})$ is defined, generally speaking, not on the entire set E_n^k . There are different before the definition in the class of functions $F(\tilde{x})$, multi-valued logic, not equivalent to each other.

Our task is to find the simplest ones, in a certain sense, before definitions.

For $F(\tilde{x})$, select all maximal intervals $N_{B_j^i}$, ($i = \overline{1, m}$, $j = \overline{0, I_i}$) contained in $E_n^k \setminus \bigcup_{v=0}^{i-1} M_v$ that have non-empty intersection with M_i such that the value of B_j^i is equal to γ_i .

D.n.f. $\mathfrak{M} = \bigvee_{i=1}^m \bigvee_{j=1}^{I_i} B_j^i$ is called the reduced normal form for $F(\tilde{x})$. It is easy to see that d.n.f. $\eta_{\Sigma TF}$ is uniquely determined by the function F .

Let us now indicate the points at which, when the values of the function F change (transition to F'), the values of $\eta_{\Sigma TF}$ change (transition to $\eta_{\Sigma TF'}$).

3 Monotone functions of k -valued logic

Let's consider some order on the set ε_k . For two sets $\mathfrak{S} = (\alpha_1, \alpha_2, \dots, \alpha_n)$ and $\tilde{\beta} = (\beta_1, \beta_2, \dots, \beta_n)$ the precedence relation $\mathfrak{S} \leq \tilde{\beta}$ is satisfied if $\alpha_i \leq \beta_i$ in this order for any $i = \overline{1, n}$.

Definition 1. A k -valued logic function $f(x_1, x_2, \dots, x_n)$ is said to be monotonic with respect to a given order if for any tuples α and β such that ($\mathfrak{S} \leq \tilde{\beta}$) we have $f(\alpha) \leq f(\beta)$.

If $0 < 1 < 2 < \dots < k - 1$, then the set of functions that are monotone in this order constitutes the class of monotone functions of k -valued logic.

Theorem 1. Abbreviated d.n.f. monotone function f_γ of k -valued logic in n variables

a) consists of e.c. K^A , and only elementary formulas of the form $J_{[a, k-1]}(x)$, $0 \leq a \leq k - 1$ are used;

b) Is the only minimal (shortest) d.n.f. of the function f .

Proof.

a) Let $K = J_{T_1}(x_1) \cdot J_{T_2}(x_2) \cdot \dots \cdot J_{T_n}(x_n) \cdot \gamma$, where $T_j = [a_j, k - 1]$, $j \neq i$, $0 \leq a_j \leq k - 1$, $T_i = [b_i] \cup [a_i, k - 1]$, $b_i \leq a_i$.

Then the conjunction K , and hence the function f_γ , takes the value γ on the set $\tilde{a} = (a_1, a_2, \dots, a_{i-1}, a_i, a_{i+1}, \dots, a_n)$.

b) It follows from the monotonicity condition for the function f_γ that for any set \tilde{b} such that $\tilde{b} \geq \tilde{a}$, $f_\gamma(\tilde{b}) = \gamma$ therefore, there exists an e.c. $K' = J_{T'_1}(x_1) \cdot J_{T'_2}(x_2) \cdot \dots \cdot J_{T'_n}(x_n) \cdot \gamma$, where $T'_j = T_j$, $j \neq i$, $T'_i = [b_i, k - 1]$, for which $U_K \subset U_{K'} \subseteq U_{f_\gamma}$, and e.c. K is not maximal for U_{f_γ} .

c) As proved, each maximum e.c. K functions has the form $K = J_{[a_1, k-1]}(x_1) \cdot J_{[a_2, k-1]}(x_2) \cdot \dots \cdot J_{[a_n, k-1]}(x_n) \cdot \gamma$, $0 \leq a_j \leq k-1$, $j = \overline{1, n}$.

Let us show that the set $\tilde{a} = (a_1, a_2, \dots, a_n)$ is core for the function f_γ , etc. in the abbreviated d.n.f. the function f_γ has no e.c., except for K , which takes the value γ on this set.

Indeed, if in the reduced d.n.f. function f_γ was an e.c. K' , which takes the values γ on the tuple \tilde{a} , then it would follow from the monotonicity condition for the function f_γ that the e.c. K' takes the value γ on all tuples \tilde{b} such that $\tilde{b} \geq \tilde{a}$, then $U_K \subseteq U_{K'}$, which contradicts the maximum e.c. K .

The theorem is proved.

Corollary. Abbreviated d.n.f. monotone function f of k -valued logic in n variables consists of e.c. K^A and is the only minimal d.n.f. functions f .

Proof. A monotone function f has the following obvious properties: for any comparable collections $\tilde{a} \in N_{f_\gamma}$ and $\tilde{b} \in N_{f_\theta}$ we have $\tilde{b} > \tilde{a}$ for $\gamma < \theta$. Therefore, e.c. K , is included in the abbreviated d.n.f. functions f_γ ($\gamma \in \{\varepsilon_k/0\}$) do not contain elementary formulas of type $J_T(x)$, where the set T is a disconnected set of points from ε_k .

The second assertion is proved by the method of theorem 1, and the core sets for the function f are the sets $\tilde{a} = (a_1, a_2, \dots, a_n)$ in the e.c. $K = J_{[a_1, b_1]}(x_1) \cdot J_{[a_2, b_2]}(x_2) \cdot \dots \cdot J_{[a_n, b_n]}(x_n) \cdot \gamma$.

Corollary proven. On the set ε_k we introduce a partial order $0 < 1, 0 < 2, \dots, 0 < k-1$ where i is incomparable with j if $i, j \in \{\varepsilon_k/0\}$.

The set of functions of k -valued logic f in n variables, monotone in a given order, is combined into the class S . Let us estimate the cardinality of the class S .

The set ε_k is associated with a basic graph - a directed graph with K vertices corresponding to the elements of the set ε_k , in which there is an arc (i, j) if and only if $i > j$.

Let us introduce the Z axis on the plane. Associate each point A of the plane with the number Z_A , the projection of A onto the Z axis. In particular, if the basis graph is drawn on the plane, then each vertex corresponds to the number Z_i . An image of a basic graph is called admissible if for any arc (i, j) of the graph $Z_i - Z_j \geq 1$.

Consider a random variable $\xi = Z_A$, where the point A can fall into any vertex of the graph with probability $\frac{1}{k}$ then the expectation is $M\xi = Z_{cp} = \frac{Z_1 + \dots + Z_k}{k}$ and the variance is

$$D\xi = \frac{1}{k} \sum_{i=1}^k (Z_i - Z_{cp})^2.$$

We will consider the image of the graph shifted so that $M\xi = 0$.

In older articles an estimate is obtained for finding the number $\psi(n)$ of monotone functions of n variables from an arbitrary partially ordered set of k elements:

$$\psi(n) = d^{\frac{1}{\sqrt{2\pi D}} \cdot \frac{k^n}{\sqrt{n}} (1 + \varepsilon(n))} \quad (5)$$

where $\varepsilon(n) \rightarrow 0$ at $n \rightarrow \infty$; $D = \inf D\xi$; $d = \max(|H_1|, \dots, |H_s|)$, $H_0 \leq H_1 \leq \dots \leq H_{s+1}$, all $H_i \subseteq \varepsilon_k$, $s \geq 1$, $|H_0| = |H_{s+1}| = 1$ and $H_i \neq H_j$, at $i \neq j$ ($H_i \leq H_j$ if $a \leq b$ for any $a \in H_i$, $b \in H_j$), the maximum is taken over all possible chains. This estimate is also valid for the class of functions S .

For the order in ε_k we have:

$$\begin{cases} Z_1 - Z_0 \geq 1 \\ \dots \dots \dots \\ Z_{k-1} - Z_0 \geq 1 \end{cases} \quad (6)$$

$$Z_{cp} = \frac{Z_0 + Z_1 + \dots + Z_{k-1}}{k} = 0, \quad D\xi = \frac{1}{k} \sum_{i=0}^{k-1} Z_i^2 \quad (7)$$

It follows that $Z_0 \leq -\frac{k-1}{k}$ and $Z_i \geq \frac{1}{k}$, $i = \overline{1, k-1}$, so $D\xi \geq \frac{k-1}{k^2}$ and $D \geq \frac{k-1}{k^2}$.

On the set ε_k for the introduced order there is only $(k-1)$ chain

$$\begin{cases} \{0\} < \{0, 1\} < \{1\} \\ \dots \dots \dots \\ \{0\} < \{0, k-1\} < \{k-1\} \end{cases} \quad (8)$$

It is obvious that in the considered case $d = 2$.

Consequently

$$\left\{ \psi(n) = d^{\frac{1}{\sqrt{2\pi(k-1)}} \cdot \frac{k^{n+1}}{\sqrt{n}} (1+\varepsilon(n))} \right. \quad (9)$$

where $\varepsilon(n) \rightarrow 0$ at $n \rightarrow \infty$.

For functions of class S , e.c. consists of elementary formulas of the form $J_T(x)$, where $T \subseteq \{\varepsilon_k/0\}$.

If for monotone functions f of k -valued logic the abbreviated d.n.f. is the only minimal one, then for functions of the class S this property does not hold, which is demonstrated by the following.

Example. $k = 3$, $n = 3$.

Let the function $f(x_1, x_2, x_3)$ take the values 1 on the sets $(0, 1, 1)$, $(1, 1, 1)$, $(1, 2, 1)$, $(2, 1, 1)$, $(1, 2, 2)$ and 0 in other cases.

Abbreviated d.n.f. function f has the form:

$$D_C(f) = J_1(x_2) \cdot J_1(x_3) \vee J_1(x_1) \cdot J_2(x_2) \cdot J_{[1,2]}(x_3) \quad (10)$$

and the minimum:

$$D_M(f) = J_1(x_2) \cdot J_1(x_3) \vee J_1(x_1) \cdot J_{[1,2]}(x_2) \cdot J_1(x_3) \quad (11)$$

The process of transition from the abbreviated d.n.f. functions f of a k -valued logic to a dead-end one can be divided into elementary steps, each of which is a removal from the d.n.f.

D obtained in the previous step, one e.c. K . Removed e.c. is such that $U_K \subseteq \bigcup_{j=1}^m U_{K_j}$, where

K_j are some e.c. from d.s.f. D different from K .

In older articles the criterion for covering an interval by the sum of other intervals for functions f of k -valued logic is described. For functions f of class S , this criterion has a simpler form.

E.c. K_1 and K_2 are called orthogonal if $K_1 \cdot K_2 = 0$. In other words, conjunctions K_1 and K_2 are orthogonal if and only if $U_{K_1} \cap U_{K_2} = \emptyset$. Obviously, when studying the absorption, some sets of e.c. $\{K_j\}$, $j = \overline{1, m}$ e.c. K it suffices to consider only those e.c. that are non-orthogonal to K . To check orthogonality, it is easiest to use the following properties: two e.c. are orthogonal if and only if there exists a variable x_j for which $T_j^1 \cap T_j^2 = \emptyset$ is satisfied in the elementary formulas $J_{T_j^1}(x_1)$ and $J_{T_j^2}(x_2)$.

D.n.f. D realizing the function f absorbs the e.c. K if $K(\tilde{x}) \leq D(\tilde{x})$ for any $\tilde{x} = \varepsilon_k^n$.

So let $K = J_{T_1}(x_1) \cdot J_{T_2}(x_2) \cdot \dots \cdot J_{T_t}(x_t) \cdot \gamma$.

Obviously, K can be absorbed only by those sets of e.c. $\{K_j\}$, which take values from $\{0, \gamma\}$, so let's consider the absorption process using the example of the quasi-Boolean function f_γ .

For each e.c. $\{K_j\}$, $j = \overline{1, m}$ construct an e.c. K_j , replacing the elementary formulas $J_T(x)$ occurring in K_j with $J_{[1, k-1]}(x)$.

It's obvious that $U_{K_j} \subseteq U_{K_j}$, $U_{K_j} \cap (U_D/U_{K_j}) = \emptyset$.

Let us introduce into consideration the set $\varepsilon_k^{n,t}$ - the collection of all sets from ε_k^n , in which the t first coordinates take values from $\{\varepsilon_k/0\}$, and the rest are arbitrary.

Theorem 2. The disjunction $D = \bigvee_{j=1}^m K_j$ absorbs the e.c. K if and only if $\bigvee_{j=1}^m K_j = \gamma$ for any $\tilde{x} = \varepsilon_k^{n,t}$, etc. if $\bigvee_{j=1}^m K_j = \varepsilon_k^{n,t}$.

Proof. *Need.* Let D absorb the e.c. K . Let us prove that in this case $\bigvee_{j=1}^m K_j = \gamma$ for any $\tilde{x} = \varepsilon_k^{n,t}$. Let us assume that this is not the case, etc. there is a collection \mathfrak{S} such that $\bigvee_{j=1}^m K_j(\mathfrak{S}) = 0$. Denote by x_{i_1}, \dots, x_{i_p} the variables that are not included in any of the e.c. from D . Obviously, the values of the remaining variables do not affect the value of the expression $\bigvee_{j=1}^m K_j$.

The value of the function f on the tuples \mathfrak{S} will be denoted by $[f]\mathfrak{S}$. Then one can write

$$\left[\bigvee_{j=1}^m K_j \right] \{\mathfrak{S}\} = 0 \quad (12)$$

where $\{\mathfrak{S}\}$ is the set of sets whose (x_1, x_2, \dots, x_t) coordinates take all possible values from $\{\varepsilon_k/0\}$, and the remaining $(n-t)$ coordinates are such that (12) is satisfied. hence we get that $[K_j]\{\mathfrak{S}\} = 0$ for all $j = \overline{1, m}$, so $[D]\mathfrak{S} = 0$.

Let us determine the values of the remaining variables entering K ($K \neq 0$ on U_D , since K is not orthogonal to D) so that K turns into γ on these sets. The intersection of these two sets determines the values of all variables in such a way that D takes the value 0 on this set, and e.c. K value γ . This contradicts the condition $K(\tilde{x}) \leq D(\tilde{x})$ for any $\tilde{x} = \varepsilon_k^n$, hence the assumption that $\bigvee_{j=1}^m K_j \neq \gamma$ on $\varepsilon_k^{n,t}$ is false, and the necessity of the condition of the theorem is proved.

Adequacy. Let the condition of the theorem be satisfied etc., $\bigcup_{j=1}^m U_{K_j} = \varepsilon_k^{n,t}$. Then $U_K \subseteq$

$$\bigcup_{j=1}^m U_{K_j}, \text{ but } U_K \cap \left(\bigcup_{j=1}^m U_{K_j} / \bigcup_{j=1}^m U_{K_j} \right) = \emptyset. \text{ Consequently, } U_K \subseteq \bigcup_{j=1}^m U_{K_j}.$$

The theorem has been proven.

4 Conclusions

The paper proposes a representation of k -valued functions in the class of disjunctive normal forms. Monotone functions of k -valued logic are investigated. We prove theorems on the coincidence of abbreviated and shortest d.n.f. k -valued functions. For a certain class of k -valued monotone functions, the number of functions from this class is calculated. Criteria for the absorption of elementary conjunctions by a first-order neighborhood are proposed.

References

- [1] A. Kabulov, I. Yarashov, A. Otakhonov Algorithmic Analysis of the System Based on the Functioning Table and Information Security // 2022 IEEE International IOT, Electronics and Mechatronics Conference (IEMTRONICS), Toronto, ON, Canada, 2022, pp. 1-5, doi: 10.1109/IEMTRONICS55184.2022.9795746.
- [2] A. Kabulov, I. Saymanov, I. Yarashov, A. Karimov Using Algorithmic Modeling to Control User Access Based on Functioning Table // 2022 IEEE International IOT, Electronics and Mechatronics Conference (IEMTRONICS), Toronto, ON, Canada, 2022, pp. 1-5, doi: 10.1109/IEMTRONICS55184.2022.9795850.
- [3] E. Navruzov, A. Kabulov Detection and analysis types of DDoS attack // 2022 IEEE International IOT, Electronics and Mechatronics Conference (IEMTRONICS), Toronto, ON, Canada, 2022, pp. 1-7, doi: 10.1109/IEMTRONICS55184.2022.9795729.
- [4] A. Kabulov, I. Saymanov, I. Yarashov and F. Muxammadiev Algorithmic method of security of the Internet of Things based on steganographic coding // 2021 IEEE International IOT, Electronics and Mechatronics Conference (IEMTRONICS), Toronto, ON, Canada, 2021, pp. 1-5, doi: 10.1109/IEMTRONICS52119.2021.9422588.
- [5] A. Kabulov, I. Normatov, E. Urumbaev, F. Muhammadiev Invariant Continuation of Discrete Multi-Valued Functions and Their Implementation // 2021 IEEE International IOT, Electronics and Mechatronics Conference (IEMTRONICS), Toronto, ON, Canada, 2021, pp. 1-6, doi: 10.1109/IEMTRONICS52119.2021.9422486.
- [6] A. Kabulov, I. Normatov, A. Seytov, A. Kudaybergenov Optimal Management of Water Resources in Large Main Canals with Cascade Pumping Stations // 2020 IEEE International IOT, Electronics and Mechatronics Conference (IEMTRONICS), Vancouver, BC, Canada, 2020, pp. 1-4, doi: 10.1109/IEMTRONICS51293.2020.9216402.
- [7] Kabulov, A. V., Normatov, I. H. (2019). About problems of decoding and searching for the maximum upper zero of discrete monotone functions // Journal of Physics: Conference Series, 1260(10), 102006, 2019. doi:10.1088/1742-6596/1260/10/102006.
- [8] Kabulov, A. V., Normatov, I. H., Ashurov A.O. Computational methods of minimization of multiple functions // Journal of Physics: Conference Series, 1260(10), 10200, 2019. doi:10.1088/1742-6596/1260/10/102007.
- [9] Anvar Kabulov, Alimdzhhan Babadzhanov, Islambek Saymanov Correct models of families of algorithms for calculating estimates // AIP Conference Proceedings 8 June 2023; 2781 (1): 020010. <https://doi.org/10.1063/5.0144830>.
- [10] Anvar Kabulov, Alimdzhhan Babadzhanov, Islambek Saymanov Completeness of the linear closure of the voting model // AIP Conference Proceedings 8 June 2023; 2781 (1): 020020. <https://doi.org/10.1063/5.0144832>.
- [11] Anvar Kabulov, Mansur Berdimurodov Gost R 34.12-2015 (Kuznechik) analysis of a cryptographic algorithm // AIP Conference Proceedings 8 June 2023; 2781 (1): 020046. <https://doi.org/10.1063/5.0145975>.
- [12] Valeri Sklyarov, Iouliia Skliarova, Anvar Kabulov Hardware accelerators for solving computationally intensive problems over binary vectors and matrices // AIP Conference Proceedings 8 June 2023; 2781 (1): 020013. <https://doi.org/10.1063/5.0145125>.
- [13] Preface: International Conference on Modern Problems of Applied Mathematics and Information Technology // AIP Conference Proceedings 8 June 2023; 2781 (1): 010001. <https://doi.org/10.1063/12.0017180>.
- [14] Normatov I. Principle of Independence of Continuation of Functions Multivalued Logic from Coding // Journal of Physics: Conference Series, 2019, 1210(1), 012107. doi:10.1088/1742-6596/1210/1/012107.
- [15] I. Normatov, E. Kamolov Development of an algorithm for optimizing the technological process of kaolin enrichment // 2020 IEEE International IOT, Electronics and Mechatronics Conference (IEMTRONICS), Vancouver, BC, Canada, 2020, pp. 1-4, doi: 10.1109/IEMTRONICS51293.2020.9216371.

IRSTI 27.35.14, 27.35.21

DOI: <https://doi.org/10.26577/JMMCS202412115>**B.E. Kanguzhin^{1,2}** , **Zh.A. Kaiyrbek^{1,2*}** , **B. Uaissov³** ¹Al-Farabi Kazakh National University, Kazakhstan, Almaty²Institute of Mathematics and Mathematical Modeling, Kazakhstan, Almaty³Academy of logistics and transport, Kazakhstan, Almaty

*e-mail: kaiyrbek.zhalgas@gmail.com

IN ONE SCENARIO, THE DEVELOPMENT OF A DEFECT IN THE ATTACHMENT OF THE ROD

This article discusses the issue of the origin of a rod fastening defect. At the beginning of operation, the rod is rigidly fixed at the edges. During operation, over time, certain defects may appear at the ends of the rod. We need to find out what defects may occur? Then it is necessary to trace the further behavior of the emerging defects at the ends of the rod. This paper discusses the diagnostics of types of fastening of a structure made of interconnected rods. In this work, the state of fastening types in individual parts of the structure is determined and a number of results are obtained using mathematical analysis. Most of them assume how failures begin at the end connections of the rods, and then the scenario for their further development. Mathematical models are presented to determine the state of the rod attachments relative to the proposed scenario, and then the state in which they are in is carefully examined. Defects in fastening objects made from a system of rods are investigated using identification problems. The difference between this article and other works is that instead of the shape of the area, the size of the object, or the state of its location, defects that occur in fasteners are studied. This work is devoted to the search for types of fastening that provide the required range of vibration frequencies.

Key words: Euler-Bernoulli equation, rod, defect, Taylor formula.

Б.Е. Кангузин^{1,2}, **Ж.А. Қайырбек^{1,2*}**, **Б. Уайсов³**¹Әл-Фараби атындағы Қазақ ұлттық университеті, Қазақстан, Алматы қ.²Математика және математикалық модельдеу институты, Қазақстан, Алматы қ.³Логистика және көлік академиясы, Қазақстан, Алматы қ.

*e-mail: kaiyrbek.zhalgas@gmail.com

Стержень бекітуіндегі ақаудың пайда болып дамуының сценарийі туралы

Бұл мақалада стерженьдердің ақауының шығу тегі туралы мәселе қарастырылады. Жұмыстың басында стержень ұштарында қатаң бекітіледі. Уақыт өте келе стержень ұштарында белгілі бір ақаулар пайда болуы мүмкін. Бізге қандай ақаулар пайда болуы мүмкін екенін анықтау керек? Содан кейін стержень ұштарында пайда болатын ақаулардың одан әрі әрекеті туралы айтылады. Осы жұмыста өзара байланысқан стерженьдерден құралған конструкцияның бекіту түрлеріне диагностика жасау қарастырылған. Бұл жұмыста конструкцияның жеке бөлшектерінде бекіту түрлерінің ақуалы анықталды және бірқатар нәтижелер математикалық жолмен талдау арқылы алынған. Олардың көбі стерженьдердің шеттік бекітулерінде ақау қалай басталады және одан кейін олар ары қарай қандай сценаримен дамтыны ұсынылған. Ұсынылған сценарийге байланысты стерженьнің шеттік бекітуінің күйін анықтауға математикалық модельдер көрсетілген және одан кейін олар қандай күйде болатыны мұқият зерттелген. Стерженьдер жүйесінен құрастырылған объектілердің бекітуіндегі ақауларын идентификациялау есептері бойынша зерттелінген. Осы мақаланың басқа жұмыстардан өзгешелігі – облыс формасы, объект көлемі немесе орналасу жағдайының орнына бекітулерде пайда болатын ақаулар зерттеледі. Бұл жұмыста тербеліс жиілігінің қажетті диапазонын қамтамасыз ететін бекіту түрлерін іздеу қарастырылады.

Түйін сөздер: Эйлер-Бернулли теңдеуі, стержень, ақау, Тейлор формуласы.

Б.Е. Кангужин^{1,2}, Ж.А. Кайырбек^{1,2*}, Б. Уайсов³

¹Казахский Национальный университет им. аль-Фараби, Казахстан, г. Алматы

²Институт математики и математического моделирования, Казахстан, г. Алматы

³Академия логистики и транспорта, Казахстан, г. Алматы

*e-mail: kaiyrbek.zhalgas@gmail.com

Об одном сценарии зарождения развития дефекта крепление стержня

В данной статье обсуждается вопрос зарождения дефекта крепления стержня. Вначале эксплуатации стержень по краям жестко закреплен. В процессе эксплуатации с течением времени могут появляться те или иные дефекты на концах стержня. Надо выяснить какие дефекты могут возникать? Затем надо проследить дальнейшее поведение возникающего дефектов на концах стержня. В данной работе рассматривается диагностика видов крепления конструкции из соединенных между собой стержней. В данной работе определено состояние типов крепления в отдельных частях конструкции и методом математического анализа получен ряд результатов. Большинство из них предполагают, как начинаются разрушения в концевых соединениях стержней, а затем сценарий их дальнейшего развития. Представлены математические модели для определения состояния крепления стержня относительно предложенного сценария, а затем тщательно изучено, в каком состоянии они находятся. Дефекты крепления объектов, изготовленных из системы стержней, исследуются по задачам идентификации. Отличие данной статьи от других работ состоит в том, что вместо формы области, размера объекта или состоянии его расположения изучаются дефекты, возникающие в креплениях. Данная работа посвящена поиску типов крепления, обеспечивающих необходимый диапазон частот вибрации.

Ключевые слова: Уравнение Эйлера-Бернулли, стержень, дефект, формула Тейлора.

1 Introduction

Acoustic diagnostics is the determination of the technical condition of equipment in working order based on the parameters of vibration processes. Acoustic diagnostic methods are widely used to determine the strength of various materials and the location of incipient, incipient and developing cracks. The acoustic diagnostic method is used to determine the technical condition of a structure in various environments. Acoustic diagnostic methods make it possible to study the structure itself as a whole without dismantling it. This work is devoted to the search for types of fastening that provide the required range of vibration frequencies. Such problems relate to the problems of mathematical acoustics outlined above. Even in this case, it is necessary to identify parameters that describe the state of fixation by natural frequency. More precisely, the diagnostics of the states of the edge fastenings of the rods based on the frequencies of transverse vibrations is considered.

Transverse oscillations of the rod are described by the Euler-Bernoulli equation [1], which is written in the form

$$\frac{\partial^2}{\partial x^2} \left(EJ \frac{\partial^2 w}{\partial x^2} \right) + A\rho \frac{\partial^2 w}{\partial t^2} = q(x, t) \quad (1)$$

relative to the transverse deflection $w(x, t)$.

Here are E, J, A, ρ standard physical characteristics of the material from which the rod is made. At the beginning, we consider that both ends of the rod are rigidly fixed. This means that relations

$$w(0, t) = 0, \quad \frac{\partial w(0, t)}{\partial x} = 0, \quad w(l, t) = 0, \quad \frac{\partial w(l, t)}{\partial x} = 0$$

are fulfilled. In this case, the length of the rod is chosen equal to l . Over time, defects may appear along the rod. We believe that, first of all, defects can arise at one of the ends of the rod.

A comparative analysis of literary [1–3] sources indicates that it is easier to bend a rod than to stretch it or rotate it around the axis of the rod. The mathematically specified phenomenon is characterized by the asymptotic behavior of $w_1(x, t)$, $w_2(x, t)$ transverse and $w_3(x, t)$ longitudinal deviations in the form of

$$\frac{1}{h^2}(\vec{e}_1 \cdot w_1(x) + \vec{e}_2 \cdot w_2(x)) + \frac{1}{h} \cdot \vec{e}_3(w_3(x) - \eta_1 \frac{\partial}{\partial x} w_1(x) - \eta_2 \frac{\partial}{\partial x} w_2(x)) + \frac{1}{h}(\eta_1 \vec{e}_2 - \eta_2 \vec{e}_1) \quad (2)$$

Here \vec{e}_3 direction is along the rod, and \vec{e}_1, \vec{e}_2 directions are perpendicular to the rod axis [3]. In expression 2 there is also $w_4(x, t)$, which characterizes the torsion around the axis of the rod. Parameter h is also involved here, which characterizes the diameter of the cross section of the rod. Taking into account the above-mentioned effect, given by expression 2, we can now proceed to the study of physical phenomena occurring near the fixed end of the rod.

2 Methods and materials

2.1 The scenario of the occurrence and development of defects at the point of attachment of the rod

In this point, one of the possible variants of occurrence at the end points of the rod attachment is attached. The scenario consists of four stages of emergence and development of a defect at one end of a rod. The defect at the point of attachment of the rod undergoes the following stages. At the beginning, the end of the rod is rigidly fixed, then during the operation of the rod, the conditions of rigid fixation of the rod are weakened due to the bending moment. The next stage is characterized by the fact that the actions of transverse forces cause "backlash" at the point of attachment. Each stage of the defect corresponds to its own individual frequency of transverse oscillations of the rod. The indicated natural oscillations of the rod can be measured by acoustic means. Thus, based on the measured natural frequencies of the transverse oscillations of the rod, the stage of the defect in the end fixings of the rod can be determined.

Now consider the neighborhood of rod $x = 0$. That is, x is between 0 and h . Then the Taylor formula [4]

$$w(x, t) = w(0, t) + \frac{\partial w(0, t)}{\partial x} x + \frac{1}{2} \frac{\partial^2 w(0, t)}{\partial x^2} x^2$$

$$\frac{\partial w(x, t)}{\partial x} \approx \frac{\partial w(0, t)}{\partial x} + \frac{\partial^2 w(0, t)}{\partial x^2} x + \frac{1}{2} \frac{\partial^3 w(0, t)}{\partial x^3} x^3$$

we use for the rigidly fixed edge $x = 0$, and we get

$$\begin{cases} w(h, t) \approx \frac{1}{2} \frac{\partial^2 w(0, t)}{\partial x^2} h^2 \\ \frac{\partial w(h, t)}{\partial x} \approx \frac{\partial^2 w(0, t)}{\partial x^2} h + \frac{1}{2} \frac{\partial^3 w(0, t)}{\partial x^3} h^3 \end{cases} \quad (3)$$

We know that torque is equal to the theory of elasticity

$$M(0) = -EJ \frac{\partial^2 w(0, t)}{\partial x^2}$$

and is equal to the transverse force

$$Q(0) = EJ \frac{\partial^3 w(0, t)}{\partial x^3}$$

Therefore, from equation 3 the relations are fulfilled

$$\begin{cases} w(h, t) \approx \frac{-h^2}{2EJ} M(0) \\ \frac{\partial w(h, t)}{\partial x} \approx -\frac{h}{EJ} M(0) + \frac{h^3}{2EJ} Q(0) \end{cases}$$

for moment and transverse force [5].

Now we can predict how a defect will appear at edge $x = 0$ of the rod and according to what scenario it will develop.

Let there be at the beginning a rigid fastening of the edge $x = 0$ of the rod

$$w(0, t) = 0, \quad \left. \frac{\partial w(0, t)}{\partial x} \right|_{x=0} = 0. \quad (4)$$

During operation (after some time) conditions

$$w(0, t) = 0, \quad \left. \frac{\partial w(0, t)}{\partial x} \right|_{x=0} = \alpha_1 \frac{\partial^2 w(0, h)}{\partial x^2} \quad (5)$$

are carried out taking into account relation 4. Since h — is small, the following hierarchy

$$h \frac{\partial^2 w(0, t)}{\partial x^2} \gg \frac{h^2}{2} \frac{\partial^2 w(0, t)}{\partial x^2} \gg \frac{h^3}{2} \frac{\partial^3 w(0, t)}{\partial x^3}$$

will be executed. Therefore, we will first consider $h \frac{\partial^2 w(0, t)}{\partial x^2}$, and $\frac{h^2}{2} \frac{\partial^2 w(0, t)}{\partial x^2}$, $\frac{h^3}{2} \frac{\partial^3 w(0, t)}{\partial x^3}$ are very small quantities. That is, it can be considered zero.

Here α_1 is the parameter. In this case, fastening 4 is transferred to condition 5. This is where edge defect $x = 0$ begins to appear. In this case, it shows that the value of $h \frac{\partial^2 w(0, t)}{\partial x^2}$ and $h^3 \frac{\partial^3 w(0, t)}{\partial x^3}$ is very small. Therefore, condition 5 is satisfied. The mechanical meaning of this condition 5 is to take into account the influence of angular momentum $M(0)$ on the value of the angle of inclination $\frac{\partial w(0, t)}{\partial x}$. Therefore, instead of condition 4, condition 5 should be taken into account. If previously there was a rigid mount, now it is necessary to take into account the influence of torque. If you have observed such a situation, then you can continue to use the rod. Due to the impact of torque, the rigid mount was changed to the mount under condition 4, but we continue to operate. At this stage [6], there is no need to stop

using the rods, even though the angle of inclination appears. That is, it does not require repair.

But one thing should be noted: the natural frequencies of horizontal oscillations according to conditions 4 change when the natural frequencies are conditions 5. If we continue to use the rods without repair, then we will call the transition from state 4 to state 5 a level 1 defect and assume that this defect does not yet require repair. So, let us assume that conditions 5 are satisfied at edge $x = 0$. From the asymptotic relations 2, the boundary conditions 5 change to the following conditions:

$$\begin{cases} w(0, t) = \alpha_2 \frac{\partial^2 w(0, t)}{\partial x^2} \\ \frac{\partial w(0, t)}{\partial x} = \alpha_1 \frac{\partial^2 w(0, t)}{\partial x^2} \end{cases} \quad (6)$$

here $0 < \alpha_2 < \alpha_1$. In this case, we consider that a level 2 defect has occurred on edge $x = 0$ in which case the repair time will be reduced. Therefore, the risk is even higher than the previous level. Previously, the degree of destruction varied under the influence of torque. Now we need to take into account the action of the transverse force $Q(0)$. If we take these points into account [7], the rod goes through 4 stages during operation.

3 Conclusion

At stage 1 there will be a rigid fastening. At this moment, the equation of the rod is described by equation

$$w(0) = 0, \quad \frac{\partial w(0)}{\partial x}(0) = 0.$$

At this stage the rod is in a horizontal position. After the 1st stage, after rigid fastening, it moves on to bending. At this moment the equation of the rod will be

$$w(0) = 0, \quad \frac{\partial w(0)}{\partial x} = \alpha_1 \frac{\partial^2 w(0)}{\partial x^2}.$$

At this stage, the rod deviates from the horizontal position and acquires an inclined angle.

At this stage there is no need for repairs. Here the rigid fastening is maintained. Here the edge binding remains as rigid as before. Bending occurs only along the rod. That is, the rod retains its original fastening.

After the 2nd stage, edge $x = 0$ is weakened. At this stage, you can continue using the rod. We must remember that repairs must be made there in the future. That is, the edges of the rod change from a rigid attachment to a slightly looser edge. Therefore, as the ends of the rod are weakened from the rigid fastenings, play occurs. The resulting play does not completely release the rod. When there is play in the rigid fasteners, a hole appears. The equation of the rod for backlash has the form [6]

$$w(0) = \beta \frac{\partial^2 w(0)}{\partial x^2}, \quad \frac{\partial w(0)}{\partial x} = \alpha_1 \frac{\partial^2 w(0)}{\partial x^2}, \quad \alpha \gg \beta.$$

At this time we must remember the work ahead. After the 3rd stage it moves from bend to fracture. The rod at this time is described by the equation [6]

$$w(0) = \beta \frac{\partial^2 w(0)}{\partial x^2}, \quad \frac{\partial w(0)}{\partial x} = \alpha_1 \frac{\partial^2 w(0)}{\partial x^2} + \frac{\partial^3 w(0)}{\partial x^3}, \quad \alpha \gg \beta \gg \gamma.$$

At this time, a transverse force acts on the rod. As a result, the rod will break.

That is, we see here that at the end there is a transverse force. This shear force will cause the rod to break. Then from these stages we draw the following conclusions: First of all, the rod bends under the influence of a torque, under the influence of which its edges become loose, and the rod breaks under the action of a transverse force. At this time, it is necessary to urgently repair the rod. All this follows from the Taylor formula of the form of the equation of state of the rods.

4 Acknowledgement

This research has been funded by the Science Committee of the Ministry of Science and Higher Education of the Republic of Kazakhstan (Grant No. AP19175972 and No. AP19678089).

References

- [1] Nazarov S.A. General scheme for averaging self-adjoint elliptic systems in multidimensional domains, including thin ones // Algebra and analysis.- 1995. - P. 681–748.
- [2] Kozlova M.V. Averaging of a three-dimensional elasticity problem for a thin inhomogeneous beam // Bulletin of Moscow State University. - 1989. - P. 6-10.
- [3] Kozlova S.V., Panasenko G.P. Homogenization of a three-dimensional problem of the theory of elasticity in an inhomogeneous rod // Journal of Computational Mathematics and Mathematical Physics. – 1991. – P. 1592–1596.
- [4] Maz'ya V., Nazarov S.A., Plamenevskij B.A. Asymptotic theory of elliptic boundary value problems in singularly perturbed domains - Birkhauser. - 2000.
- [5] Nazarov S.A. Asymptotic analysis of thin plates and rods. Dimensionality reduction and integral estimates- Novosibirsk. - 2002.
- [6] Kanguzhin B.E., Ghulam Hazrat A.R., Kaiyrbek Zh.A. Identification of the Domain of the Sturm–Liouville Operator on a Star Graph // Symmetry. - 2021. - P. 1-15.
- [7] Kanguzhin B.E., Akanbay Y.N., Kaiyrbek Zh. A. On the Uniqueness of the Recovery of the Domain of the Perturbed Laplace Operator // Lobachevskii J. of Math.. - 2022. - P. 1532–1535.

IRSTI 27.41.19

DOI: <https://doi.org/10.26577/JMMCS202412116>**A. Karimov** , **K. Imanberdiyev*** 

Al-Farabi Kazakh National University, Kazakhstan, Almaty

*e-mail: kanzharbek75ikb@gmail.com

INTEGRO-INTERPOLATION METHOD OF CONSTRUCTING A DIFFERENCE SCHEME IN A PROBLEM WITH A MOVING BOUNDARY

Working with systems that involve moving boundaries can be a very difficult task. Not only do we have to solve the equations describing the system, but we also have to find the region the system occupies at each step. One of the common moving-boundary classes, Stefan problems are systems of diffusion or heat-conduction where the boundaries between the different phases in the system change over time [1, 2]. Unfortunately, since Stefan problems can be so complex that an analytical solution of the system is often impossible. Therefore, approximate analytical methods or numerical methods, which are the most practical for working with these problems, are often used. This work is devoted to numerical investigation of nonlinear fluid filtration. Hydrodynamic study of non-Newtonian fluid filtration requires solving nonlinear differential equations with partial derivatives. The integration of these equations is associated with serious mathematical difficulties caused by moving boundaries, the dependence of the physical properties on the coordinates and time, the specifics of the boundary conditions. Therefore, in the works devoted to the study of nonlinear effects of filtering liquid and gas, approximate methods are used (quasistationary approximation, the integral relations and numerical). Among them, we can note the simplicity and versatility of finite difference method, which, however, requires the solution of a complex system of algebraic equations with simple computational algorithms. In our problem, in order to close the mathematical system, another equation is required is a type of Stefan's condition. This is the law of conservation of momentum balance, which determines the position of the moving interface. Note that this moving boundary is an unknown surface. Consequently, the problem we are considering is an example of a free boundary problem [3].

Key words: nonlinear fluid filtration, non-newtonian fluid, movable boundary, region of the grids, numerical solution, finite difference method, approximate analytical solution.

А. Каримов, Қ. Иманбердиев*

Әл-Фараби атындағы Қазақ ұлттық университеті, Қазақстан, Алматы қ.

*e-mail: kanzharbek75ikb@gmail.com

Шекарасы жылжымалы есептің айырымдық схемасын құрудың интегро-интерполяция әдісі

Жүйе жылжымалы шекаралар бойынша берілсе күрделі есепке жатады. Мұнда жүйені сипаттайтын теңдеуді шешіп қоймай, жүйенің өзгеріс аймағын білу қажет. Осындай көп тараған жылжымалы шекарасымен берілген есептердің диффузиялық немесе жылуөткізгіштік процестерде кездесуі Стефан типтес есептерге жатады. Бұндай жүйеде әртүрлі фазалардың шекарасы уақытқа байланысты өзгеріп отырады [1, 2]. Өкінішке орай, Стефан есептері күрделі болғандықтан аналитикалық шешімдерін анықтау мүмкіндігі қиын. Сондықтан мұндай есептерде жуық аналитикалық шешімі және тәжірибеде ыңғайлы сандық жуық шешімдері қолданылады. Бұл есеп сызықты емес флюидтің филтрленуінің сандық зерттеу жұмысына жатады. Ньютондық емес сұйықтардың филтрленуінің гидродинамикасын зерттеу сызықты емес дербес туындылы дифференциалдық теңдеудің шешіміне байланысты күрделі болады. Мұндай есептердің интегралын анықтау келесі математикалық қиындықтар тудырады: процесті сипаттайтын физикалық шамалардың кеңістік координаттарына және уақытқа байланысты өзгерісі, жылжымалы шекаралардың және шекаралық шарттардың ерекшелігіне байланысты болады. Сондықтан сұйықтардың филтрленуінің сызықты емес эффектілігін

зерттеуде жуық шығару әдістері (квазисызықты, интегралдық қатынас немесе сандық) қолданылады. Бұлардың ішінде қарапайымдылығымен және жетімділігімен ақырлы-айырымдық әдіс ерекше орын алады. Бірақ есептеу алгоритмінің жеңілдігіне қарамастан күрделі алгебралық теңдеулер жүйесін құрып шығару керек. Біздің есепті тұйықталған математикалық жүйеге келтіру үшін Стефан шартында кездесетін теңдеу қажет. Бұл жерде сұйықтық қозғалысының шекарасына байланысты қозғалыс мөлшерінің сақталу импульс заңын беретін теңдеу болу керек. Мұндай есеп белгісіз шекараға байланысты жылжымалы бетті береді. Сондықтан еркін жылжытын шекараға байланысты шартпен берілген есепке мысал бола алады [3].

Түйін сөздер: сызықты емес сұйықтықты фильтрациялау, Ньютондық емес сұйықтық, жылжымалы шекара, тор аймағы, сандық шешім, шекті айырмдық әдіс, жуықталған аналитикалық шешім.

А. Каримов, К. Иманбердиев*

Казахский национальный университет имени аль-Фараби, Казахстан, г. Алматы

*e-mail: kanzharbek75ikb@gmail.com

Интегро-интерполяционный метод построения разностной схемы в задаче с подвижной границей

Работа с системами, которые имеют подвижные границы, может оказаться очень сложной задачей. Нужно не только решить уравнения, описывающие систему, но и найти область, которую система занимает на каждом шаге. Один из распространенных классов задач с движущимися границами, задачи Стефана – это системы диффузии или теплопроводности, в которых границы между различными фазами в системе меняются с течением времени [1,2]. К сожалению, поскольку задачи Стефана могут быть настолько сложными, что аналитическое решение системы часто оказывается невозможным. Поэтому часто используются приближенные аналитические методы или численные методы, которые наиболее практичны для работы с такими задачами. Данная работа посвящена численному исследованию нелинейной фильтрации флюида. Гидродинамическое исследование фильтрации неньютоновской жидкости ставит перед необходимостью решения нелинейных дифференциальных уравнений с частными производными. Интегрирование таких уравнений связано с серьезными математическими трудностями, обусловленными подвижными границами, зависимостью физических свойств от координат и времени, спецификой краевых условий. Поэтому в работах, посвященных исследованию нелинейных эффектов фильтрации флюида, применяются приближенные методы (квазистационарное приближение, интегральные соотношения и численные). Среди них простотой и универсальностью отличается метод конечных разностей, который, однако, требует решения громоздкой системы алгебраических уравнений при простоте вычислительных алгоритмов. В нашей задаче, чтобы замкнуть математическую систему, требуется еще одно уравнение – типа условия Стефана. Это закон сохранения баланса импульса движения, который определяет положение движущейся границы раздела. Заметим, что эта движущаяся граница является неизвестной поверхностью. Следовательно, рассматриваемая нами задача является примером задачи со свободной границей [3].

Ключевые слова: нелинейная фильтрация жидкости, неньютоновская жидкость, подвижная граница, область сеток, численное решение, метод конечных разностей, приближенное аналитическое решение.

1 Introduction

Oils of Western Kazakhstan, containing a relatively large amount of paraffin-asphaltene-resinous substances, belong to non-Newtonian fluids. The study of the structural and mechanical properties of such oils is of great interest for solving various issues of oil production. The study of the rheological characteristics of non-Newtonian oils on a capillary

viscometer (copper capillary tubes with a diameter of 2, 3 and 4 mm and a length of 200, 300 and 400 mm) was carried out according to a well-known technique, [4–6]. For oil with a 25% resin content at temperatures of 16, 18 and 210 C, the characteristic dependence $\vartheta = \vartheta(|\nabla P|)$ Figure 1 shows the curve, [7, 8]. For the test oil, the plot of dependence is nonlinear and passes through the origin, and it is convexed downwards at small pressure gradients, and at large it has a linear shape. Models of viscous and viscous-plastic media and various types of dependence were used to describe the structural behavior of the fluid. So, for example, the flow curve shown in Figure 1 can be approximated by two straight lines, in particular, one straight line OA , passing through the origin, and another AC , cutting off on the abscissa axis segment OB , corresponding to the limiting shear gradient g_* . If we restrict research to $|\nabla P| > g_*$, then we obtain a model similar to the Shvedov–Bingham model, and for $|\nabla P| < g_*$ is viscous fluid flow model.

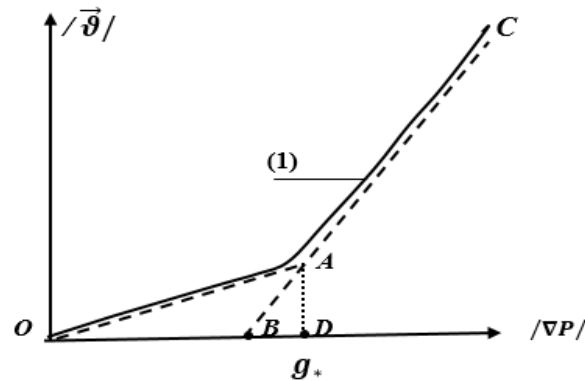


Figure 1

Figure 1. Shows the experimental dependence of the $\vartheta = \vartheta(|\nabla P|)$ fluid filtration rate (solid curve 1) and its approximation (dashed lines) BC or OAC . If the rate of fluid filtration at low pressure gradients cannot be neglected, then it is necessary to use filtration models that take into account the fluid flow at such gradients. These models include those based on polygonal or other approximations of the indicator curve

$$\vartheta = \vartheta(|\nabla P|).$$

When using the experimental curve (1), the velocity of fluid movement in a porous medium can be described by the nonlinear equation, [5, 8]:

$$\vec{\vartheta} = -\frac{k}{\mu} F(|\nabla P|) \frac{\nabla P}{|\nabla P|}. \quad (1)$$

In this case $F(|\nabla P|)$ is a continuous positive, monotonically increasing function ($F'(|\nabla P|) > 0$), derivative of which can have a finite number of discontinuities of the first kind.

Figure 1 (curve 1) shows a model of a viscous medium with an apparent viscosity [7] depending on the pressure gradient. In this case, the polygon fits into the indicator curve in such a way that its first link passes through the origin and characterizes filtration at low pressure gradients, and the second link coincides with the asymptote of the graph $\vartheta = \vartheta(|\nabla P|)$ and characterized the flow of fluids at large pressure gradients.

To calculate the filtration of a Newtonian fluid, along with mathematical methods, simulators (analog computers) are widely used, however, electric simulation of the flow of a non-Newtonian fluid in a porous medium using conventional simulators is in most cases impossible. In work [9] similarity criteria are derived and an analog simulator based on the well-known electrohydrodynamic analogy is described. In the case when the movements of the liquid at small pressure gradients are not taken into account, i.e. the curve is approximated by a half-line BC , cutting off on the abscissa axis a segment of OB .

Thus, approximation by a two-link polygon will give the following model of nonlinear filtering [8].

$$\vec{v} = \begin{cases} -\frac{k}{\nu}\nabla P, & |\nabla P| < g_*, \\ -\frac{k}{\mu}(|\nabla P| - \mu_*g_*)\frac{\nabla P}{|\nabla P|}, & |\nabla P| > g_*. \end{cases} \quad (2)$$

Here $\mu_* = (1 - \frac{\mu}{\nu})$ is the apparent viscosity, and μ and ν are dynamic viscosities at small and large pressure gradients.

In other works [8], approximate analytical solutions for this problem were obtained using various approximations: either the half-line BC or the polygon OAC . To obtain approximate solutions, usually use the method of integral relations proposed by G.I. Barenblatt [6] and the method based on applying the Laplace transform. With the help of the Laplace transform, the approximate solution of the problem is limited to the initial stage of the process (quasi-stationary approximation).

2 Methods and materials

2.1 System of equations describing isothermal fluid filtration

It is assumed that the terrestrial rock is elastic, and the fluid belongs to the class of weakly compressible liquids. Under these assumptions, the mathematical model can be represented in the form of the following system of equations: continuity equation $\frac{\partial m\rho}{\partial t} + \text{div}(\rho\vec{v}) = 0$; equation of the porous medium state is $dm = \beta_r dP$; equation for the fluid state is $\rho = \rho_0 \exp[\beta_f(P - P_0)]$.

Then the equation of continuity, taking into account the equations of state of the porous medium and fluid becomes

$$\beta^* \frac{\partial P}{\partial t} + \text{div} \vec{v} = 0. \quad (3)$$

In the above formulas, the following designations are adopted: k is permeability coefficient, $\beta^* = \beta_r + \beta_f$ is reservoir coefficient of elasticity, β_r and β_f are rock and fluid compressibility factors.

2.2 Mathematical model of nonlinear fluid filtration

Let's now consider the problem of fluid filtration, i.e. with polygonal approximation of the experimental flow rate is depression curve (Figure 1). Let an isotropic layer of unit thickness and width be filled with a homogeneous liquid. Under the long-term influence of the temperature field, the liquid acquired structural and mechanical properties that were

unequal along the length of the formation. In this case, the value of the gradient at the boundary of the viscosity discontinuity can depend on the x coordinate. If the structural and mechanical properties of liquid particles are distributed during their transfer, we will assume that the magnitude of the gradient at the viscosity discontinuity boundary $g(x, t)$ will change in proportion to the speed of the liquid. Then, taking into account the filtration law (2), the continuity equation (3) in a one-dimensional formulation for the case $g(x, 0) = g_* = \text{const}$ is reduced to solving the equations [7, 8]. Thus, it is required to find the function $P_1(x, t)$, $P_2(x, t)$, $\xi(t)$ from the conditions:

$$c_1 \frac{\partial P_1}{\partial t} = \frac{\partial}{\partial x} \left[k_1(x, t) \left(\frac{\partial P_1}{\partial x} - \mu_* g_* \right) \right], \quad x_0 < x \leq \xi(t), \quad t > 0, \quad (4)$$

$$c_2 \frac{\partial P_2}{\partial t} = \frac{\partial}{\partial x} \left[k_2(x, t) \frac{\partial P_2}{\partial x} \right], \quad \xi(t) \leq x \leq L, \quad t > 0. \quad (5)$$

where $c_1 = \mu\beta^*$, $c_2 = \nu\beta^*$.

Under the initial condition

$$P_2(x, 0) = \varphi(x), \quad x_0 < x < L, \quad \xi(0) = x_0, \quad (6)$$

and the condition of matching the initial values P_1 and P_2 : $\lim_{t \rightarrow 0} P_1(x, t) = \varphi(x_0)$.

Under the following conditions on the unknown boundary $\xi = \xi(t)$:

$$\lim_{x \rightarrow \xi-0} P_1(x, t) = \lim_{x \rightarrow \xi+0} P_2(x, t), \quad t > 0, \quad (7)$$

$$\lim_{x \rightarrow \xi-0} \frac{\partial}{\partial x} P_1(x, t) = \lim_{x \rightarrow \xi+0} \frac{\partial}{\partial x} P_2(x, t) = g_*, \quad t > 0. \quad (8)$$

and the corresponding condition on the gallery

$$\alpha_1 \frac{k}{\mu} \left(\frac{\partial P_1(x_0, t)}{\partial x} - \mu_* g_* \right) + \beta_1 P_1(x_0, t) = q_1(t), \quad t > 0, \quad (9)$$

$$P_2(L, t) = \varphi(L), \quad t > 0. \quad (10)$$

where $\alpha_1 \cdot \beta_1 = 0$, $\alpha_1 + \beta_1 = 1$.

Unlike problems [10–12], here there is no explicit equation for determining the free boundary, however, the known value of the gradient at the viscosity discontinuity boundary allows us to construct a difference scheme that allows us to determine the position of the boundary.

It should be noted that in a layer of finite length L , filtration is divided into two periods. The first period is at $0 \leq t \leq T$, where T is the moment in time when the boundary reaches the right end of the formation ($\xi(T) = L$), the second period at $t \geq T$ is characterized by the solution of equation (4). An approximate solution of the problem by the method of integral relations was considered, for example, in [8].

In the case of rectilinear-parallel motion of the medium and $g_* = \text{const}$, taking into account the following dimensionless parameters:

$$\bar{x} = \frac{x}{L}, \quad \bar{\xi} = \frac{\xi}{L}, \quad \bar{u} = \frac{P_i(x, t)}{P_0}, \quad k_1(\bar{x}, \bar{t}) = \frac{k_1(x, t)}{k_0},$$

$$k_2(\bar{x}, \bar{t}) = \frac{\mu_0 k_2(x, t)}{k_0}, \quad \bar{t} = \frac{t}{t_0}, \quad \bar{g}_* = \frac{g_* L}{P_0}, \quad \bar{q}_1 = \left(\frac{\mu q_1}{k_1} + \mu_* g_* \right) \cdot \frac{L}{P_0},$$

$$t_0 = \frac{\mu \beta^* L^2}{k_0}, \quad \mu_0 = \frac{\nu}{\mu}, \quad c_1 = 1, \quad c_2 = 1, \quad i = 1, 2.$$

For P_1, P_2 in dimensionless form, one notation $\bar{u}(\bar{x}, \bar{t})$ is adopted, since they are defined in non-intersecting areas, and the continuity conditions are satisfied at the interface. It is necessary to define the functions $u(x, t)$ so that they satisfy the filtration equation. Let's write the equations by omitting the dashes above the variables

$$c \frac{\partial u}{\partial t} = \frac{\partial}{\partial x} \left(k \frac{\partial u}{\partial x} \right), \quad t > 0. \quad (11)$$

Moreover, the functions u, c and k are defined in the intervals $0 < x < \xi(t)$ and $\xi(t) < x < 1$, i.e.

$$k = \begin{cases} k_1(x, t), & 0 < x < \xi(t), \\ k_2(x, t), & \xi(t) < x < 1, \end{cases} \quad 0 < k_i \leq k_{i0};$$

$$c = \begin{cases} c_1(x, t), & 0 < x < \xi(t), \\ c_2(x, t), & \xi(t) < x < 1, \end{cases} \quad 0 < c_i \leq c_{i0}. \quad (12)$$

Note that the functions c and k may have a discontinuity at $x = \xi(t)$. In addition to equation (11), the functions $u(x, t)$ and $\xi(t)$ at the interface $x = \xi(t)$ must satisfy the conditions of continuity of the desired function

$$u(\xi - 0, t) = u(\xi + 0, t),$$

and matching gradients at the viscosity discontinuity boundary:

$$\frac{\partial}{\partial x} u(\xi - 0, t) = \frac{\partial}{\partial x} u(\xi + 0, t) = g_*. \quad (13)$$

Initial conditions

$$u(x, 0) = \varphi(x), \quad \xi(0) = x_0, \quad (14)$$

and boundary conditions

$$l_1 u(x_0, t) = q_1(t), \quad u(1, t) = 1. \quad (15)$$

Here the operator corresponds to plane-parallel filtration

$$l_1 = \alpha_1 \left(k_1 \frac{\partial u}{\partial x} \right) + \beta_1 u.$$

Assuming that problem (11)–(15) is posed correctly and we assume that $\xi(t)$ is a monotonically increasing function $t \in (0, T]$, $\varphi'(x) \geq 0$ and $q_1(t) < 0$.

2.3 Difference scheme

For the numerical solution of the considered nonlinear problem, we construct an iterative implicit difference scheme based on the idea of the method of attaching a moving boundary $\xi = \xi(t)$ to grid node [11, 13, 14]. The domain for solving the problem is the half-grid $D = \{x, t | x_0 \leq x \leq 1, t \geq 0\}$. On the segment $[0, 1]$, we introduce a quasi-uniform grid of basic and flow nodes:

$$\{x_i = x_{i-1} + h, i = \overline{1, n-1}; x_0 = 0; x_N = 1\},$$

$$\{x_{i-1/2} = x_{i-1} + 0.5h, i = \overline{1, n-1}; x_0 = x_{-1/2}; x_N = x_{N+1/2}\}.$$

The area $[0, 1]$ of streaming nodes is split into cells $i = [x_{i-1/2}, x_{i+1/2}]$, $i = \overline{0, n}$. The line $x = \xi(t)$ in the solution area is the dividing one. Here we consider a uniform mesh in x and a non-uniform mesh in time $\widehat{\omega}_{h,\tau} = \{x_i, t_k | x_i = x_0 + ih, h > 0, i = \overline{0, n}, t_k = t_{k-1} + \tau_k, \tau_k = \sum_{j=0}^k \Delta\tau_j, \Delta\tau_j > 0, k \geq 1, n \geq 3\}$. In this case the time step τ_k we will take depending on k so that the end of the broken line approximating the movable boundaries $x = \xi(t)$ for any $\tau_k = \sum_{j=0}^k \Delta\tau_j$ would hit the node of the difference grid.

The initial boundary value problem (11)–(15) corresponds to the following conservative, purely implicit two-layer difference scheme [7, 11]. Let us consider the case $c_1 = c_2 = 1$. Then we write (11) at all points except the point $x = \xi(t)$ in the form of

$$\frac{\partial u}{\partial t} = \frac{\partial}{\partial x} \left(k \frac{\partial u}{\partial x} \right), \quad t > 0. \quad (16)$$

Integrate it within $(\xi_k - h_1/2), (\xi_k + h_1/2)$,

$$\int_{\xi_k - h_1/2}^{\xi_k + h_1/2} \frac{\partial u}{\partial t} dx = \int_{\xi_k - h_1/2}^{\xi_k} \frac{\partial}{\partial x} \left(k_1 \frac{\partial u}{\partial x} \right) dx + \int_{\xi_k}^{\xi_k + h_1/2} \frac{\partial}{\partial x} \left(k_2 \frac{\partial u}{\partial x} \right) dx. \quad (17)$$

Applying the mean value theorem to the integral on the left, we obtain

$$h_1 \frac{\partial u}{\partial t} = k_2 \frac{\partial u}{\partial x} \Big|_{\xi_k + h_1/2} - k_1 \frac{\partial u}{\partial x} \Big|_{\xi_k - h_1/2}. \quad (18)$$

Here the condition from the point of discontinuity is divided into two, which reduces the approximation error arising from the inaccurate determination of the interface. Moreover, if we divide (18) by h_1 and go to the difference derivatives [15], for the point $x = \xi(t)$ we get:

$$y_{\bar{t}} = (\bar{k} y_{\bar{x}})_x, \quad (19)$$

where under \bar{k} is considered

$$\bar{k} = \begin{cases} k_1(x - h_1/2, t) & \text{given that } 0 < x < \xi(t), \\ k_2(x + h_1/2, t) & \text{given that } \xi(t) < x < 1. \end{cases}$$

Passing to the difference derivatives in (16) and comparing them with (19), we obtain a homogeneous difference scheme over the entire interval $[0, 1]$. Combining it with the initial and boundary conditions, we arrive at the difference problem in the entire domain:

$$\begin{aligned} y_{\bar{i}} &= (\bar{k}y_{\bar{x}})_x, \quad y_i^{(0)} = \varphi(x_i), \\ \ell_1 y &= q_1(t_k) \quad \text{given that } x = 0, \\ y &= 1 \quad \text{given that } x = 1. \end{aligned} \quad (20)$$

The operator ℓ_1 is determined by the balance method by integrating (16) on the segments $(0, h/2)$ and using the boundary condition. As is known, in this case, the approximation error will be $o(h^2)$.

Difference problem (20) is supplemented by the condition within which $x = \xi(t)$. For this in the area D_ξ taking into account the condition on the fracture line of the fluid viscosity (13), at $t = t_k$, calculate the integral for a cell with a node of $i = i_k$. Then the equation (16) becomes:

$$\begin{aligned} \int_{x_{i-\frac{1}{2}}}^{x_{i+\frac{1}{2}}} \frac{\partial u}{\partial t} dx &= (1 - \delta_i) \frac{\partial u}{\partial t} \Big|_{x_{i-\frac{1}{2}}}^{x_{i+\frac{1}{2}}} + \delta_i \left[\bar{k} \frac{\partial u}{\partial x} \Big|_{x_{i-\frac{1}{2}}}^{x_{i+\frac{1}{2}}} + \bar{k} \frac{\partial u}{\partial x} \Big|_{\xi_{k+0}}^{\xi_{k-0}} \right] \\ &= k_{i+\frac{1}{2}} \frac{\partial u}{\partial x} \Big|_{x_{i+\frac{1}{2}}} - k_{i-\frac{1}{2}} \frac{\partial u}{\partial x} \Big|_{x_{i-\frac{1}{2}}} + \delta_i \left(k_{i-\frac{1}{2}} \frac{\partial u}{\partial x} \Big|_{\xi_{k-0}} - k_{i+\frac{1}{2}} \frac{\partial u}{\partial x} \Big|_{\xi_{k+0}} \right) \\ &= k_{i+\frac{1}{2}} \frac{\partial u}{\partial x} \Big|_{x_{i+\frac{1}{2}}} - k_{i-\frac{1}{2}} \frac{\partial u}{\partial x} \Big|_{x_{i-\frac{1}{2}}} + \delta_i \left(k_{i-\frac{1}{2}} - k_{i+\frac{1}{2}} \right) g_*. \end{aligned}$$

Here: given $\delta_i = 1$, $\xi \in [x_{i-\frac{1}{2}}, x_{i+\frac{1}{2}}]$ and $\delta_i = 0$, $\xi \notin [x_{i-\frac{1}{2}}, x_{i+\frac{1}{2}}]$.

We denote the grid function $y_{i_k} = u(x_i, t_k)$ and $\check{y}_{i_k} = u(x_i, t_{k-1})$.

Then we have:

$$\left(\frac{y_{i_k} - \check{y}_{i_k}}{\Delta\tau_k} \right) h_1 = k_{i_k+\frac{1}{2}} \frac{y_{i_k+1} - y_{i_k}}{h_1} - k_{i_k-\frac{1}{2}} \frac{y_{i_k} - y_{i_k-1}}{h_1} + \delta_i \left(k_{i_k-\frac{1}{2}} - k_{i_k+\frac{1}{2}} \right) g_*.$$

Hence, when the interface of two viscosities is displaced by one step, we find the corresponding time

$$\frac{h_1}{\Delta\tau_k^{(s+1)}} = \frac{\left[k_{i_k+\frac{1}{2}} \frac{y_{i_k+1}^{(s)} - y_{i_k}^{(s)}}{h_1} - k_{i_k-\frac{1}{2}} \frac{y_{i_k}^{(s)} - y_{i_k-1}^{(s)}}{h_1} + \left(k_{i_k-\frac{1}{2}} - k_{i_k+\frac{1}{2}} \right) g_* \right]}{\left(y_{i_k}^{(s)} - \check{y}_{i_k} \right)}, \quad (21)$$

where $\delta_i = 1$, s is t .

The computational algorithm is based on a counter sweep. Difference equation (20) over the entire grid region is then reduced to the form:

$$a_{z,i} y_{z,i-1} - b_{z,i} y_{z,i} + c_{z,i} y_{z,i+1} = d_{z,i}, \quad z = 1, 2. \quad (22)$$

Then, to determine the pressure value at the interface between two viscosities, we obtain a system of algebraic equations.

a) from left to right, using the right sweep formulas, we determine the sweeping coefficients

$$\alpha_i = \frac{c_{1,i}}{b_{1,i} - a_{1,i}\alpha_{i-1}}, \quad \beta_i = \frac{a_{1,i}\beta_{i-1} - d_{1,i}}{b_{1,i} - a_{1,i}\alpha_{i-1}}, \quad i = \overline{1, i_k - 1}, \quad i_k \geq 2; \quad (23)$$

b) from right to left, calculate the sweep coefficients of the left sweep

$$\psi_i = \frac{a_{2,i}}{b_{2,i} - c_{2,i}\psi_{i+1}}, \quad \eta_i = \frac{c_{2,i}\eta_{i+1} - d_i}{b_{2,i} - c_{2,i}\psi_{i+1}}, \quad i = \overline{n-1, i_k}. \quad (24)$$

For the movable unit $\ll i = i_k \gg$, based on the formula of right and left runs

$$y_{1,i-1} = \alpha_{i-1}y_{1,i} + \beta_{i-1}, \quad i = \overline{i_k, -n_k}; \quad (25)$$

$$y_{2,i+1} = \psi_{i+1}y_{2,i} + \eta_{i+1}, \quad i = \overline{i_k, n_k}, \quad (26)$$

and taking into account (13), we find the required function $y_{1,i_k} = y_{2,i_k} = y_{i_k}^*$,

$$y_{i_k}^* = \frac{\beta_{i_k-1} + \eta_{i_k+1}}{2 - (\psi_{i_k+1} + \alpha_{i_k-1})}. \quad (27)$$

Wherein α_0 , β_0 and ψ_n , η_n are determined depending on the setting of the boundary conditions.

Thus, when passing from the $(k-1)$ time layer, calculations are performed in the following order

$$\begin{aligned} \Delta\tau_{k-1}^{(0)} &\Rightarrow (20) \Rightarrow (22) \Rightarrow (21) \Rightarrow (18) \Rightarrow \\ &\Rightarrow \left| \Delta\tau_k^{(s)} - \Delta\tau_k^{(s-1)} \right| < \varepsilon_\tau \wedge \max_i \left| y_i^{(s)} - y_i^{(s-1)} \right| < \varepsilon_p. \end{aligned}$$

If the convergence condition is satisfied, we assume that $\Delta\tau_{k-1} = \Delta\tau_{k-1}^{(s)}$ and $\xi_{k+1} = \xi_k + h_1$ and go to the next time layer, and if the inequalities are not satisfied, we repeat the iterative process.

2.4 Numerical solution results

For illustration, the numerical solution of the problem was carried out for a constant shear gradient $g_* = \text{const}$. This problem has an approximate analytical solution [8], and for a quasi-stationary approximation of a physical process, we execute the law of variation of the moving boundary.

When the gallery is set on the constant pressure of $\Delta p = p_0 - p_c$, then the solution has the form of:

$$\xi(t) = 2\sqrt{\varkappa_\mu t \ln \left(\frac{(1-\varepsilon)\Delta p}{(g_*\sqrt{\pi\varkappa_\mu t})} \right)}, \quad \varepsilon = \frac{(\sqrt{\varkappa_\mu} - \sqrt{\varkappa_\nu})}{(\sqrt{\varkappa_\mu} + \sqrt{\varkappa_\nu})}. \quad (28)$$

If the production gallery is set to a constant flow rate $D = g_* + \mu \cdot \frac{q_1}{k}$, then the solution has the following form:

$$\xi(t) = C\sqrt{\varkappa_\mu t},$$

$$\text{where } p_0 + D\sqrt{t} \cong p_0 + 2\sqrt{\frac{\varkappa_\mu t}{\pi}} \left[(1 + \varepsilon) \varepsilon \left(x e^{-C^2} - C\sqrt{\pi} \operatorname{erfc} C \right) - 1 \right]. \quad (29)$$

Here $\varkappa_\mu = \frac{k}{(\mu \cdot \beta^*)}$, $\varkappa_\nu = \frac{k}{(\nu \cdot \beta^*)}$, $g_* = 5 \cdot 10^{-3} \text{atm/m}$, $p_0 = 150 \text{atm}$, $p_c = 120 \text{atm}$, $\mu = 2.5 \text{cPs}$, $\nu = 3.6 \text{cPs}$, $k = 0.4 \text{D}$, $\beta^* = 16 \cdot 10^{-6} \text{atm}^{-1}$, $q_1 = 6.077 \cdot 10^2 \text{cm}^3/\text{sec}$, $L = 10^3 \text{m}$, $t_0 = 10^6 \text{sec}$, \varkappa_μ , \varkappa_ν are the piezoconductivity coefficients at high and low pressure gradients.

Position of the movable boundary versus time during operation with a given constant pressure on the gallery and at a constant gradient value $g_* = 5 \cdot 10^{-3} \text{atm/m}$ at the discontinuity of viscosities boundary is shown in Figure 2. Here, the absolute error, defined as the difference between the numerical and approximate analytical solutions depending on the operating time, varies from $1.73 \cdot 10^{-2}$ to $7.22 \cdot 10^{-2}$.

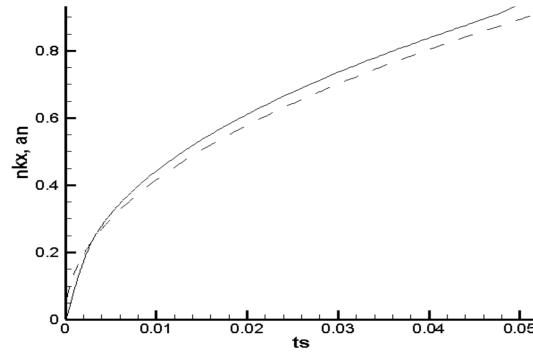


Figure 2

Figure 2. Graph of a moving border $\xi = \xi(t)$ depending on the time when the gallery is operated with constant pressure. The solid line corresponds to the numerical solution, and the dashed line to the approximate analytical solution (28).

The coordinate of the moving boundary depending on the time during operation with a given flow rate and at $g_* = 5 \cdot 10^{-3} \text{atm/m}$ is shown in Figure 3. Here, the absolute error of the solution, depending on the operation time, varies from $1.92 \cdot 10^{-2}$ to $8.15 \cdot 10^{-2}$.

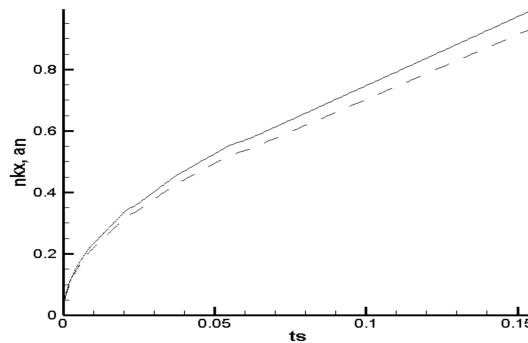


Figure 3

Figure 3. Graph of a moving border $\xi = \xi(t)$ depending on the time when the gallery is operating with a constant flow rate. The solid line corresponds to the numerical solution, and the dashed line to the approximate analytical solution (29).

For the value of the gradient at the boundary of the discontinuity of viscosities $g_* = 5 \cdot 10^{-3} \text{atm/m}$ at $\Delta p = p_0 - p_c = 30 \text{atm}$ the moving front $\xi(t)$ reaches the right end of the formation $L = 10^3 \text{m}$ in 19.4 hours. If the value of the gradient at the boundary of the discontinuity of viscosities increases, then the time to reach the moving boundary $\xi(t)$ the right end of the layer is correspondingly growing. Calculations were carried out for various constant values of the shear gradient: $7 \cdot 10^{-3} \text{atm/m}$; $8 \cdot 10^{-3} \text{atm/m}$ and $9 \cdot 10^{-3} \text{atm/m}$. The time to reach the moving front $\xi(t)$ of the right end of the reservoir $L = 10^3 \text{m}$ is growing: 22.2 hours; 25 hours and 27.7 hours; respectively. In the case of the first stage of fluid filtration, the change in pressure as a function of time is shown in Figures 4 and 5 at $g_* = 5 \cdot 10^{-3} \text{atm/m}$.

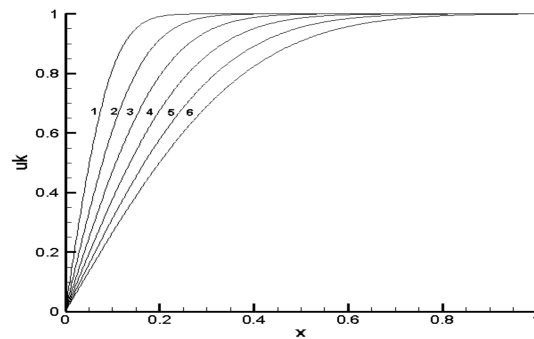


Figure 4

Figure 4. Pressure change graphs during gallery operation with constant pressure for various values of dimensionless time: 1 – $0.2924\text{E} - 02$; 2 – $0.6866\text{E} - 02$; 3 – $0.1275\text{E} - 01$; 4 – $0.2078\text{E} - 01$; 5 – $0.3118\text{E} - 01$; 6 – $0.4404\text{E} - 01$.

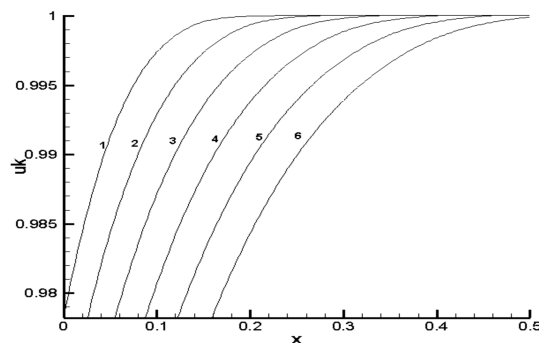


Figure 5

Figure 5. Graphs of pressure changes during gallery operation with constant flow rate for various values of dimensionless time: 1 – $0.3165\text{E} - 02$; 2 – $0.5959\text{E} - 02$; 3 – $0.9645\text{E} - 02$; 4 – $0.1425\text{E} - 01$; 5 – $0.1972\text{E} - 01$; 6 – $0.2611\text{E} - 01$.

3 Conclusion

Analysis of the results showed that the number of iterations depends on the step size of the grid region. In this case, the step along the spatial coordinate is selected depending on the

value of the fracture gradient of the fluid viscosity. With a large shear gradient, one should take a smaller step along the spatial coordinate. In a numerical experiment, formula (21) was used to find the appropriate time for fishing in the node of the movable boundary. The results presented showed that the proposed method can be used to determine the free boundary in similar problems with conditions (7), (8), implicitly determining its position.

References

- [1] Stefan J., Uber einige Probleme der Theorie der Warmeleitung, *Sitzungsber Wien. Akad. Mat. Natur.*, 98 (1889): 473–484.
- [2] Stefan J., Uber die Diffusion von Sauren und Basen gegen einander, *Sitzungsber Wien. Akad. Mat. Natur.*, 98 (1889): 616–634.
- [3] Crank J., *Free and Moving Boundary Problems*, – Oxford: Clarendon Press, 1984, 425 p.
- [4] Mirzajanzade A.Kh., Mirzoyan A.A., Gevinyan G.M., Seid-Rza M.K., *Hydraulics of clay and cement mortars*, – M.: Nedra, 1966, 231 p. (in Russian)
- [5] Pleshchinsky B.I., Nazarovskiy G.A., Molokovich Yu.M., Study of filtration of non-Newtonian fluid in a heterogeneous medium, *Research on underground hydromechanics*, Kazan, Kazan University Publishing House, 1 (1976): 194–201. (in Russian) <https://www.mathnet.ru/rus/kuipg/v1/p194>
- [6] Barenblatt G.I., On some approximate methods in the theory of one-dimensional unsteady filtration of fluid in elastic mode, *Izvestia AN USSR, OTN*, 9 (1954): 35–50. (in Russian)
- [7] Karimov A., *Numerical methods of modelling nonlinear processes of heat and mass transfer in computers*, Almaty, Kazakh University, (2014): 199 p. (in Russian)
- [8] Molokovich Yu.M., Skvortsov E.V., Approximate solutions of one-dimensional problems of filtration of elastic non-Newtonian fluid, – M.: VNIIONG, (1970): 139–151. (in Russian)
- [9] Korniltsev Yu.A., Molokovich Yu.M., Electrical modeling of rectilinear-parallel problems of filtration of non-Newtonian fluids, *Scientific notes of Kazan State University*, 130:1 (1970): 33–44. (in Russian) <https://www.mathnet.ru/rus/uzku/v130/i1/p33>
- [10] Vladimirov L.A., Solution of the problem of the motion of the interface between two fluids, *Journal of Computational Mathematics and Mathematical Physics*, Vol. 6, addition to № 4 (1966): 267–271. (in Russian)
- [11] Budak B.M., Vasiliev F.P., Egorova A.T., On one version of an implicit difference scheme with trapping the phase front at a grid node for solving Stefan-type problems, *In the collection Computational methods and programming, Moscow State University Publishing House*, 6 (1967): 231–241. (in Russian)
- [12] Furzeland R.M., A Comparative Study of Numerical Methods for Moving Boundary Problems, *IMA Journal of Applied Mathematics*, 26:4 (1980): 411–429. <https://doi.org/10.1093/imamat/26.4.411>.
- [13] Caldwell J., Kwan Y.Y., Numerical methods for one-dimensional Stefan problems, *Communications in Numerical Methods in Engineering*, 20:7 (2004): 535–545. <https://doi.org/10.1002/cnm.691>.
- [14] Whye-Teong Ang, A numerical method based on integro-differential formulation for solving a one-dimensional Stefan problem, *Numerical Methods for Partial Differential Equations*, 24:3 (2008): 939–949. <https://doi.org/10.1002/num.20298>.
- [15] Samarsky A.A., Nikolaev E.S., *Methods for solving grid equations*, – M.: Nauka, 1978, 589 c. (in Russian)

Литература

- [1] Stefan J., Uber einige Probleme der Theorie der Warmeleitung, *Sitzungsber Wien. Akad. Mat. Natur.*, 98 (1889): 473–484.
- [2] Stefan J., Uber die Diffusion von Sauren und Basen gegen einander, *Sitzungsber Wien. Akad. Mat. Natur.*, 98 (1889): 616–634.
- [3] Crank J., *Free and Moving Boundary Problems*, – Oxford: Clarendon Press, 1984, 425 p.
- [4] Мирзаджанзаде А.Х., Мирзоян А.А., Гевинян Г.М., Сеид-Рза М.К., *Гидравлика глинистых и цементных растворов*, – М.: Недра, 1966, 231 с.
- [5] Плесчинский Б.И., Назаровский Г.А., Молокович Ю.М., Исследование фильтрации неньютоновской жидкости в неоднородной среде, *Исследования по подземной гидромеханике*, Казань, Издательств Казанского университета, 1 (1976): 194–201. <https://www.mathnet.ru/rus/kuiipg/v1/p194>
- [6] Баренблатт Г.И., О некоторых приближенных методах в теории одномерной неустановившейся фильтрации жидкости при упругом режиме, *Известия АН СССР, ОТН*, 9 (1954): 35–50.
- [7] Каримов А., *Численные методы моделирования нелинейных процессов тепло- и массообмена*, Алматы, Казах университети, (2014): 199 с.
- [8] Молокович Ю.М., Скворцов Э.В., Приближенные решения одномерных задач фильтрации упругой неньютоновской жидкости, – М.: ВНИИОНГ, (1970): 139–151.
- [9] Корнильцев Ю.А., Молокович Ю.М., Электромоделирование прямолинейно-параллельных задач фильтрации неньютоновских жидкостей, *Ученые записки Казанского государственного университета*, 130:1 (1970): 33–44. <https://www.mathnet.ru/rus/uzku/v130/i1/p33>
- [10] Владимиров Л.А., Решение задачи о движении границы раздела двух жидкостей, *Журнал вычислительной математики и математической физики*, Т. 6, дополнение к № 4 (1966): 267–271.
- [11] Будаков Б.М., Васильев Ф.П., Егорова А.Т., Об одном варианте неявной разностной схемы с ловлей фазового фронта в узел сетки для решения задач типа Стефана, *В сборнике Вычислительные методы и программирование*, Издательство МГУ, 6 (1967): 231–241.
- [12] Furzeland R.M., A Comparative Study of Numerical Methods for Moving Boundary Problems, *IMA Journal of Applied Mathematics*, 26:4 (1980): 411–429. <https://doi.org/10.1093/imamat/26.4.411>.
- [13] Caldwell J., Kwan Y.Y., Numerical methods for one-dimensional Stefan problems, *Communications in Numerical Methods in Engineering*, 20:7 (2004): 535–545. <https://doi.org/10.1002/cnm.691>.
- [14] Whye-Teong Ang, A numerical method based on integro-differential formulation for solving a one-dimensional Stefan problem, *Numerical Methods for Partial Differential Equations*, 24:3 (2008): 939–949. <https://doi.org/10.1002/num.20298>.
- [15] Самарский А.А., Николаев Е.С., *Методы решения сеточных уравнений*, – М.: Наука, 1978, 589 с.

IRSTI 27.39.21

DOI: <https://doi.org/10.26577/JMMCS202412117>A.M. Manat , N.T. Orumbayeva* Karaganda University of the name of academician E.A. Buketov, Kazakhstan, Karaganda
*e-mail: orumbayevanurgul@gmail.com

ON ONE SOLUTION OF A NONLOCAL BOUNDARY VALUE PROBLEM FOR A NONLINEAR PARTIAL DIFFERENTIAL EQUATION OF THE THIRD ORDER

In this paper, a nonlocal boundary value problem for the Benjamin-Bona-Mahony-Burgers equation is studied in a rectangular domain. By introducing new functions, the nonlocal boundary value problem for a nonlinear third-order partial differential equation is reduced to a boundary value problem for a second-order hyperbolic equation with a mixed derivative and functional relations. Before using the approximate method, the nonlinear problem under consideration is examined for the presence of solutions, it is necessary to clarify where these solutions are located, that is, to find the region of isolation of solutions. The isolation area of the solution in our case is a ball in which there is a unique solution to the problem. Next, an algorithm for finding a solution to a nonlocal boundary value problem is proposed. In terms of the initial data, conditions for the convergence of the algorithms are established, which simultaneously ensure the existence and isolation of a solution to a nonlinear nonlocal boundary value problem. Estimates between the exact and approximate solutions of the problem under consideration are obtained. The results obtained are of a theoretical nature and can be used in the construction of computational algorithms for solving nonlocal boundary value problems for the Benjamin-Bona-Mahony-Burgers equation.

Key words: Benjamin-Bona-Mahony-Burgers equation, differential equations with partial derivatives, algorithm, approximate solution.

A.M. Манат, Н.Т. Орумбаева*

Академик Е.А. Бөкетов атындағы Қарағанды университеті, Қазақстан, Қарағанды қ.

*e-mail: orumbayevanurgul@gmail.com

Үшінші ретті дербес туындылы сызықтық емес дифференциалдық теңдеу үшін бейлокал шеттік есебінің бір шешімі жайында

Бұл жұмыста тікбұрышты облыста Бенджамин-Бона-Махони-Бюргерс теңдеуі үшін бейлокал шеттік есебі зерттеледі. Жаңа функциялар енгізе отырып үшінші ретті дербес туындылы сызықтық емес дифференциалдық теңдеу үшін бейлокал шеттік есебі аралас туындылы екінші ретті гиперболалық теңдеу үшін бастапқы-шеттік есепке келтіріледі. Жуық әдісті қолданбас бұрын қарастырылып отырған сызықтық емес есептің шешімінің бар болуын зерттейміз, шешімдердің қайда орналасқанын, яғни шешімнің оқшауланған облысын анықтау қажет. Біздің жағдайымызда оқшауланған облыс - есептің шешімі бар және жалғыз болатын шар болып табылады. Әрі қарай бейлокал шеттік есептің шешімін табу алгоритмі ұсынылады. Бастапқы берілгендер терминінде сызықтық емес бейлокал шеттік есептің шешімінің бар болуы мен оқшауланғанын қамтамасыз ететін алгоритмдердің жинақтылық шарттары алынған. Қарастырылып отырған есептің нақты және жуық шешімі арасындағы бағалаулар табылған. Алынған нәтижелер теориялық сипатқа ие және үшінші ретті дербес туындылы сызықтық емес дифференциалдық теңдеулер үшін бейлокал шеттік есептерді шешуде есептеу алгоритмдерін құру үшін қолданысын таба алады.

Түйін сөздер: Бенджамин-Бона-Махони-Бюргерс теңдеуі, дербес туындылы дифференциалдық теңдеулер, алгоритм, жуық шешімі.

А.М. Манат, Н.Т. Орумбаева*

Карагандинский университет имени академика Е.А. Букетова, Казахстан, г. Караганда

*e-mail: orumbayevanurgul@gmail.com

Об одном решении нелокальной краевой задачи для нелинейного дифференциального уравнения в частных производных третьего порядка

В данной работе в прямоугольной области исследуется нелокальная краевая задача для уравнения Бенджамина-Бона-Махони-Бюргерса. Вводя новые функций нелокальная краевая задача для нелинейного дифференциального уравнения в частных производных третьего порядка сводится к начально-краевой задаче для гиперболического уравнения второго порядка со смешанной производной и функциональным соотношениям. Прежде чем использовать приближенный метод рассматриваемая нелинейная задача исследуется на наличие решений, необходимо уточнить, где эти решения находятся, то есть найти область изоляции решений. Область изоляции решения в нашем случае является шар, в котором решения задачи существует и единственно. Далее, предложен алгоритм нахождения решения нелокальной краевой задачи. В терминах исходных данных установлены условия сходимости алгоритмов, одновременно обеспечивающие существование и изолированность решения нелинейной нелокальной краевой задачи. Получены оценки между точным и приближенным решениями рассматриваемой задачи. Полученные результаты носят теоретический характер и могут быть использованы при построении вычислительных алгоритмов решения нелокальных краевых задач для нелинейных дифференциальных уравнений в частных производных третьего порядка.

Ключевые слова: уравнение Бенджамина-Бона-Махони-Бюргерса, дифференциальные уравнения в частных производных, алгоритм, приближенное решение.

1 Introduction

The article considers a nonlocal boundary value problem for a third-order nonlinear partial differential equation or the Benjamin-Bona-Mahony-Burgers equation. Various types of the BBMB equation were studied in [1]-[14]. Despite the presence of a large number of works devoted to the study of solving problems for the BBMB equation, interest in them has not waned to this day. This is due to the fact that the Benjamin-Bona-Mahony-Burgers equations represent an interesting and important object of study, combining wave theory, mathematical physics and practical applications. Previously, the authors used the parameterization method [15]-[17] to study more general boundary value problems for a system of linear [18]-[19] and nonlinear third-order pseudoparabolic equations. Constructive algorithms for finding approximate solutions to the problems under study were proposed and necessary and sufficient conditions for the existence of a solution were established. Subsequently, a nonlocal boundary value problem for the Benjamin-Bona-Mahony equation was studied [20]. Due to the fact that the problems under consideration are nonlinear, direct use of previously obtained results is not always possible. In this article, the Benjamin-Bona-Mahony-Burgers equation with general nonlocal boundary conditions that differ from the conditions specified in [20] is investigated. An algorithm for finding an approximate solution is proposed and conditions for the solvability of the problem under study are obtained.

2 Statement of the initial boundary problem

A nonlocal boundary value problem for the nonlinear Benjamin-Bona-Mahony-Burgers equation is considered.

$$\frac{\partial^3 w}{\partial x^2 \partial y} = \frac{\partial w}{\partial y} - \alpha \frac{\partial^2 w}{\partial x^2} + \beta \frac{\partial w}{\partial x} + w \frac{\partial w}{\partial x}, \quad (x, y) \in \Omega = [0, X] \times [0, Y], \quad (1)$$

$$w(x, 0) = \varphi(x), \quad x \in [0, X], \quad (2)$$

$$w(0, y) = \gamma(y)w(X, y) + \psi(y), \quad y \in [0, Y], \quad (3)$$

$$\frac{\partial w(0, y)}{\partial x} = \theta(y), \quad y \in [0, Y], \quad (4)$$

here α, β -const, function $\varphi(x)$ continuously differentiable on $[0, X]$, functions $\psi(y), \theta(y), \gamma(y)$ are continuously differentiable on $[0, Y]$, $\gamma(y) \neq 1$.

Let $C(\Omega, R)$ be the set of functions $w : \Omega \rightarrow R$. continuous on Ω

Function $w(x, y) \in C(\Omega, R)$ having partial derivatives $\frac{\partial w(x, y)}{\partial x} \in C(\Omega, R)$, $\frac{\partial w(x, y)}{\partial y} \in C(\Omega, R)$, $\frac{\partial^2 w(x, y)}{\partial x \partial y} \in C(\Omega, R)$, $\frac{\partial^2 w(x, y)}{\partial x^2} \in C(\Omega, R)$, $\frac{\partial^3 w(x, y)}{\partial x^2 \partial y} \in C(\Omega, R)$ is called a solution to problem (1)-(4) if it satisfies equation (1), for all $(x, y) \in \Omega$, and boundary conditions (2)-(4).

To find solutions to problem (1)-(4) we introduce new functions

$$w(0, y) = \mu(y), \quad z(x, y) = w(x, y) - \mu(y).$$

Then problem (1)-(4) can be written in the form (5)-(9)

$$\frac{\partial^3 z(x, y)}{\partial x^2 \partial y} = \frac{\partial z(x, y)}{\partial y} + \mu'(y) - \alpha \frac{\partial^2 z(x, y)}{\partial x^2} + \beta \frac{\partial z(x, y)}{\partial x} + [z(x, y) + \mu(y)] \frac{\partial z(x, y)}{\partial x}, \quad (5)$$

$$z(0, y) = 0, \quad y \in [0, Y], \quad (6)$$

$$z(x, 0) + \lambda(0) = \varphi(x), \quad \mu(0) = \varphi(0), \quad (7)$$

$$\mu(y) = \frac{\gamma(y)z(X, y) + \psi(y)}{1 - \gamma(y)}, \quad y \in [0, Y], \quad (8)$$

$$\frac{\partial z(0, y)}{\partial x} = \theta(y), \quad y \in [0, Y]. \quad (9)$$

3 Methods and materials

Differentiating equation (8) with respect to the variable y we obtain equation (10).

$$\mu'(y) = \frac{\gamma'(y)}{[1 - \gamma(y)]^2} z(X, y) + \frac{\gamma(y)}{1 - \gamma(y)} \frac{\partial z(X, y)}{\partial y} + \frac{\psi'(y)}{[1 - \gamma(y)]^2}. \quad (10)$$

By reintroducing the new function $v(x, y) = \frac{\partial z(x, y)}{\partial x}$, problem (5)-(9) and relation (10) can be written in the following form

$$\frac{\partial^2 v(x, y)}{\partial x \partial y} = \int_0^x \frac{\partial v(\xi, y)}{\partial y} d\xi + \mu'(y) - \alpha \frac{\partial v(x, y)}{\partial x} + \beta v(x, y) + \left[\int_0^x v(\xi, y) d\xi + \mu(y) \right] v(x, y), \quad (11)$$

$$v(x, 0) = \varphi'(x), \quad x \in [0, X], \quad (12)$$

$$\mu(y) = \frac{\gamma(y)}{1 - \gamma(y)} \int_0^X v(x, y) dx + \frac{\psi(y)}{1 - \gamma(y)}, \quad (13)$$

$$\mu'(y) = \frac{\gamma'(y)}{[1 - \gamma(y)]^2} \int_0^X v(x, y) dx + \frac{\gamma(y)}{1 - \gamma(y)} \int_0^X \frac{\partial v(x, y)}{\partial y} dx + \frac{\psi'(y)}{[1 - \gamma(y)]^2}, \quad (14)$$

$$v(0, y) = \theta(y), \quad y \in [0, Y], \quad (15)$$

where $z(x, y) = \int_0^x v(\xi, y) d\xi$. In (11), integrating over the variable x and taking into account conditions (15), we obtain

$$\begin{aligned} \frac{\partial v(x, y)}{\partial y} = & \theta'(y) - \alpha v(x, y) + \alpha \theta(y) + \mu'(y)x + \int_0^x \left(\int_0^\xi \frac{\partial v(\xi_1, y)}{\partial y} d\xi_1 + \right. \\ & \left. + \left[\int_0^\xi v(\xi_1, y) d\xi_1 + \mu(y) \right] v(\xi, y) + \beta v(\xi, y) \right) d\xi. \end{aligned} \quad (16)$$

After repeated integration over the variable y and application of condition (12), we obtain the following:

$$\begin{aligned} v(x, y) = & \varphi'(x) + \int_0^y \left(\theta'(\eta) - \alpha v(x, \eta) + \alpha \theta(\eta) + \mu'(\eta)x + \int_0^x \int_0^\xi \frac{\partial v(\xi_1, \eta)}{\partial \eta} d\xi_1 d\xi + \right. \\ & \left. + \int_0^x \left[\int_0^\xi v(\xi_1, \eta) d\xi_1 + \mu(\eta) \right] v(\xi, \eta) d\xi + \beta \int_0^x v(\xi, \eta) d\xi \right) d\eta. \end{aligned} \quad (17)$$

Assuming that $v(x, y) = \varphi'(x)$, from equations (13) and (14) we determine

$$\begin{aligned} \mu^{(0)}(y) &= \frac{\gamma(y)}{1 - \gamma(y)} [\varphi(X) - \varphi(0)] + \frac{\psi(y)}{1 - \gamma(y)}, \\ \mu'^{(0)}(y) &= \frac{\gamma'(y)}{[1 - \gamma(y)]^2} [\varphi(X) - \varphi(0)] + \frac{\psi'(y)}{[1 - \gamma(y)]^2}. \end{aligned}$$

Using equation (16) under the condition $\mu(y) = \mu^{(0)}(y)$, we can find

$$\begin{aligned} \frac{\partial v^{(0)}(x, y)}{\partial y} &= \theta'(y) - \alpha\varphi'(x) + \alpha\theta(y) + \\ &+ \mu'^{(0)}(y)x + \int_0^x \left[\int_0^\xi \varphi'(\xi_1) d\xi_1 + \mu^{(0)}(y) \right] \varphi'(\xi) d\xi + \beta \int_0^x \varphi'(\xi) d\xi = \\ &= \theta'(y) - \alpha\varphi'(x) + \alpha\theta(y) + \mu'^{(0)}(y)x + \int_0^x \left[\varphi(\xi) - \varphi(0) + \mu^{(0)}(y) \right] \varphi'(\xi) d\xi + \beta \int_0^x \varphi'(\xi) d\xi. \end{aligned}$$

Next, from equation (17) it follows

$$\begin{aligned} v^{(0)}(x, y) &= \varphi'(x) + \int_0^y \left(\theta'(\eta) - \alpha\varphi'(x) + \alpha\theta(\eta) + \mu'^{(0)}(y)x + \right. \\ &\left. + \int_0^x \left[\varphi(\xi) - \varphi(0) + \mu^{(0)}(\eta) \right] \varphi'(\xi) d\xi + \beta \int_0^x \varphi'(\xi) d\xi \right) d\eta. \end{aligned}$$

Taking the found functions $\mu^{(0)}(y)$ and $v^{(0)}(x, y)$, the numbers $r_1 > 0$ and $r_2 > 0$, we construct the following sets:

$$\begin{aligned} S(\mu^{(0)}(y), r_1) &= \left\{ \mu(y) \in C([0, Y], R) : \|\mu(y) - \mu^{(0)}(y)\| < r_1 \right\}, \\ S(v^{(0)}(x, y), r_2) &= \left\{ v(x, y) \in C(\Omega, R) : \|v(x, y) - v^{(0)}(x, y)\| < r_2, (x, y) \in \Omega \right\}, \\ G^0(r_1, r_2) &= \left\{ (x, y, w, v) : (x, y) \in \Omega, \left\| w(x, y) - \int_0^x v^{(0)}(\xi, y) d\xi - \mu^{(0)}(y) \right\| < \right. \\ &\left. < r_1 + r_2, \|v(x, y) - v^{(0)}(x, y)\| < r_2 \right\}. \end{aligned}$$

Let $U(l_1, l_2, x, y)$ denote the collection of quadruples $\left(\mu^{(0)}(y), v^{(0)}(x, y), r_1, r_2 \right)$, for which the function $f(x, y, w, v)$ in $G^0(r_1, r_2)$ has continuous partial derivatives $f'_w(x, y, w, v)$, $f'_v(x, y, w, v)$ and $\|f'_w(x, y, w, v)\| \leq l_1$, $\|f'_v(x, y, w, v)\| \leq l_2$, $l_{1,2} - const$. Taking the pair $\{\lambda^{(0)}(y), v^{(0)}(x, y)\}$ as the initial approximation of problem (11)-(15), we construct successive approximations using the algorithm

1. Assuming $v(x, y) = v^{(k-1)}(x, y)$, from (13) and (14) we determine $\mu'^{(k)}(y)$ и $\mu^{(k)}(y)$.
2. Using equation (16), $\mu(y) = \mu^{(k)}(y)$, we find $\frac{\partial v^{(k)}(x, y)}{\partial y}$.
3. Then, using equation (17) we find $v^{(k)}(x, y)$.

As a result, we get the system $\left\{ \mu'^{(k)}(y), \mu_r^{(k)}(x), \frac{\partial v^{(k)}(x, y)}{\partial y}, v_r^{(k)}(x, t) \right\}, k = 1, 2, \dots$

The following statement ensures the feasibility and convergence of the proposed algorithm, as well as the solvability of problem (11)-(15).

Theorem 1. Let the following conditions be satisfied

- a) the function $\varphi(x)$ is continuously differentiable on $[0, X]$,
- b) the functions $\gamma(y), \psi(y), \theta(y)$ are continuously differentiable on $[0, Y]$, $\gamma(y) \neq 1$,
- c) $q = \alpha Y + \frac{X^2 Y \gamma}{1-\gamma} + \frac{X^2 \gamma}{1-\gamma} + \frac{X^2}{2} + \frac{X^2 Y l_2}{2} + X^2 Y \frac{l_2 \gamma}{1-\gamma} + (l_1 + \beta) X Y < 1$,
- d) $\frac{\sigma}{1-q} \frac{\gamma}{1-\gamma} X Y^2 < r_1$, $\frac{q Y \sigma}{1-q} < r_2$,

where $\gamma = \max_{y \in [0, Y]} \|\gamma(y)\|$, $\psi = \max_{y \in [0, Y]} \|\psi(y)\|$, $\theta = \max_{y \in [0, Y]} \|\theta(y)\|$, $\alpha, \beta - const$,

$$\begin{aligned} \sigma = & \theta' + \alpha \max_{x \in [0, X]} \|\varphi'(x)\| + \alpha \theta + X \left(\frac{\gamma'}{[1-\gamma]^2} [\varphi(X) - \varphi(0)] + \frac{\psi'}{[1-\gamma]^2} \right) + \\ & + X \max_{x \in [0, X]} \|\varphi(x)\| \max_{x \in [0, X]} \|\varphi'(x)\| + X \left(\frac{\gamma}{1-\gamma} [\varphi(X) - \varphi(0)] + \frac{\psi}{1-\gamma} \right) \max_{x \in [0, X]} \|\varphi'(x)\| + \\ & + \beta \int_0^X \varphi'(x) dx, \end{aligned}$$

then the sequence of functions $\{\mu_r^{(k)}(x), v_r^{(k)}(x, t)\}$, $k = 1, 2, \dots$, determined by the algorithm is contained in $S(\mu^{(0)}(y), r_1) \times S(v^{(0)}(x, y), r_2)$, converges to $\{\mu^*(x), v^*(x, t)\}$ - solving problem (11)-(15). Moreover, any solution to problem (11)-(15) in $S(\mu^{(0)}(y), r_1) \times S(v^{(0)}(x, y), r_2)$ isolated and fair estimates:

- a) $\|\mu^*(y) - \lambda^{(k)}(y)\| \leq \frac{\gamma}{1-\gamma} \frac{X Y^2}{2} \sum_{i=k}^{\infty} q^i \sigma$,
- b) $\|v^*(x, y) - v^{(k)}(x, y)\| \leq Y \sum_{i=k+1}^{\infty} q^i \sigma$.

Proof. For $k = 0$ the following inequalities hold

$$\|\mu^{(0)}(y)\| \leq \frac{\gamma}{1-\gamma} [\varphi(X) - \varphi(0)] + \frac{\psi}{1-\gamma},$$

$$\left\| \mu'^{(0)}(y) \right\| \leq \frac{\gamma'}{[1-\gamma]^2} [\varphi(X) - \varphi(0)] + \frac{\psi'}{[1-\gamma]^2},$$

$$\left\| \frac{\partial v^{(0)}(x, y)}{\partial y} \right\| \leq \theta' + \alpha \max_{x \in [0, X]} \|\varphi'(x)\| + \alpha \theta + X \left(\frac{\gamma'}{[1-\gamma]^2} [\varphi(X) - \varphi(0)] + \frac{\psi'}{[1-\gamma]^2} \right) +$$

$$\begin{aligned} & + X \max_{x \in [0, X]} \|\varphi(x)\| \max_{x \in [0, X]} \|\varphi'(x)\| + X \left(\frac{\gamma}{1-\gamma} [\varphi(X) - \varphi(0)] + \frac{\psi}{1-\gamma} \right) \max_{x \in [0, X]} \|\varphi'(x)\| + \\ & + \beta \int_0^X \varphi'(x) dx = \sigma, \end{aligned}$$

$$\|v^{(0)}(x, y) - \varphi'(x)\| \leq \int_0^y \left\| \frac{\partial v^{(0)}(x, \eta)}{\partial \eta} \right\| d\eta.$$

For $k = 1$, when $v(x, y) = v^{(0)}(x, y)$, the following inequalities follow

$$\|\mu^{(1)}(y) - \mu^{(0)}(y)\| \leq \frac{\gamma'}{1-\gamma} \int_0^X \|v^{(0)}(x, \eta) - \varphi'(x)\| dx < \frac{\gamma}{1-\gamma} XY\sigma < r_1,$$

$$\left\| \mu'^{(1)}(y) - \mu'^{(0)}(y) \right\| \leq \frac{\gamma'}{[1-\gamma]^2} \int_0^X \|v^{(0)}(x, y) - \varphi'(x)\| dx + \frac{\gamma}{1-\gamma} \int_0^X \left\| \frac{\partial v^{(0)}(x, y)}{\partial y} \right\| dx,$$

$$\left\| \frac{\partial v^{(1)}(x, y)}{\partial y} - \frac{\partial v^{(0)}(x, y)}{\partial y} \right\| \leq$$

$$\leq \alpha \int_0^y \left\| \frac{\partial v^{(0)}(x, \eta)}{\partial \eta} \right\| d\eta + \frac{\gamma'x}{[1-\gamma]^2} \int_0^y \left\| \frac{\partial v^{(0)}(x, \eta)}{\partial \eta} \right\| d\eta +$$

$$+ \frac{\gamma x}{1-\gamma} \int_0^X \left\| \frac{\partial v^{(0)}(x, y)}{\partial y} \right\| dx + \int_0^x \int_0^\xi \left\| \frac{\partial v^{(0)}(\xi_1, y)}{\partial \eta} \right\| d\xi_1 d\xi +$$

$$+ l_2 \int_0^x \int_0^\xi \int_0^y \left\| \frac{\partial v^{(0)}(\xi_1, \eta)}{\partial \eta} \right\| d\eta d\xi_1 d\xi + \frac{\gamma l_2 x}{1-\gamma} \int_0^y \int_0^X \left\| \frac{\partial v^{(0)}(x, \eta)}{\partial \eta} \right\| dx d\eta +$$

$$+ l_1 \int_0^x \int_0^y \left\| \frac{\partial v^{(0)}(\xi, \eta)}{\partial \eta} \right\| d\eta d\xi + \beta \int_0^x \int_0^y \left\| \frac{\partial v^{(0)}(\xi, \eta)}{\partial \eta} \right\| d\eta d\xi \leq$$

$$\leq \left(\alpha Y + \frac{X^2 Y \gamma}{1-\gamma} + \frac{X^2 \gamma}{1-\gamma} + \frac{X^2}{2} + \frac{X^2 Y l_2}{2} + X^2 Y \frac{l_2 \gamma}{1-\gamma} + (l_1 + \beta) XY \right) \max_{(x,y) \in \Omega} \left\| \frac{\partial v^{(0)}(x, y)}{\partial y} \right\| \leq$$

$$\leq q \max_{(x,y) \in \Omega} \left\| \frac{\partial v^{(0)}(x, y)}{\partial y} \right\| \leq q\sigma.$$

$$\|v^{(1)}(x, y) - v^{(0)}(x, y)\| \leq \int_0^y \left\| \frac{\partial v^{(1)}(x, \eta)}{\partial \eta} - \frac{\partial v^{(0)}(x, \eta)}{\partial \eta} \right\| d\eta \leq \int_0^y q\sigma < r_2.$$

For $k = 2$ the following estimates hold:

$$\|\mu^{(2)}(y) - \mu^{(1)}(y)\| \leq \frac{\alpha}{1-\alpha} \int_0^X \|v^{(1)}(x, y) - v^{(0)}(x, y)\| dx \leq$$

$$\begin{aligned}
&\leq \frac{\gamma}{1-\gamma} \int_0^y \int_0^X q\sigma dx d\eta \leq \frac{\gamma}{1-\gamma} \frac{XY}{2} q\sigma, \\
\left\| \frac{\partial v^{(2)}(x, y)}{\partial y} - \frac{\partial v^{(1)}(x, y)}{\partial y} \right\| &\leq q \max_{(x, y) \in \Omega} \left\| \frac{\partial v^{(1)}(x, y)}{\partial y} - \frac{\partial v^{(0)}(x, y)}{\partial y} \right\| \leq q^2 \max_{(x, y) \in \Omega} \left\| \frac{\partial v^{(0)}(x, y)}{\partial y} \right\| \leq q^2 \sigma, \\
\|v^{(2)}(x, y) - v^{(1)}(x, y)\| &\leq \int_0^y \left\| \frac{\partial v^{(2)}(x, \eta)}{\partial \eta} - \frac{\partial v^{(1)}(x, \eta)}{\partial \eta} \right\| d\eta \leq Y q^2 \sigma. \\
\|\mu^{(2)}(y) - \mu^{(0)}(y)\| &\leq \frac{\gamma}{1-\gamma} \frac{XY}{2} q\sigma + \frac{\gamma}{1-\gamma} \frac{XY}{2} \sigma \leq \frac{\gamma}{1-\gamma} \frac{XY}{2} (1+q)\sigma < r_1, \\
\left\| \frac{\partial v^{(2)}(x, y)}{\partial y} - \frac{\partial v^{(0)}(x, y)}{\partial y} \right\| &\leq (1+q) \max_{(x, y) \in \Omega} \left\| \frac{\partial v^{(1)}(x, y)}{\partial y} - \frac{\partial v^{(0)}(x, y)}{\partial y} \right\| \leq \\
&\leq (q+q^2) \max_{(x, y) \in \Omega} \left\| \frac{\partial v^{(0)}(x, y)}{\partial y} \right\| \leq (q+q^2)\sigma. \\
\|v^{(2)}(x, y) - v^{(0)}(x, y)\| &\leq Y(q^2+q)\sigma < r_2.
\end{aligned}$$

At the $k+1$ -th step of the algorithm, for $v(x, y) = v^{(k)}(x, y)$, the following estimates hold

$$\|\mu^{(k+1)}(y) - \mu^{(k)}(y)\| \leq \frac{\gamma}{1-\gamma} \int_0^y \int_0^X \|v^{(k)}(x, \eta) - v^{(k-1)}(x, \eta)\| dx d\eta, \quad (18)$$

$$\left\| \mu'^{(k+1)}(y) - \mu'^{(k)}(y) \right\| \leq \frac{\gamma}{1-\gamma} \int_0^X \|v^{(k)}(x, y) - v^{(k-1)}(x, y)\| dx, \quad (19)$$

$$\left\| \frac{\partial v^{(k+1)}(x, y)}{\partial y} - \frac{\partial v^{(k)}(x, y)}{\partial y} \right\| \leq q \max_{(x, y) \in \Omega} \left\| \frac{\partial v^{(k)}(x, y)}{\partial y} - \frac{\partial v^{(k-1)}(x, y)}{\partial y} \right\|, \quad (20)$$

$$\|v^{(k+1)}(x, y) - v^{(k)}(x, y)\| \leq \int_0^y \left\| \frac{\partial v^{(k+1)}(x, \eta)}{\partial \eta} - \frac{\partial v^{(k)}(x, \eta)}{\partial \eta} \right\| d\eta. \quad (21)$$

$$\begin{aligned}
&\|\mu^{(k+1)}(y) - \mu^{(0)}(y)\| \leq \\
&\leq \frac{\gamma}{1-\gamma} \int_0^y \int_0^X \|v^{(k)}(x, \eta) - \varphi'(x)\| dx d\eta \leq \frac{\gamma}{1-\gamma} \frac{XY}{2} \sum_{i=0}^k q^i \sigma < r_1,
\end{aligned}$$

$$\|v^{(k+1)}(x, y) - v^{(0)}(x, y)\| \leq Y \sum_{i=1}^{k+1} q^i \sigma < r_2.$$

Consequently, from inequalities (18)-(21) and $q < 1$ it follows that the sequence $\{\mu^{(k)}(y), v^{(k)}(x, y)\}$ at $k \rightarrow \infty$, converges to $\{\mu^*(y), v^*(x, y)\}$ — solution of problem (10)-(14) in $S(\mu^{(0)}(y), r_1) \times S(v^{(0)}(x, y), r_2)$.

Let's establish inequalities

$$\|\mu^{(k+p)}(y) - \mu^{(k)}(y)\| \leq \frac{\gamma}{1-\gamma} \frac{XY}{2} \sum_{i=k}^{k+p-1} q^i \sigma, \quad (22)$$

$$\|v^{(k+p)}(x, y) - v^{(k)}(x, y)\| \leq Y \sum_{i=k+1}^{k+p} q^i \sigma. \quad (23)$$

for $p \rightarrow \infty$ we obtain estimates a), b) of Theorem 1.

Let's prove uniqueness. The uniqueness of the solution of problem (1)-(4) is proved similarly to the proof of Theorem 1 from [18]. Theorem 1 is proved.

The function $w^{(k)}(x, y)$, $k = 1, 2, 3, \dots$ is determined from the equality

$$w^{(k)}(x, y) = \mu^{(k)}(x, y) + \int_0^x v^{(k)}(\xi, y) d\xi, \quad (x, y) \in \Omega.$$

Let $S_1(w^{(0)}(x, y), r_1 + r_2x)$ denote the set of continuously differentiable with respect to x, y functions $w : \Omega \rightarrow R$, satisfying the inequality $\|w(x, y) - w^{(0)}(x, y)\| < r_1 + r_2x$.

In view of the equivalence of problems (1)-(4) and (11)-(15), Theorem 1 implies.

Theorem 2. If the conditions of Theorem 1 are satisfied, then the sequence of functions $w^{(k)}(x, y)$, $k = 1, 2, \dots$, is contained in $S(w^{(0)}(x, y), r_1 + r_2)$ converges to the unique solution $w^*(x, y)$ of problem (1)-(4) in $S(w^{(0)}(x, y), r_1 + r_2)$ and the inequality

$$\|w^*(x, y) - w^{(k)}(x, y)\| \leq \frac{\gamma}{1-\gamma} \frac{X^2Y^2}{2} \sum_{i=k+1}^{\infty} q^i \sigma + Y \sum_{i=k}^{\infty} q^i \sigma.$$

4 Conclusion

Thus, the third-order nonlinear Benjamin-Bona-Mahony-Burgers equation with nonlocal conditions has been studied. The Benjamin-Bona-Mahony-Burgers equation describes the propagation of small amplitude waves in a nonlinear dispersive medium when simulating unidirectional plane waves. In this paper, an algorithm for searching for an approximate solution to the problem under consideration is proposed and the conditions for the convergence of the proposed algorithm are determined. An estimate between the exact and approximate solution of the nonlinear problem is obtained.

5 Acknowledgements

This research is funded by the Science Committee of the Ministry of Education and Science of the Republic of Kazakhstan (Grants No. AP23488729, 2024-2026)

References

- [1] Benjamin T.B., Bona J.L., Mahony J.J., *Model equations for long waves in nonlinear dispersive systems*, *Philosophical transactions of the royal society a mathematical, physical and engineering sciences*, 1220, (1972), 47-78. <https://doi.org/10.1098/rsta.1972.0032>.
- [2] Al-Khaled K., Momani S., Alawneh A., *Approximate wave solutions for generalized Benjamin-Bona-Mahony-Burgers equations*, *Applied Mathematics and Computation*, 171, (2005) 281-292. <https://doi.org/10.1016/j.amc.2005.01.056>
- [3] Arora G., Mittal R.C., Singh B.K., *Numerical solution of BBM-Burger equation with quadratic b-spline collocation method*, *Journal of Engineering Science and Technology*, 9 (2014), 104-116.
- [4] Dehghan M., Abbaszadeh M., Mohebbi A., *The numerical solution of nonlinear high dimensional generalized Benjamin-Bona-Mahony-Burgers equation via the meshless method of radial basis functions*, *Computer and Mathematics with Applications*, 68, (2014), 212-237. <https://doi.org/10.1016/j.camwa.2014.05.019>
- [5] Chunhuan Xiang, Honglei Wang, *New Exact Solutions for Benjamin-Bona-Mahony-Burgers Equation*, *Open Journal of Applied Sciences*, 10, (2020), 543-550. <https://doi.org/10.4236/ojapps.2020.108038>
- [6] Hajiketabi M., Abbasbandy S., Casas F., *The Lie-group method based on radial basis functions for solving nonlinear high dimensional generalized Benjamin-Bona-Mahony-Burgers equation in arbitrary domains*, *Applied Mathematics and Computation* 321 (2018), 223-243. <https://doi.org/10.1016/j.amc.2017.10.051>
- [7] Izadi M., Samei M.E., *Time accurate solution to Open Access Benjamin-Bona-Mahony-Burgers equation via Taylor-Boubaker series scheme*, *Springer open journal*, 17, (2022), 1-29. <https://doi.org/10.1186/s13661-022-01598-x>
- [8] Kanth A.R., Deepika S., *Non-polynomial spline method for one dimensional nonlinear Benjamin-Bona-Mahony-Burgers equation*, *Int. J. Nonlinear Sci. Numer. Simul*, 18(3-4), (2017), 277-284. <https://doi.org/10.1515/ijnsns-2016-0136>
- [9] Korpusov M. O., Panin A. A., *Local solvability and solution blowup for the Benjamin-Bona-Mahony-Burgers equation with a nonlocal boundary condition*, *Theoretical and Mathematical Physics* 175:2 (2013), 580-591. <https://doi.org/10.4213/tmf8417>
- [10] Mei M., *Large-time behavior of solution for generalized Benjamin-Bona-Mahony Burgers equations*, *Nonlinear Analysis: Theory, Methods and Applications* **33** (1998), 699-714. [https://doi.org/10.1016/S0362-546X\(97\)00674-3](https://doi.org/10.1016/S0362-546X(97)00674-3)
- [11] Kozhanov A.I., Lukina G.A., *Pseudoparabolic and pseudohyperbolic equations in noncylindrical time domains*, *Mathematical Notes NEFU*, 3(26), (2019), 15-30. <https://doi.org/10.25587/SVFU.2019.17.12.002>
- [12] Oruc O., *A new algorithm based on Lucas polynomials for approximate solution of 1D and 2D nonlinear generalized Benjamin-Bona-Mahony-Burgers equation*, *Computer and Mathematics with Applications*, 74, (2017), 3042-3057. <https://doi.org/10.1016/j.camwa.2017.07.046>
- [13] Shallu V.K.K., *Numerical treatment of Benjamin-Bona-Mahony-Burgers equation with fourth-order improvised b-spline collocation method*, *Journal of Ocean Engineering and Science*, 7, (2021), 99-111. <https://doi.org/10.1016/j.joes.2021.07.001>
- [14] Zhao T., Zhang X., Huo, J., Su, W., Liu, Y., Wu, Y., *Optimal error estimate of Chebyshev-Legendre spectral method for the generalised Benjamin-Bona-Mahony-Burgers equations*, *Abstract and Applied Analysis*, (2012). <http://dx.doi.org/10.1155/2012/106343>
- [15] Asanova A. T., Dzhumabaev D. S., *Well-posedness of nonlocal boundary value problems with integral condition for the system of hyperbolic equations*, *Journal of Mathematical Analysis and Applications*, 402:1 (2013), 167-178. <https://doi.org/10.1016/j.jmaa.2013.01.012>
- [16] Dzhumabayev D. S., *Criteria for the unique solvability of a linear boundary-value problem for an ordinary differential equation*, *USSR Computational Mathematics and Mathematical Physics*, 29:1 (1989), 34-46. [https://doi.org/10.1016/0041-5553\(89\)90038-4](https://doi.org/10.1016/0041-5553(89)90038-4)
- [17] Dzhumabaev D. S., Temesheva S. M., *A parametrization method for solving nonlinear two-point boundary value problems*, *Computational Mathematics and Mathematical Physics*, 47:1 (2007), 37-61. <https://doi.org/10.1134/S096554250701006X>
- [18] Orumbayeva N.T., Keldibekova A.B. *On One Solution of a Periodic Boundary-Value Problem for a Third-Order Pseudoparabolic Equation*, *LOBACHEVSKII JOURNAL OF MATHEMATICS*, 41(9) (2020), 1864-1872. <http://dx.doi.org/10.1134/S1995080220090218>

-
- [19] Keldibekova A. B., *Solvability of a semi-periodic boundary value problem for a third order differential equation with mixed derivative*, *Bulletin of the Karaganda University Mathematics Series*, 98(2), (2020), 84-99. <http://dx.doi.org/10.31489/2020M2/84-99>
- [20] Manat A.M., Orumbayeva N.T., *On one approximate solution of nonlocal boundary value problem for the Benjamin-Bona-Mahony equation*, *Bulletin of the Karaganda University Mathematics Series*, 2(110), (2023), 84-92. <http://dx.doi.org/10.31489/2023M2/84-92>

IRSTI 20.15.05

DOI: <https://doi.org/10.26577/JMMCS202412118>

A.R. Ryskan^{1,2*} , Z.O. Arzikulov^{3,4} , T.G. Ergashev^{4,5} 
¹Abai Kazakh National Pedagogical University, Kazakhstan, Almaty
²Narxoz University, Kazakhstan, Almaty
³Fergana Polytechnic Institute, Uzbekistan, Fergana
⁴TIIAME National Research University, Uzbekistan, Tashkent
⁵Ghent University, Ghent, Belgium
*e-mail: ryskan.a727@gmail.com

PARTICULAR SOLUTIONS OF MULTIDIMENSIONAL GENERALIZED EULER-POISSON-DARBOUX EQUATIONS OF ELLIPTIC-HYPERBOLIC TYPE

The primary outcome of this study is the construction of partial solutions for a class of multidimensional partial differential equations with multiple singular coefficients of the second order. We consider the generalized multidimensional second-order Euler-Poisson-Darboux equation. Employing a well-known method, we reduce the generalized Euler-Poisson-Darboux equation to a second-order partial differential equation of the hypergeometric type. The solutions to this second order hypergeometric equation comprise 2^n functions that contain the first Lauricella hypergeometric function. The Lauricella function, also known as an n-dimensional series, incorporates three distinct parameters - the Pochhammer polynomials. To study the properties of these particular solutions, we require a decomposition formula expressing the first Lauricella function as the product of simpler hypergeometric functions with fewer variables. Through this study of particular solutions and the determination of singularity order at the origin, we establish the uniqueness of these solutions. Thus, having proved the peculiarity of particular solutions at the origin, it can be argued that the constructed particular solutions are fundamental solutions of the generalized multidimensional second-order Euler-Poisson-Darboux equation.

Key words: multidimensional generalized Euler-Poisson-Darboux equation, particular solutions, Lauricella's hypergeometric function, expansion formula, order of the singularity.

А.Р. Рысқан^{1,2*}, З.О. Арзикулов^{3,4}, Т.Г. Эргашев^{4,5}

¹Абай атындағы Қазақ ұлттық педагогикалық университеті, Қазақстан, Алматы қ.

²Нархоз университеті, Қазақстан, Алматы қ.

³Ферғана политехникалық институты, Өзбекстан, Ферғана қ.

⁴ТIIАШМИ Ұлттық зерттеу университеті, Өзбекстан, Ташкент қ.

⁵Гент университеті, Бельгия, Гент қ.

*e-mail: ryskan.a727@gmail.com

Эллиптикалық-гиперболалық типтегі Эйлер-Пуассон-Дарбу көпөлшемді жалпыланған теңдеулердің дербес шешімдері

Осы жұмыстың негізгі нәтижесі екінші ретті бірнеше сингулярлық коэффициенттері бар көп айнымалы дербес туындылы дифференциалдық теңдеулер класы үшін дербес шешімдерді құру болып табылады. Эйлер-Пуассон-Дарбудың екінші ретті жалпыланған көп өлшемді теңдеуі қарастырылады. Белгілі әдіс көмегімен Эйлер-Пуассон-Дарбу жалпыланған теңдеуі гипергеометриялық типтегі екінші ретті дербес туындылы дифференциалдық теңдеуге әкеледі. Екінші ретті гипергеометриялық теңдеудің шешімдері құрамында Лауричелланың алғашқы гипергеометриялық функциясы бар 2^n функциялар болып табылады.

Лауричелланың функциясы деп аталатын функция бұл үш түрлі параметрден тұратын, яғни Похгаммер көпмүшелерінен құрылған n -өлшемді қатар. Дербес шешімдердің қасиеттерін зерттеу үшін Лауричелланың бірінші функциясын аз айнымалылары бар бірнеше қарапайым гипергеометриялық функциялардың көбейтіндісі түрінде келтіретін ыдырау формуласы қажет. Дербес шешімдердің қасиеттері зерттеледі, осылайша координаттардың басындағы ерекшеліктің реті анықталады. Координаттардың басында дербес шешімдердің ерекшелігін дәлелдей отырып, құрылған дербес шешімдер Эйлер-Пуассон-Дарбудың жалпыланған екінші ретті көп өлшемді теңдеуінің іргелі шешімдері болып табылады деп айтуға болады.

Түйін сөздер: Эйлер-Пуассон-Дарбудың көпөлшемді жалпыланған теңдеуі, ерекше шешімдер, Лауричелла гипергеометриялық функциясы, жіктеу формуласы, ерекшелік реті.

А.Р. Рысқан^{1,2*}, З.О. Арзикулов^{3,4}, Т.Г. Эргашев^{4,5}

¹Казахский национальный педагогический университет имени Абая, Казахстан, г. Алматы

²Университет Нархоз, Казахстан, г. Алматы

³Ферганский политехнический институт, Узбекистан, г. Фергана

⁴Национальный исследовательский университет ТИИМСХ, Узбекистан, г. Ташкент

⁵Гентский университет, Бельгия, г. Гент

*e-mail: ryskan.a727@gmail.com

Частные решения многомерных обобщенных уравнений Эйлера-Пуассона-Дарбу эллиптико-гиперболического типа

Основным результатом настоящей работы является построение частных решений для класса многомерных уравнений в частных производных с несколькими сингулярными коэффициентами второго порядка. Рассматривается обобщенное многомерное уравнение второго порядка Эйлера-Пуассона-Дарбу. С помощью известного метода обобщенное уравнение Эйлера-Пуассона-Дарбу приводится к дифференциальному уравнению в частных производных второго порядка гипергеометрического типа. Решениями гипергеометрического уравнения второго порядка являются 2^n функций, которые содержат в себе первую гипергеометрическую функцию Лауричелла. Так называемая функция Лауричелла представляет собой n -мерный ряд, содержащий три разных параметра - многочлены Похгаммера. Для исследования свойств частных решений необходима формула разложения, которая выражала бы первую функцию Лауричелла в терминах произведения нескольких более простых гипергеометрических функций, содержащих меньшее количество переменных. Изучаются свойства частных решений, таким образом определяется порядок особенности в начале координат. Доказав особенность частных решений в начале координат, можно утверждать о том, что построенные частные решения являются фундаментальными решениями обобщенного многомерного уравнения второго порядка Эйлера-Пуассона-Дарбу.

Ключевые слова: многомерное обобщенное уравнение Эйлера-Пуассона-Дарбу, частные решения, гипергеометрическая функция Лауричелла, формула разложения, порядок особенности.

1 Introduction

It is known that particular solutions have an essential role in studying partial differential equations. In case of the singular elliptic equations, the role of particular solutions is played by fundamental solutions. Formulation and solving of many local and non-local boundary value problems are based on these solutions. The explicit form of particular solutions gives a possibility to study the considered equation in detail. For example, in the works of Barros-Neto and Gelfand [1–3] fundamental solutions for Tricomi operator in the plane were explicitly calculated.

Particular solutions of generalized Euler-Poisson-Darboux equation

$$u_{xx} + u_{yy} + \frac{2\alpha}{x}u_x + \frac{2\beta}{y}u_y = u_{tt} + \frac{2\gamma}{t}u_t, \quad x > 0, y > 0, t > 0$$

were found in [4], where α , β and γ are constants ($0 < 2\alpha, 2\beta, 2\gamma < 1$).

It is well known [5] that all linearly-independent fundamental solutions of the singular elliptic equation

$$\sum_{j=1}^m \frac{\partial^2 u}{\partial x_j^2} + \sum_{j=1}^n \frac{2\alpha_j}{x_j} \frac{\partial u}{\partial x_j} = 0, \quad m \geq 2, n \leq m \quad (1)$$

in the first hyperoctant $x_1 > 0, \dots, x_n > 0$ are expressed explicitly by a hypergeometric function $F_A^{(n)}$ in n variables introduced by Lauricella [6]. Fundamental solutions of the equation (1) in its various special cases were constructed by many authors [7–10] and applied to the solution of boundary value problems for the equation (1) up to dimension $m \leq 4$ [11–13]. Further applications of fundamental solutions of the equation (1) can be found in the works [14–16].

In this paper, we construct a particular solutions of multidimensional generalized Euler-Poisson-Darboux equation

$$\sum_{j=1}^k \frac{\partial^2 u}{\partial x_j^2} + \sum_{j=1}^k \frac{2\alpha_j}{x_j} \frac{\partial u}{\partial x_j} = \sum_{j=k+1}^n \frac{\partial^2 u}{\partial x_j^2} + \sum_{j=k+1}^n \frac{2\alpha_j}{x_j} \frac{\partial u}{\partial x_j}, \quad k = \overline{1, n-1} \quad (2)$$

in the n -dimensional cone

$$\Omega = \{(x_1, \dots, x_n) : x_1^2 + \dots + x_k^2 > x_{k+1}^2 + \dots + x_n^2, \quad k = \overline{1, n-1}\},$$

where α_j are constants ($0 < 2\alpha_j < 1$, $j = \overline{1, n}$). It turns out that particular solutions of the equation (2) are also expressed in terms of the Lauricella function $F_A^{(n)}$ with variables, however, which differ from the variables of the functions involved in the fundamental solutions of the singular elliptic equation (1).

In investigation of the particular solutions for the singular partial differential equations, we need expansions for hypergeometric functions of several variables in terms of simpler hypergeometric functions of (for example) the Gauss and Appell types.

The familiar operator method of Burcnall and Chaundy [17, 18] has been used by them rather extensively for finding decomposition formulas for hypergeometric functions of two variables in terms of the classical Gauss hypergeometric function of one variable.

Following the works [17, 18], Hasanov and Srivastava [19, 20] introduced operators generalizing the Burcnall-Chaundy operators and found expansion formulas for many triple hypergeometric functions, and they proved recurrent formulas when the dimension of hypergeometric function exceeds three. However, due to the recurrence, additional difficulties may arise in the applications of those decomposition formulas. For two Lauricella hypergeometric functions in n variables are proved new expansion formulas which are free from the recurrence [21]. The most recent properties of Lauricella's hypergeometric function F_A^n can be found in [22].

The plan of this paper is as follows. In Section 2 we briefly give some preliminary information, which will be used later: definitions of Pochhammer symbol, Gaussian and Lauricella hypergeometric functions; a system of PDE satisfied by Lauricella hypergeometric function $F_A^{(n)}$ and its linearly-independent solutions. In Section 3 the expansion formula for the Lauricella function and consequences from this formula are given.

In Section 4 we describe the method of finding particular solutions for the considered equation and in Section 5 we show what order of singularity the found solutions will have.

2 Preliminaries

Below we give definition of Pochhammer symbol and some formulas for Gauss hypergeometric function, definition of Lauricella hypergeometric function $F_A^{(n)}$ and system of partial differential equations which can be satisfied by the Lauricella function $F_A^{(n)}$.

First we define a Pochhammer symbol and Gaussian hypergeometric function.

A symbol $(\kappa)_\nu$ denotes the general Pochhammer symbol or the shifted factorial, since $(1)_l = l!$ ($l \in N \cup \{0\}$; $N := \{1, 2, 3, \dots\}$), which is defined (for $\kappa, \nu \in C$), in terms of the familiar Gamma function, by

$$(\kappa)_\nu := \frac{\Gamma(\kappa + \nu)}{\Gamma(\kappa)} = \begin{cases} 1 & (\nu = 0; \kappa \in C \setminus \{0\}) \\ \kappa(\kappa + 1)\dots(\kappa + l - 1) & (\nu = l \in N; \kappa \in C), \end{cases}$$

it being understood conventionally that $(0)_0 := 1$ and assumed tacitly that the Γ -quotient exists.

A function

$$F(a, b; c; x) \equiv F \left[\begin{matrix} a, b \\ c \end{matrix}; x \right] = \sum_{k=0}^{\infty} \frac{(a)_k (b)_k}{(c)_k} \frac{x^k}{k!}, \quad |x| < 1 \quad (3)$$

is known as the Gauss hypergeometric function and an equality

$$F(a, b; c; 1) = \frac{\Gamma(c)\Gamma(c-a-b)}{\Gamma(c-a)\Gamma(c-b)}, \quad c \neq 0, -1, -2, \dots, \operatorname{Re}(c-a-b) > 0 \quad (4)$$

holds [23, p.73,(14)]. Moreover, the following Boltz formula [23, p.76,(22)]

$$F(a, b; c; x) = (1-x)^{-b} F \left(c-a, b; c; \frac{x}{x-1} \right) \quad (5)$$

is valid.

Lauricella hypergeometric function $F_A^{(n)}$ in $n \in N$ (real or complex) variables is defined as following [6]

$$F_A^{(n)}(a, \mathbf{b}; \mathbf{c}; \mathbf{x}) \equiv F \left[\begin{matrix} a, \mathbf{b} \\ \mathbf{c} \end{matrix}; \mathbf{x} \right] = \sum_{|\mathbf{k}|=0}^{\infty} (a)_{|\mathbf{k}|} \prod_{j=1}^n \frac{(b_j)_{k_j}}{(c_j)_{k_j}} \frac{x_j^{k_j}}{k_j!}, \quad \sum_{j=1}^n |x_j| < 1, \quad (6)$$

where

$$\mathbf{a} := (a_1, \dots, a_n), \quad \mathbf{b} := (b_1, \dots, b_n), \quad \mathbf{c} := (c_1, \dots, c_n);$$

$$\mathbf{x} := (x_1, \dots, x_n); |\mathbf{k}| := k_1 + \dots + k_n, k_1 \geq 0, \dots, k_n \geq 0.$$

In definition (6), as usual, the denominator parameters c_1, \dots, c_n are neither zero nor a negative integer.

Lauricella function $\omega(\mathbf{x}) = F_A^{(n)}(a, \mathbf{b}; \mathbf{c}; \mathbf{x})$ satisfies the system of equations [24, p. 117]

$$\begin{aligned} x_j(1-x_j) \frac{\partial^2 \omega}{\partial x_j^2} - x_j \sum_{\substack{i=1 \\ i \neq j}}^n x_i \frac{\partial^2 \omega}{\partial x_i \partial x_j} - b_j \sum_{\substack{i=1 \\ i \neq j}}^n x_i \frac{\partial \omega}{\partial x_i} \\ + [c_j - (a + b_j + 1)x_j] \frac{\partial \omega}{\partial x_j} - ab_j \omega = 0, \quad j = \overline{1, n} \end{aligned} \quad (7)$$

and, in turn, this system has 2^n linearly independent solutions [24, p.118]

$$\begin{aligned} 1 : & \left\{ F_A^{(n)} \left[\begin{array}{c} a, b_1, \dots, b_n; \\ c_1, \dots, c_n; \end{array} \mathbf{x} \right], \right. \\ n : & \left\{ \begin{array}{l} x_1^{1-c_1} F_A^{(n)} \left[\begin{array}{c} a+1-c_1, b_1+1-c_1, b_2, \dots, b_n; \\ 2-c_1, c_2, \dots, c_n; \end{array} \mathbf{x} \right], \\ \dots \\ x_n^{1-c_n} F_A^{(n)} \left[\begin{array}{c} a+1-c_n, b_1, \dots, b_{n-1}, b_n+1-c_n; \\ c_1, \dots, c_{n-1}, 2-c_n; \end{array} \mathbf{x} \right], \\ \dots \\ x_1^{1-c_1} x_2^{1-c_2} F_A^{(n)} \left[\begin{array}{c} a+2-c_1-c_2, b_1+1-c_1, b_2+1-c_2, b_3, \dots, b_n; \\ 2-c_1, 2-c_2, c_3, \dots, c_n; \end{array} \mathbf{x} \right], \\ \dots \\ x_1^{1-c_1} x_n^{1-c_n} F_A^{(n)} \left[\begin{array}{c} a+2-c_1-c_n, b_1+1-c_1, b_2, \dots, b_{n-1}, b_n+1-c_n; \\ 2-c_1, c_2, \dots, c_{n-1}, 2-c_n; \end{array} \mathbf{x} \right], \\ \dots \\ x_2^{1-c_2} x_3^{1-c_3} F_A^{(n)} \left[\begin{array}{c} a+2-c_2-c_3, b_1, b_2+1-c_2, b_3+1-c_3, b_4, \dots, b_n; \\ c_1, 2-c_2, 2-c_3, c_4, \dots, c_n; \end{array} \mathbf{x} \right], \\ \dots \\ x_{n-1}^{1-c_{n-1}} x_n^{1-c_n} \times \\ \quad \times F_A^{(n)} \left[\begin{array}{c} a+2-c_{n-1}-c_n, b_1, \dots, b_{n-2}, b_{n-1}+1-c_{n-1}, b_n+1-c_n; \\ c_1, \dots, c_{n-2}, 2-c_{n-1}, 2-c_n; \end{array} \mathbf{x} \right], \\ \dots \\ x_1^{1-c_1} \dots x_n^{1-c_n} F_A^{(n)} \left[\begin{array}{c} a+n-c_1-\dots-c_n, b_1+1-c_1, \dots, b_n+1-c_n; \\ 2-c_1, \dots, 2-c_n; \end{array} \mathbf{x} \right]. \end{array} \right. \end{aligned}$$

3 Methods and materials. Expansions of Lauricella function $F_A^{(n)}$

For a given multivariable function, it is useful to find a decomposition formula which would express the multivariable hypergeometric function in terms of products of several simpler hypergeometric functions involving fewer variables.

Burchnell and Chaundy [17, 18] systematically presented a number of expansion and decomposition formulas for some double hypergeometric functions in series of simpler

hypergeometric functions. For example, the Appell function

$$F_2 \left[\begin{matrix} a, b_1, b_2; \\ c_1, c_2; \end{matrix} x, y \right] = \sum_{m,n=0}^{\infty} \frac{(a)_{m+n} (b_1)_m (b_2)_n}{(c_1)_m (c_2)_n} \frac{x^m y^n}{m! n!}, \quad |x| + |y| < 1$$

has the expansion [17]

$$F_2 \left[\begin{matrix} a, b_1, b_2; \\ c_1, c_2; \end{matrix} x, y \right] = \sum_{r=0}^{\infty} \frac{(a)_r (b_1)_r (b_2)_r}{r! (c_1)_r (c_2)_r} x^r y^r F \left[\begin{matrix} a+r, b_1+r; \\ c_1+r; \end{matrix} x \right] F \left[\begin{matrix} a+r, b_2+r; \\ c_2+r; \end{matrix} y \right].$$

Following the works [17, 18] Hasanov and Srivastava found a decomposition formulas for all four Lauricella functions of three variables [19] and proved a recurrence formulas at arbitrary $n \in N \setminus \{1\}$ [20]. However, due to the recurrence of Hasanov-Srivastava's decomposition formulas, additional difficulties may arise in the applications of this expansions. Further study of the properties of the Lauricella function $F_A^{(n)}$ showed that known decomposition formula can be reduced to a more convenient (nonrecurrence) form.

With any natural numbers $n \in N \setminus \{1\}$ the following expansion formula holds true [22]:

$$F_A^{(n)}(a, \mathbf{b}; \mathbf{c}; \mathbf{x}) = \sum_{|\mathbf{m}_n|=0}^{\infty} \frac{(a)_{A(n,n)}}{M_{i,j}!} \prod_{k=1}^n \frac{(b_k)_{B(k,n)}}{(c_k)_{B(k,n)}} x_k^{B(k,n)} F \left[\begin{matrix} a + A(k, n), b_k + B(k, n); \\ c_k + B(k, n); \end{matrix} x_k \right], \quad (8)$$

where

$$|\mathbf{m}_n| = \sum_{i=2}^n \sum_{j=i}^n m_{i,j}, \quad m_{i,j} \geq 0, \quad 2 \leq i \leq j \leq n;$$

$$M_{i,j}! = m_{2,2}! m_{2,3}! \cdots m_{i,j}! \cdots m_{n,n}!, \quad 2 \leq i \leq j \leq n;$$

$$A(k, n) = \sum_{i=2}^{k+1} \sum_{j=i}^n m_{i,j}, \quad B(k, n) = \sum_{i=2}^k m_{i,k} + \sum_{i=k+1}^n m_{k+1,i}.$$

In case $n = 1$, the formula (8) is greatly simplified and coincides with the definition of the single hypergeometric function (3).

Using expansion (8) and Boltz formula (5), it is easy to derive an analogue of the Boltz formula for the Lauricella hypergeometric function in the form

$$F_A^{(n)}(a, \mathbf{b}; \mathbf{c}; \mathbf{x}) = \sum_{|\mathbf{m}_n|=0}^{\infty} \frac{(a)_{A(n,n)}}{M_{i,j}!} \prod_{k=1}^n \frac{(b_k)_{B(k,n)}}{(c_k)_{B(k,n)}} \left(\frac{x_k}{1-x_k} \right)^{B(k,n)} \times \\ \times \prod_{k=1}^n (1-x_k)^{-b_k} F \left[\begin{matrix} c_k - a + B(k, n) - A(k, n), b_k + B(k, n); \\ c_k + B(k, n); \end{matrix} \frac{x_k}{x_k - 1} \right]. \quad (9)$$

Let a, b_1, \dots, b_n are real numbers with $a \neq 0, -1, -2, \dots$ and $a > |\mathbf{b}|$, where $|\mathbf{b}| := b_1 + \dots + b_n$. Then $n = 1, 2, \dots$, the following summation formula holds true [21]

$$\sum_{|\mathbf{m}_n|=0}^{\infty} \frac{(a)_{A(n,n)}}{M_n!} \prod_{k=1}^n \frac{(b_k)_{B(k,n)} (a - b_k)_{A(k,n) - B(k,n)}}{(a)_{A(k,n)}} = \frac{\Gamma(a - |\mathbf{b}|)}{\Gamma(a)} \prod_{k=1}^n \frac{\Gamma(a)}{\Gamma(a - b_k)}. \quad (10)$$

It is easy to see that formula (10) is a natural generalization of the well-known summation formula (4).

Let a, b_k, c_k be real numbers, where $c_k \neq 0, -1, -2, \dots$ and $a > |\mathbf{b}| > 0$ and $c_k > b_k$. Then for $n = 1, 2, \dots$, the following limit correlation is true

$$\lim_{\varepsilon \rightarrow 0} \left\{ \varepsilon^{-b_1 - \dots - b_n} F_A^{(n)} \left(a, \mathbf{b}; \mathbf{c}; 1 - \frac{z_1(\varepsilon)}{\varepsilon}, \dots, 1 - \frac{z_n(\varepsilon)}{\varepsilon} \right) \right\} = \frac{\Gamma(a - |\mathbf{b}|)}{\Gamma(a)} \prod_{k=1}^n \frac{|z_k(0)|^{-b_k} \Gamma(c_k)}{\Gamma(c_k - b_k)}. \quad (11)$$

where $z_k(\varepsilon)$ are arbitrary functions, and $z_k(0) \neq 0$.

Limit correlation (11) directly follows from decomposition (9) and summation formula (10).

4 Particular solutions

Consider equation (2) in Ω . Let $x := (x_1, \dots, x_n)$ be any point and $x_0 := (x_{01}, \dots, x_{0n})$ be any fixed point of Ω . We search for a solution of (2) as follows:

$$u_k(x, x_0) = P(r_k) \omega(\xi_k), \quad k = \overline{1, n}, \quad (12)$$

where ω is unknown function and

$$P(r_k) = r_k^{-2\beta}, \quad \beta = \frac{n-2}{2} + \sum_{j=1}^n \alpha_j; \quad (13)$$

$$r_k^2 = \sum_{i=1}^n \operatorname{sgn}(k-i)(x_i - x_{0i})^2, \quad \operatorname{sgn}(z) := \begin{cases} 1, & \text{if } z \geq 0, \\ -1, & \text{if } z < 0; \end{cases} \quad (14)$$

$$\xi_k := (\xi_{k1}, \xi_{k2}, \dots, \xi_{kn}), \quad \xi_{kj} = \operatorname{sgn}(k-j) \frac{r_k^2 - r_{kj}^2}{r_k^2}, \quad (15)$$

$$r_{kj}^2 = \operatorname{sgn}(k-j)(x_j + x_{0j})^2 + \sum_{\substack{i=1 \\ i \neq j}}^n \operatorname{sgn}(k-i)(x_i - x_{0i})^2, \quad k, j = \overline{1, n}.$$

In what follows for brevity, we omit the index (letter) k in the notations $u_k, r_k, \xi_{k1}, \dots, \xi_{kn}$.

Let us calculate the necessary derivatives of the desired solution

$$\frac{\partial u}{\partial x_j} = \omega \frac{\partial P}{\partial x_j} + P \sum_{i=1}^n \frac{\partial \omega}{\partial \xi_i} \frac{\partial \xi_i}{\partial x_j}, \quad j = \overline{1, n},$$

$$\frac{\partial^2 u}{\partial x_j^2} = P \sum_{i=1}^n \sum_{l=1}^n \frac{\partial \xi_i}{\partial x_j} \frac{\partial \xi_l}{\partial x_j} \frac{\partial^2 \omega}{\partial \xi_i \partial \xi_l} + \sum_{i=1}^n \left(2 \frac{\partial P}{\partial x_j} \frac{\partial \xi_i}{\partial x_j} + P \frac{\partial^2 \xi_i}{\partial x_j^2} \right) \frac{\partial \omega}{\partial \xi_i} + \omega \frac{\partial^2 P}{\partial x_j^2}, \quad j = \overline{1, n}$$

and substitute into equation (2):

$$\sum_{i=1}^n A_{ik} \frac{\partial^2 \omega}{\partial \xi_i^2} + \sum_{i=1}^n \sum_{l=i+1}^n B_{ilk} \frac{\partial^2 \omega}{\partial \xi_i \partial \xi_l} + \sum_{i=1}^n C_{ik} \frac{\partial \omega}{\partial \xi_i} + D_k \omega = 0, \quad (16)$$

where

$$A_{ik} = P \sum_{j=1}^n \operatorname{sgn}(k-j) \left(\frac{\partial \xi_i}{\partial x_j} \right)^2, \quad (17)$$

$$B_{ilk} = 2P \sum_{j=1}^n \operatorname{sgn}(k-j) \frac{\partial \xi_i}{\partial x_j} \frac{\partial \xi_l}{\partial x_j},$$

$$C_{ik} = \sum_{j=1}^n \operatorname{sgn}(k-j) \left(2 \frac{\partial P}{\partial x_j} \frac{\partial \xi_i}{\partial x_j} + P \frac{\partial^2 \xi_i}{\partial x_j^2} + P \frac{2\alpha_j}{x_j} \frac{\partial \xi_i}{\partial x_j} \right), \quad (18)$$

$$D_k = \sum_{j=1}^n \operatorname{sgn}(k-j) \left(\frac{\partial^2 P}{\partial x_j^2} + \frac{2\alpha_j}{x_j} \frac{\partial P}{\partial x_j} \right).$$

Now we consider A_k . Since

$$\xi_{kj} = -\operatorname{sgn}(k-j) \frac{4x_j x_{0j}}{r^2}$$

and

$$\frac{\partial \xi_i}{\partial x_j} = -\operatorname{sgn}(k-i) \frac{4x_{0j}}{r^2} \delta_{ij} - \operatorname{sgn}(k-j) \frac{2(x_j - x_{j0})}{r^2} \xi_i, \quad (19)$$

where

$$\delta_{ij} = \begin{cases} 1, & i = j, \\ 0, & i \neq j \end{cases}$$

is the Kronecker delta, we have

$$\left(\frac{\partial \xi_i}{\partial x_j} \right)^2 = \frac{16x_{i0}^2}{r^4} \delta_{ij} + \frac{16(x_j - x_{j0})x_{i0}}{r^4} \delta_{ij} \xi_i + \frac{4(x_j - x_{j0})^2}{r^4} \xi_i^2, \quad (20)$$

Substituting (20) into (17), we get

$$A_{ik} = -\frac{4Px_{i0}}{x_i r^2} \xi_i (1 - \xi_i). \quad (21)$$

Using the product of the derivatives $\frac{\partial \xi_i}{\partial x_j}$ and $\frac{\partial \xi_l}{\partial x_j}$ in the form

$$\frac{\partial \xi_i}{\partial x_j} \frac{\partial \xi_l}{\partial x_j} = \left(-\frac{4(x_i - x_{i0})}{x_i r^2} - \frac{4(x_l - x_{l0})}{x_l r^2} + \frac{8}{r^2} \right) \xi_i \xi_l, \quad l \geq i + 1,$$

we have

$$B_{ilk} = P \left(\frac{4x_{i0}}{x_i r^2} + \frac{4x_{l0}}{x_l r^2} \right) \xi_i \xi_l. \quad (22)$$

Substituting the following derivatives

$$\frac{\partial P}{\partial x_j} = -2\beta \operatorname{sgn}(k - j) P \frac{x_j - x_{j0}}{r^2},$$

$$\frac{\partial^2 \xi_i}{\partial x_j^2} = -\operatorname{sgn}(k - j) \frac{4(x_j - x_{j0})}{x_i r^2} \delta_{ij} \xi_i - \operatorname{sgn}(k - j) \frac{2\xi_i}{r^2} + \frac{8(x_j - x_{j0})^2}{r^4} \xi_i$$

and (19) into (18), we get

$$C_{ik} = -P \left(-(\beta + 1) \frac{4x_{i0}}{x_i r^2} \xi_i + 2\alpha_i \frac{4x_{i0}}{x_i r^2} - \xi_i \sum_{j=1}^n \alpha_j \frac{4x_{j0}}{x_j r^2} \right). \quad (23)$$

Taking into account first derivative (14) of P and its second derivative

$$\frac{\partial^2 P}{\partial x_j^2} = 2\beta \operatorname{sgn}(k - j) P \left[2(\beta + 1) \frac{(x_j - x_{j0})^2}{r^4} - \frac{1}{r^2} \right],$$

it is not difficult to find the expression

$$D_k = 4\beta P \sum_{j=1}^n \frac{\alpha_j x_{j0}}{x_j r^2}. \quad (24)$$

Now substituting (21)–(24) into equation (16), we obtain the following equation

$$\begin{aligned} & \sum_{i=1}^n \frac{x_{i0}}{x_i} \left[\xi_i (1 - \xi_i) \frac{\partial^2 \omega}{\partial \xi_i^2} + [2\alpha_i - (\beta + 1)\xi_i] \frac{\partial \omega}{\partial \xi_i} - \alpha_i \beta \omega \right] \\ & - \sum_{i=1}^n \sum_{l=i+1}^n \left(\frac{x_{i0}}{x_i} + \frac{x_{l0}}{x_l} \right) \xi_i \xi_l \frac{\partial^2 \omega}{\partial \xi_i \partial \xi_l} - \sum_{i=1}^n \xi_i \frac{\partial \omega}{\partial \xi_i} \sum_{j=1}^n \frac{\alpha_j x_{j0}}{x_j} = 0, \end{aligned}$$

which is equivalent to the system:

$$\xi_j (1 - \xi_j) \frac{\partial^2 \omega}{\partial \xi_j^2} - \xi_j \sum_{\substack{i=1 \\ i \neq j}}^n \xi_i \frac{\partial^2 \omega}{\partial \xi_i \partial \xi_j} - \alpha_j \sum_{\substack{i=1 \\ i \neq j}}^n \xi_i \frac{\partial \omega}{\partial \xi_i}$$

$$+ [2\alpha_j - (\beta + \alpha_j + 1)\xi_j] \frac{\partial \omega}{\partial \xi_j} - \alpha_j \beta \omega = 0, \quad j = \overline{1, n}. \quad (25)$$

Thus, the multidimensional generalized Euler-Poisson-Darboux equation (2) equivalently reduced to the system (25).

Comparing the system (25) with the system (7) and by virtue of (12), we obtain 2^n particular solutions of equation (2):

$$u_{k,1}(x; x_0) = \gamma_1 r_k^{-2\beta} F_A^{(n)} \left[\begin{matrix} \beta, \alpha_1, \dots, \alpha_n; \\ 2\alpha_1, \dots, 2\alpha_n; \end{matrix} \xi_k \right], \quad (26)$$

$$u_{k,2}(x; x_0) = \gamma_2 \frac{(x_1 x_{01})^{1-2\alpha_1}}{r_k^{2\beta+2-4\alpha_1}} F_A^{(n)} \left[\begin{matrix} \beta + 1 - 2\alpha_1, 1 - \alpha_1, \alpha_2, \dots, \alpha_n; \\ 2 - 2\alpha_1, 2\alpha_2, \dots, 2\alpha_n; \end{matrix} \xi_k \right], \quad (27)$$

$$u_{k,3}(x; x_0) = \gamma_3 \frac{(x_2 x_{02})^{1-2\alpha_2}}{r_k^{2\beta+2-4\alpha_2}} F_A^{(n)} \left[\begin{matrix} \beta + 1 - 2\alpha_2, \alpha_1, 1 - \alpha_2, \alpha_3, \dots, \alpha_n; \\ 2\alpha_1, 2 - 2\alpha_2, 2\alpha_3, \dots, 2\alpha_n; \end{matrix} \xi_k \right], \quad (28)$$

.....

$$u_{k,n}(x; x_0) = \gamma_n \frac{(x_{n-1} x_{0n-1})^{1-2\alpha_{n-1}}}{r_k^{2\beta+2-4\alpha_{n-1}}} F_A^{(n)} \left[\begin{matrix} \beta + 1 - 2\alpha_{n-1}, \alpha_1, \dots, \alpha_{n-2}, 1 - \alpha_{n-1}, \alpha_n; \\ 2\alpha_1, \dots, 2\alpha_{n-2}, 2 - 2\alpha_{n-1}, 2\alpha_n; \end{matrix} \xi_k \right], \quad (29)$$

$$u_{k,n+1}(x; x_0) = \gamma_{n+1} \frac{(x_n x_{0n})^{1-2\alpha_n}}{r_k^{2\beta+2-4\alpha_n}} F_A^{(n)} \left[\begin{matrix} \beta + 1 - 2\alpha_n, \alpha_1, \dots, \alpha_{n-1}, 1 - \alpha_n; \\ 2\alpha_1, \dots, 2\alpha_{n-1}, 2 - 2\alpha_n; \end{matrix} \xi_k \right], \quad (30)$$

$$u_{k,n+2}(x; x_0) = \gamma_{n+2} \frac{(x_1 x_{01})^{1-2\alpha_1} (x_2 x_{02})^{1-2\alpha_2}}{r_k^{2\beta+4-4\alpha_1-4\alpha_2}} \times \\ \times F_A^{(n)} \left[\begin{matrix} \beta + 2 - 2\alpha_1 - 2\alpha_2, 1 - \alpha_1, 1 - \alpha_2, \alpha_3, \dots, \alpha_n; \\ 2 - 2\alpha_1, 2 - 2\alpha_2, 2\alpha_3, \dots, 2\alpha_n; \end{matrix} \xi_k \right], \quad (31)$$

.....

$$u_{k,(n^2+n+2)/2}(x; x_0) = \gamma_{(n^2+n+2)/2} \frac{(x_{n-1} x_{0n-1})^{1-2\alpha_{n-1}} (x_n x_{0n})^{1-2\alpha_n}}{r_k^{2\beta+4-4\alpha_{n-1}-4\alpha_n}} \times \\ \times F_A^{(n)} \left[\begin{matrix} \beta + 2 - 2\alpha_{n-1} - 2\alpha_n, \alpha_1, \dots, \alpha_{n-2}, 1 - \alpha_{n-1}, 1 - \alpha_n; \\ 2\alpha_1, \dots, 2\alpha_{n-2}, 2 - 2\alpha_{n-1}, \dots, 2 - 2\alpha_n; \end{matrix} \xi_k \right], \quad (32)$$

.....

$$u_{k,2^n}(x; x_0) = \gamma_{2^n} \frac{\prod_{j=1}^n (x_j x_{0j})^{1-2\alpha_j}}{r_k^{2\beta+2n-4\alpha_1-\dots-4\alpha_n}} F_A^{(n)} \left[\begin{matrix} \beta + n - 2\alpha_1 - \dots - 2\alpha_n, 1 - \alpha_1, \dots, 1 - \alpha_n; \\ 2 - 2\alpha_1, \dots, 2 - 2\alpha_n; \end{matrix} \xi_k \right], \quad (33)$$

where β , r_k and ξ_k are defined in (13), (14) and (15), respectively; γ_i ($i = \overline{1, 2^n}$) are constants to be selected in a special way based on the applied problem under consideration.

5 Some properties of particular solutions

It can be directly shown that the particular solutions (26) – (33) satisfy the equation (2) with respect to the variables (x_1, \dots, x_n) and (x_{01}, \dots, x_{0n}) , however, these functions with respect to variables (x_1, \dots, x_n) do not satisfy the adjoint equation

$$\sum_{j=1}^k \frac{\partial^2 u}{\partial x_j^2} - \sum_{j=1}^k \frac{\partial u}{\partial x_j} \left(\frac{2\alpha_j u}{x_j} \right) = \sum_{j=k+1}^n \frac{\partial^2 u}{\partial x_j^2} - \sum_{j=k+1}^n \frac{\partial u}{\partial x_j} \left(\frac{2\alpha_j u}{x_j} \right), \quad x_1 > 0, \dots, x_n > 0. \quad (34)$$

In this connection, according to Sabitov's proposal [25], we multiply the functions (26) – (33) by $x^{(2\alpha)} := x_1^{2\alpha_1} \dots x_n^{2\alpha_n}$, since the product $x^{(2\alpha)} u_{k,j}(x; x_0)$ is a solution of equation (34) whenever $u_{k,j}(x; x_0)$ is a solution of the original equation (2). Thus, if $u_{k,j}(x; x_0)$ are functions defined in (26) – (33), then we obtain 2^n particular solutions

$$q_{k,j}(x; x_0) = x^{(2\alpha)} u_{k,j}(x; x_0), \quad j = \overline{1, 2^n}, \quad (35)$$

which are satisfy the equation (2) and adjoint equation (34) with respect to the variables (x_{01}, \dots, x_{0n}) and (x_1, \dots, x_n) , respectively.

Theorem 1. If $0 < 2\alpha_j < 1$ ($j = \overline{1, n}$), then particular solutions (26) – (33) have a singularity of the order $\frac{1}{r^{n-2}}$ at $r \rightarrow 0$.

Proof. We will consider the first particular solution, the singularity of the remaining solutions is proved in a similar way. By virtue of (26) and (35), we have

$$q_{k,1}(x; x_0) = \gamma_1 x^{(2\alpha)} r_k^{-2\beta} F_A^{(n)} \left[\begin{matrix} \beta, \alpha_1, \dots, \alpha_n; \\ 2\alpha_1, \dots, 2\alpha_n; \end{matrix} \xi_k \right].$$

Taking into account the expression (13) for β , one can rewrite particular solution $q_{k,1}(x; x_0)$ in the form

$$q_{k,1}(x; x_0) = \frac{1}{r^{n-2}} \tilde{q}_{k,1}(x; x_0),$$

where

$$\tilde{q}_{k,1}(x; x_0) = \gamma_1 \frac{x^{(2\alpha)}}{r_k^{2\alpha}} F_A^{(n)} \left[\begin{matrix} \beta, \alpha_1, \dots, \alpha_n; \\ 2\alpha_1, \dots, 2\alpha_n; \end{matrix} \frac{4x_1 x_{01}}{r_k^2}, \dots, \frac{4x_k x_{0k}}{r_k^2}, -\frac{4x_{k+1} x_{0k+1}}{r_k^2}, \dots, -\frac{4x_n x_{0n}}{r_k^2} \right]. \quad (36)$$

Now we show that $\tilde{q}_{k,1}(x; x_0)$ is bounded at $r \rightarrow 0$. On the right side (36) we make a replacement $x_j - x_{0j} = \varepsilon t_j$ ($j = \overline{1, n}$), where $t := (t_1, \dots, t_n)$ are new variables and $\varepsilon \geq 0$, then

$$\tilde{q}_{k,1}(x; x - \varepsilon t) = \gamma_1 \frac{x^{(2\alpha)} \varepsilon^{-2\alpha}}{T_k^{2\alpha}} F_A^{(n)} \left[\begin{matrix} \beta, \alpha_1, \dots, \alpha_n; \\ 2\alpha_1, \dots, 2\alpha_n; \end{matrix} 1 - \frac{z_1(\varepsilon)}{\varepsilon^2}, \dots, 1 - \frac{z_n(\varepsilon)}{\varepsilon^2} \right].$$

where

$$z_j(\varepsilon) = \frac{T_k^2 \varepsilon^2 + \text{sgn}(k - j) \cdot 4x_j (x_j - \varepsilon t_j)}{T_k^2},$$

$$T_k^2 = \sum_{j=1}^k t_j^2 - \sum_{j=k+1}^n t_j^2, \quad j = \overline{1, n}.$$

Using the limit correlation (11), we have

$$\lim_{\varepsilon \rightarrow 0} \tilde{q}_{k,1}(x; x - \varepsilon t) = \gamma_1 \frac{\Gamma(\beta - \alpha)}{4^{2\alpha} \Gamma(\beta)} \prod_{j=1}^n \frac{\Gamma(2\alpha_j)}{\Gamma(\alpha_j)} < \infty.$$

Thus the function $\tilde{q}_{k,1}(x; x_0)$ is bounded, hence the function $q_{k,1}(x; x_0)$ has the singularity of the order $\frac{1}{r^{n-2}}$ at $r \rightarrow 0$. Q.E.D.

6 Conclusion

This study focused on constructing particular solutions for the generalized multidimensional Euler-Poisson-Darboux equation. The method utilized for constructing particular solutions was derived from the renowned monograph by Appel and Campet de Ferrier. Each particular solution contains the first hypergeometric Lauricella function. Furthermore, the singularity of the obtained particular solutions at the origin was proved.

7 Acknowledgments

This research was funded by the Science Committee of the Ministry of Education and Science of the Republic of Kazakhstan (Grant No. AP14972818).

References

- [1] Barros-Neto J.J., Gelfand I.M., "Fundamental solutions for the Tricomi operator", *Duke Math.J.* 98 (3) (1999): 465-483.
- [2] Barros-Neto J.J., Gelfand I.M., "Fundamental solutions for the Tricomi operator II", *Duke Math.J.* 111 (3) (2001): 561-584.
- [3] Barros-Neto J.J., Gelfand I.M., "Fundamental solutions for the Tricomi operator III", *Duke Math.J.* 128 (1) (2005): 119-140.
- [4] Seilkhanova R.B., Hasanov A., "Particular solutions of generalized Euler-Poisson-Darboux equation", *Electronic Journal of Differential Equations* Vol. 2015, No. 9 (2015): 1-10.
- [5] Ergashev T.G., "Fundamental Solutions for a Class of Multidimensional Elliptic Equations with Several Singular Coefficients", *Journal of Siberian Federal University. Mathematics and Physics* 13 (1) (2020): 48-57.
- [6] Lauricella G., "Sulle Funzione Ipergeometriche a piu Variabili", *Rend. Circ. Mat. Palermo* 7 (1893): 111-158.
- [7] Hasanov A., Karimov E.T., "Fundamental solutions for a class of three-dimensional elliptic equations with singular coefficients", *Applied Mathematics Letters* 22 (2009): 1828-1832.
- [8] Rassias J.M., Hasanov A., "Fundamental solutions of two degenerated elliptic equations and solutions of boundary value problems in infinite area", *Int. J. Appl. Math. and Stat.* Vol.8, No. 7 (2007): 87-95.
- [9] Weinstein A., "On a singular differential operator", *Ann. Mat. Pura Appl.* Vol. 49 (1960): 359-365.
- [10] Itagaki M., "Higher order three-dimensional fundamental solutions to the Helmholtz and the modified Helmholtz equations", *Eng. Anal. Bound. Elem.* 15 (1995): 289-293.

-
- [11] Berdyshev A.S., Ryskan A., "The Neumann and Dirichlet problems for one four-dimensional degenerate elliptic equation", *Lobachevskii Journal of Mathematics* Vol. 41, No. 6 (2020): 1051–1066.
- [12] Berdyshev A.S., Ryskan A.R., "Boundary value problem for the four-dimensional Gellerstedt equation", *Bulletin of the Karaganda University. Mathematics series*. No. 4 (104) (2021): 35-48.
- [13] Karimov E.T., Nieto J.J., "The Dirichlet problem for a 3D elliptic equation with two singular coefficients", *Computers and Mathematics with Applications* 62 (2011): 214-224.
- [14] Ergashev T.G., "The fourth double-layer potential for a generalized bi-axially symmetric Helmholtz equation", *Tomsk State University Journal of Mathematics and Mechanics* 50 (2017): 45-56.
- [15] Srivastava H.M., Hasanov A., Choi J., "Double-layer potentials for a generalized bi-axially symmetric Helmholtz equation", *Sohag J. Math.* 2 (1) (2015): 1-10.
- [16] Baishemirov Z., Berdyshev A., Ryskan A.A., "Solution of a Boundary Value Problem with Mixed Conditions for a Four-Dimensional Degenerate Elliptic Equation", *Mathematics* 10, 1094 (2022).
- [17] Burchinal J.L., Chaundy T.W., "Expansions of Appell's double hypergeometric functions", *The Quarterly Journal of Mathematics, Oxford, Ser. 11* (1940): 249-270.
- [18] Burchinal J.L., Chaundy T.W., "Expansions of Appell's double hypergeometric functions(II)", *The Quarterly Journal of Mathematics, Oxford, Ser. 12* (1941): 112-128.
- [19] Hasanov A., Srivastava H., "Some decomposition formulas associated with the Lauricella function $F_A^{(r)}$ and other multiple hypergeometric functions", *Applied Mathematic Letters* 19 (2) (2006): 113-121.
- [20] Hasanov A., Srivastava H., "Decomposition Formulas Associated with the Lauricella Multivariable Hypergeometric Functions", *Computers and Mathematics with Applications* 53:7 (2007): 1119-1128.
- [21] Hasanov A., Ergashev T.G., "New decomposition formulas associated with the Lauricella multivariable hypergeometric functions", *Montes Taurus Journal of Pure and Applied Mathematics* 3 (3) (2021): 317-326.
- [22] Ryskan A., Ergashev T., "On Some Formulas for the Lauricella Function", *Mathematics* 11, 4978 (2023).
- [23] Erdelyi A., Magnus W., Oberhettinger F., Tricomi F.G., *Higher Transcendental Functions* (New York, Toronto and London: McGraw-Hill Book Company, Vol.I, 1953).
- [24] Appell P. and Kampe de Fériet J., *Fonctions Hypergeometriques et Hyperspheriques; Polynomes d'Hermite* (Paris: Gauthier - Villars, 1926).
- [25] Sabitov K.B., "Generalization of the Kelvin theorem for solutions of elliptic equations with singular coefficients and applications", *Differential equations* 58 (1) (2022): 53-64.

2-бөлім

Раздел 2

Section 2

Механика

Механика

Mechanics

IRSTI 30.17.35, 27.35.45

<https://doi.org/10.26577/JMMCS202412119>B.A. Berdenova 

Al-Farabi Kazakh National University, Kazakhstan, Almaty

e-mail: Bakytur.Berdenova@kaznu.edu.kz

SIMULATION OF CARBON DIOXIDE ADSORPTION ONTO CONSOLIDATED ACTIVATED CARBON IN 2D AXISYMMETRIC SYSTEM

The research work is devoted to the kinetics of adsorption. Needless to say that physical adsorption is of great interest in heat industry according to the number of research papers published in the area annually. The working pair of carbon dioxide and consolidated tablet of AC was considered. The mathematical model built for a cylindrical coordinate system, so the computational domain is a rectangle corresponding to the radial section of the tablet. The rate of adsorption implemented using the LDF (linear driving force) model. The temperature map was constructed for analyzing the behavior of the temperature field. Curves of instantaneous uptake and simulated average temperature are obtained. Simulation results are compared with experimental data and shows good agreement. The study also presents findings of a grid sensitivity analysis. The developed solver is the subject to further expansion to consider more quantities, such as change in porosity, volatile gas concentration, etc.

Key words: activated carbon, adsorption, axisymmetric, carbon dioxide, numerical modeling.

Б.А. Берденова

әл-Фараби атындағы қазақ ұлттық университеті, Қазақстан, Алматы қ.

e-mail: Bakytur.Berdenova@kaznu.edu.kz

Нығыздалған белсендірілген көмірге көмірқышқыл газының адсорбциясын 2D осьтік симметриялық жүйеде модельдеу

Зерттеу жұмысы адсорбция кинетикасына арналған. Жыл сайын аталған бағытта жарияланатын ғылыми еңбектердің санына қарасақ, физикалық адсорбцияның жылу өнеркәсібінде үлкен қызығушылық тудыратынын айтудың қажеті жоқ. Көмірқышқыл газы және нығыздалған белсендірілген көмір таблеткасының жұмысшы жұбы қарастырылды. Математикалық модель цилиндрлік координаттар жүйесі үшін құрылды, сондықтан есептеу облысы таблетканың радиалды қимасына сәйкес келетін тік бұрышты төртбұрыш болып табылады. Адсорбция жылдамдығы LDF (сызықтық қозғаушы күш) моделін қолдану арқылы жүзеге асырылды. Жұмыста температура өрісінің өзгеру қарқыны талданды, лездік жұтылу және модельденген орташа температура қисықтары тұрғызылды. Модельдеу нәтижелері эксперименттік деректермен салыстырылды және жақсы сәйкес келетіні анықталды. Зерттеу жұмысы сонымен қатар есептеу нәтижелерінің тордың өлшеміне тәуелділігіне талдау нәтижелерін ұсынады. Өзірленген есептегіш құралды адсорбциялық жұтылу кезіндегі кеуектілік өзгерісі, ұшқыш газ концентрациясы және тағы басқа өзекті шамаларды ескеретіндей етіп ұлғайту күтіледі.

Түйін сөздер: белсендірілген көмір, адсорбция, осьтік симметрия, көмірқышқыл газы, сандық модельдеу.

Б.А. Берденова

Казахский национальный университет имени аль-Фараби, Казахстан, г. Алматы
e-mail: Bakytnur.Berdenova@kaznu.edu.kz

Симуляция адсорбции диоксида углерода на консолидированный активированный уголь в 2D осесимметричной системе

Научно-исследовательская работа посвящена кинетике адсорбции. Излишне говорить, что физическая адсорбция представляет большой интерес в теплоэнергетике, судя по количеству научных работ, публикуемых ежегодно в этой области. Рассмотрена рабочая пара углекислого газа и консолидированной таблетки активированного угля. Математическая модель построена для цилиндрической системы координат, поэтому расчетная область представляет собой прямоугольник, соответствующий радиальному сечению таблетки. Скорость адсорбции реализована с использованием модели LDF (линейная движущая сила). Проведен анализ поведения поля температуры. Получены кривые мгновенного поглощения и моделируемой средней температуры. Результаты моделирования согласуются с результатами экспериментального исследования. В работе также представлены результаты анализа чувствительности сетки. Разработанный решатель подлежит дальнейшему расширению для учета большего количества величин, таких как изменение пористости, концентрации летучего газа и т.д.

Ключевые слова: активированный уголь, адсорбция, осевая симметрия, углекислый газ, численное моделирование.

1 Introduction

The process of adsorption has a wide range of applications, it is used in cooling/heating systems, gas separation, gas purification, water filtration, carbon capture, etc. Here is an overview of some recent research findings on adsorption and its use in refrigeration systems. Automotive adsorption-based air conditioning systems are a promising alternative to traditional systems from an environmental and energy saving perspective. Such systems can operate using exhaust heat from an engine. An example of a designed and tested adsorption chiller prototype can be found in Verde et al. [1]. The adsorption system working on a two-bed silica gel was able to produce 2.1 kW cooling capacity.

Ben-Mansour et al. [2] presented a review on the application of the adsorption process on CO₂ separation from typical power plant exhaust gases. The work discusses the candidate materials for post-combustion carbon capture, the experimental investigations that have been carried out, and numerical models developed to simulate the gas separation. Authors indicate gaps in experimental investigations and in simulation studies considering one dimensional flow. More research work is needed that doesn't not ignore the radial or 3D thermal and adsorption behaviors.

The established patterns in equilibrium adsorption curves in adsorption theory are of an empirical nature. A new approach to constructing equilibrium uptake equations was proposed by the following authors. Yin et al. [3] introduced a new model correlating and predicting adsorption equilibrium concentrations using machine learning method. Sellaoui et al. [4] established theoretical expressions to fit the adsorption isotherms of ibuprofen on activated carbon using grand canonical ensemble. Unlike conventional isotherms models (Langmuir, Freundlich, etc.) the expressions involve physicochemical parameters and are thermodynamically consistent. Sghaier et al. [5] used statistical physics formalism with the grand canonical ensemble to construct isotherm equations. The study performed by applying four expressions and the best isotherm equation fitting experimental data was found. Also

the authors used the statistical physics for expressing and calculating the coefficient of performance (COP) of ethanol/activated carbon systems.

Cai et al. [6] demonstrated silica gel (SG)-water adsorption refrigeration device and compared the performance of three types of composite adsorbents in the refrigeration system. The composites fabricated by mixing SG with MOFs to improve mass transfer characteristics and either with copper chips (CCs) or foamed copper (CFs) of different mass ratio to improve thermal characteristics. Development of new materials by mixing different substances permits limitless possibilities in the field of adsorption application.

Pena and de Lemos [7] numerically investigated unsteady multidimensional heat transfer problem with internal heat generation. The simulation is carried out in a two-dimensional axisymmetric domain and involved reaction and phase transition phenomena. In [8] recent study, we presented results of simulation of CO_2 gas adsorption onto consolidated AC tablet, with the calculation geometry simplified to a one-dimensional case. The mathematical model involved more quantities, such as change in porosity, volatile gas concentration, and accordingly, more equations were solved. The current work investigates the process of CO_2 adsorption by the composite under constant pressure and temperature conditions in 2D axisymmetric system. The energy balance equation and the adsorbed phase balance equations have been solved at a moment, and the solver is subject to further expansion to account for more associated accompanying phenomena.

2 Mathematical model and problem description

The calculation domain is schematically illustrated in Figure 1. The mathematical model built for a cylindrical coordinate system, so the computational domain is a rectangle corresponding to the radial section of the tablet.

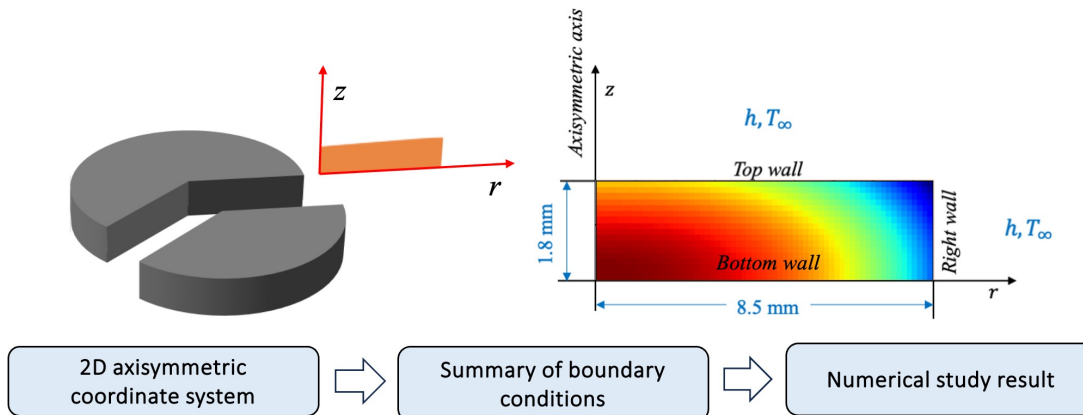


Figure 1: Schematic illustration of calculation domain

The energy conservation equation for the solid adsorbent is as equation (1). The adsorption rate is assumed to follow the Linear Driving Force model, equation (2). The thermal conductivity and capacity of the adsorbent vary with temperature and adsorption rate, since the composition of a unit volumes change with adsorption, also due to the

exothermic nature of the process for the working pair of CO₂/AC. But in the current study they are considered constant due to lack of experimental data.

$$\rho c_p \frac{\partial T}{\partial t} = \frac{1}{r} \frac{\partial}{\partial r} \left(kr \frac{\partial T}{\partial r} \right) + \frac{\partial}{\partial z} \left(k \frac{\partial T}{\partial z} \right) + \dot{e}_{\text{gen}} \quad (1)$$

$$\frac{\partial q}{\partial t} = k_{\text{LDF}}(T) (q_{\text{eq}} - q) \quad (2)$$

Boundary conditions:

$$-k \frac{\partial T}{\partial z} \Big|_{z=H} = h [T - T_{\infty}] \quad (3)$$

$$\frac{\partial T}{\partial z} \Big|_{z=0} = 0 \quad (4)$$

$$-k \frac{\partial T}{\partial r} \Big|_{r=R} = h [T - T_{\infty}] \quad (5)$$

For the nodes along the longitudinal axis equation (6) is solved.

$$\rho c_p \frac{\partial T}{\partial t} = k \left(2 \cdot \frac{\partial^2 T}{\partial r^2} + \frac{\partial^2 T}{\partial z^2} \right) + \dot{e}_{\text{gen}} \quad (6)$$

Initial conditions, equation (7) and equation (8):

$$q|_{t=0} = 0 \quad (7)$$

$$T|_{t=0} = T_{\infty} \quad (8)$$

Problem parameters used for simulation. Dimensions of the tablet used in the simulation: tablet radius 8.5 mm, height 1.8 mm (see Figure 1). The characteristics of the composite consolidated activated carbon taken from previous studies [8,9] and illustrated in Table 1.

The expression for the rate constant of LDF model:

$$k_{\text{LDF}}(T) = k_0 \exp \left(-\frac{E_a}{RT} \right) \quad (9)$$

Where R is the gas constant, 8.314 J mol⁻¹ K⁻¹. The activation energy and pre-exponential factor are:

$$E_a = -17.34 \text{ kJ mol}^{-1} \quad (10)$$

Table 1: The characteristics of the composite for numerical calculations

Property	Unit	Value
Heat conductance	$\text{W m}^{-1} \text{K}^{-1}$	0.22
Thermal capacity	$\text{J g}^{-1} \text{K}^{-1}$	0.821
Isosteric heat of adsorption	kJ mol^{-1}	19.02
Porosity	-	0.482
Skeletal density	g cm^{-3}	0.917
Apparent density	g cm^{-3}	0.475
Equilibrium uptake	g g^{-1}	0.274

$$k_0 = 1.58 \times 10^{-5} \text{ s}^{-1} \quad (11)$$

The heat transfer coefficient depends on the difference in temperature between the surface of the heated object and the surrounding temperature T_∞ , and on the thermal properties of the medium. The properties of carbon dioxide under given conditions of temperature and pressure are shown in Table 2.

Dimensionless numbers, [10]:

$$Ra = Gr \cdot Pr \quad (12)$$

$$Gr = \frac{\beta \cdot \Delta T \cdot g \cdot L^3}{\nu^2} \quad (13)$$

$$Pr = \frac{\mu_g \cdot c_{p,g}}{k_g} \quad (14)$$

Table 2: Properties of carbon dioxide at 293.15 °C and 0.535 MPa

Property	Unit	Value
Pressure	bar	5.35
Temperature	Celsius	20
Density	kg m^{-3}	9.96
Specific isobar heat capacity	$\text{kJ kg}^{-1} \text{K}^{-1}$	0.88
Isobar coefficient of thermal expansion	$10^{-3} (\text{K}^{-1})$	3.75
Heat conductance	$10^{-3} (\text{W m}^{-1} \text{K}^{-1})$	16.44
Dynamic viscosity	$10^{-6} (\text{Pa s})$	14.72
Kinematic viscosity	$10^{-6} (\text{m}^2 \text{s}^{-1})$	1.478

The system of equations has been solved in Python (Version 3.11.5) using the explicit finite difference scheme. Volume average of quantity f found as below:

$$\Theta(f) = \int_0^H \int_0^R (2\pi r \cdot f(r, z)) dr dz = \sum_{i=1}^n \sum_{j=1}^m 2\pi \cdot r_j^* \cdot f(r_j^*, z_i^*) \cdot \Delta r \cdot \Delta z \quad (15)$$

$$T_{\text{ave}} = \frac{\int T dV}{V} \quad (16)$$

$$q_{\text{ave}} = \frac{\int q dV}{V} \quad (17)$$

3 Results and discussion

The temperature field behaves as expected, the outer boundaries are colder than the core. Figure 2 shows the instantaneous temperature field at the same time instant 18 seconds calculated using 8x32 nodes, 12x48 nodes and 16x64 nodes. The results illustrated upside down due to peculiarity of the visualization library. The proper grid sensitivity analysis was performed to avoid grid size dependent results, Appendix A. The grid refinement allows more accurate calculation and detailed temperature map.

The calculation result of the previous study obtained using non-isothermal pore change model for the 1D case illustrated for comparison [8]. Two temperature profiles are shown in Figure 3, one obtained using 2D axial symmetric geometry in scope of the current study, and the other obtained using abovementioned 1D non-isothermal pore change model. The non-isothermal pore change model counts the effects associated with change in porosity, and mobile gas penetration into the tablet. But due to the 1D geometry the convective heat loss through the side wall cannot be determined. When using a 2D case the cooling occurs faster indicating the heat loss through the sides. The findings are reasonable and consistent with recent results.

According to the experimental measurement the adsorption rate is high during the first 300 seconds and declined rapidly thereafter. It achieves a plateau at around 600 seconds and remains constant, when no further change in adsorption uptake is noticed. Therefore, only the first 600 seconds are of interest as a simulation time. The instantaneous average simulated uptake compared with experimental data.

Figure 4 illustrates the adsorption uptake over time. Black dots indicate the experimental data, the dashed blue line indicates simulation result of the current study. Solid purple line shows the result obtained in previous study using non-isothermal pore change model.

4 Conclusions

Recent review articles point to the need for more experimental and numerical studies that do not ignore the radial or 3D thermal and adsorption behaviours. The present paper shows simulation results obtained for a cylindrical coordinate system, so the computational domain is the radial section of the tablet. Currently the energy balance equation and the adsorbed phase balance equations are solved. The validation of the developed solver is performed via comparison with the results obtained experimentally and using one-dimensional model of recently published study. The developed solver is the subject to further expansion to consider more quantities, such as change in porosity, volatile gas concentration, etc. In-situ measurements of the sample's temperature and thermal properties are challenging

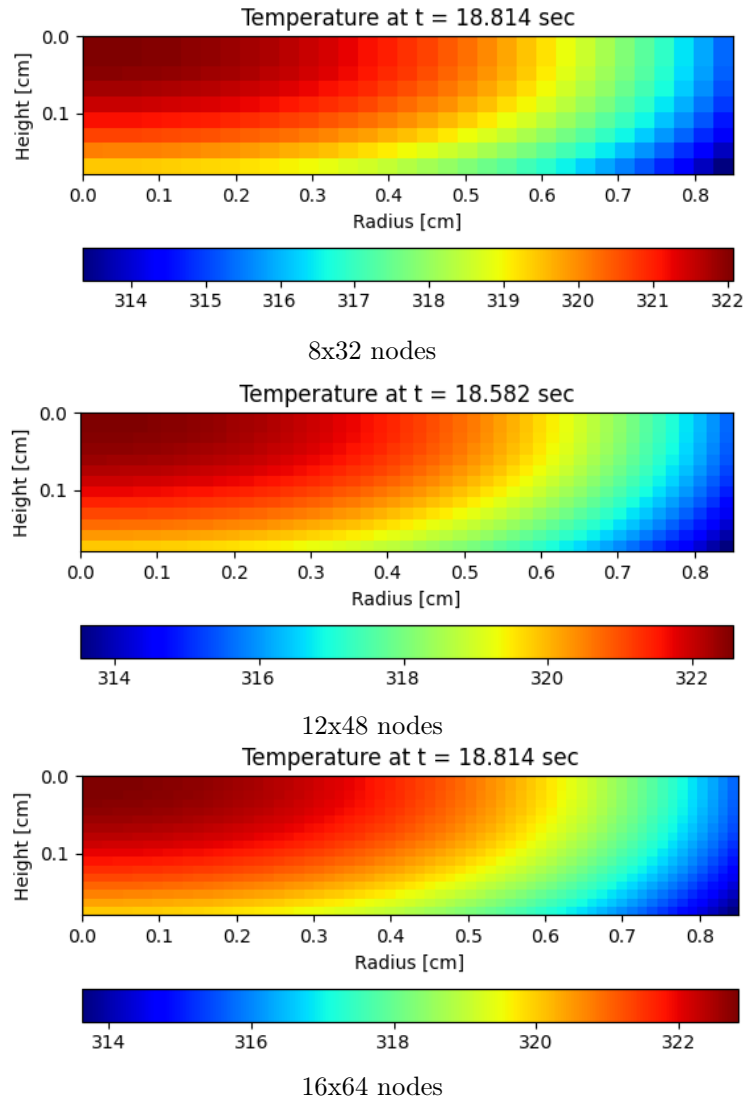


Figure 2: Instantaneous temperature field at 18 seconds calculated using different mesh refinements: (a) 8x32 nodes, (b) 12x48 nodes, (c) 16x64 nodes

experimental investigation work. The validation of the simulated temperature profiles with experimental data is of great interest.

Research highlights

- Gas adsorption onto activated carbon tablet simulated in 2D axisymmetric system.
- Dynamics curves for key parameters were constructed and compared with results of a recent one-dimensional numerical study.
- Adsorption uptake curves were compared with experimental data.

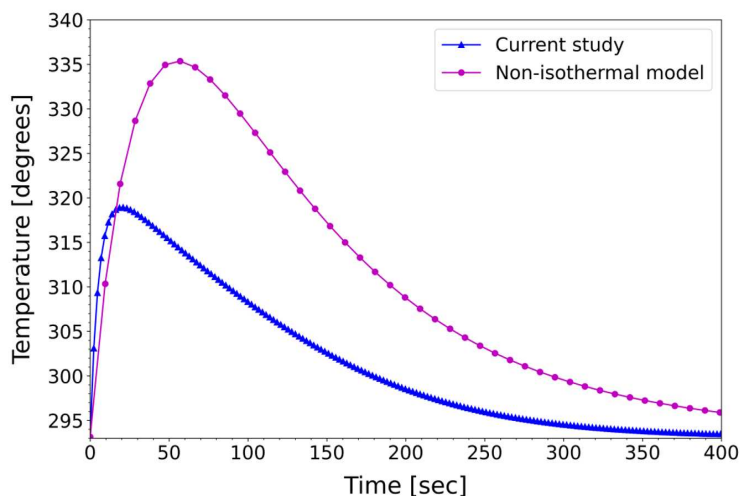


Figure 3: Mean temperature profiles obtained using 2D axial symmetric geometry (blue line), and 1D non-isothermal pore change model (purple line) [8]

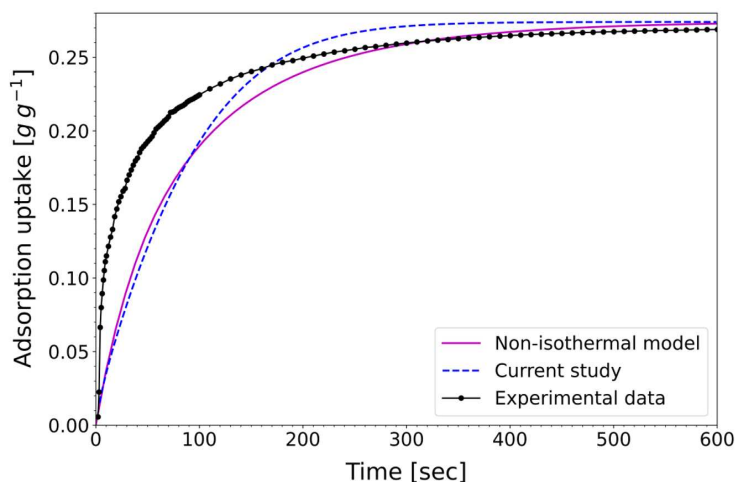


Figure 4: Adsorption uptake obtained using 2D axial symmetric geometry (dashed blue line) and 1D non-isothermal pore change model (solid purple line). Black line corresponds to the experimental data

Declaration of Competing Interest

The author declares that she has no known competing financial interests or personal relationships that could have appeared to influence the work reported in this paper.

Acknowledgement

The author wish to acknowledge the financial support received from JSC Center for International Programs – Bolashaq, the research was performed on scope of "500 scholars" fellowship program. Also, the author would like to express her gratitude to Prof. Bidyut Baran Saha for his valuable advice.

Appendix A. Interim Results

Figure 5 shows the average temperature profiles obtained for 3 different cases: (a) for adaptive $k_{LDF}(T)$ and $h(T)$, (b) for fixed k_{LDF} and adaptive $h(T)$, and (c) for both fixed k_{LDF} and h . The mean temperature T_{ave} varies over time according to the Figure 6. The calculation results for 4 different grid sizes illustrated. The grid sensitivity analysis shows good convergence of the curves towards the result obtained on the finest grid, Table 3. The grid size cannot be reduced indefinitely. The computational result is reasonable for 12x48 nodes. Further refinements increase the calculation time only, and do not affect much on the temperature profiles.

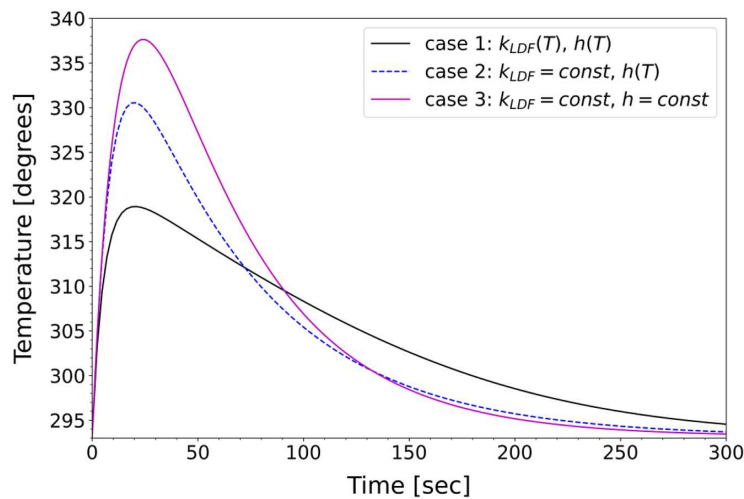


Figure 5: Temperature profile obtained using 3 different cases

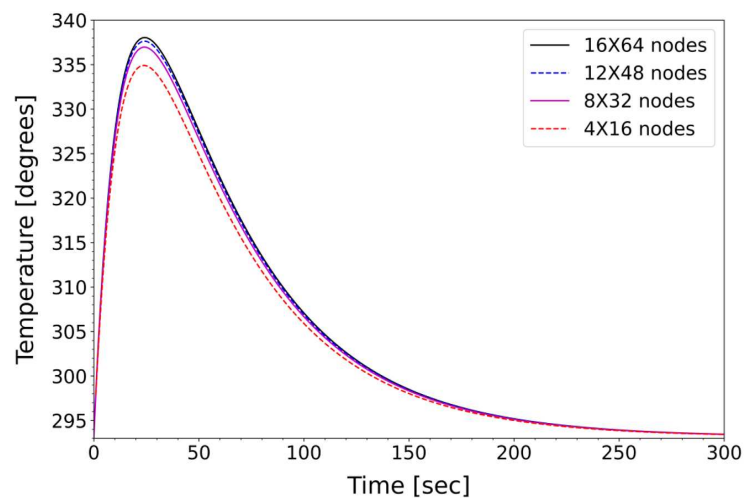


Figure 6: Grid sensitivity analysis. Mean temperature over time.

Table 3: Maximum temperature observed for different grid sizes

Number of nodes	16x64	12x48	8x32	4x16
T_{\max}	338.04	337.64	336.97	334.69

References

- [1] Verde M., Harby K., de Boer R., Corberán J.M., "Performance evaluation of a waste-heat driven adsorption system for automotive air-conditioning: Part I – Modeling and experimental validation", *Energy*, 116 (2016): 526-538. Doi: <https://doi.org/10.1016/j.energy.2016.09.113>, Url: <https://www.sciencedirect.com/science/article/pii/S0360544216313858>.
- [2] Ben-Mansour R., Habib M.A., Bamidele O.E., Basha M., Qasem N.A.A., Peedikakkal A., Laoui T., Ali M., "Carbon capture by physical adsorption: Materials, experimental investigations and numerical modeling and simulations – A review", *Applied Energy*, 161 (2016): 225-255. Doi: <https://doi.org/10.1016/j.apenergy.2015.10.011>, Url: <https://www.sciencedirect.com/science/article/pii/S0306261915012386>.
- [3] Yin G., Jameel Ibrahim Alazzawi F., Mironov S., Reegu F., El-Shafay A.S., Lutfor Rahman M., Su C-H., Lu Y-Z., Chinh Nguyen H., "Machine learning method for simulation of adsorption separation: Comparisons of model's performance in predicting equilibrium concentrations", *Arabian Journal of Chemistry*, 15(3) (2022): 1878-5352. Doi: <https://doi.org/10.1016/j.arabjc.2021.103612>, Url: <https://www.sciencedirect.com/science/article/pii/S1878535221006274>.
- [4] Sellaoui L., Guedidi H., Knani S., Reinert L., Duclaux L., Ben Lamine A., "Application of statistical physics formalism to the modeling of adsorption isotherms of ibuprofen on activated carbon", *Fluid Phase Equilibria*, 387 (2015): 103-110. Doi: <https://doi.org/10.1016/j.fluid.2014.12.018>, Url: <https://www.sciencedirect.com/science/article/pii/S0378381214006992>.
- [5] Sghaier W., Ben Torkia Y., Bouzid M., Ben Lamine A., "Thermodynamic analysis of cooling cycles based on statistical physics modeling of ethanol adsorption isotherms", *International Journal of Refrigeration*, 141 (2022): 119-131. Doi: <https://doi.org/10.1016/j.ijrefrig.2022.05.022>, Url: <https://www.sciencedirect.com/science/article/pii/S014070072200175X>.
- [6] Cai S., Hua Zh., Dai M., Li S., Luo X., Tu Zh., "Performance analysis of adsorption refrigeration using a composite adsorbent with improved heat and mass transfer", *International Journal of Heat and Mass Transfer*, 216 (2023): 124523. Doi: <https://doi.org/10.1016/j.ijheatmasstransfer.2023.124523>, Url: <https://www.sciencedirect.com/science/article/pii/S0017931023006683>.
- [7] Pena Fabrício J., De Lemos Marcelo J., "Simulation of multidimensional unsteady heat transfer with aluminothermic reaction and phase transition", *International Journal of Heat and Mass Transfer*, 213 (2023): 124365. Doi: <https://doi.org/10.1016/j.ijheatmasstransfer.2023.124365>, Url: <https://www.sciencedirect.com/science/article/pii/S0017931023005112>.
- [8] Berdenova B., Pal F., Saha B.B., Kaltayev A., "Non-isothermal pore change model predicting CO2 adsorption onto consolidated activated carbon", *International Journal of Heat and Mass Transfer*, 177 (2021): 121480. Doi: <https://doi.org/10.1016/j.ijheatmasstransfer.2021.121480>, Url: <https://www.sciencedirect.com/science/article/pii/S0017931021005834>.
- [9] Berdenova B., Pal A., Muttakin M., Mitra S., Thu K., Saha B.B., Kaltayev A., "A comprehensive study to evaluate absolute uptake of carbon dioxide adsorption onto composite adsorbent", *International Journal of Refrigeration*, 100 (2019): 131-140. Doi: <https://doi.org/10.1016/j.ijrefrig.2019.01.014>, Url: <https://www.sciencedirect.com/science/article/pii/S0140700719300143>.
- [10] Maragkos G., Beji T., "Review of Convective Heat Transfer Modelling in CFD Simulations of Fire-Driven Flows", *Applied Sciences*, 11 (2021): 5240. Doi: [10.3390/app11115240](https://doi.org/10.3390/app11115240), Url: <https://www.mdpi.com/2076-3417/11/11/5240>.

3-бөлім

Раздел 3

Section 3

Информатика

Информатика

Computer
Science

IRSTI 20.15.05

DOI: <https://doi.org/10.26577/JMMCS2024121110>

A. Makulova¹ , B. Sharipova² , M. Othman³ , A. Pyrkova⁴ ,
G. Ordabayeva^{4*} 

¹Narxoz university, Kazakhstan, Almaty

²Almaty technological university, Kazakhstan, Almaty

³Universiti Putra Malaysia, Malaysia, Selangor D.E.

⁴Al-Farabi Kazakh national university, Kazakhstan, Almaty

*e-mail: gulzi200988@mail.ru

DETECTION OF OPERATING SYSTEM VULNERABILITIES AND NETWORK TRAFFIC ANALYSIS METHODS

Researchers and experts on information protection develop antivirus programs and applications to improve the security of operating systems and security policies. Threats will be relevant to organizations that do not consider security policies and regular software updates. This paper discusses applications for scanning and analyzing network traffic, such as Netdiscover, Wireshark, and Nmap. The model network is based on a virtual machine. This research aims to determine methods for scanning and analyzing network traffic and detecting network vulnerabilities. This study conducted a penetration test for Windows 10 using the Kali Purple operating system and identified the vulnerability of the operating system. The calculation of network traffic is performed with (1) the determination of the arithmetic means of network traffic, (2) the calculation of the variance, and (3) the determination of the magnitude of fluctuations relative to the average M , the range of maximum and minimum values of D , and the Hurst coefficient. As a result of the conducted research on students enrolled in the educational program 6B06301 – Information Security Systems at Farabi University, the proficiency in MS Excel and C# skills amounted to 77.11%. The research results can be used in the field of information security systems.

Key words: network traffic, penetration, analysis, vulnerability, exploit, attack, Kali Linux, Windows.

A. Мақулова¹, Б. Шарипова², М. Othman³, А. Пыркова⁴, Г. Ордабаева^{4*}

¹Нархоз университеті, Қазақстан, Алматы қ.

²Алматы технологиялық университеті, Қазақстан, Алматы қ.

³Putra университеті, Малайзия, Селангор Д.Е.

⁴Әл-Фараби атындағы Қазақ ұлттық университеті, Қазақстан, Алматы қ.

*e-mail: gulzi200988@mail.ru

Операциялық жүйе осалдығын анықтау және трафикті талдау әдістері

Зерттеушілер мен ақпаратты қорғау жөніндегі сарапшылар операциялық жүйелердің қауіпсіздігін және қауіпсіздік саясатын арттыру үшін вирусқа қарсы бағдарламалар мен қосымшалар әзірлейді. Мақалада Netdiscover, Wireshark және Nmap сияқты желілік трафикті сканерлеуге және талдауға арналған қосымшалар қарастырылды. Желілік трафикті талдай білу – киберқорғаудың алғашқы желісі. Виртуалды кеңістік – деректерді қорғау технологиясы саласындағы оқыту сценарийлерін іске асыруға арналған орын. Осы зерттеудің мақсаты желілік трафикті талдау әдістерін және желінің осалдығын анықтау. Зерттеуде Kali Purple операциялық жүйесінің көмегімен Windows 10 жүйесіне ену тесті жүргізілді және операциялық жүйенің осалдығы анықталды. Сондай-ақ, желілік трафиктің орташа арифметикалық мәнін (1), дисперсияны есептеу (2), орташа M (3) қатысты ауытқу мәнін анықтау, D максималды және минималды мәнінің диапазоны және Херст коэффициентіне талдау жүргізілді.

Желілік трафикті талдаудың және осалдықтарды анықтаудың ұсынылған әдістемесі Ethernet жергілікті желісіне шабуылдарды неғұрлым жоғары дәлдікпен және толықтықпен анықтауға және бұғаттауға мүмкіндік берді. Нәтижеде анықталған Херст коэффициентінің мәні ($\leq 0,5$) өзіндік ұқсастығы жоқ эргодикалық қатар екені айқындалды. Сонымен қатар, орындалған зертханалық жұмыс нәтижесінде Farabi университетінің 6B06301 – Ақпараттық қауіпсіздік жүйелері білім беру бағдарламасы бойынша студенттердің MS Excel және C# бойынша біліктілігі 77,11% тең болды. Алынған зерттеу нәтижелері ақпараттық қауіпсіздік жүйесі саласында пайдаланылуы мүмкін.

Түйін сөздер: желілік трафик, ену, талдау, осалдық, эксплуат, шабуыл, Kali Linux, Windows.

А. Мақулова¹, Б. Шарипова², М. Othman³, А. Пыркова⁴, Г. Ордабаева^{4*}

¹Университет Naqhoz, Қазақстан, г. Алматы

²Алматинский технологический университет, Қазақстан, г. Алматы

³Университет Putra, Малайзия, Селангор Д.Е.

⁴Қазақский национальный университет имени аль-Фараби, Қазақстан, г. Алматы

*e-mail: gulzi200988@mail.ru

Обнаружения уязвимости операционной системы и методы анализа сетевого трафика

Исследователи и эксперты по защите информации разрабатывают антивирусные программы и приложения для повышения безопасности операционных систем и политик безопасности. В данной статье рассматриваются приложения для сканирования и анализа сетевого трафика, такие как Netdiscover, Wireshark и Nmap. Умение анализировать сетевой трафик – первая линия защиты от киберугроз. Виртуальное пространство – место для реализации сценариев обучения в области технологии защиты данных. Цель данного исследования определить методы анализа сетевого трафика и обнаружение уязвимости сети. В данном исследовании с помощью операционной системы Kali Purple проведен тест на проникновение в Windows 10 и определена уязвимость операционной системы. Также, проведен расчет сетевого трафика с определением: среднеарифметическое значение сетевого трафика (1), вычисление дисперсии (2), определение значения колебаний относительно среднего M (3), диапазон максимального и минимального значения D и коэффициент Херста. Предложенная методика анализа сетевого трафика и обнаружения уязвимостей позволила с более высокой точностью и полнотой выявить и заблокировать атаки на локальную сеть Ethernet. По результатам показателя Херста ($\leq 0,5$) определен эргодический ряд, который не обладает самоподобием. В результате проведенного исследования студентов по образовательной программе 6B06301 – Системы информационной безопасности университета Farabi навыки работы с MS Excel и C# составили 77,11%. Полученные результаты исследования могут быть использованы в области системы информационной безопасности.

Ключевые слова: сетевой трафик, проникновение, анализ, уязвимость, эксплуат, атака, Kali Linux, Windows.

1 Introduction

Today, data transmission is developing rapidly. This means the availability of the local network and easy connection of users. The local data transmission environment also creates conditions for listening to network traffic and connecting attackers to the network. Unregistered port numbers make network traffic monitoring and intrusion detection difficult.

Klenilmar L. Dias et al. [7] consider a module for classifying video traffic based on machine learning. The proposed naive Bayes algorithm is used to relax the independence hypothesis and in quality assurance schemes for computer networks. The results of this module are applied in real-time scenarios.

Some other authors [4] propose an effective statistical approach to attack detection based on traffic characteristics and an algorithm for dynamic detection of threshold values. The data

from the MIT Lincoln Laboratory DARPA and developments of the university laboratory using this algorithm were used to derive attributes based on distributed denial-of-service characteristics.

Markus Ring et al. [13] proposed a new methodology for generating real network traffic based on the flow for evaluating network-based intrusion detection systems (NIDS). The data is based on Generative Adversarial Networks (GANs), which are used to generate images. The new method proposed for estimating generated network traffic based on the flow of the CIDDS-001 dataset has shown the ability to generate high-quality data.

In this paper, the algorithms for modeling network graphs are considered, and applications for network analysis are used. The experimental part shows the analysis of network traffic based on a virtual machine and the use of network traffic filtering. In order to protect the information, an exploit of the Windows operating system was identified, and a vulnerability scan module was searched. Based on the results of the network traffic calculation, the Hurst index ($\leq 0,5$) is obtained.

2 Methods and materials

In the research by N. Clarke et al. [1], traffic metadata is used to identify users. The results of the experiments conducted to investigate the relationship between user actions and network signals are shown in Table 1.

F. Pacheco et al. [11] have studied the methods of machine learning and Deep Learning (DL) for the classification of Internet traffic. The platform under study is satellite communications, where encrypted, unencrypted, and tunnel communications are considered.

Table 1: Services and interaction with users [1].

Services	User interaction
Bbc	Watching video clips, TV programs, listening to audio clips, commenting, sharing news
Dropbox	Uploading files, general viewing of files, folders
Facebook, Twitter	Posting, commenting, sharing, finding friends, attaching files, chatting, messaging
Google	Keyword searching, creating, editing, deleting online documents
Hotmail	Downloading and uploading file attachments, composing an email, deleting content, replying to email
Skype	Sending text messages, transferring files, changing online presence
YouTube	Searching, watching videos, downloading songs and videos, writing comments
Wikipedia	Searching, reading articles

Y. Kawasaki et al. [6] propose a state-space model that estimates the traffic state over a two-dimensional network with alternative routes. This method also employs sequential Bayesian filtering with a cell transmission model GTM for the flow model.

The article by Makarenko S.I. et al. [9] presents a comparative analysis of foreign and Russian penetration testing methodologies and standards, such as The Open Source Security Testing Methodology (OSSTMM), Information System Security Assessment Framework

(ISSAF), Open Web Application Security Project (OWASP), Penetration Testing Execution Standard (PTES), Technical Guide to Information Security Testing and Assessment (NIST SP 800-115), Study a Penetration Testing Model (BSI), Methodology of Information Systems Security Penetration Testing (PETA), Penetration Testing Framework (PTF), and Positive Technologies. Additionally, definitions of basic terminology are provided.

Ethical hacking (pentest, pentesting) involves authorized simulated attacks on computer systems to identify weaknesses in the security system. It is also used to assess the security of operating systems, network security, web applications, and wireless systems. To protect the system, professional pentesters utilize various tools and methods that malicious actors use for hacking. Stages of penetration testing:

- 1) Information gathering – detecting network hosts, open ports, etc.;
- 2) Vulnerability analysis – checking for unpatched systems, misconfigurations, etc.;
- 3) Exploitation – gaining access using discovered vulnerabilities;
- 4) Post-exploitation – maintaining access using backdoors, rootkits, etc.;
- 5) Reporting – presenting results and recommendations for preventing identified vulnerabilities.

A research study was conducted at the Faculty of Information Technology of Farabi University to identify vulnerabilities in the Windows 10 operating system. The research consisted of two parts: conducting a penetration test and calculating the Hurst exponent using Wireshark.

For the study, students specializing in information security systems at the Faculty of Information Technology were selected. A survey was conducted among the students, which included the following questions: 1) participation in CTF competitions; 2) knowledge of scanning tools; 3) practical experience in identifying OS vulnerabilities. Data analysis involved observing 86 participants. According to the survey results, 21% of students participated in CTF competitions, 62% possessed practical skills in scanning tools, and 17% had practical experience in identifying OS vulnerabilities.

3 Results and discussion

The experimental part of the work analyzes network traffic based on a virtual machine. Data connection type is a network bridge. In order to analyze network traffic, we use the *Kali Purple* operating system.

The *Netdiscover* utility discovering network interfaces without an IP address configuration was used to determine the nodes available on the network.

One of the key features of the Wireshark utility is traffic interception. The Wireshark utility fixes the problem with the network, debugging of web applications, network programs, and sites and allows viewing the packet data at all OSI levels.

The Wireshark window consists of panels: Packet List, Packet Details, and Packet Bytes. In the window, one can see the traffic related to the wireless access point and which protocols are used.

In the *Filter* menu, entering the command `ip.src==192.168.137.136` and pressing *Enter* make it possible to get only those packets that came from the specified IP address and the results of filtering.

The *Statistics-Capture File Properties* command shows the average number of packets per second, the average packet size, and the traffic intensity.

Traffic results are as follows: packet intensity $\lambda = 2.5$ packets/s, average packet size $L = 159$ bytes, and traffic intensity $a = 3159$ kb/s.

An open-source network scanner used in Windows and Kali Purple operating systems is Network Mapper (*Nmap*). This utility determines the devices connected to the network, installed programs, the type of operating system, and the types of filters applied. *Nmap* opens a port on a computer and uses incoming connections to connect to another program.

Yu.V.Markin [10] considers a table with the results of network analyzers (Table 2):

Table 2: Summary table of the overview of network analyzers [10].

Objectives	Wireshark	Snort	Bro	ntopng
Thread recovery	+/-	-/+	+	-
Analysis of encrypted data	+	-	-	-
Analysis of nested tunnels	+	-	+	-
Adding protocol support	-/+	+/-	+/-	+/-

In order to achieve the set goals, the following requirements have been developed:

1. Difference in data flows when sending and recovering;
2. Supported format of archived and classified traffic;
3. Supported tunnel protocols with arbitrary stack configuration.

Based on the analysis performed to protect the information, exploits for the Windows 7 operating system were identified, and a search for the exploit/multi/handler vulnerability scanning module was performed (Fig. 1).

```

msf5 exploit(multi/handler) > set LHOST 192.168.137.136
LHOST => 192.168.137.136
msf5 exploit(multi/handler) > show options

Module options (exploit/multi/handler):

  Name  Current Setting  Required  Description
  ----  -
  LHOST 192.168.137.136 yes       The listen address (an interface may be specified)
  LPORT 4444             yes       The listen port

Payload options (generic/shell_reverse_tcp):

  Name  Current Setting  Required  Description
  ----  -
  LHOST 192.168.137.136 yes       The listen address (an interface may be specified)
  LPORT 4444             yes       The listen port

Exploit target:

  Id  Name
  --  ---
  0   Wildcard Target

View the full module info with the info, or info -c command.

msf5 exploit(multi/handler) >

```

Figure 1: Defining exploits

The use of certain network layer vulnerabilities is based on the IEEE 802.11 standard. For the experiment, a test local private wireless network Broadcom 802.11 n Network Adapter

was used. The attack generation environment uses a virtual machine with the installed Kali Purple distribution version kali-linux-2024.1-installer-purple-amd64.iso with a set of special utilities for testing for network penetration. A virtual machine with Windows 7 OS was used to analyze the attacks. Metasploit Exploitation Framework tool was used to test for penetration.

The results of exploits that can be applied in the tested are shown in Fig. 2.

```

msf5 > exploit(multi/handler) > set payload windows/meterpreter/reverse_tcp
payload => windows/meterpreter/reverse_tcp
msf5 > exploit(multi/handler) > show options

Module options (exploit/multi/handler):



| Name     | Current Setting | Required | Description                                               |
|----------|-----------------|----------|-----------------------------------------------------------|
| EXITFUNC | process         | yes      | Exit technique (Accepted: '', seh, thread, process, none) |
| LHOST    | 192.168.137.136 | yes      | The listen address (an interface may be specified)        |
| LPORT    | 4444            | yes      | The listen port                                           |



Payload options (windows/meterpreter/reverse_tcp):



| Name     | Current Setting | Required | Description                                               |
|----------|-----------------|----------|-----------------------------------------------------------|
| EXITFUNC | process         | yes      | Exit technique (Accepted: '', seh, thread, process, none) |
| LHOST    | 192.168.137.136 | yes      | The listen address (an interface may be specified)        |
| LPORT    | 4444            | yes      | The listen port                                           |



Exploit target:



| ID | Name            |
|----|-----------------|
| 0  | Wildcard Target |



View the full module info with the info, or info -c command.

msf5 > exploit(multi/handler) > █

```

Figure 2: Results of the vulnerability definition

On Windows 7, a hack was detected using the Servis apache2 (Fig. 3-4)

```

(root@kali)~# service apache2 status
o apache2.service - The Apache HTTP Server
  Loaded: loaded (/usr/lib/systemd/system/apache2.service; disabled; preset: disabled)
  Active: inactive (dead)
  Docs: https://httpd.apache.org/docs/2.4/

(root@kali)~# service apache2 start
o apache2.service - The Apache HTTP Server
  Loaded: loaded (/usr/lib/systemd/system/apache2.service; disabled; preset: disabled)
  Active: active (running) since Sat 2024-03-30 19:37:20 CDT; 4s ago
  Docs: https://httpd.apache.org/docs/2.4/
  Process: 37352 ExecStart=/usr/sbin/apachectl start (code=exited, status=0/SUCCESS)
  Main PID: 37369 (apache2)
  Tasks: 6 (limit: 9396)
  Memory: 19.7M (peak: 20.2M)
  CPU: 185ms
  CGroup: /system.slice/apache2.service
          └─37369 /usr/sbin/apache2 -k start
             └─37372 /usr/sbin/apache2 -k start
                └─37373 /usr/sbin/apache2 -k start
                   └─37374 /usr/sbin/apache2 -k start
                      └─37375 /usr/sbin/apache2 -k start
                         └─37376 /usr/sbin/apache2 -k start

```

Figure 3: Loading the Servis apache2



Figure 4: Open apache2 in the Windows 10

In our research paper, we used the Hurst definition of R/S statistics to calculate network traffic per second. The traffic load results are shown in Fig. 5. The simulation duration is 330 seconds, and the number of packets is 3093. This value can be changed to study the nature of the traffic.

Address	Port	Packets	Bytes	Total Packets	Percent Filtered	Tx Packets	Tx Bytes	Rx Packets	Rx Bytes
64.233.166.84	443	13	4 kB	35	37.14%	0	0 bytes	13	4 kB
80.241.0.72	128	1	90 bytes	2	50.00%	0	0 bytes	1	90 bytes
142.250.184.206	443	231	40 kB	1,633	14.15%	0	0 bytes	231	40 kB
142.250.184.246	443	9	2 kB	19	47.37%	0	0 bytes	9	2 kB
142.250.185.102	443	10	2 kB	20	50.00%	0	0 bytes	10	2 kB
142.250.185.106	443	12	3 kB	26	46.15%	0	0 bytes	12	3 kB
142.250.185.163	443	10	3 kB	21	47.62%	0	0 bytes	10	3 kB
142.250.185.164	443	9	3 kB	22	40.91%	0	0 bytes	9	3 kB
142.250.185.195	443	7	2 kB	15	46.67%	0	0 bytes	7	2 kB
142.250.185.226	443	10	3 kB	25	40.00%	0	0 bytes	10	3 kB
142.250.186.138	443	27	6 kB	78	34.62%	0	0 bytes	27	6 kB
142.250.186.174	443	10	2 kB	21	47.62%	0	0 bytes	10	2 kB
172.217.38.99	443	45	8 kB	90	50.00%	0	0 bytes	45	8 kB
192.168.137.2	53	50	4 kB	102	49.02%	0	0 bytes	50	4 kB
192.168.137.136	33419	2	190 bytes	4	50.00%	2	190 bytes	0	0 bytes
192.168.137.136	34519	10	3 kB	21	47.62%	10	3 kB	0	0 bytes
192.168.137.136	34600	2	146 bytes	4	50.00%	2	146 bytes	0	0 bytes
192.168.137.136	34900	2	160 bytes	4	50.00%	2	160 bytes	0	0 bytes
192.168.137.136	35894	2	194 bytes	4	50.00%	2	194 bytes	0	0 bytes
192.168.137.136	36535	2	148 bytes	4	50.00%	2	148 bytes	0	0 bytes
192.168.137.136	36617	2	142 bytes	4	50.00%	2	142 bytes	0	0 bytes
192.168.137.136	36622	2	170 bytes	4	50.00%	2	170 bytes	0	0 bytes
192.168.137.136	36654	2	170 bytes	4	50.00%	2	170 bytes	0	0 bytes
192.168.137.136	36777	12	3 kB	26	46.15%	12	3 kB	0	0 bytes
192.168.137.136	37196	2	150 bytes	4	50.00%	2	150 bytes	0	0 bytes
192.168.137.136	38458	2	154 bytes	4	50.00%	2	154 bytes	0	0 bytes
192.168.137.136	38947	10	2 kB	20	50.00%	10	2 kB	0	0 bytes
192.168.137.136	40734	1	73 bytes	2	50.00%	1	73 bytes	0	0 bytes
192.168.137.136	41734	10	3 kB	25	40.00%	10	3 kB	0	0 bytes
192.168.137.136	42220	9	2 kB	19	47.37%	9	2 kB	0	0 bytes

Figure 5: Traffic under study for calculation

The following packets were received according to the analysis results: Ethernet – 2, TCP – 43, IPv4 – 22, and UDP – 55. The calculations of the results obtained are shown in Table 3.

Traffic duration $m = 330$ seconds, $N = 330/(3093/330) \approx 35$

Where, N is the number of blocks, and 3093 is the number of packets.

$i = 1$, time = 150 s – 31, packet = 345

$P1 = 345/(150 * 31) = 0.074$

$i = 2$, time = 210 s – 46, packet = 417

$$\begin{aligned}
P2 &= 417/(210 * 6) = 0.043 \\
i = 3, \text{ time} &= 270 \text{ s} - 113, \text{ packet} = 2961 \\
P3 &= 2961/(270 * 113) = 0.097 \\
i = 4, \text{ time} &= 330 \text{ s} - 141, \text{ packet} = 3093 \\
P4 &= 3093/(330 * 14) = 0.066
\end{aligned}$$

Table 3: Summary table of Network Analyzer overview.

Xi	1	2	3	4
Pi	0.074	0.043	0.097	0.066

The arithmetic mean of network traffic is determined by the following formula:

$$M = \frac{1}{N} \sum_{i=1}^N X_i \quad (1)$$

$$M = 0.07$$

Calculating the variance:

$$S^2 = \frac{1}{N} \sum_{i=1}^N (X_i - M)^2 \quad (2)$$

$$S = 0.019$$

Determination of the value of the oscillations relative to the mean M :

$$\begin{aligned}
D_j &= \sum_k^j X_k - j \cdot M \\
D1 &= X1 - N \cdot M = 0.004 \\
D2 &= X1 + X2 - N \cdot M = -0.023 \\
D3 &= X1 + X2 + X3 - N \cdot M = 0.004 \\
D4 &= X1 + X2 + X3 + X4 - N \cdot M = 0
\end{aligned} \quad (3)$$

Maximum and minimum D value range:

$$R = \max \{D_j\} - \min \{D_j\} \quad (4)$$

$$R = 0.004$$

The Hurst coefficient is determined by the following formula:

$$H = \frac{\ln \left(\frac{R}{S} \right)}{\ln N} \quad (5)$$

$$H = -1.1$$

This traffic calculation can be performed using the C# compiler (Fig. 6).

```

using System;
using System.Text;

class HelloWorld {
    static void Main() {
        Console.OutputEncoding = Encoding.UTF8;
        int[] packet = new int[4];
        int[] time = new int[4];
        int[] second = new int[4];
        double[] Pi = new double[4];
        double S, H, D;
        double[] D = new double[4];

        for (int i = 0; i < 4; i++) {
            Console.WriteLine($"Packet {i+1}: ");
            packet[i] = int.Parse(Console.ReadLine());
            Console.WriteLine($"Time {i+1}: ");
            time[i] = int.Parse(Console.ReadLine());
            Console.WriteLine($"Second {i+1}: ");
            second[i] = int.Parse(Console.ReadLine());
        }

        for (int i = 0; i < 4; i++) {
            Pi[i] = (double)packet[i] / (second[i] * time[i]);
            Console.WriteLine($"Pi[{i+1}] = " + Math.Round(Pi[i], 3));
        }

        S = 0.074;
        H = 0.043;
        D[1] = 0.097;
        D[2] = 0.066;
        M = 0.07;
        S = 0.019;
        D[1] = 0.004;
        D[2] = -0.023;
        D[3] = 0.004;
        D[4] = 0;
        H = 0.004;
        H = -1.1;
        H equal an anti-persistent or ergodic series that does not have self-similarity
    }
}

```

Figure 6: Results C#

Based on the results of the Hurst indicator (H), the following processes are determined:

- $H \leq 0.5$ – an anti-persistent or ergodic series that does not have self-similarity;
- $H = 0.5$ – complete random series with particle displacement in classical Brownian motion;
- $H \geq 0.5$ – a persistent (self-sustaining) process that has a long memory and is self-similar [12].

According to the results, we have $H \leq 0.5$, and this process is anti-persistent and does not have self-similarity.

In the following studies, the vulnerability analysis of the modules of the biometric voice identification system is conducted, and a block diagram of the system of voice identification of the user by voice with enhanced protection against attacks is proposed. This scheme for the use of elementary speech units in the developed identification systems allows improving computational performance, reducing subjective decisions in biometric systems, and increasing security against attacks on voice biometric identification systems with a probability of the first and second errors of the kind of 0.025 and 0.005 [15].

Using the MS Excel and C# compiler, the calculation was carried out by 77.11% of students (Fig. 7).

Computer Emergency Response Team (KZ-CERT) is a center that collects and analyzes information on computer incidents and provides advisory and technical support to users in preventing computer security threats. Together with Nitro Team LLP, more than 170 potentially vulnerable Microsoft Exchange IP addresses were discovered in the republican segment. Attackers can gain access to any Microsoft Exchange Server email account using these vulnerabilities. KZ-CERT experts sent instructions on identifying vulnerable software to all government agencies and operational information security centers [8].

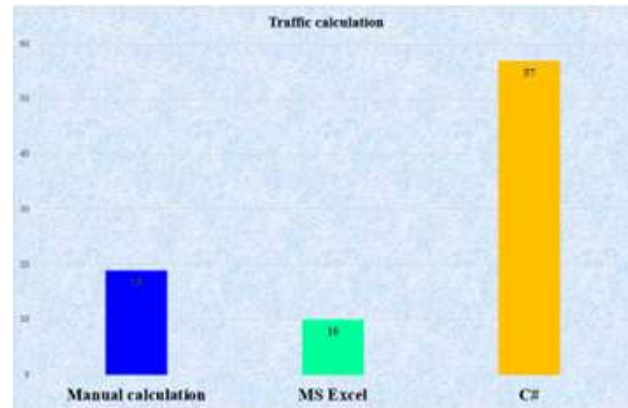


Figure 7: Methods of traffic calculation

Emrah Yasasin et al. [16] examine the vulnerability of software packages and the impact of exploits. Based on the National Vulnerability Database (NVD), the authors used mean absolute error (MAE) and root-mean-square error (RMSE) to measure prediction accuracy using single, double, and triple exponential smoothing, Croston's methodology, ARIMA, and the neural network approach. The results have shown that the optimal forecasting methodology depends on the software, and forecasting accuracy is reliable within the two applied forecasting error metrics.

Darshana Upadhyay et al. [14] investigate the vulnerability of the Supervisory Control and Data Acquisition (SCADA) network. In the scientific work, real incidents of SCADA vulnerabilities registered in standard databases are considered, and recommendations for SCADA security are given.

4 Conclusion

The goal of this research was to identify effective utilities for analyzing network traffic and detecting network vulnerabilities. Based on the analysis, the following threats were identified: broadcast scanning; interception of network traffic; modification and implementation of network traffic; getting information about the device; changing the ARP-spoofing table; implementation of a false DHCP server.

Identification of vulnerabilities in Windows 10 is done using the Kali Purple distribution. The following categories of attacks were identified: violation of the network perimeter; violation of integrity; violation of confidentiality; accessibility violation; link layer attack; Ethernet network layer attacks.

The analysis revealed the lack of full protection against harmful network activity. The developed methodology for detecting vulnerabilities and cracking the OS is based on the IDEF0 and IDEF1X methodology.

The proposed method of analyzing network traffic and detecting vulnerabilities allows you to identify and block attacks on the local Ethernet network with higher accuracy and completeness. The obtained results of the Hurst exponent ($H \leq 0.5$) determined an ergodic series that does not have self-similarity.

The vulnerability database grows every year. Organizations are undergoing changes

that are associated with a security risk. Information security management automates the inventory of resources and the identification of vulnerabilities using modern security tools. Each vulnerability must be verified. Thus, the proposed methods of analyzing and scanning the vulnerability of network resources are the first step towards security. This is a cyclical process, and the regularity of the process allows minimizing the risk of attacks on private, corporate infrastructure.

Further research will continue to study new types of attacks in local networks and improve the architecture of the information security system.

References

- [1] Clarke N., Li F., Furnell S., "A novel privacy preserving user identification approach for network traffic", *Computers & Security*, 70 (2017): 335–350.
- [2] Gorodnichev M.G., et al, "Machine learning in the tasks of identifying unwanted content", *In: Wave electronics and its application in information and telecommunication systems (WECONF)*, Saint-Petersburg (2019).
- [3] Gubareva O.Yu., Bourdine A.V., Evtushenko A.S., et al, *Secure data transmission channel protected by special fiber optic link based on optical crypto-fibers*. (2018). DOI:10.1117/12.2318579.
- [4] Jisa D., Ciza T., "Efficient DDoS flood attack detection using dynamic thresholding on flow-based network traffic", *Computers & Security*, 82 (2019): 284–295.
- [5] Kali Linux, Penetration Testing and Ethical Hacking Linux Distribution. [Electronic resource]. URL: <https://www.kali.org/> (Date: 25.02.2024).
- [6] Kawasaki Y., Hara Y., Kuwahara M., "Traffic state estimation on a two-dimensional network by a state-space model", *Transportation Research Part C: Emerging Technologies*, 113 (2020): 176–192.
- [7] Klenilmar L., Dias M.A., Pongelupe W.M., "An innovative approach for real-time network traffic classification", *Computer Networks*, 158 (2019): 143–157.
- [8] KZ-CERT (2021) 170 IP addresses of potentially vulnerable Microsoft Exchange mail servers found in Kaznet. <https://cert.gov.kz/news/11/1441>.
- [9] Makarenko S.I., Smirnov G.E., "Analysis of penetration testing standards and methodologies", *Systems of Control, Communication and Security*, 4 (2020): 44–72 (in Russian). DOI: 10.24411/2410-9916-2020-10402.
- [10] Markin Yu.V., "Methods and means of in-depth analysis of network traffic", *Dissertation, V.P. Ivannikov Institute of System Programming of the Russian Academy of Sciences*, (2017).
- [11] Pacheco F., Exposito E., Gineste M., "A framework to classify heterogeneous Internet traffic with machine learning and deep learning techniques for satellite communications", *Computer Networks*, 173 (2020): 107213.
- [12] Paramonov A.I., "Development and research of a complex of traffic models for public communication networks", *Dissertation, St. Petersburg State University of Telecommunications named after Professor M. A. Bonch-Bruевичh*, (2014).
- [13] Ring M., Schlör D., Landes D., et al, "Flow-based network traffic generation using. Generative Adversarial Networks", *Computers & Security*, 82 (2019): 156–172
- [14] Upadhyay D., Sampalli S., "SCADA (Supervisory Control and Data Acquisition) systems: Vulnerability assessment and security recommendations", *Computers & Security*, 89 (2020): 101666.
- [15] Vanyushina A.V., "Classification of IP traffic in a computer network using machine learning algorithms", *Dissertation, Moscow Technical University of Communications and Informatics*, (2019).
- [16] Yasasin E., Prester J., Wagner G., et al, "Forecasting IT security vulnerabilities – An empirical analysis", *Computers & Security*, 88 (2020): 101610.

IRSTI 81.96.00

DOI: <https://doi.org/10.26577/JMMCS2024121111>

Sh.Zh. Mussiraliyeva , M.A. Bolatbek , A.N. Zhumakhanova* ,
G. Baispay , Zh. Medetbek 
Al-Farabi Kazakh National University, Kazakhstan, Almaty
*e-mail: aygerim129@gmail.com

CREATING A MODEL OF SEMANTIC ANALYSIS OF EXTREMIST TEXTS IN THE KAZAKH LANGUAGE

Presently, there is a significant emphasis on the utilization of semantic analysis to scrutinize texts and viewpoints expressed in the Kazakh language within the realm of social networks, with the primary objective of identifying content of a suspicious or extremist nature. This research article is dedicated to exploring the application of machine learning and deep learning techniques in the realm of extremist content detection within textual data.

The investigation takes into account several critical factors, including oversampling and undersampling during the feature processing phase, the nuanced differentiation between extremist and neutral subjects, and the handling of imbalanced classification challenges. These considerations culminate in the development of a sophisticated deep learning model for text classification. The study encompasses the deployment of various machine learning models to discern extremist content within textual materials. Additionally, a comprehensive comparative analysis of machine learning methodologies is conducted to ascertain the most effective approach for this task, taking into consideration oversampling and undersampling techniques for addressing data imbalance issues.

The research endeavors are delineated into two core subtasks: the formulation of a machine learning model specialized in the detection of extremist content within text, and the construction of a deep learning model that factors in the unique characteristics of the Kazakh language and the available dataset.

Furthermore, the study delves into the intricacies of feature processing, culminating in a comparative assessment of outcomes derived from a range of machine learning algorithms used to classify religious extremism, each leveraging distinct feature combinations. The methodologies explored encompass decision trees, random forests, support vector machines, k-nearest neighbors, logistic regression, and naive Bayes.

This research significantly contributes to the spheres of text mining, artificial intelligence, and machine learning, offering practical recommendations for the processing and categorization of texts linked to religious extremism. Moreover, it underscores the contemporary significance of conducting semantic analyses on extremist texts written in the Kazakh language.

Key words: internet extremism, machine learning, deep learning, social networks, neural networks.

Ш.Ж. Мусиралиева, М.А. Болатбек, А.Н. Жумаханова*, Г. Байспай, Ж. Медетбек
Әл-Фараби атындағы Қазақ ұлттық университеті, Қазақстан, Алматы қ.
*e-mail: aygerim129@gmail.com

Қазақ тіліндегі экстремистік мәтіндерді семантикалық талдау моделін құру

Қазіргі уақытта әлеуметтік желілерде қазақ тіліндегі мәтіндер мен көзқарастарды зерттеу үшін семантикалық талдауды қолдануға көп көңіл бөлінуде, оның басты мақсаты күдікті немесе экстремистік сипаттағы мазмұнды анықтау болып табылады. Бұл зерттеу мақаласы мәтіндік деректердегі экстремистік мазмұнды анықтау саласында машиналық оқыту мен терең оқыту әдістерін қолдануды зерттейді.

Зерттеу бірнеше маңызды факторларды ескереді, соның ішінде функцияларды өңдеу сатысында артық іріктеу және жеткіліксіз таңдау, экстремистік және бейтарап субъектілер арасындағы нәзік саралау және теңгерімсіз жіктеу мәселелерін шешу. Бұл пайымдаулар мәтінді жіктеу үшін күрделі терең оқыту моделін әзірлеумен аяқталады. Зерттеу мәтіндік материалдардағы экстремистік мазмұнды анықтау үшін әртүрлі машиналық оқыту үлгілерін пайдалануды қамтиды. Бұдан басқа, деректердің теңгерімсіздігі мәселелерін шешу үшін артық іріктеу және жеткіліксіз таңдау әдістерін ескере отырып, осы тапсырмаға ең тиімді тәсілді анықтау үшін машиналық оқыту әдістемелерінің кешенді салыстырмалы талдауы жүргізіледі.

Зерттеу жұмыстары екі негізгі қосалқы міндетке бөлінген: мәтіндегі экстремистік мазмұнды анықтауға мамандандырылған машиналық оқыту моделін әзірлеу және қазақ тілінің бірегей сипаттамалары мен қолжетімді деректер жиынтығын ескере отырып, терең оқыту моделін құру.

Зерттеу сонымен қатар, діни экстремизмді жіктеу үшін пайдаланылатын машиналық оқыту алгоритмдерінің ауқымынан алынған нәтижелерді салыстырмалы бағалаумен аяқталатын, әрқайсысында ерекше белгілердің комбинациясын пайдалана отырып, мүмкіндіктерді өңдеудің қыр-сырын зерттейді. Зерттелген әдістерге шешім ағаштары, кездейсоқ ормандар, тірек векторлық машиналар, k-ең жақын көршілер, логистикалық регрессия және аңғал Бейс кіреді.

Бұл зерттеу діни экстремизмге қатысты мәтіндерді өңдеу бойынша тәжірибелік нұсқаулар ұсына отырып, мәтінді өңдеу, жасанды интеллект және машиналық оқыту салаларына елеулі үлес қосады. Оның үстіне бұл қазақ тілінде жазылған экстремистік мәтіндерге семантикалық талдау жүргізудің заманауи маңыздылығын көрсетеді.

Түйін сөздер: интернет экстремизмі, машиналық оқыту, терең оқыту, әлеуметтік желілер, нейрондық желілер.

Ш.Ж. Мусиралиева, М.А. Болатбек, А.Н. Жумаханова*, Г. Байспай, Ж. Медетбек
Казахский национальный университет имени аль-Фараби, Казахстан, г. Алматы
*e-mail: aygerim129@gmail.com

Создание модели семантического анализа текстов экстремистской направленности на казахском языке

В настоящее время большое внимание уделяется использованию семантического анализа для изучения текстов и точек зрения, выраженных на казахском языке в социальных сетях, с основной целью выявления контента подозрительного или экстремистского характера. Эта исследовательская статья посвящена изучению применения методов машинного обучения и глубокого обучения в области обнаружения экстремистского контента в текстовых данных.

В исследовании учитываются несколько важных факторов, в том числе избыточная и недостаточная выборка на этапе обработки признаков, тонкая дифференциация между экстремистскими и нейтральными субъектами, а также решение проблем несбалансированной классификации. Эти соображения завершаются разработкой сложной модели глубокого обучения для классификации текста. Исследование включает в себя использование различных моделей машинного обучения для выявления экстремистского содержания в текстовых материалах. Кроме того, проводится всесторонний сравнительный анализ методологий машинного обучения для определения наиболее эффективного подхода к этой задаче с учетом методов передискретизации и недостаточной выборки для решения проблем дисбаланса данных.

Исследовательские усилия разделены на две основные подзадачи: разработка модели машинного обучения, специализирующейся на обнаружении экстремистского контента в тексте, и построение модели глубокого обучения, учитывающей уникальные характеристики казахского языка и доступный набор данных.

Кроме того, исследование углубляется в тонкости обработки признаков, кульминацией которых является сравнительная оценка результатов, полученных с помощью ряда алгоритмов машинного обучения, используемых для классификации религиозного экстремизма, каждый из которых использует отдельные комбинации признаков. Исследованные методологии включают деревья решений, случайные леса, машины опорных векторов, k-ближайших соседей, логистическую регрессию и наивный байесовский подход.

Это исследование вносит значительный вклад в области анализа текста, искусственного интеллекта и машинного обучения, предлагая практические рекомендации по обработке и категоризации текстов, связанных с религиозным экстремизмом. Более того, это подчеркивает современную значимость проведения семантического анализа экстремистских текстов, написанных на казахском языке.

Ключевые слова: интернет экстремизм, машинное обучение, глубокое обучение, социальные сети, нейронные сети.

1 Introduction

Semantic text analysis is one of the main problems of both the theory of creating artificial intelligence systems associated with natural language processing and computer linguistics. Syntactic and morphological analysis is usually used in the primary processing of texts using an automatic machine method. Turning to semantic analysis, scientists not only consider the text as a set of words and sentences, but also try to create a complete semantic image created by the author.

Machine learning is considered a branch of artificial intelligence. Its main idea is that the computer is not limited to using a pre-written algorithm, but learns to solve the problem on its own. Any work can be classified into one of three levels depending on the relative availability of machine learning technology. The first level is when it is available to various technology giants at the level of Google or IBM. The second level is when a student who has certain knowledge can apply it. The third level is when even grandparents can handle it. Now that machine learning is at the intersection of the second and third levels, the pace of changing the world with the help of this technology is increasing every day [1].

To create methods in machine learning, mathematical statistics, numerical methods, mathematical analysis, optimization methods, probability theory, graphical theories, and various methods of working with numerical data are used. As the processing power of computers has increased, the laws and predictions they create have become many times more complex, and the range of problems and problems that can be solved using machine learning has expanded. With machine learning, we use different methods and select the most suitable method for a given task.

The task is divided into 2 subtasks: 1) creating a machine learning model for detecting extremism in text and 2) creating a deep learning model.

In general, many deep learning methods have sufficient performance and can solve many problems that previously could not be solved effectively, for example, they are often used in computer vision, machine translation, and speech recognition tasks. Using deep learning, we develop a model taking into account the characteristics of the Kazakh language and data set [2].

2 Material and methods

Using machine learning to detect extremism in text

In this section, we compare the results of using different machine learning algorithms to classify religious extremism using different combinations of features. Modern research considers the following most common methods for constructing and training classifiers:

decision tree, random forest, support vector machine, k-nearest neighbors, logistic regression, naive Bayes (Figure 1).

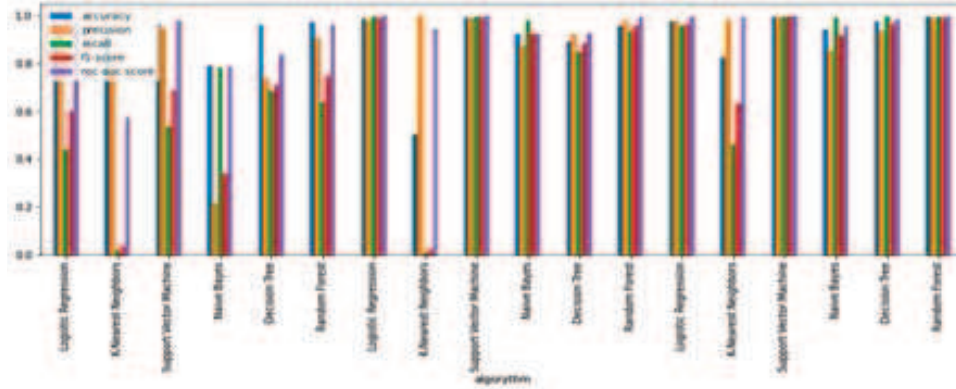


Figure 1: Comparison of results of classification algorithms

Table 1 shows the comparison results between different methods using different features. As shown in the table, the performance of all methods improves by combining more functions together. This observation confirms the informativeness and effectiveness of the acquired features. However, the contribution of each feature varies significantly, indicating variations in the results of individual methods [3].

Table 1: Comparison of different methods using different features

Methods	Features	ACC.	Prec.	Recall	F1	AUC
SVM	Statistical Features +TF-IDF	0.8204	0.2423	0.7593	0.3673	0.8622
	Statistical Features +TF-IDF+POS	0.8412	0.2512	0.6625	0.3643	0.8263
	Statistical Features +TF-IDF+POS+LIWC	0.1065	0.0641	0.8834	0.1196	0.5357
	Statistical Features +TF-IDF	0.9444	0.9529	0.201	0.332	0.6472
Decision tree	Statistical Features +TF-IDF+POS	0.9444	0.8969	0.2159	0.348	0.6395
	Statistical Features +TF-IDF+POS+LIWC	0.9444	0.8812	0.2208	0.3532	0.6274
	Statistical Features	1234	1234	1234	1234	1234
	Statistical Features +TF-IDF	0.9368	1.0	0.0794	0.1471	0.9179
KNN	Statistical Features +TF-IDF+POS+LIWC	0.9364	1.0	0.0744	0.1386	0.914
	Statistical Features +TF-IDF	0.9335	0.8421	0.0397	0.0758	0.5847
	Statistical Features +TF-IDF+POS	0.9354	0.8158	0.0769	0.1406	0.6105
	Statistical Features +TF-IDF+POS+LIWC	0.9351	0.7037	0.0943	0.1663	0.701

	Statistical Features +TF-IDF	0.9681	0.8942	0.6079	0.7238	0.9739
Simplified Bayes algorithm	Statistical Features +TF-IDF+POS	0.9625	0.806	0.598	0.6866	0.9687
	Statistical Features +TF-IDF+POS+LIWC	0.9543	0.7304	0.531	0.6149	0.9599
	Statistical Features +TF-IDF	0.9601	0.9568	0.4392	0.602	0.9759
Logistic regression	Statistical Features +TF-IDF+POS	0.9598	0.9418	0.4417	0.6014	0.9759
	Statistical Features +TF-IDF+POS+LIWC	0.9409	0.6647	0.2804	0.3944	0.9336

The AUC performance measurement in each classification is the area under the receiver operating characteristic curve with all extracted features. In the last column of Table 4, AUC tends to increase with more combined features. The logistic regression method obtains the highest AUC of 0.9759, while most other methods have a very similar AUC value above 0.9.

To evaluate the classification of texts related to extremism with other specific online communities, we expanded our corpus and tested our models in "news" and "jokes". As the results show, most models show an accuracy of more than 75%, and the model trained with KNN methods detects extremist texts with an accuracy of more than 95% in tests on both datasets. This means our model can work in real environments with an accuracy of about 95% [4].

Using deep learning to detect extremism

Deep learning is ideal for natural language processing (NLP) tasks such as sentiment analysis, text classification, machine translation. For text classification, we use the following deep learning methods: convolutional neural network (CNN) and recurrent neural network LSTM.

Our dataset includes labeled texts. Each text was assigned a label: 0 for neutral text or 1 for extremist text. Since in our case the data is text, we considered filtering and vectorization to prepare the data. Text filtering is performed to reduce noise and outliers.

The following algorithm was used to filter the texts:

- 1) bringing all characters to the same case and removing unnecessary characters,
- 2) exclusion of common words (stop words),
- 3) perform stemming and lemmatization,
- 4) indicate the tokenization pattern (breaking the text into words - tokens) and the n-gram model of words (the number of possible words in a token).

Neural networks can only learn to find patterns in numeric data, and so before we feed text into the neural network as input, we converted each word into a numeric value. This process is called word encoding or tokenization.

For tokenization, we used word embeddings. This method represents words as dense word vectors (also called word embeddings). This means that the word "embedding" collects more information into fewer dimensions. Their goal is to map semantic meaning into geometric

space. This geometric space is called the embedding space. This will display semantically similar words close to the embedding space, such as numbers or colors.

To tokenize the data, we used the Tokenizer utility class in Keras, which can vectorize a text corpus into a list of integers.

```
from keras.preprocessing.text import Tokenizer
from keras.preprocessing.sequence import pad_sequences
from keras.preprocessing import text, sequence

tokenizer = Tokenizer(num_words=20000)
tokenizer.fit_on_texts(list(X_train))

X_train = tokenizer.texts_to_sequences(X_train)
X_test = tokenizer.texts_to_sequences(X_test)

X_train = sequence.pad_sequences(X_train, maxlen=200)
X_test = sequence.pad_sequences(X_test, maxlen=200)

print('X_train shape:', X_train.shape)
print('X_test shape: ', X_test.shape)
```

In Tokenizer we used two parameters: `num_words` which is responsible for setting the size of the dictionary and `pad_sequence()` which simply pads the sequence of words with zeros. The `pad_sequence()` parameter is used to solve the problem of different word lengths in a text sequence. We add the `num_words` parameter, which is responsible for setting the size of the dictionary. We set the value of `num_words` to 20000. One of our problems is that each text sequence in most cases has a different word length. And we'll also add the `maxlen` parameter to indicate how long the sequences should be. This cuts out sequences larger than this number [5-6].

3 Literature review

The objective of this literature review is to bridge an existing knowledge gap by conducting a comparative examination of machine learning algorithms utilized for the identification of extremist content in the Kazakh language. By amalgamating and critically assessing prior research, this review seeks to provide insights into the strengths, limitations, and potential avenues for future exploration within this field. Ultimately, this endeavor contributes to the advancement of robust tools aimed at countering the proliferation of extremism within the Kazakh online sphere.

Article [7] underscores the importance of identifying and categorizing tweets associated with extremism, as extremist groups employ social media platforms to disseminate their ideologies and recruit adherents. The article introduces a system designed to analyze content related to terrorism, with a specific focus on classifying tweets into extremist and non-extremist categories. This approach harnesses deep learning-based sentiment analysis techniques to construct a tweet classification system. Encouragingly, the experimental results

suggest the potential effectiveness of this structural framework. The article addresses the pressing need for effective methodologies to detect extremist content on prominent social networks like Facebook and Twitter. It makes a substantial contribution to the domain of extremism studies by presenting a framework that aids in monitoring and combating the propagation of extremist ideologies online. Furthermore, this work offers prospective researchers a blueprint for advancing the field of identifying and categorizing extremist content on social media platforms.

In Article [8], the significance of researching online extremism to monitor the proliferation of hate on social media platforms is articulated. The author highlights the limitations of existing research, emphasizing its ideological bias and its propensity to utilize simplistic binary or tertiary classifications. The research within this article endeavors to establish a balanced dataset encompassing various ideologies, with a particular focus on extremist tweets. The resulting dataset, referred to as Merged ISIS/Jihadist-White Supremacist (MIWS), is evaluated employing pretrained BERT and its variants (RoBERTa and DistilBERT), achieving a notable f1 score of 0.72. This study underscores the increasing emphasis on natural language processing employing deep learning techniques within extremism detection research.

Article [9] delves into the role of uncertainty in political, religious, and social matters in inciting extremism among individuals, which manifests through their expressions on social networks. Acknowledging the dominance of English in social media interactions, this research underscores the importance of considering sentiments expressed in other local languages to gain a more comprehensive understanding of the data. The study concentrates on sentiment analysis of multilingual textual data sourced from social networks to gauge the intensity of extremist sentiment. It introduces a multilingual dictionary complete with intensity weightings, achieving a validation accuracy of 88%. For classification, Polynomial Naive Bayes and Linear Support Vector Classifiers are deployed, with the Linear Support Vector Classifier attaining an 82% accuracy rate on a multilingual dataset. This research advances our comprehension of extremist sentiments expressed in multiple languages on social networks, offers insights into the levels of extremism, and underscores the effectiveness of the classification algorithms employed.

The subsequent article [10] accentuates the menace posed by online extremists on social media platforms and acknowledges the limitations associated with suspending their accounts, as they can readily create new ones. This study proffers operational solutions to confront this challenge, with a particular focus on formulating behavioral patterns for Twitter accounts linked to the "Islamic State of Iraq and Syria" (ISIS). These patterns are employed to track existing extremist users by identifying pairs of accounts attributed to the same individual.

In summation, these articles collectively enrich the landscape of detecting extremist content through the application of machine learning and deep learning techniques. They encompass diverse facets such as sentiment analysis, language models, social network analysis, and deep learning architectures. By engaging with these articles, readers can acquire a comprehensive comprehension of the subject matter, along with insights into the diverse methodologies and algorithms employed in this domain.

4 Results and discussion

In neural network, we know several terms such as input layer, hidden layer and output layer. Thus, the difference between deep learning and neural network architecture is the specified number of hidden layers. A simple neural network has only 1 hidden layer, whereas Deep Learning has more than 1 hidden layer (Figure 2).

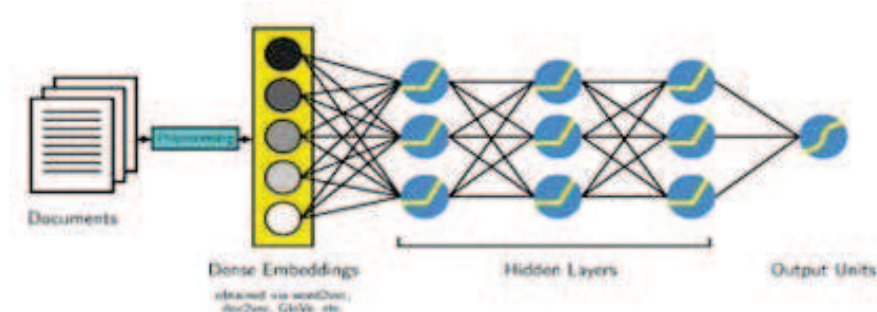


Figure 2: Deep Learning Model Architecture

We start with a layer of input neurons, where we enter our feature vectors, and then the values are transferred to the hidden layer. Each time we connect, we pass the value forward while the value is multiplied by the weight and the offset is added to the value. This happens on every connection, and at the end we get the value of the output layer. The output layer consists of one or more output nodes. In our case, one node, since we have a binary classification task.

Neural network formula: To calculate the values for each output node, we must multiply each input node p by the weight W and add a bias b . All this must then be summed up and passed to function f . This function is considered an activation function, and there are various functions. Typically, a rectified linear unit (ReLU) is used for hidden layers, a sigmoid function for the output layer in a binary classification problem, or a softmax function for the output layer in multiclass classification problems. We use the sigmoid function. The algorithm starts by initializing the weights with random values and then trains them using a method called backpropagation. This is done using optimization techniques (also called an optimizer), such as gradient descent, to reduce the error between the calculated output and the desired output (also called the target output). The error is determined by the loss function, the losses of which we want to minimize using the optimizer. Here we use the "Adam" optimizer and the "cross entropy" loss function [11].

Development of a convolutional neural network for text classification

Convolutional neural networks have revolutionized image classification and computer vision by being able to extract features from images and use them in neural networks. The properties that make them useful for image processing also make them useful for sequence processing. In the case of text classification using CNN, the convolutional kernel slides over word embeddings, only its task is to look at embeddings for several words at once. The dimensions of the convolutional kernel must also change to suit this task.

To look at word embedding sequences, we want the window to look at multiple (usually 3 or 5) word embeddings in the sequences. The cores will be a wide rectangle with dimensions

like 3x300 or 5x300 (with an embedding length of 300). In our case 4x200 because we set the sequence length to 200 when tokenizing. Each kernel cell has a corresponding weight. As the kernel slides over the word embedding, the kernel's weights are multiplied by the value of the word embedding, then all the multiplied values are summed to produce the output value.

The convolutional neural network will include many of these kernels, and as the network is trained, these kernel weights are learned. Each core is designed to view a word and surrounding words in a sequential window. Thus, the convolution operation can be considered as window-based feature extraction. There is another nice property of this convolution operation. Recall that similar words will have similar embeddings, and the convolution operation is simply a linear operation on these vectors. So, when a convolutional kernel is applied to different sets of similar words, it will produce the same output value [12].

To process the entire sequence of words, these kernels will sequentially traverse the list of word embeddings. This is called 1D Convolution because the kernel only moves in one dimension: time. One core will move one by one through the list of input embeddings, looking at the first word embedding, then the next word embedding, the next, and so on. The resulting output will be a feature vector.

The maximum values obtained by processing each of our convolutional feature vectors will be concatenated and passed to the last layer. This is called MaxPooling. And this is what our convolutional neural network looks like (Figure 3).

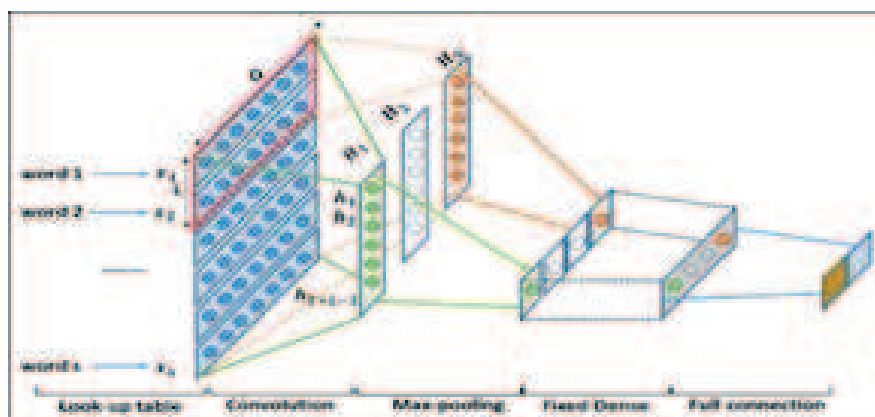


Figure 3: Proposed Convolutional Neural Network

Now let's see how we can use this network in Keras. First, we need to add an embedding layer with the parameters `input_dim` - the size of the dictionary, the number of unique words we want to use; `input_length` - sequence length; `output_dim` - dimension of the embedded variable. We then set an exclusion layer to exclude 50% of the nodes. Now we add a convolutional layer that has 100 filters with a kernel size of 4, so that each convolution takes into account a window of 4 word embeddings and a relu activation function. Before we add the Max Pooling layer, we add a normalization layer. After the pooling layer, we add a dense layer to get a pin size of 8 and use the relu activation function. Finally, we set up the output layer. Since we are doing binary classification, we use the sigmoid activation function and get 1 result in the output layer.

Here we used the "Adam" optimizer and the "cross entropy" loss function. And we got the following result for 4 epochs (Figure 4) [13]:

```

cnn_model = Sequential()
cnn_model.add(Embedding(input_dim=20000, input_length=200, output_dim=128))
cnn_model.add(SpatialDropout1D(0.5))
cnn_model.add(Conv1D(filters=100, kernel_size=4, activation='relu'))
cnn_model.add(BatchNormalization())
cnn_model.add(GlobalMaxPool1D())
cnn_model.add(Dropout(0.5))
cnn_model.add(Dense(8, activation='relu'))
cnn_model.add(Dense(1, activation='sigmoid'))

cnn_model.compile(loss='binary_crossentropy', optimizer=Adam(0.01),
                  metrics=['accuracy'])
cnn_hist = cnn_model.fit(X_train, Y_train, batch_size=256,
                          epochs=4, validation_split=0.2)

```

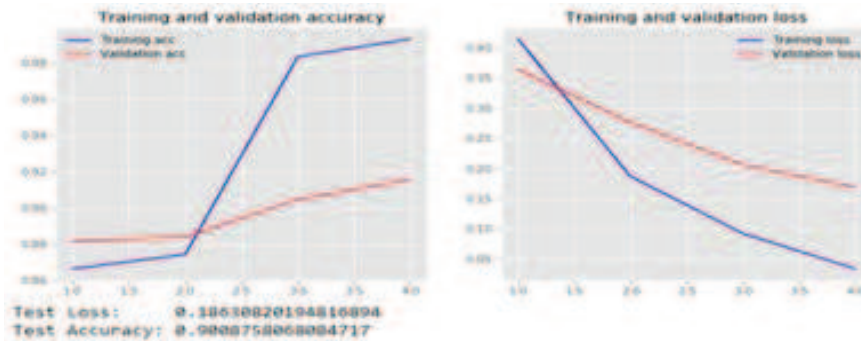


Figure 4: Result for 4 epochs

Application of a recurrent neural network

A recurrent neural network is a deep learning algorithm designed to solve a variety of complex computer problems, such as object classification and speech detection. RNNs are designed to process a sequence of events that occur sequentially, making sense of each event based on information from previous events. RNNs are rarely used in real-world scenarios due to the vanishing gradient problem. This is one of the biggest challenges for RNN performance. In practice, the RNN architecture limits its long-term memory capabilities, which are limited to remembering only a few sequences at a time.

LSTM (Long short-term memory) is designed to solve the vanishing gradient problem and allow them to retain information for longer periods of time compared to traditional RNNs. Therefore, we use LSTM rather than a traditional recurrent neural network. The LSTM architecture is shown below (Figure 5).

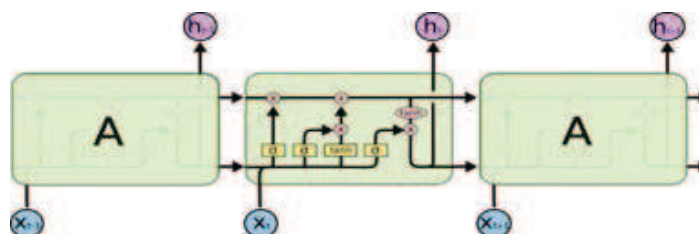


Figure 5: LSTM architecture

We will classify text data using a deep learning network with long short-term memory (LSTM). Text data is naturally sequential. A piece of text is a sequence of words between which there may be dependencies. To learn and use long-term dependencies to classify sequence data, we use an LSTM neural network. An LSTM network is a type of recurrent neural network (RNN) that can learn long-term dependencies between time steps, as shown above, of sequence data.

To input text into an LSTM network, you first need to convert the text data into numeric sequences. We already converted the text into numeric values when we built the convolutional neural network model. Next we will work with those numerical values.

We created exactly the same model for this neural network as for the convolutional neural network. Only instead of a convolutional layer, a bidirectional LSTM layer was added.

Bidirectional LSTMs are an extension of traditional LSTMs that can improve model performance in sequence classification tasks. In problems where all time slots of the input sequence are available, bidirectional LSTMs train two LSTMs instead of one in the input sequence. The first one refers to the input sequence as is, and the second one refers to an inverted copy of the input sequence. With this form of generative deep learning, the output layer can simultaneously receive information from the backward and forward states (Figure 6).

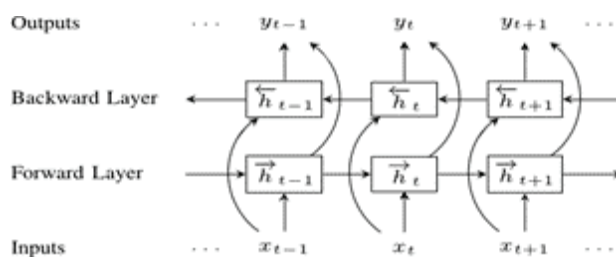


Figure 6: LSTM architecture

A convolutional neural network (CNN) is limited by the local window size and can only extract local text features. For long texts such as news, CNN cannot learn the long-term dependency of long text. A deep learning recurrent neural network model based on long short-term memory (LSTM) can learn the long-term dependency of text. The test data classification results are shown in Figure 7 [14].

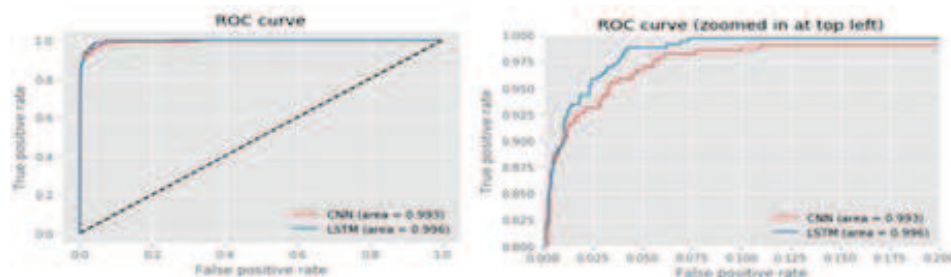


Figure 7: Test data classification result

5 Conclusion

As a result of this article, the following results were obtained: a) different machine learning models were applied to the task of detecting extremism in text content; b) a comparative analysis of machine learning methods was carried out to select the optimal method for a given task; c) oversampling and undersampling methods were carried out to eliminate the problem of data imbalance; d) a deep learning model (convolutional and recurrent neural networks) was developed to detect extremism in Kazakh texts.

Funding Statement. This research was carried out within the framework of the project "Multi-classification of ideological directions of cyber extremism in the Kazakh language using artificial intelligence methods", funded by the Science Committee of the Ministry of Science and Higher Education of the Republic of Kazakhstan (grant No. AP19676342, project leader Sh. Zh. Mussiraliyeva).

References

- [1] Bolatbek M.A., Mussiraliyeva Sh.Zh., "Identification of extremist texts using machine learning methods", *Bulletin of KazUTZU* 6 (130) (2018): 300–304.
- [2] Yntykbai B.N., Mussiraliyeva Sh.Zh., Bolatbek M.A., "Analysis of security and confidentiality in social networks using machine learning methods", *Materials of the International Scientific Conference of Students and Young Students "Farabi World"* Almaty: Kazakh University, (2021): 119.
- [3] Chesnokov V.O., "The application of the algorithm of selection of communities in information warfare in social networks", *Questions of cyber security*, 1 (19) (2017): 37–44.
- [4] Ripeanu, Beznosov K., Santos-Neto E., "Thwarting fake OSN accounts by predicting their victims", *Proceedings of the 8th ACM Workshop on Artificial Intelligence and Security*, (2015): 81–89.
- [5] Basu A., "Social network analysis: A methodology for studying terrorism", *Social Networking, ser. Intelligent Systems Reference Library*, 65 (2014): 215–242.
- [6] Freeman M., "The Sources of Terrorist Financing: Theory and Typology", *Studies in Conflict & Terrorism*, 34 (2011): 461–475. Doi:10.1080/1057610X.2011.571193.
- [7] Ahmad S., Asghar M.Z., Alotaibi F.M., Awan I., "Detection and classification of social media-based extremist affiliations using sentiment analysis techniques", *Human-centric Computing and Information Sciences*, 9 (24) (2019): 1–23. Q1.
- [8] Mayur G., Swati A., Ketan K., Ajith A., "Multi-ideology Multi-class Extremism Classification using Deep Learning Techniques", *IEEE Access*, (2022). Q1.
- [9] Asif M., Ishtiaq A., Ahmad H., Aljuaid H., Shah J., "Sentiment analysis of extremism in social media from textual information", *Telematics Informat.*, 48 (2020): 101345. Q1.
- [10] Klausen J., Marks C.E., Zaman T., "Finding extremists in online social networks", *European Journal of Operational Research*, 66 (4) (2018): 957–976. Q1.
- [11] Taha K., Yoo P.D., "Shortlisting the influential members of criminal organizations and identifying their important communication channels", *IEEE Transactions on Information Forensics and Security*, 14 (8) (2019): 1988–1999.
- [12] Devyatkin D.A., Smirnov I.V., Ananyeva M.I., Kobozeva M.V., Chepovskiy A.M., Solovyev F.N., "Exploring linguistic features for extremist texts detection (on the material of Russian-speaking illegal texts)", *IEEE International Conference on Intelligence and Security Informatics (ISI)*, (2017): 188–190.
- [13] Bissaliyev M.S., Nyussupov A.T., Mussiraliyeva Sh.Zh., "Enterprise Security Assessment Framework for Cryptocurrency Mining Based on Monero", *Vestnik KazNU Series "Mathematics, Mechanics, Informatics"*, 2 (98) (2018): 67–76.
- [14] Nouh M., Nurse J., "Identifying Key Players in Online Activist Groups on Facebook Social Network", *IEEE Computer Society*, (2015): 969–978.

IRSTI 27.47.23

DOI: <https://doi.org/10.26577/JMMCS2024121112>**I. Saymanov** 

National University of Uzbekistan named after Mirzo Ulugbek, Uzbekistan, Tashkent
Engineering Federation of Uzbekistan, Uzbekistan, Tashkent
e-mail: islambeksaymanov@gmail.com

LOGICAL AUTOMATIC IMPLEMENTATION OF STEGANOGRAPHIC CODING ALGORITHMS

The main goal of steganography is to ensure secure communication while keeping the communicative act "invisible". The origin of this term dates back to Ancient Greece and translates as "hidden writing". A simple yet effective method of steganography in antiquity, considering the frequent use of wax tablets, involved cutting out the message on the wooden bottom of the tablet and then writing a decoy message on the wax. Technological evolution has led to human ingenuity, allowing the use of this powerful tool for both message transmission and watermarking products during the transition from physical to digital media. There are various forms of steganography, including injective, generative, substitutive, selective, and constructive. The steganography we employ is injective, as it is more suitable for our task of hiding information in image pixels. After various searches, we decided to use BMP (Bitmap Picture) 3 (Microsoft Windows NT) and later versions as the image file format, as this version, especially in 24-bit and 32-bit encodings, represents a single color component. Each byte allows for altering the least significant bits without changing the external appearance of the image.

Key words: logical automatic implementation, steganographic coding, algorithms, RGB (Red, Green, Blue), LSB (Least Significant Bit), PSNR (peak signal to-noise ratio).

И. Сайманов

Мирзо Улугбек атындағы Өзбекстан Ұлттық университеті, Өзбекстан, Ташкент қ.
Өзбекстанның инженерлік федерациясы, Өзбекстан, Ташкент қ.
e-mail: islambeksaymanov@gmail.com

Стеганографиялық кодтау алгоритмдерін логикалық автоматты жүзеге асыру

Стеганографияның негізгі мақсаты коммуникативті актіні "көрінбейтін" сақтай отырып, қауіпсіз байланысты қамтамасыз ету. Бұл терминнің шығу тегі Ежелгі Грециядан басталады және "жасырын жазу" деп аударылады. Ежелгі дәуірде балауыз таблеткаларын жиі қолдануды ескере отырып, стеганографияның қарапайым, бірақ тиімді әдісі планшеттің ағаш түбіндегі хабарламаны кесіп алуды, содан кейін балауызға алдау хабарламасын жазуды қамтиды. Технологиялық эволюция адамның тапқырлығына әкеліп соқты, бұл қуатты құралды физикалық медиадан цифрлық тасымалдағышқа көшу кезінде хабарларды жіберу үшін де, өнімдерді су таңбалау үшін де пайдалануға мүмкіндік берді. Стеганографияның инъекциялық, генеративті, алмастырушы, селективті және конструктивті сияқты әртүрлі формалары бар. Біз қолданатын стеганография инъекциялық болып табылады, өйткені ол кескін шикселдеріндегі ақпаратты жасыру міндетімізге қолайлырақ. Түрлі іздеулерден кейін біз BMP 3 (Microsoft Windows NT) және одан кейінгі нұсқаларын кескін файлының пішімі ретінде пайдалануды шештік, өйткені бұл нұсқа, әсіресе 24-биттік және 32-биттік кодтауларда, бір түсті құрамдас бөлікті білдіреді. Әрбір байт кескінің сыртқы көрінісін өзгертпестен ең аз маңызды биттерді өзгертуге мүмкіндік береді.

Түйін сөздер: логикалық автоматты іске асыру, стеганографиялық кодтау, алгоритмдер, RGB (Қызыл, Жасыл, Көк), LSB (Ең аз маңызды бит), PSNR (сигналдың шуылға қатынасы шыңы).

И. Сайманов

Национальный университет Узбекистана имени Мирзо Улугбека, Узбекистан, г. Ташкент
 Инженерная Федерация Узбекистана, Узбекистан, г. Ташкент
 e-mail: islambeksaymanov@gmail.com

Логическая автоматная реализация алгоритмов стеганографического кодирования

Основная цель стеганографии обеспечить безопасную связь, сохраняя при этом коммуникативный акт "невидимым". Происхождение этого термина восходит к Древней Греции и переводится как "скрытое письмо". Простой, но эффективный метод стеганографии в древности, учитывая частое использование восковых табличек, заключался в вырезании сообщения на деревянном дне таблички, а затем написании ложного сообщения на воске. Технологическая эволюция привела к человеческой изобретательности, позволившей использовать этот мощный инструмент как для передачи сообщений, так и для нанесения водяных знаков на продукты при переходе от физических носителей к цифровым. Существуют различные формы стеганографии, включая инъективную, генеративную, замещающую, селективную и конструктивную. Используемая нами стеганография является инъективной, поскольку она больше подходит для нашей задачи по сокрытию информации в пикселях изображения. После различных поисков мы решили использовать в качестве формата файла изображения BMP 3 (Microsoft Windows NT) и более поздние версии, так как эта версия, особенно в 24-битной и 32-битной кодировке, представляет собой единую цветовую составляющую. Каждый байт позволяет изменять младшие биты без изменения внешнего вида изображения.

Ключевые слова: логическая автоматическая реализация, стеганографическое кодирование, алгоритмы, RGB (красный, зеленый, синий), LSB (младший значащий бит), PSNR (пиковое отношение сигнал/шум).

1 Introduction

The ability to utilize Arduino and any components that can be implemented sparked our interest in creating a useful and intriguing project for our participants [1]. Initially, the idea was to create a universal remote control panel that could be used in electronic equipment by using an infrared remote control to manage ecological process automation. After discussing other ideas, it was concluded that injective steganography could be an excellent tool to achieve the goal [2–8].

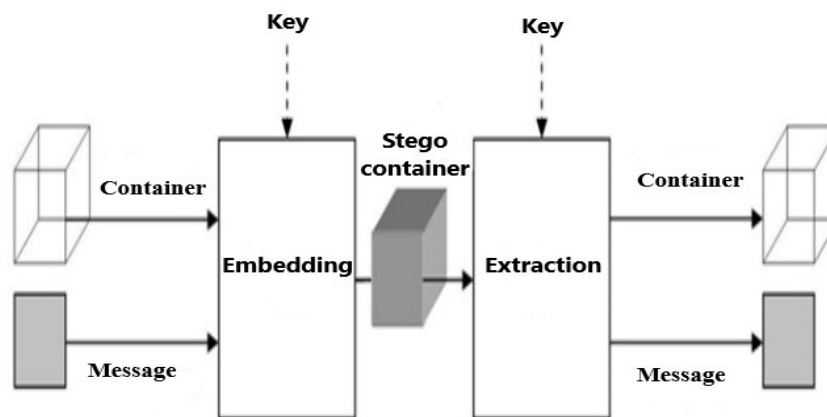


Figure 1: Generalized model of a steganographic system

The main goal of steganography is to ensure secure communication while keeping the communicative act "invisible". The origin of this term dates back to Ancient Greece and translates as "hidden writing". A simple yet effective method of steganography in antiquity, considering the frequent use of wax tablets, involved cutting out the message on the wooden bottom of the tablet and then writing a decoy message on the wax [9–14]. Technological evolution has led to human ingenuity, allowing the use of this powerful tool for both message transmission and watermarking products during the transition from physical to digital media [15–17]. There are various forms of steganography, including injective, generative, substitutive, selective, and constructive. The steganography we employ is injective, as it is more suitable for our task of hiding information in image pixels [18–24]. After various searches, we decided to use BMP 3 (Microsoft Windows NT) and later versions as the image file format, as this version, especially in 24-bit and 32-bit encodings, represents a single color component. Each byte allows for altering the least significant bits without changing the external appearance of the image. Therefore, supported raster images are 24-bit and 32-bit, because altering 8, 4, or 1 bit would be noticeable.

BMP format is one of the simplest formats jointly developed by Microsoft and IBM. A raster image file records the image as a table of points (pixels). It manages colors both in RGB (Red Green Blue) and through an indexed palette.

Our developed steganographer, as mentioned earlier, is compatible with both 32-bit and 24-bit raster image formats because we decided to use 4 image bytes to hide 1 byte of text. Of these 4 bytes, the first three are modified, and the last one should remain unchanged.

In the case of the 32-bit format (where R represents the red byte, G represents the green byte, B represents the blue byte), the least significant bit of the bytes will be modified in RGB.

The research provided systematic activities for image steganography, including hiding/embedding secret messages, revealing messages, as well as a systematic step-by-step approach to ensuring the execution of these steps. The research begins with explaining the new system, thereby giving a hint about its contents [25–29].

The proposed system employs a robust approach, involving embedding a secret message into one of the three RGB image color channels, bitwise processing, bit shuffling, a secret key, and cryptography to develop a new algorithm for steganography system. The new algorithm will provide the following important aspects of data security enhancement. Before matching the secret message to the image carrier by means of transposition, the intruder is misled.

The encryption of the secret key and data is encrypted using a reliable repetitive algorithm to ensure secure protection that cannot be easily cracked or broken.

The secret data will be hidden by matching them with the blue color frequency in the carrier image using a modification method for gray color.

Enhance file security on the Internet through efficient encryption and embedding of a secret message that can only be revealed by authorized third parties.

To ensure effective hiding of the secret message on the selected cover image, a different encryption method will be used. These modules include file matching and encryption methods to hide the secret message and ensure its security. A general diagram explaining the new methodology is presented in Figure 2 below.

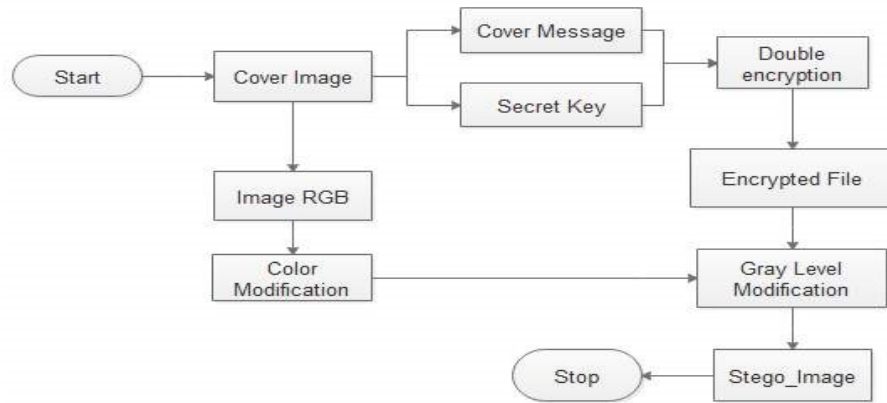


Figure 2: Steps of Text Concealment and Display on Image

2 Encryption Algorithm

This is a step-by-step approach used for concealing a message within an innocent image. This algorithm represents a procedural methodology developed to protect against malicious attacks on files over the Internet. The encryption algorithm is employed for concealment in this algorithm, precisely providing the first step in ensuring file security on the Internet, as well as serving as the first stage of image steganography adopted for this research. The algorithm begins by taking input about image concealment and outputs an encrypted stego-image with secret data and key bits. The encryption algorithm schema is presented below.

Inputs: original color image and document.

Output: Stego_Image consisting of a secret message.

Step 1: Select what needs to be concealed and the required encryption key.

Step 2: Convert the selected key into a one-dimensional array (1D array).

Step 3: Use logic 1 to apply the bitxor process to one bit of the secret key array with logical 1.

Step 4: Rearrange the encrypted bits from bitxor by swapping even and odd bits from step 2.

Logic: If the secret key bit = 1, perform the bitxor process with logical 1. Otherwise, do not implement the bitxor process.

Step 5: Repeat step 4 until all secret data bits are encrypted.

3 Cartographic module

The mapping procedure has been adopted for efficiently placing a secret message into a pixel of the carrier/cover image for final encryption. The cover image channels are transformed, followed by a 1-to-1 mapping to place the secret data into the cover image, preserving the bits and pixels of the original cover image to obtain the output steganographic image.

Input: cover image, secret message

Output: Stego_Image Step 1: Choose the carrier image.

Step 2: Transform the cover image from step 1.

Step 3: Select the secret file.

Step 4: Perform a 1-to-1 mapping to conceal the message from step 3 into the image from step 2.

Step 5: Stego image.

Concealment Algorithm.

Input: color image as cover, secret data, and key.

Output: Stego_image

Step 1: Choose the cover color image and divide it into red, green, and blue channels.

Step 2: Apply image transposition to all three channels of the input image.

Step 3: Encrypt the secret key and secret data according to encryption module 3.1.

Step 4: Transform pixel values for the blue channel by adding 1 if the first bit of the cover image equals one (1). If the pixel value is even, add one to the pixel.

Step 5: Map secret data from step 4 based on secret key bits (SKB) as follows: If secret key bits are even, the system adds one (1) to the pixel value. If pixel value equals the secret key bit value of 0 or is odd, subtract 1 from the pixel value. If pixel value of the secret bit equals 1 or is even, the system adds 1 to the pixel value.

Step 6: Repeat step 5 until all secret bits are mapped to gray levels of the carrier image.

Step 7: Transpose all three planes and combine them to make the steganographic image.

Convert the decoding algorithm of the LSB method to algebraic form as follows:

$$\begin{array}{lll}
 Y_0 = Y_1 = 1; & Y_6 = \overline{X_1 X_3}; & Y_{11} = \overline{X_1 X_3 X_4 X_6 X_7 X_8}; \\
 Y_2 = X_1 X_2; & Y_7 = \overline{X_1 X_3 X_4 X_5}; & Y_{12} = \overline{X_2 X_3 X_5 X_6 X_7 X_8}; \\
 Y_3 = \overline{X_1}; & Y_8 = \overline{X_1 X_3 X_4}; & Y_{13} = \overline{X_1 X_3 X_4 X_6 X_9}; \\
 Y_4 = \overline{X_1}; & Y_9 = \overline{X_1 X_3 X_4 X_6 X_7}; & Y_{14} = \overline{X_1 X_3 X_4 X_6 X_9}; \\
 Y_5 = \overline{X_1 X_3}; & Y_{10} = \overline{X_1 X_3 X_4 X_6 X_7 X_8}; & Y_k = \overline{X_1 X_3 X_4 X_5 X_6} \vee \overline{X_1 X_3 X_4 X_5}
 \end{array}$$

Unfortunately, it seems like the matrix scheme you mentioned is not provided in the text you provided. If you have the matrix scheme or any specific details you'd like to discuss or analyze regarding the LSB (Least Significant Bit) encoding and decoding algorithm, please feel free to provide them, and I'd be happy to assist you further.

$$\begin{array}{ll}
 Y_0 = Y_1; & Y_8 = Y_9; \\
 Y_1 = X_1 X_2 Y_2 \vee \overline{X_1} Y_3; & Y_9 = X_5 Y_{10} \vee \overline{X_5} X_6 X_7 Y_{11} \vee \overline{X_5} X_6 \overline{X_7} Y_{12} \vee \overline{X_5} X_6; \\
 Y_2 = X_1 X_2 Y_2 \vee \overline{X_1} Y_3; & Y_{10} = Y_9; \\
 Y_3 = Y_4; & Y_{11} = Y_{13}; \\
 Y_4 = X_3 Y_5 \vee \overline{X_3} Y_6; & Y_{12} = Y_{13}; \\
 Y_5 = Y_4; & Y_{13} = X_6 X_7 \overline{X_8} Y_{11} \vee X_6 \overline{X_7} \overline{X_8} Y_{12} \vee X_8 Y_{14} \vee \overline{X_6} \overline{X_8} Y_{15}; \\
 Y_6 = X_4 Y_7 \vee \overline{X_4} Y_8; & Y_{14} = \overline{X_6} Y_{15}; \\
 Y_7 = X_4 Y_7 \vee \overline{X_4} Y_8; & Y_{15} = Y_k;
 \end{array}$$

4 Extracting Algorithm.

The extraction algorithm delineates the sequential steps outlined in a flowchart aimed at extracting text from an image. The user is required to input both the key file and the steganographic image generated earlier. It is imperative that the same key file is employed during both the hiding and extraction phases. Subsequently, upon user input, the provided data undergoes scrutiny and validation for any potential exceptions. In the event of

exception detection, the process iterates from the beginning. Conversely, if no exceptions are encountered, the algorithm proceeds with the extraction process by implementing modifications to retrieve the secret message from the image file. This extracted secret message is then displayed on the screen or saved in a file.

```

Color pixel = bmp.GetPixel(j, i);
for (int n = 0; n < 3; n++)
{
    switch (colorUnitIndex % 3)
    {
        case 0:
        {
            charValue = charValue * 2 + pixel.R % 2;
        } break;
        case 1:
        {
            charValue = charValue * 2 + pixel.G % 2;
        } break;
        case 2:
        {
            charValue = charValue * 2 + pixel.B % 2;
        } break;
    }
    colorUnitIndex++;
    if (colorUnitIndex % 8 == 0)
    {
        charValue = reverseBits(charValue);
        if (charValue == 0)
        {
            // End of the secret message
            return secretData;
        }
        secretData.Append((char)charValue);
        charValue = 0;
    }
}
}

```

Figure 3: Extract the least significant bit of the blue channel.

5 Assessment of picture quality

This aspect involves examining the original image and the developed stego_image to determine whether any detectable changes or physical modifications to the original image will occur, thus verifying the effectiveness of the algorithms and steps taken in developing steganography. The quality of each (i.e., the original image and the resulting steganographic file) is carefully analyzed using common measures used for comparing the degree of quality.

The new steganographic algorithm has a high embedding capacity and low visual distortion. Encryption methods are resistant to malicious attacks, including adding noise, smoothing, quantization, and ordinary grid editing. Besides reliability, the new algorithm provides acceptable embedding capacity without noticeable visual distortion after embedding.

The efficacy of the novel encryption and steganography techniques is assessed in relation to their embedding capacity, embedding distortion, and reliability. The discrepancy in embedding distortion between the initial grid and its corresponding counterpart is scrutinized through metrics such as the root mean square error (RMSE), peak signal-to-noise ratio (PSNR), signal-to-noise ratio (SNR), and extracted reliability.

Mean Squared Error (MSE) is employed as a measure of similarity between images, elucidating the degree of distortion between the original and Stego_image. It serves as a signal

image quality metric, extensively utilized for assessing image quality due to its simplicity in determination, effectiveness in gauging image optimization, and ease of parameter calculation.

$$MSE = \frac{1}{MN} \sum_{x=1}^M \sum_{y=1}^N (S_{xy} - C_{xy})^2$$

The computation of the Mean Squared Error (MSE) between two images adheres to the aforementioned equation, wherein M and N represent the number of rows and columns of the cover image, respectively. Y and X denote the signals of the Stego image and the original image, respectively.

It is imperative to note that the Mean Squared Error is significantly influenced by the intensity scaling of the image. For instance, an MSE value of 100.0 achieved in an 8-bit image context (with pixel values ranging from 0 to 255) is deemed satisfactory. Conversely, an MSE value of 100.0 attained in a 10-bit image context (with pixel values ranging from 0 to 1023) is scarcely discernible and lacks substantial significance.

The Peak Signal-to-Noise Ratio (PSNR) provides an explanation of image quality by offering the ratio of the image signal to the power of image distortion in a logarithmic scale. It is also considered as a relative explanation of human perception of image quality. The higher the PSNR, the higher the image quality.

The PSNR is calculated by scaling the Mean Squared Error according to the image range.

$$PSNR = 10 \log \left[\frac{255^2}{MSE} \right]$$

Peak Signal-to-Noise Ratio (PSNR) values are conventionally expressed in decibels (dB). PSNR serves as a robust measure for comparing the outcomes of recovering identical images from various manipulations or compression processes. However, it's important to note that comparing PSNR values between different images holds lesser significance due to factors such as image content, resolution, and compression artifacts, which can significantly influence the perceived quality of the images. Therefore, while PSNR is valuable for assessing the fidelity of image recovery within the same context, its utility diminishes when used for comparing the quality of distinct images.

Signal-to-Noise Ratio (SNR) provides the ratio of signal power to noise power. It is an index that indicates the level of changes and influence on images based on a specific effect (such as steganography), providing a measure of the quantity/level of image transformation.

SNR is expressed in the formula below:

$$SNR = 10 \log_{10} \frac{signal}{noise}$$

Normalized Cross-Correlation (NCC) compares two images based on their common relationships. It is used to measure how two images deviate from or relate to each other. NCC is expressed in the formula below:

$$NCC = \frac{\sum_{x=1}^M \sum_{y=1}^N (S(x,y) \cdot C(x,y))}{\sum_{x=1}^M \sum_{y=1}^N (S(x,y))}$$

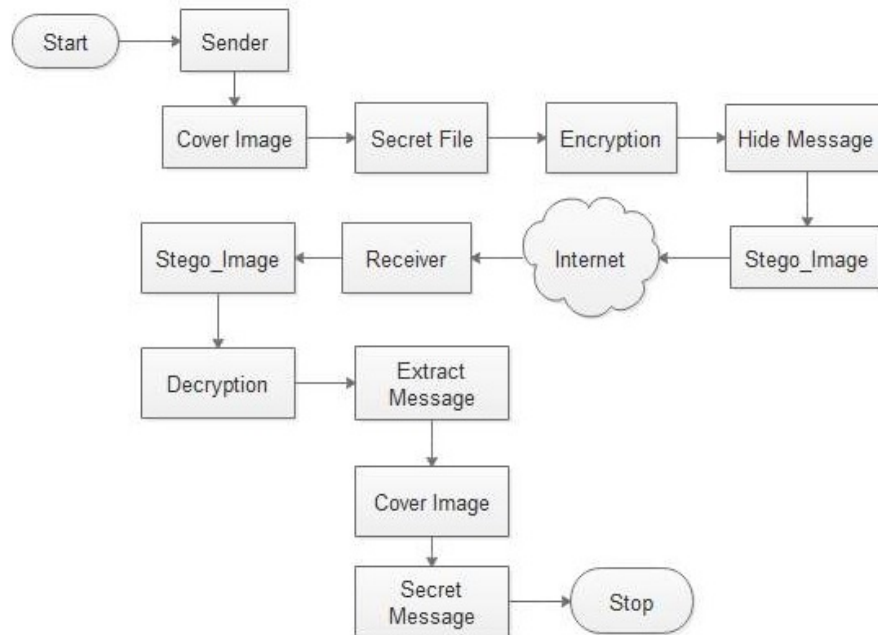


Figure 4: Extract the least significant bit of the blue channel.

The user is required to upload an image file, then select the level of security. The transmitted message is entered into the message field, after which the user enters their password for encrypting and embedding the secret message into the image (see Figure 4).

Finally, the user clicks the "Write Message to Image" button. After the appropriate measures have been taken, the user will need to upload a new image containing the secret message, i.e., the "Crypto-Stego Image". The algorithm used for the LSB method greatly complicates the detection of changes in images sent and received over the Internet by the human eye.

6 Conclusion

A logical method of steganographic encoding has been developed for the secure storage and transmission of images based on Boolean functions in the class of disjunctive normal forms using microcontrollers and CAD systems for designing programmable logic controllers. Methods and algorithms of steganographic encoding have been developed and implemented for the secure storage and transmission of images in an ecological system based on IoT technologies.

References

- [1] Kabulov A., Saymanov I., Yarashov I. and Muxammadiev F., "Algorithmic method of security of the Internet of Things based on steganographic coding 2021 *IEEE International IOT, Electronics and Mechatronics Conference (IEMTRONICS)*, (2021): 1-5, doi: 10.1109/IEMTRONICS52119.2021.9422588.

-
- [2] Kabulov A., Normatov I., Urunbaev E., Muhammadiev F., "Invariant Continuation of Discrete Multi-Valued Functions and Their Implementation 2021 IEEE International IOT, Electronics and Mechatronics Conference (IEMTRONICS), (2021): 1-6, doi: 10.1109/IEMTRONICS52119.2021.9422486.
- [3] Kabulov A., Normatov I., Seytov A., Kудaybergenov A., "Optimal Management of Water Resources in Large Main Canals with Cascade Pumping Stations 2020 IEEE International IOT, Electronics and Mechatronics Conference (IEMTRONICS), 2020: 1-4, doi: 10.1109/IEMTRONICS51293.2020.9216402.
- [4] Kabulov, A. V., Normatov, I. H., "About problems of decoding and searching for the maximum upper zero of discrete monotone functions *Journal of Physics: Conference Series*, 1260(10), 102006, 2019. doi:10.1088/1742-6596/1260/10/102006.
- [5] Kabulov, A. V., Normatov, I. H., Ashurov A.O., "Computational methods of minimization of multiple functions *Journal of Physics: Conference Series*, 1260(10), 10200, 2019. doi:10.1088/1742-6596/1260/10/102007.
- [6] Саџџ™ed Abed, Al-Mutairi Mohammed, Al-Watyan Abdullah, Al-Mutairi Omar, AlEnizy Wesam, Al-Noori Aisha, "An Automated Security Approach of Video Steganography-Based LSB Using FPGA Implementation" *Journal of Circuits, Systems and Computers*, Vol. 28, no. 05, (2019): 1950083.
- [7] Abdulrahman Abdullah Alghamdi, "Computerized Steganographic Technique Using Fuzzy Logic" *International Journal of Advanced Computer Science and Applications*, Vol. 9, no. 3, (2018): 155-159.
- [8] Bruno Carpentieri, Castiglione Arcangelo, De Santis Alfredo, Palmieri Francesco, Pizzolante Raffaele, "Compression-Based Steganography" *Concurrency and Computation: Practice and Experience*, Vol. 32, no. 8, (2020).
- [9] Mathivanan P., et al., "QR Code Based Color Image Stego-Crypto Technique Using Dynamic Bit Replacement and Logistic Map" *Optik*, Vol. 225, (2021): 1-24.
- [10] Gurunath R., Alahmadi Ahmed H., Debabrata Samanta, Mohammad Zubair Khan, Abdulrahman Alahmadi, "A Novel Approach for Linguistic Steganography Evaluation Based on Artificial Neural Networks" *IEEE Access*, Vol. 9 (2021): 120869ББ"120879.
- [11] MegГas David, Wojciech Mazurczyk, Minoru Kuribayashi, "Data Hiding and Its Applications: Digital Watermarking and Steganography" *Applied Sciences*, (2021): 1ББ"7.
- [12] Kabulov A., Yarashov I., Otakhonov A., "Algorithmic Analysis of the System Based on the Functioning Table and Information Security 2022 IEEE International IOT, Electronics and Mechatronics Conference (IEMTRONICS), (2022): 1-5, doi: 10.1109/IEMTRONICS55184.2022.9795746.
- [13] Kabulov A., Saymanov I., Yarashov I., Karimov A., "Using Algorithmic Modeling to Control User Access Based on Functioning Table 2022 IEEE International IOT, Electronics and Mechatronics Conference (IEMTRONICS), (2022): 1-5, doi: 10.1109/IEMTRONICS55184.2022.9795850.
- [14] Navruzov E., Kabulov A., "Detection and analysis types of DDoS attack 2022 IEEE International IOT, Electronics and Mechatronics Conference (IEMTRONICS), (2022): 1-7, doi: 10.1109/IEMTRONICS55184.2022.9795729.
- [15] Wenhao Chen, Lin Li, Newman Jennifer, Guan Yong, "Automatic Detection of Android Steganography Apps via Symbolic Execution and Tree Matching" *In 2021 IEEE Conference on Communications and Network Security (CNS)*, (2021): 254ББ"262.
- [16] Chiung-Wei Huang, Chou Changmin, Chiu Yu-Che, Chang Cheng-Yuan, et al., "Embedded FPGA Design for Optimal Pixel Adjustment Process of Image Steganography" *Mathematical Problems in Engineering*, (2018): 1-8.
- [17] Lili Tang, Xie Jialiang, Wu Dongrui, "An Interval Type-2 Fuzzy Edge Detection and Matrix Coding Approach for Color Image Adaptive Steganography" *Multimedia Tools and Applications*, Vol. 81, no. 27, (2022): 39145ББ"39167.
- [18] Merve Varol Arsoy, "LZW-CIE: A High-Capacity Linguistic Steganography Based on LZW Char Index Encoding" *Neural Computing and Applications*, Vol. 34, no. 21, (2022): 19117 19145.
- [19] Hala Salih Yusuf, Hani Hagrass, "Towards Image Steganography Using Type-2 Fuzzy Logic and Edge Detection *In 2018 10th Computer Science and Electronic Engineering (CEECS)*, (2018): 75-78.
- [20] Mukherjee Nabanita Goutam Paul, Sanjoy Kumar Saha, "An Efficient Multi-Bit Steganography Algorithm in Spatial Domain with Two-Layer Security *Multimedia Tools and Applications*, Vol. 77, (2018): 18451-18481.
- [21] Xiang Lingyun, Rong Wang, Zhongliang Yang, Yuling Liu, "Generative Linguistic Steganography: A Comprehensive Review *KSII Transactions on Internet and Information Systems*, Vol. 16, no. 3, (2022): 986-1005.

-
- [22] Zhongliang Yang, Zhang Pengyu, Jiang Minyu, Huang Yongfeng, Zhang Yu-Jin, "Rits: Real-Time Interactive Text Steganography Based on Automatic Dialogue Model *In International Conference on Cloud Computing and Security*, (2018): 253-264.
- [23] Roseline Oluwaseun Ogundokun, Oluwakemi Christiana Abikoye, "A Safe and Secured Medical Textual Information Using an Improved LSB Image Steganography *International Journal of Digital Multimedia Broadcasting*, (2021): 1-8.
- [24] Tibor Gabor Attila, Jozsef Katona, "Development of Multi-Platform Steganographic Software Based on Random-LSB *Programming and Computer Software*, Vol. 49, no. 8, (2023): 922-941.
- [25] Jayapandiyam Jagan Raj, Kavitha C., Sakthivel K., "Enhanced Least Significant Bit Replacement Algorithm in Spatial Domain of Steganography Using Character Sequence Optimization *IEEE Access*, (2020): 136537-136545.
- [26] Sathish Shet K., Aswath A.R., Hanumantharaju M.C., Gao Xiao-Zhi, "Novel High-Speed Reconfigurable FPGA Architectures for EMD-Based Image Steganography *Multimedia Tools and Applications*, Vol. 78, no. 13, (2019): 18309-18338.
- [27] Iluminada Baturone, Barriga Angel, Jimenez-Fernandez Carlos, Lopez Diego R., Sanchez-Solano Santiago, "Microelectronic Design of Fuzzy Logic-Based Systems *CRC press*, (2018): 338.
- [28] Safdar Munir M., Bajwa Imran Sarwar, Cheema Sehrish Munawar, "An Intelligent and Secure Smart Watering System Using Fuzzy Logic and Blockchain *Computers and Electrical Engineering*, Vol. 77, (2019): 109-119.
- [29] Khan Muhammad, Jamil Ahmad, Muhammad Sajjad, Muhammad Zubair, "Secure Image Steganography using Cryptography and Image Transposition arXiv:1510.04413.

МАЗМҰНЫ – СОДЕРЖАНИЕ – CONTENTS

1-бөлім	Раздел 1	Section 1
Математика	Математика	Mathematics
<i>Akhymbek M.E., Tastankul R.A., Ozbekbay B.O.</i>		
Spectrum of the Hilbert transform on Orlicz spaces over \mathbb{R}		3
<i>Burgumbayeva S., Zhussupova D., Koshkarova B.</i>		
Mathematical modelling of the process of natural gas transportation via pipe networks using crossing-branch method		12
<i>Jenaliyev M.T., Kassymbekova A.S.</i>		
On the initial boundary problem for hyperbolic equations with exponential degeneration $t^{12/7}$		27
<i>Kabulov A., Baizhumanov A., Berdimurodov M.</i>		
On the minimization of k -valued logic functions in the class of disjunctive normal forms		37
<i>Kanguzhin B.E., Kaiyrbek Zh.A., Uaissov B.</i>		
In one scenario, the development of a defect in the attachment of the rod		46
<i>Karimov A., Imanberdiyev K.</i>		
Integro-interpolation method of constructing a difference scheme in a problem with a moving boundary		52
<i>Manat A.M., Orumbayeva N.T.</i>		
On one solution of a nonlocal boundary value problem for a nonlinear partial differential equation of the third order		65
<i>Ryskan A.R., Arzikulov Z.O., Ergashev T.G.</i>		
Particular solutions of multidimensional generalized Euler-Poisson-Darboux equations of elliptic-hyperbolic type		76
2-бөлім	Раздел 2	Section 2
Механика	Механика	Mechanics
<i>Berdenova B.A.</i>		
Simulation of carbon dioxide adsorption onto consolidated activated carbon in 2D axisymmetric system		89
3-бөлім	Раздел 3	Section 3
Информатика	Информатика	Computer Science
<i>Makulova A., Sharipova B., Othman M., Pyrkova A., Ordabayeva G.</i>		
Detection of operating system vulnerabilities and network traffic analysis methods		99
<i>Mussiraliyeva Sh.Zh., Bolatbek M.A., Zhumakhanova A.N., Baispay G., Medetbek Zh.</i>		
Creating a model of semantic analysis of extremist texts in the kazakh language		110
<i>Saymanov I.</i>		
Logical automatic implementation of steganographic coding algorithms		122